LIMIT STATE DESIGN OF OIL AND GAS WELL CASINGS

XIAOGUANG HUANG MSc BSc

Engineering Design & Simulation Group
School of Engineering and Built Environment
University of Wolverhampton

A thesis submitted in partial fulfilment of the
requirements of the University of Wolverhampton
for the degree of Doctor of Philosophy

This research programme was carried out
in collaboration with BG Technology
(now Advantica Technology)

Jan 2002

Abstract

The casing is widely used as a protective conduit during all phases of drilling operations and production in the oil and gas industry. Traditionally casings were designed using working stress design, which had a number of shortcomings such as poor economics, inflexibility and uneven risk. This thesis was initiated by the increasing demand for an improved design of casings for the oil and gas industry. A new approach using the concept of limit state design is proposed to remedy the limitations of the present design code. Limit state design employs the probability of failure rather than the usage of a safety factor, from which the designer can gain an overall idea of the safety and adequacy of the design. The main objective of this thesis is to set up a set of limit state design equations for casings under different loadings. This objective is tackled by way of investigations into three fundamental casing failure modes, i.e. casing collapse, casing burst and casing axial tensile failure.

Simple equations are proposed for the calculation of the load terms in the limit state design equations for the three failure modes. A comprehensive finite element methodology is developed to investigate the ultimate strength of casings with imperfections under different loadings. Extensive comparisons between finite element models and historical experimental data demonstrate that, if the variables are known, the ultimate strength of a casing can be predicted to a satisfactory degree of accuracy using the finite element method. Detailed parametric studies have been performed to investigate the effects of major factors (i.e., the ratio of outside diameter to wall thickness, ovality, eccentricity, material hardening, anisotropy and residual stress) on the casing strength.

Existing design equations are assessed by means of full-scale test data, where they are found to be only accurate within a certain region. The investigations for new limit state design equations have been performed by employing a new concept of generalized material behaviour, which is constructed from experimental data and implemented in the finite element simulation. A set of limit state design equations are derived after regression analysis of the numerical results. Comparisons demonstrate that, the new design equations are capable of providing more accurate predictions of

casing strength without compromising safety. The limit state design approach is provided in a structured way with a detailed design flow chart to enable a casing designer with a conventional engineering background to assess casing design using the limit state design methodology. It is anticipated that the implementation of a limit state design methodology in the design of casings will lay the foundation for an increased safety awareness whilst enhancing cost savings.

Acknowledgements

I would like to express my sincere appreciation to my supervisors, Professor Musa Mihsein, Dr Kevin Kibble and Professor Richard Hall, for their merit guidance and help throughout my stay at the University of Wolverhampton. Without their valuable advice, continual encouragement and support, it would have been impossible to complete this study.

General support from the School of Engineering and Built Environment at the University of Wolverhampton is most gratefully acknowledged. In particular, I would like to express my gratitude to the school secretary, Mrs Amrit Chodda, for her assistance during the course. I would also like to thank BG Technology (now Advantica Technology) at Loughborough for the financial support to this research. Thanks to Mr Mark Nunn, senior engineer of BG Technology, for his technical help on casing design. Thanks to the library of Institute of Petroleum Engineering, Technical University Clausthal, Germany, for kindly providing casing test data. Special thanks go to Mr Andrea Assanelli, senior engineer of Siderca Plc., Argentina, for many valuable discussions and advice on casing collapse.

To my parents and my sisters, I offer heartily thanks for their love and their continuous support throughout the years. Without them, I would not be where I am today. I would also like to thank my wife, Yanyun, for her support and care. It would not have been possible to go through those sleepless nights without her by my side.

Finally, I would like to thank all the Chinese fellows in the University of Wolverhampton for their encouragement. Special thanks go to Mr Stefan Scholze (fellow PhD student) for his kind help on finding the casing test data.

CONTENTS

PAGE NUMBERING AS ORIGINAL

Nomenclature

English letters

A_{ann}	Annulus area, m^2
A_s	Cross sectional area of casing, m^2
CVN	Charpy V-notch impact value, N m
d	Casing shoe depth at stuck point, m
$\{d\}$	Vector of unknown nodal displacements
d_1	Influx depth, m
d_2	Depth of relevant inspection point, m
d_{packer}	Packer depth, m
d_{perfs}	Perforation depth, m
d_{shoe}	Shoe depth, m
d_{toc}	Top of cement depth, m
d_{wh}	Wellhead depth, m
D	Casing outside diameter, m
D_o^{loc}	Local outside diameter, m
D_{max}	Maximum measured outside diameter, m
D_{min}	Minimum measured outside diameter, m
E	Young's modulus, Pa
E_t	Tangent modulus, Pa
$f_Z(Z)$	Probability density function of basic variables
$\{f\}$	Vector of applied nodal forces
F_A	Axial force, N
g	The gravity acceleration, m s^{-2}
gr	Kick gas gravity at standard temperature and pressure
$G(Z)$	Limit state response
H_{CSD}	The vertical casing setting depth, m
Ki	Kick intensity
K_{Ic}	Critical mode I stress intensity factor threshold value, Pa $m^{\frac{1}{2}}$
$[K]$	Stiffness matrix
l	Length of mud column inside the casing, m
L	Casing length, m
L_{at}	Ultimate load of casing axial tension, N
L_c	Critical casing length, m
L_{char}	Characteristic value of the load effect
L_f	Load design factor
L_w	The worst case load, N

$L(Z)$	Load effect contribution
modu	Modelling uncertainty
M	Safety margin between two quantities
n	Hardening parameter
N_N	Interpolation function
Ob	Overbalance
P_2	Pressure at the inspection point, Pa
P_{b-gk}	Burst load due to gas kick, Pa
P_{b-pt}	Burst limit state load in pressure test, Pa
P_{b-tl}	Burst load due to tubing leak, Pa
P_{BA}	Burst strength with axial tensile stress, Pa
P_{B0}	Burst strength without axial tensile stress, Pa
P_{cs}	Collapse load of surface casing at casing seat, Pa
P_{CI}	Collapse load of intermediate casing, Pa
P_{EA}	Elastic collapse pressure under axial loading, Pa
P_{E0}	Elastic collapse pressure without axial loading, Pa
P_{exp}	Experimental collapse strength, Pa
P_{FEM}	Predicted collapse strength from FEM, Pa
P_{frac}	Formation fracture pressure, Pa
$P(F)$	Probability of failure of a particular limit state
P_{GA}	General yield pressure under axial loading, Pa
P_{G0}	General yield pressure without axial loading, Pa
P_{op}	The overpull force, N
P_{res}	Reservoir pressure, Pa
P_{test}	Test pressure, Pa
P_{yA}	Yield onset collapse pressure under axial loading, Pa
P_{y0}	Yield onset collapse pressure without axial loading, Pa
r	Inside radius of casing, m
R	Outside radius of casing, m
R_{char}	Characteristic value of the resistance
R_f	Resistance design factor
R_{ij}	Anisotropy yield stress ratios
R_{min}	Minimum resistance, Pa
R_{min} / SF	The safe working stress of a casing
$R(Z)$	Resistance contribution
S	Surface bounding a volume
SF	Safety factor
t	Wall thickness of casing, m
td	Thermal degradation
t_{max}	Maximum wall thickness, m
t_{min}	Minimum wall thickness , m

T	Temperature at point of interest, ^{0}C
T_1	Absolute temperature at influx depth, ^{0}C
T_2	Absolute temperature at the relevant inspection point, ^{0}C
T_{ref}	Reference temperature for thermal degradation, ^{0}C
u	Initial ovality
u^N	Nodal variable
V	Volume occupied by a part of the solid body, m^3
V_i	Shut-in influx volume, m^3
V_t	The transition volume, m^3
$w(\theta)$	Initial pattern of ovality
W_n	Nominal weight of casings, N
Y/T	Ratio of yield strength to ultimate tensile strength
Z	Generalized design variables in a limit state function

Greek letters

α, β	Material constants
δ	Distance measured from the eccentric centres, m
δv	Virtual velocity, m s^{-1}
ε	True strain
ε^{el}	True elastic strain
ε_{nom}	Nominal strain
ε^{pl}	True plastic strain
ε^{t}	Total true strain
ε_{uts}	Strain corresponding to ultimate tensile stress
λ	Anisotropy parameter
μ	Mean value of a variable
θ	Angular dimension
ρ_{air}	Air density at standard temperature and pressure, Kg m^{-3}
ρ_{cement}	Cement slurry density, Kg m^{-3}
ρ_f	Formation density, Kg m^{-3}
ρ_i	Inside mud density, Kg m^{-3}
ρ_m	Mud density, Kg m^{-3}
ρ_{ml}	Mud density used to drill the next hole, Kg m^{-3}
ρ_o	Fluid density outside casing, Kg m^{-3}
ρ_{pf}	Production fluid density, Kg m^{-3}
ρ_s	Density of steel, Kg m^{-3}
σ	True stress, Pa
σ_A	Applied axial stress, Pa
σ_E	Elastic proportional limit, Pa
σ_x	Yield stress in the axial direction, Pa
σ_{nom}	Nominal stress, Pa

σ_0	Reference yield stress, Pa
σ_R	Residual stress in the circumference, Pa
$\sigma_{R\theta op}$	Optimum residential stress, Pa
σ_s	Yield stress in the circumference, Pa
σ_{uts}	Ultimate tensile stress, Pa
σ_y	Yield strength, Pa
$\frac{d\sigma}{d\varepsilon}$	Current slope in the stress-strain curve
ϕ	Standard deviation
υ	Poisson's ratio
ψ	Initial eccentricity

Abbreviations

AIS	Asymptotic Importance Sampling
API	American Petroleum Institute
BEM	Boundary Element Method
COV	Coefficient of Variance
DCE	Design Check Equation
DEA	Drilling Engineer Association
FEM	Finite Element Method
FORM	First Order Reliability Method
ISO	International Standard Organisation
LRFD	Load and Resistance Factor Design
LSD	Limit State Design
MTR	Mill Test Reports
PDF	Probability Density Function
QRA	Quantitative Risk Assessment
SLS	Serviceability Limit State
SORM	Second Order Reliability Method
TRL	Tolerable Risk Levels
ULS	Ultimate Limit State
UTS	Ultimate Tensile Stress
WSD	Working Stress Design

List Of Tables

List Of Figures

Chapter 1

Introduction

1.1 General

The casing is widely used as a protective conduit during all phases of drilling operations and production in the oil and gas industry. Casing design impacts greatly on how safe a well operates, and thus is one of the most important aspects of a well plan. As the casing is often designed to withstand many severe operating and production conditions, procedures for casing design must be sufficiently flexible to meet all potential requirements. Therefore, casing design requires a sound knowledge of the operating conditions imposed on the casing surface as well as a working understanding of various concepts related to the casing properties. Casing design engineers must be aware of these concepts before beginning the actual casing design. These concepts include items such as the casing manufacturing process, physical properties, and testing procedures. As the casing usually accounts for between 10% to 30% of the total cost of a well and thus represents a major capital investment, casing design will also have a significant impact on well performance, price and productivity.

With the increasing need for safety awareness and cost reduction in casing design due to the competitiveness of today's market, the size and the number of investigations on how to improve the casing design criterion have been growing rapidly in recent years. The objective of a casing design is to estimate the casing strength and the possible loads during the service life, in order to make sure that they are separated by an adequate safety margin. Therefore, a casing design engineer needs to find out the casing strength and load uncertainties. Casing strength uncertainty arises due to the inherent variability of material properties of casings, workmanship, and the handling of casings during installation. While the load uncertainty is associated with a casing designer's inability to estimate the possible loads precisely.

A casing experiences a variety of loads from various operations during the service life. In particular, casings are subjected to pressure loads induced by contained moving fluids both inside and outside the casing, forces due to self-weight and end constraint, and accidental loads caused by the loss of drilling fluids. In addition, variation of temperature along the length of a casing during installation and operating conditions may induce additional loads. These loads can be reduced into a few fundamental forces such as the external and internal pressures. Analysis shows that the important casing failures include casing collapse under excessive external pressure, casing burst under excessive internal pressure and casing tensile failure under an axial tensile load.

1.2 Problems In Casing Design

Two of the most important factors in any casing design are safety and cost. Throughout the oil and gas industry, the importance of control and optimisation of these factors has been long recognized.

Traditionally casing design uses the working stress design (WSD) method, a deterministic approach, which defines the load as an estimate of the maximum anticipated load, while the casing strength is defined as a lower bound of material strength. According to this method, a designer must assure that the maximum possible load will not exceed the minimum casing strength. A safety factor is therefore used as a contingency since there are always many uncertainties during the service life of a casing. The safety factor is fixed by various design standards. An individual company may set up its own guidelines based on experience, which may be totally different from one company to another. However, in the majority of cases, this possible worst case scenario will not be realised. Conversely, there are rare instances that the actual load does exceed the strength, and the casing fails.

Although the working stress design method uses a safety factor to estimate the worst case scenario, the true safety margin in the casing design is largely unknown because this safety factor is not a direct measure of safety or risk. This deterministic approach

cannot answer the fundamental question of how often a failure will occur. Safety factors are used because of uncertainties in the design parameters, so maybe they are better termed 'factors of ignorance'. Therefore, a safety factor as a stand-alone design criterion for casing design is becoming increasingly outmoded in the oil and gas industry. Clearly small changes in this safety factor will have a great impact on the economics of the casing. As a result, it will be beneficial to quantify the safety factors and make use of the redundancy in the casing design process without compromising safety.

However, the true safety factor is difficult to quantify, because it requires a clear understanding of the mechanisms, which cause a casing to fail, as well as an understanding of the risk associated with the failure event. A more practical and meaningful methodology is provided by considering the probability of failure, which can be quantified as an absolute number to describe the true failure event. It is associated with the consequence of a failure (loss of equipment, life etc.), which in turn gives the overall risk of a casing design. It is noted that the risk is often a value quoted as reasonably practical to achieve within the constraints of the system. A tolerable risk level (TRL) is such an achievable number, which is used to work back in the casing design process to an acceptable probability of failure. Therefore, the fundamental question of how often a casing design will fail is answered and the need for an arbitrarily set safety margin can be removed in the casing design process.

Although working stress design is conceptually simple and has worked well in the past, it has many drawbacks particularly if a poorly estimated safety factor is used. Casing designers, using this deterministic approach, have recognized the inadequacy of the safety factor and attempted to rectify this by including as many of the load variables as can be predicted, with the operational consequence of each. It is widely accepted that it is advantageous to explore the possibility of developing a new casing design methodology on the basis of probabilistic concepts and historical data in the oil and gas industry, to remedy the limitations of the present design code. Limit state design is such a probabilistic method through which the risk of a failure inherent in an engineering design can be determined. Compared with the working stress design, it provides an overall idea of the safety and adequacy of a design. The success of the

implementation of a limit state design methodology in the casing design will lay the foundation of increased safety awareness whilst maintaining possible cost efficiency.

1.3 Objectives Of The Research

The objective of this study is to enable the limit state design to be used for casing design in the oil and gas industry. The output from this study will be a systematic toolkit of simplified limit state equations describing the limit-state responses of a casing under external pressure, internal pressure and axial tension. Such a limit state design approach will be provided in a structured way using detailed design flow charts to enable a casing designer with a conventional background to assess casing design using the limit state design methodology.

1.4 Key Components Of The Research

Limit state design is a long established concept, which has recently come to the attention of the oil and gas industry. Although the idea is quite simple, limit state design has a number of components that require detailed consideration.

(1) Available Data. The acquisition, quality control and subsequent use of all types of data are central for the adequate execution of the limit states design methodology. The relevant strength, material behaviour and geometry properties (including yield stress, outside diameter, wall thickness, eccentricity, ovality and residual stress) of samples have been accurately measured in full-scale tests. These data were collected from previous studies and industrial experience, and have been used to validate the proposed limit state models. Therefore, they are very crucial in the development of the limit state design methodology for casing design.

(2) Limit State Models. The basic building blocks for a limit state design process use a set of simplified models that describe the physical phenomena of possible failures. Plausible casing failure modes have been established and likely causes of failure exploited. Models have been developed for casing collapse, casing burst and casing tension, which vary in complexity according to each limit state.

(3) Limit State Load Determination. A series of load cases have been designed to calculate the load term for a limit state casing design on the basis of real casing operating conditions. A set of simple equations is proposed to determine the load term for each load case. This part of the research drew heavily on the experiences of British Gas Technology (the sponsor of this project).

(4) Ultimate Casing Strength Determination. On the basis of the limit state models, finite element simulations of casing failures have been carried out to determine the ultimate casing strength under different load conditions. The finite element simulations have been validated by test data collected for this research. It has been demonstrated that the simulation can predict the actual ultimate casing strength accurately, provided major variables are known. Effects of major factors on the ultimate casing strength have been studied and discussed.

(5) Limit State Design Equations. A set of limit state design equations has been derived on the basis of the finite element simulations. Existing design equations have been reviewed and assessed in terms of their background and applicability to the limit state design of casing by means of full-scale test data. The output of this phase of the study was whether to find out the most suitable equation for limit state design to use or to derive new limit state equations. The limit state design equations constitute the limit state toolkit. Guidelines are given to enable a casing designer to assess a casing string using limit state design methodology.

The above are the main contents of this thesis, which is the first part of a study to apply full quantitative risk assessment (QRA) in the limit state design of casing in collaboration with BG Technology (Now Advantica Technology) at Loughborough. This thesis will focus on the investigation of the mechanical characteristics of a casing under limit states. The other part will focus on the reliability analysis of casing design by another researcher at the University of Wolverhampton. For the limit state design

equations derived in this work, each variable in the limit state design equations will be treated as a random variable and assigned a probability distribution function. A reliability technique will be evaluated to calculate the overall risk of a limit state casing design. Furthermore, the full QRA together with the limit state design equations will be implemented in a limit state casing design software. The final outcome will be a full QRA based limit state casing design system, integrating the limit state design equations from Part 1 with the reliability analysis techniques from Part 2.

1.5 Background And Research Approach

The principal difficulty in this research was to establish the limit state models of casing failures under different loading conditions. Many concept studies (Payne and Swanson, 1990; Maes et al, 1993; Gulati et al, 1994; Lewis et al, 1995; Brand et al, 1995; Raney et al, 1997) have already concentrated on describing the advantages of limit state design and making comparison with the conventional work stress design. Though some equations from different theories have been proposed to describe the limit state response of a casing, there is a considerable mismatch between the predictions from these equations and the full-scale experimental data. The ultimate strength of a real casing is still uncertain because there are many factors (both material and geometrical imperfections) affecting the actual casing strength.

As early as 1884, Levy developed a rational expression for the collapse of long cylinders under external pressure (Clinedinst, 1939). The importance of inelastic effects was well recognized very early, as Southwell (1915) established a collapse pressure formula for D/t as low as 10 in a notable contribution. Clinedinst (1939), in his first of many contributions to casing collapse, derived an elastic collapse equation. With the development of theoretical analysis of casing collapse, many researchers (Timoshenko, 1933 and 1961; Donnell, 1956; Arbocz and Babcock, 1969; Heise and Esztergar, 1970; Small, 1978; Huang and Pattillo, 1980) recognized the importance of geometrical imperfections and performed some initial studies of their effects on the buckling of cylinders under external pressure.

Due to the limitations of classical theories, numerical methods were gradually introduced in the early 1960s and many advances have been made since then. As to ultimate casing strength, the effects of geometrical imperfections have to be investigated by numerical analysis. With the rapid increase in computing power, the finite element method (FEM) has dominated the field through its versatility and flexible ability to model complex geometry and material properties. Most researchers (Tamano et al, 1983; Tokimasa and Tanaka, 1986; Issa and Crawford, 1993; Bai et al, 1993, 1995 and 1997; Abbassian and Parfitt, 1995; Assanelli et al, 1998) investigated the ultimate collapse strength of casing using finite element analysis. In addition, considerable research efforts (Stewart et al, 1993 and 1998; Klever et al, 1993 and 1998; Paslay et al, 1998; Tallin et al, 1998) have been made for casing burst by FEM. Compared to casing collapse and burst, far fewer investigations have been carried out for casing tensile failure. However, several researchers (Pattillo and Hunag, 1982; Kyoguku et al, 1982; Tamano et al, 1982) performed numerical and experimental studies of the collapse strength under a combination of axial loading and external pressure.

The research presented in this thesis was initiated and guided by the need to establish a more accurate risk based design criterion for the oil and gas industry. A set of casing failure models has been constructed to describe each limit state response of a casing under different loadings. The ultimate casing strength has been determined by the finite element analysis. After the finite element analysis was validated by test data, a set of limit state design equations was derived. These limit state design equations have been passed on to a following study for a quantitative risk assessment of casing design.

1.6 Thesis Structure

The thesis is divided into eight chapters to investigate the limit state design of casing for the oil and gas industry. A general introduction of the research is given in Chapter 1, including the research objectives, background, key components and research approach.

In Chapter 2, the theory of limit state design, which is characterised by a limit state equation, is reviewed and discussed. In addition, it presents a review of the topics relevant to casing design. The advantages and disadvantages of each design method are highlighted in a general review and comparison of casing design methodologies.

In Chapter 3, three fundamental failure modes, i.e., casing collapse, casing burst and casing axial tension, are identified according to the predominance of a particular loading in the casing design process. On the basis of the real casing operating conditions, a set of equations are proposed for the load calculation of each failure mode, which is the load term in a limit state casing design equation.

In Chapter 4, numerical methods to study casing failures including boundary element and finite element methods are generally reviewed. In addition, a brief introduction of ABAQUS, the commercial finite element analysis package used in this research, is presented. Furthermore, several key features of the finite element analysis, including the non-linear equilibrium equation solution, Riks algorithm and material plasticity modelling, are generally described.

In Chapter 5, a comprehensive review of casing collapse is performed. In particular, attention is directed to the major factors relevant to collapse, including lobe number, ratio of length to outside diameter, ovality, eccentricity, residual stress, material hardening and material anisotropy. A brief description of the casing collapse experiment is given in correspondence with the importance of the casing collapse test for this research. A large number of finite element analyses of casing collapse are performed and validated by existing collapse test data. Furthermore, the capabilities of previous published collapse equations have been assessed using the available test data. Two empirical equations with imperfections implicitly and explicitly expressed are proposed after regression analyses of finite element results.

In Chapter 6, a brief review of published design equations for casing burst is presented. Finite element analyses of casing burst are performed, which have been validated through an extensive comparison with burst test data. Major factors have been studied, and comparisons have been performed to assess the accuracies of previous design equations for casing burst using available burst test data. An empirical burst equation is derived on the basis of FE analyses. It is proved from the

comparison that, not only is the new burst equation able to give a safe design, but also it is up to 15 percent more accurate than the API burst equation.

In Chapter 7, casing strength under axial tension alone is studied. In particular, it is found that the ultimate tensile strength of a casing can be used as the material resistance term in the limit state function for this load case. Furthermore, combined load cases, i.e. casing collapse and casing burst in the presence of axial tension load, are generally investigated.

The original contributions of the work reported in this thesis are:

1. An investigation into the criterion of limit state casing design through a comprehensive comparison with other casing design methodologies. (Chapter 2)

2. Provision of an intuitive way to calculate the load for a casing under different loading conditions. (Chapter 3)

3. Provision of a comprehensive finite element model, including geometric imperfections, material hardening and anisotropy, to study casing failure and proposition of a generalized material constitutive behaviour to simulate the casing material. (Chapters 5 and 6)

4. Provision of new design equations for the calculation of material resistance of the casing for different failure modes. (Chapters 5, 6 and 7)

5. An initial investigation into a real implementation of limit state design based quantitative risk assessment of casing failure.

Chapter 2

Review Of Casing Design

2.1 Introduction

This thesis is the first part of a study to apply full quantitative risk assessment (QRA) in the limit state design of casing in collaboration with BG Technology (Now Advantica Technology) at Loughborough. It will focus on the investigation of the mechanical characteristics of a casing under limit states. The objective of this research is to derive a systematic toolkit of simplified limit state equations describing the limit state responses of a casing under external pressure, internal pressure and axial tension.

Chapter 2 presents a review of the topics relevant to casing design in this thesis, including a detailed review, comparison of casing design methodologies, and descriptions of the limit state design concepts and limit state equation.

The design of casing requires a knowledge of the operating conditions to be imposed on the casing as well as a working understanding of various concepts related to casing properties. A drill engineer must be aware of these concepts before beginning the actual casing design operations. A general introduction of casing functions and casing properties is first presented. The analysis of the casing manufacturing process is not a part of this thesis, but the imperfections and material anisotropy induced from the manufacturing process will greatly affect the casing strength. Thus an understanding of the manufacturing process will provide a good basis for accurately estimating the casing strength. This topic is therefore briefly reviewed.

Attention is next turned to the limit state design concepts and limit state equation. Detailed descriptions are presented for casing design methods, including deterministic design method such as working stress design (WSD), reliability based design methods such as load and resistance factor design (LRFD) and quantitative risk assessment (QRA). Advantages and disadvantages of each method are highlighted. Examples are

presented to show the relationship between WSD, LRFD, and QRA designs for the same load combinations. Finally applying a full QRA methodology in the limit state design is proposed at the end of this chapter.

2.2 Basic Casing Design Concepts

2.2.1 Casing Types And Functions

The presence of high-pressure zones at different depths along the wellbore, and the presence of weak, unconsolidated formations, necessitates running casings to seal off these troublesome zones and to allow the drilling to total depth. As a result, different sizes of casing are employed and this arrangement gives a final tapered shape to the finished well. The types of casing currently in use are as follows:

- **Conductor Pipe.** Conductor pipe is run from the surface to a shallow depth to protect near surface unconsolidated formations, seal off shallow-water zones, provide protections against shallow gas flows, provide a circuit for the drilling mud and to protect the foundation of the platform in offshore operations. Conductor pipe is always cemented to the surface. It is used to support subsequent casing strings and wellhead equipment.

- **Surface Casing.** Surface casing is run to prevent caving of weak formations that are encountered at shallow depths. This casing should be set in competent rocks such as hard limestone. This will ensure that formations at the casing shoe will not fracture at the high hydrostatic pressures that may be encountered later. The surface casing also serves to provide protection against shallow blowouts. The setting depth of this string of casing is chosen so that troublesome formations, thief zones, water sands, shallow hydrocarbon zones and build-up sections of deviated wells may be protected.

- **Intermediate Casing.** Intermediate casing is usually set in the transition zone below or above an over-pressured zone, to seal off a severe-loss zone or to protect against problem formations. Good cementation of this casing must be assured to present communication behind the casing between the lower hydrocarbon zones and upper water formations. Multistage cementing may be used to cement this string of casing in order to prevent weak formations from being subjected to high hydrostatic pressure from an unbroken, long column of cement.

- **Production Casing.** Production casing is the last casing string. It is run to isolate producing zones, to provide reservoir fluid control, and to permit selective production in multi-zone production. This is the string through which the well will be completed.

- **Liner Casing.** A liner is a string of casing that does not reach the surface. Liners are hung on the intermediate casing by use of a suitable arrangement of a packer and slips called a liner-hanger. Liner casings are used frequently as a cost effective method to attain pressure or fracture gradient control without the expense of running a casing string to the surface. It is noted that the tie back liner is a section of casing extending upwards from the top of an existing liner to the surface.

Figure 2.1 shows the relationship of these casing strings. In addition, the illustration shows some of the problems and drill hazards that the casing strings are designed to control. In general, the functions of the casing can be summarised as follows:

1) To keep the hole open and to provide a support for weak, vulnerable or fractured formations.

2) To isolate porous media with different fluid/pressure regimes from contaminating the pay zone. This is basically achieved through the combined presence of cement and casing.

3) To prevent contamination of near-surface fresh water zones.

4) To provide a passage for hydrocarbon fluids.

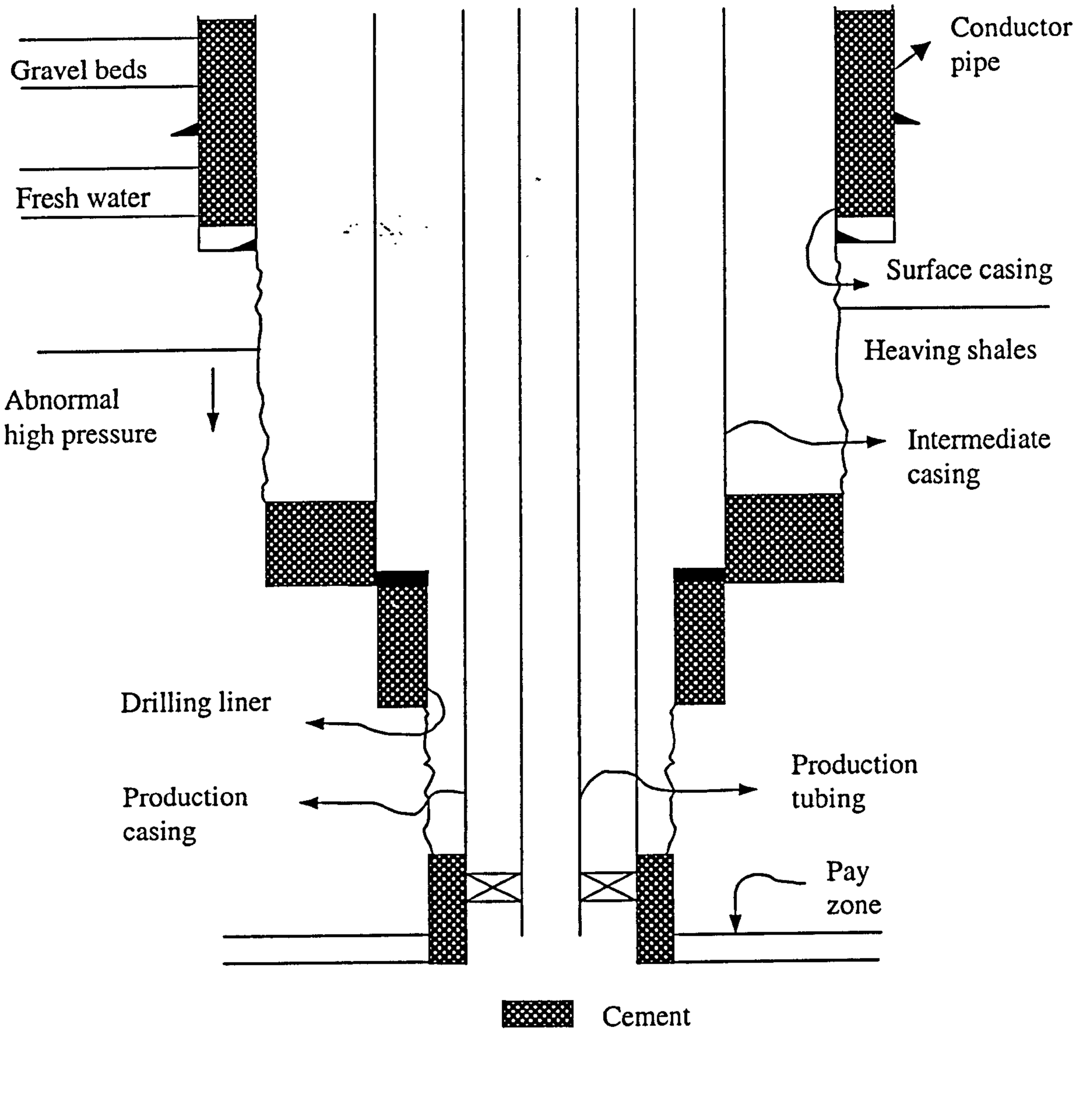

Fig. 2.1 A typical casing string relationships

5) To provide a suitable connection for the wellhead equipment. The casing also serves to connect the blowout prevention equipment, which is used to control the well while drilling.

6) To provide a hole of known diameter and depth to facilitate the running of testing and completion equipment.

2.2.2 Casing Physical Properties

The physical properties of a casing include grade, pressure resistance, diameter and weight. These properties relate to a casing's ability to meet the demand of the imposed drill conditions. The limitations of the casing properties must be considered before final casing selection.

2.2.2.1 Casing Grades

Different grades of casing are manufactured to suit different drilling situations. The casing grade is a designation that defines the casing's yield strength and certain special characteristics. The American Petroleum Institute (API) lists eight different grades of casings as shown in Table 2.1. The number in the grade designation (e.g.

Table 2.1 API casing grades

Grade	Minimum Yield Strength		Minimum Tensile Strength	
	(psi)	(MPa)	(psi)	(MPa)
H40	40,000	275.76	60,000	413.64
J55	55,000	379.17	70,000-95,000	482.58-654.93
K55	55,000	379.17	70,000-95,000	482.58-654.93
N80	80,000	551.52	100,000	689.40
L80	80,000	551.52	100,000	689.40
C75	75,000	517.05	95,000	654.93
C95	95,000	654.93	105,000	723.87
P110	110,000	758.34	125,000	861.75
Q125	125,000	861.75	135,000	930.69

H40) gives the API minimum yield strength in thousands of psi. The average yield strength of casing is usually 10,000 psi (68.9 MPa) greater than the minimum yield, for example, 90,000 psi (620.5 MPa) for N80 casing. The minimum yield strength value is used in collapse and burst resistance calculations, whereas the average is used for biaxial evaluations (Rabia, 1987).

2.2.2.2 Casing Diameter And Wall Thickness

Different casing sizes are run at different parts of the hole to allow the drilling of the well to its total depth with minimum risk. Since pressures vary along every section of the hole, it is possible to run a casing string having the same outside diameter but with different thickness or strength properties. Thus, a heavy or high grade casing can be run only along portions of the hole containing high pressures. This arrangement provides the most economical way of selecting a given casing string. A drill engineer normally considers three types of diameter data when planning the casing design, which are outside, inside and drift diameters. The inside diameter equals to the outside diameter minus twice the nominal wall thickness. The drift diameter refers to the diameter of a cylinder drift mandrel that can pass freely through the casing with reasonable exerted force equivalent to the weight of the mandrel being used for the test. In this thesis, only outside and inside diameters will be employed in the analysis.

2.2.2.3 Casing Weight

The API defines three types of casing weight: 1) nominal weight; 2) plain end weight; and 3) threaded and coupled weight. A detailed treatment of casing weights can be found in API bulletin 5C3 (API, 1992). As casing weights required for the purpose of casing design are usually reported as nominal weight, only nominal weight will be reviewed here. It is used primarily for the purpose of identification of casing types during ordering, which is normally based on the calculated, theoretical weight per foot

for a 20 ft (6.1 m) length of threaded and coupled casing joint. Therefore, the nominal weight, W_n, is calculated by,

$$W_n = 10.68(D-t)t + 0.0722D^2 \qquad lbm/ft \qquad (2.1)$$

2.2.2.4 Process Of Casing Manufacture

The following notes are extracted from API Spec 5C3 (1992). It states that casing, liner and tubing conforming to this standard must be seamless or electric welded. Seamless casing is defined as wrought steel tubular product made without a welded seam. It is manufactured by hot working steel, or if necessary, by subsequently cold finishing the hot-worked tubular product to produce the desired shape. The process may involve a plug mill or mandrel mill rolling. A typical seamless process is shown in Fig. 2.2. Different from seamless casing, an electric welded casing has one longitudinal seam formed by electric flash welding or electric resistance welding, without adding extra metal. The weld seam of electric welded casing is heat treated after welding to a minimum temperature of 1000^0F (538^0C), or processed in such a manner that no untempered martensite remains. Fig. 2.3 illustrates a typical electric weld process.

2.2.3 Some Casing Design Technical Terms

Prior to discussing the detailed casing design techniques, it is necessary to clarify some technical terms used in the casing design process. Pore pressure is defined as the pressure acting on the fluids in the pore spaces of the rock, which is the strict meaning of what is generally referred to as formation pressure. The fracture gradient is the rate of change in fracture pressure required to fracture subsurface formations. At the data collection stage in a casing design, the pore pressure, fracture gradient and mud weight can be determined from the offset well data log. Casing seat selection is to choose a casing seat that can withstand the maximum pressures to which the wellbore will be subjected during drilling of the next hole section. The casing seat selection can be determined by drawing the fracture gradient data together with pore pressure and

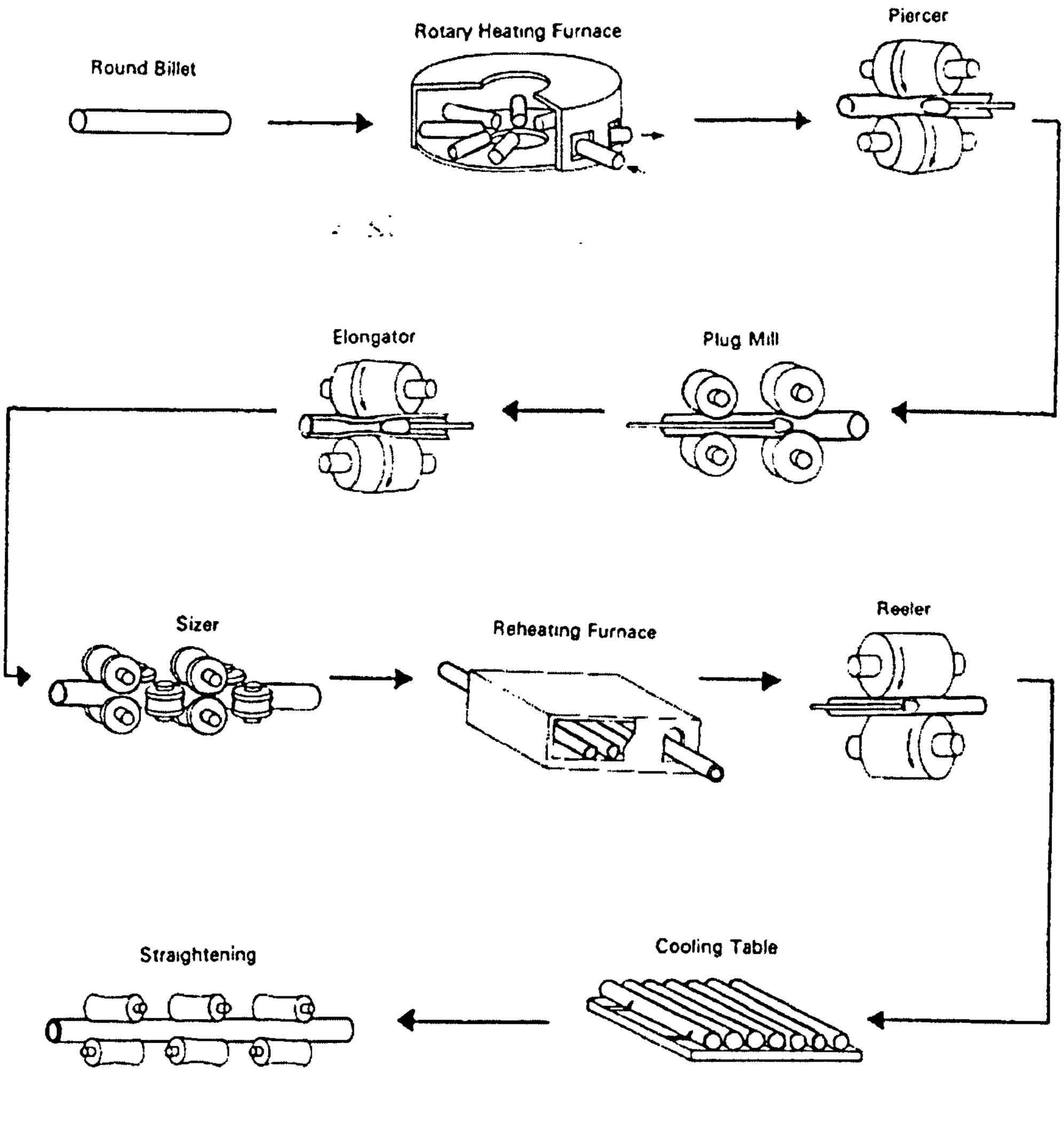

Fig. 2.2 A typical seamless casing manufacture process

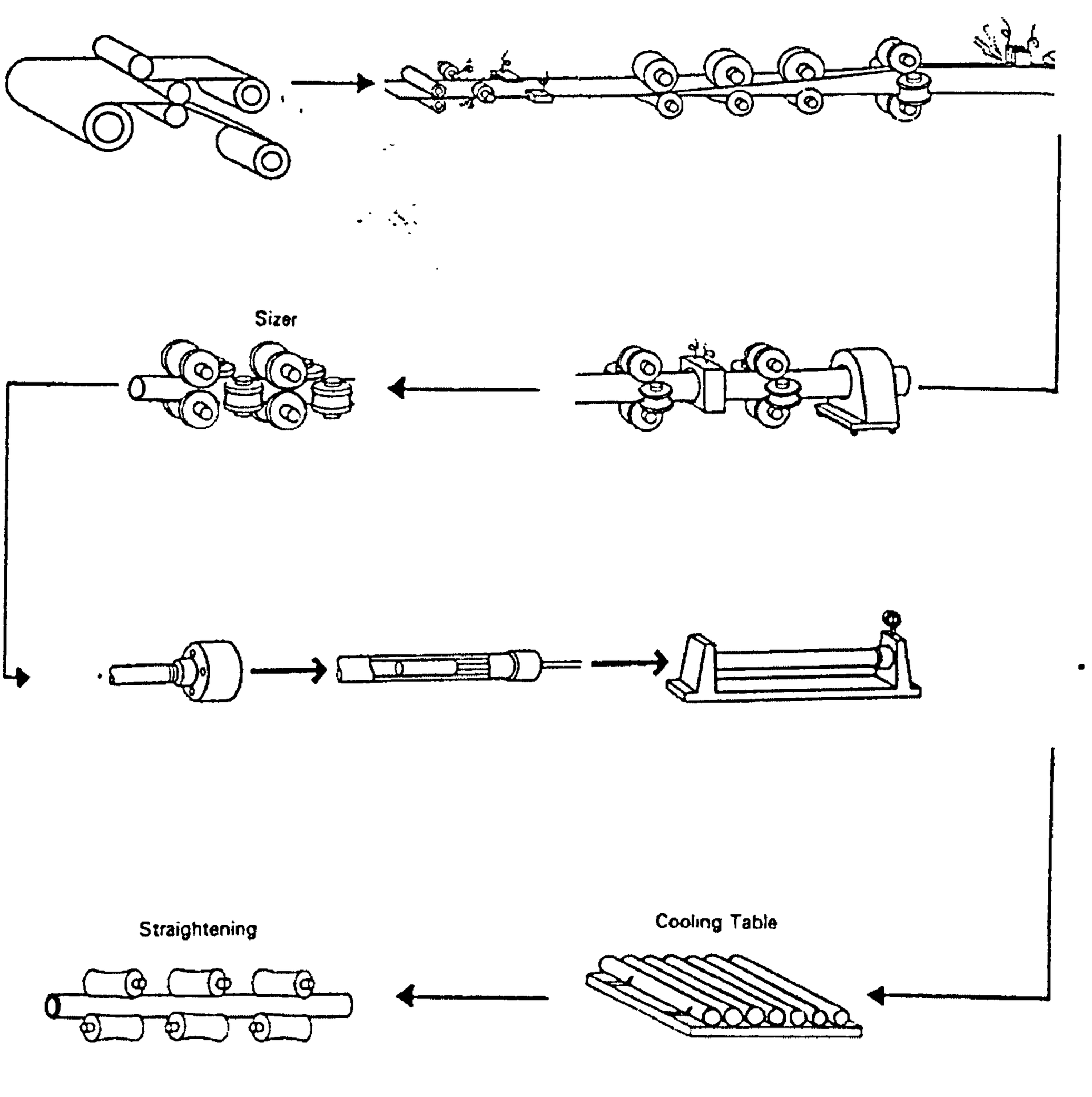

Fig. 2.3 A typical welded casing manufacture process

mud weight against depth. A kick is an accidental condition where the internal drilling fluids are replaced by lighter fluids, usually a light gas such as methane, from a high pressure zone below the casing termination point. It arises when the pressure of a permeable formation exceeds the mud weight and an influx of formation fluid enters the wellbore during drilling. For practical purpose, kick tolerance can be defined as the maximum kick size, which can be tolerated without fracturing the previous casing shoe.

2.3 Review Of Limit State Design

2.3.1 Basic Concepts Of Limit State Design

The objective of any structural design is to obtain a structural solution for safety and serviceability throughout the design life. Having been the accepted basis for steel and concrete structure design in structural engineering for some twenty-five years, limit state design theory is conveniently introduced by considering the fundamental purpose of the design so that structural design can be seen in its correct perspective.

A limit state is a condition beyond which the structure will become less than completely fit for its intended use. If this happens, the structure is said to enter into a limit state. In the structural engineering context, the best known application of limit state design is to structural steelwork. Until about 1950, steelwork design was invariably based on the result of an analysis which treated the structure as elastic. A structure is said to be safe if the maximum stress calculated on that basis is less than an allowable stress, which is a defined fraction of the yield stress of the steel. It is progressively realised that this approach is incomplete and not entirely rational. In particular, it fails to recognise that very high stress, well beyond allowable stress, occurs in small regions of the structure at quite low loads. It also leads to inconsistencies between one structure and another. For instance, two structures may both be at the allowable stress limit under a certain load, and have different factors of safety against collapse. Structural engineers resolve this problem by concentrating on

collapse, which is one of the limit states that make a structure unusable. It turns out that collapse loads can be predicted far more reliably, consistently and easily than any state that depends on an allowable stress. Moreover, design based on a limit state against plastic collapse allows for worthwhile economies in steel.

Nowadays, most design codes are based on limit state theory. More and more structural engineers are using limit state design concepts readily and comfortably. The central concepts of a limit state design theory are: (1) All the separate conditions that make the structure unfit for use are taken into account. These are the separate limit states. (2) The design is based on the actual behaviour of the materials and performance of structures and members in service. (3) Ideally, design should be based on statistical methods with a small probability of the structure reaching a limit state. Usually partial factors are used to account for the probability of the characteristic loads being exceeded and the assessed design strength not being reached. Thus limit state design simply provides a basic framework within which the performance of the structure can be assessed against various limiting conditions. When formulating procedures nowadays, it is customary to do so in a way, which recognizes the inherent variability of loads, materials, construction practices and approximations made in design. Point (3) above implies the recognition of the facts that, load and material strength vary and approximations are used in the design. In addition, imperfections in fabrication affect the strength in service. All these factors are usually realistically assessed by use of some concepts from probability theory.

Limit states are broadly divided into two categories corresponding to the two types of performance requirements, i.e, ultimate limit state (ULS) and serviceability limit state (SLS). Due to limitations of strength and stability under the imposed loads, the attainment of an ultimate limit state is regarded as an inability to sustain any increase in load. When the ULS is reached, the whole structure or part of it collapses. A serviceability limit state corresponds to impaired performance such that the functional requirements cannot be fulfilled. When the SLS is reached, the structure or part of it is unfit for normal use but does not indicate that collapse has occurred.

Generally speaking, the idea of limit state design of casing is quite simple. A designer focuses his attention on conditions which directly limit the continued safe and convenient operations of a casing, rather than on indirect factors which may be related

to limits on operations but do not immediately define those limits. Therefore, limit state design is a method through which the risks of failure inherent in a casing design can be determined. An overall idea of the safety and adequacy of the design can be thus attained. The implementation of probabilistic concepts also asks the designer to consider the real situation as opposed to a series of intuitive assumptions that may have been sufficient in the past.

2.3.2 Limit State Equation

The limiting capacity of a structural element in a particular behaviour mode while meeting its functional requirements is described by a limit state equation. It is a mathematical expression based on the mechanics of a material model, experimental results, or a combination of the two. For each limit state, a mathematical model is necessary, which incorporates variables describing uncertainties with respect to loads, structural response, geometry, the interaction of the casing components, resistance, workmanship, environment etc. The limit state equation $G(Z)$ can be normally formulated in terms of a load effect contribution $L(Z)$ and a resistance contribution $R(Z)$, which can be written as,

$$G(Z) = R(Z) - L(Z) \tag{2.2}$$

where, $Z = (Z_1, Z_2 \ldots, Z_n)$ are the design variables such as wall thickness, material yield strength and loads etc. According to the definition, a limit state function must be chosen in such a way that a negative value of G indicates that the combination of $Z = (Z_1, Z_2 \ldots, Z_n)$ results in a failure. That is,

$$G(Z)\begin{cases} > 0 & (Z \text{ belongs to the safe set}) \\ = 0 & (Z \text{ lies on the limit state surface}) \\ < 0 & (Z \text{ belongs to the failure set}) \end{cases} \tag{2.3}$$

The probability of failure $P(F)$ of a particular limit state consequently equals to,

$$P(F) = P(G(Z) \leq 0) = \int_{G(Z)\leq 0} f_Z(Z)dZ \tag{2.4}$$

where $f_Z(Z)$ is the probability density function of all the basic variables.

Design for an ultimate limit state may conveniently be explained with reference to the typical diagram shown in Fig. 2.4. It compares the strength $R(Z)$ of a number of nominally identical structures with the load spectrum $L(Z)$ that might be expected to occur during lifetime of those structures. The overlapped area stands for the probability of failure in the limit state design. The fact that both quantities appear not as single vertical lines but as curves, termed frequency distributions, is in recognition of the variability not only of the loads experienced by a structure, but also of the factors which influence the strength of the structure. The load curve is broad, reflecting the variability of loading on a structure, while the greater degree of control over its strength leads to a narrow strength curve.

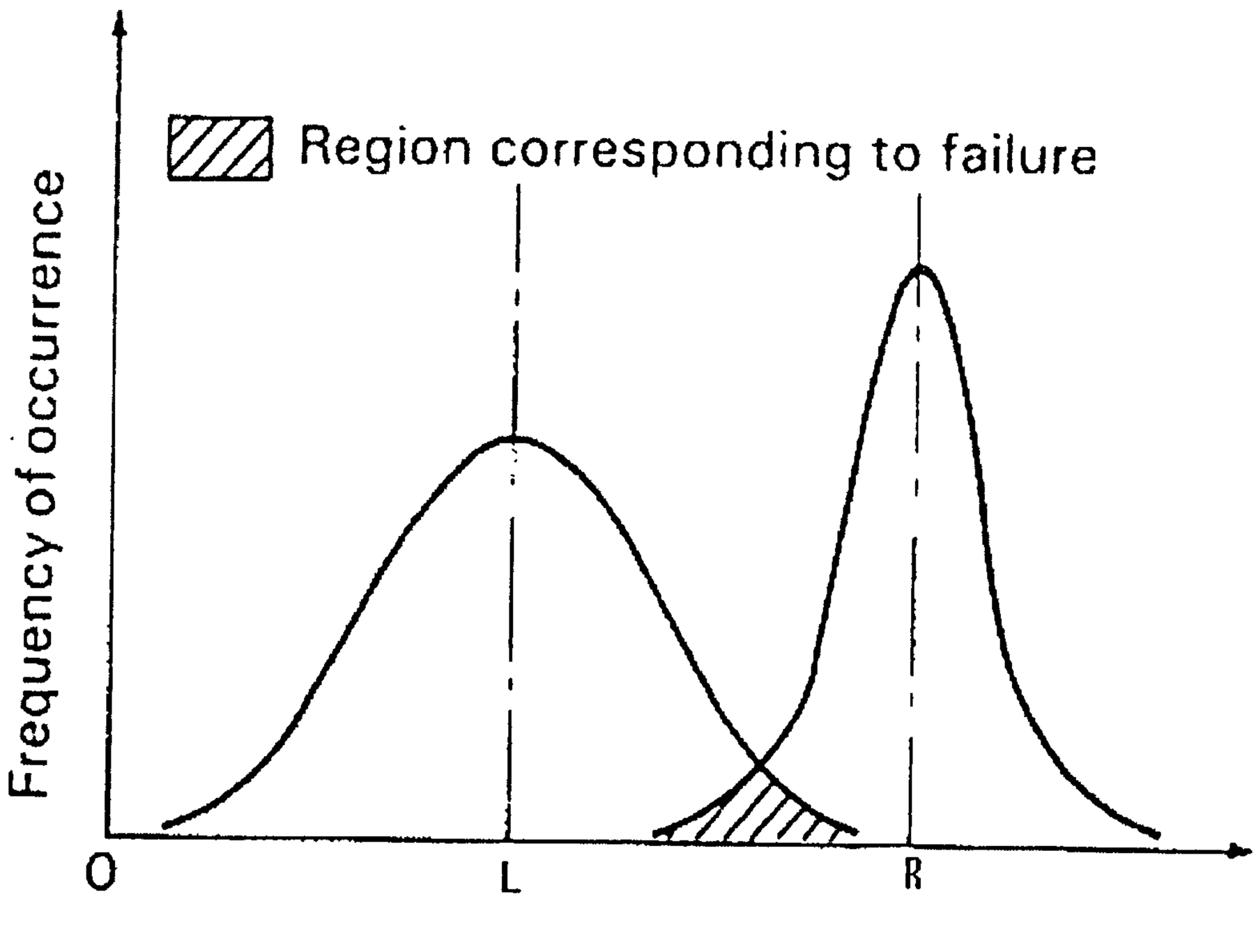

Fig. 2.4 Illustration of probability of failure for a ultimate limit state

2.4 Review Of Casing Design Methods

2.4.1 General

A primary goal of casing design is to ensure that the total effect of the applied loads is lower than that of casing strength, given the uncertainties in the estimation of the load effect, resistance and their relationship. Based on engineers' experience, almost all of the casings have been historically designed using the working stress design method (WSD) from as early as 1939 (Payne and Swanson, 1990). Recently, the need for more safety awareness as well as cost efficiency in casing design has prompted a closer investigation of the application of reliability based limit state design methods. As a result, two formats of reliability based limit state design methods, load and resistance factor design and quantitative risk assessment design, are proposed for casing design. Beginning in the late 1980's and early 1990's, load and resistance factor design (LRFD) is developed and implemented, while a first attempt to apply quantitative risk assessment to casing design is described by Reeves et al (1993). A general description of the three casing design methods as well as a comparison is given in the following sections.

2.4.2 Working Stress Design Method

The oil and gas industry has historically used working stress design method in the design of casing strings. Most of present-day design procedures of casing are still based on this deterministic methodology. It is a simple system of comparing a calculated worst case load against the rating of a casing, well understood by the average drill engineer. This design process defines the load as an estimation of the maximum anticipated load, while the strength of the casing is defined as a lower bound of material strength. According to this method, a designer must assure that the maximum possible load will not exceed the expected minimum allowable strength. A safety factor is usually used as a contingency. The origin of such a safety factor is

almost empirical, which has rarely been subjected to field or analytical verification, as shown in a review of design practice by Payne and Swanson (1990). To make matters worse, the safety factor is fixed from design experience by various design standards, which may be totally different from each other.

The primary role of a safety factor is to account for uncertainties in the design variables and parameters, especially for the load effect and the strength (or resistance in some literature) of the structure. However, these safety factors give little indication of the probability of failure of a casing in working stress design, as they do not explicitly consider the randomness of the design variables and parameters. The true safety margin in the casing design is largely unknown. In addition, it is reported (Payne and Swanson, 1990; Maes and Breitung, 1993) that small changes in the safety factor have a huge impact on the economics of drilling practice.

In general, the working stress design procedure can be expressed by the following relationship,

$$SF \times L_w(Z_i) \leq R_{\min}(Z_i) \tag{2.5}$$

where, Z_i are the variables and parameters such as pressure, diameter, yield stress etc. L_w is the worst case load, SF is the safety factor, and $R_{\min}$ is the minimum resistance. The ratio $R_{\min} / SF$ is called the safe working stress, hence the name of the design procedure.

Although working stress design is conceptually simple and has worked well in most cases in the past, it has many drawbacks. These problems are:

- It is over conservative in most cases. The casing is designed to the worst case load, with no regard to the likelihood of occurrence of the load. Moreover, working stress design uses conservative elasticity based theories and minimum strength in design. Over design leads to more costly casing purchase in practice.

- The design parameters are not tried to the risk level inherent in the resulting design. It gives the engineer no insight into the degree of risk or safety of the design, thus making it impossible to assess the risk cost balance.

- The working stress design treats all wells the same regardless of the cost or consequence. For example, consequences of a blowout due to a kick when drilling a shallow well in a remote location are different than those of drilling on an offshore platform. Working stress design does not distinguish these applications.

- There is no rigorously defensible justification for the specification of many of the parameters used in working stress design. The safety factors are based on the engineer's experience, and not on the uncertainties inherent in the load and resistance estimation.

2.4.3 Reliability Based Limit State Design Methods

The general principles of reliability based design are given in ISO 2394 (International Organisation for Standardization, 1986), and a detailed discussion of the underlying theory is given by Kapur and Lamberson (1977). In reliability based design approaches, the uncertainties and variability in each of the design variables and parameters is explicitly considered. In addition, a limit state approach is used rather than elasticity based failure criterion. Thus, the failure criterion of working stress design is replaced by a limit state that represents the true limit of a casing for a given load effect. The implementation of probabilistic theory allows the estimation of the probability of failure of a casing design, thus giving a better whilst risk consistent design.

2.4.3.1 Load And Resistance Factor Design

The load and resistance factor design (LRFD) method is a reliability based design method. Maes et al (1995), Raney et al (1997) and the ISO standard 2394 (1986) described the steps in detail of an acceptable load and resistance factor design format. In addition, Raney et al (1997) gave a flow chart of a complete LRFD process as

implemented for production tubing in the oil company Mobil. In the LRFD format, a concerted effort is made to maintain an engineering understanding of the load and resistance formulation. The limit state theory is considered in this format, however, the design procedure is greatly simplified by the use of a design check equation (DCE), which enables the designer to check a casing design. Normally a design check equation is chosen to be a simple and familiar equation, where appropriate characteristic values of the design parameters are used along with partial factors that account for the uncertainties in the load and resistance, and the difference between the design check equation and the actual limit states. Similar to the safety factors used in WSD, only one characteristic value each for the load and resistance is used, called load and resistance factors. Load and resistance factors have been developed for each load combination and risk level. Therefore, a design is said to be safe when the product of load and load design factor is less than that of resistance and its factor. The load and resistance factor design method can be represented by the following inequality,

$$L_f \times L_{char}(Z_i) \leq R_f \times R_{char}(Z_i) \tag{2.6}$$

where, L_f and R_f are the load and resistance design factors respectively. L_{char} and R_{char} represent the characteristic values of the load effect and the resistance, with Z_i being the characteristic values of each of the parameters and variables in the design procedure. A characteristic load in LRFD means a load, which has an acceptably small probability of not being exceeded during the lifetime of the structure. While a characteristic resistance refers to the specific resistance below which not more than a small percentage (typically 5%) of the results of tests may be expected to fall.

In load and resistance factor design, any design that satisfies inequality (2.6) is a valid design. The design check equation can be functionally identical to a limit state equation. The functional relationship can be specified by a simple design formula similar to that in the WSD. It is suggested by the Drilling Engineer Association (DEA) that a single design factor equation be used in the first step of implementation of the LRFD. However, it is noted that inequality (2.6) is merely a conceptual representation. In practice, it may not be possible to risk-calibrate a single design factor in the way suggested by the DEA, or to separate the load and resistance factors

in the way suggested by inequality (2.6). Moreover, several load effect and resistance terms may be presented in the design check equation, with varying uncertainties, requiring the use of several partial factors as described earlier in the limit state design theory.

It is observed from inequality (2.6) that the partial factors (e.g. load and resistance factors) are, in a sense, similar to the safety factors used in the working stress design (WSD) method. Comparing inequality (2.6) to inequality (2.5), it is noticed that both inequalities are based on deterministic values, and the safety factor in inequality (2.5) is replaced by two partial factors. Indeed, the ratio of L_f / R_f is analogous to the safety factor used in WSD, if the design check equation in LRFD happens to be identical to the WSD failure criterion. Thus, it may be said in concept that,

$$\frac{L_f}{R_f} \Rightarrow SF \tag{2.7}$$

Despite these similarities between the LRFD and WSD, there are three crucial differences. First, the load and the resistance effects in an LRFD are estimated from limit state theory, rather than conservative elasticity-based theories in the WSD. Secondly, the load and the resistance effects are treated separately, thus allowing the partial factors to separately account for the uncertainties. Finally, the most important point is that these partial factors in the LRFD are determined based on reliability theory, rather than safety factors being arbitrarily set based on experience in the WSD.

It is necessary to give a more detailed description on partial factors in the LRFD. They are determined through a process of calibration, where the deterministic design check equation with partial factors is calibrated against the probabilistic limit state equation. Partial factors are chosen such that their use in the design check equation results in a design that has a pre-selected target reliability (e.g. target probability of failure or target risk level). For the partial factors to do so, the calibration process should prescribe a scope of the application of the LRFD, and the values of the partial factors should be optimized to ensure a uniform reliability across that scope. The objective is to obtain a set of factors that result in a design of the target probability of failure. In brief, the load and resistance design may be summarized as follows:

- Choose a desired target probability of failure.

- Identify the characteristic values of each of the parameters, and the uncertainty and variability about these values.

- For an assumed set of load and resistance factors, generate a set of 'passed' designs from the DCE, across the scope of the structure, for all possible load magnitudes. In other words, all designs that 'pass' the DCE are valid designs. The passing of a design is controlled by the assumed value of the load and resistance factors.

- For each of the passed designs, estimate the probability of failure from the limit state equation, taking into account the uncertainty in each of the variables.

- Determine the statistically minimum reliability assured by the assumed set of load and resistance factors. This is the reliability, i.e. probability of failure, that results from the use of these partial factors. The probability of failure of any design that results from the use of these partial factors in the DCE will statistically be less than or equal to the target probability of failure.

- Repeat until the set of partial factors results in the desired target probability of failure. At the end of the process, a set of partial factors and their corresponding reliability are determined. If several target reliabilities are to be aimed for, the above procedure is repeated until a new set of partial factors is obtained.

A brief description of the load and resistance factor design method is given above. It is noted that calibration is usually a time-consuming and rigorous step in devising an LRFD procedure. Several reliability theories and statistical details such as uncertainty estimation, pre-processing of high reliability designs, zonation, uniformity of reliability, multiple partial factors calibration etc, were given in detail by Maes et al (1995), and thus are omitted here for brevity. The LRFD prevents some of the fundamental criticisms of WSD, by using partial factors to account for design uncertainties based on reliability theory. Thus it is better than the WSD, as the partial factors are determined from a target probability of failure. However, not only is it very difficult to determine the partial factors for the load and resistance effects, but also it is still an indirect measurement of failure, like safety factors in WSD. Although

it is simple to use in casing design, the question of why use indirect partial factors instead of the probability of failure arises. As a result, a full quantitative risk assessment (QRA) concept is developed (Adams and Glover, 1998).

2.4.3.2 Quantitative Risk Assessment

Quantitative risk assessment (QRA) is another reliability based design method. As early as 1993, one major study (Adams et al, 1998) was undertaken on casing and tubing quantitative risk assessment, in which some early results were obtained. A project proposal, DEA (E)-64 "The use of QRA in Casing/Tubing Design", was developed and presented to the Europe chapter meeting in Amsterdam in 1993, and the USA chapter meeting in Houston in 1993 (Adams et al, 1993). Since then, quantitative risk assessment has received support from major oil and gas companies including AGIP, Amerada Hess, Amoco, BG, BP, Conoco, Exxon, the HSE, Mobil, Norsk Hydro, the NPD, Phillips, Saga, Shell, Statoil, Texaco, Total and Unocal.

In quantitative risk assessment, the limit state equation is directly considered. Different from the load and resistance factor design (LRFD), the variables and parameters, which determine the load and resistance effects for the given limit state, are all treated as random variables. In the QRA design process, the probability of failure can be directly estimated if the magnitude and uncertainty of each basic variable are known. The uncertainties in the load and resistance terms in a limit state equation are calculated from the uncertainties of the basic variables and parameters, through an appropriate uncertainty propagation model such as Monte Carlo simulation (Payne and Swanson, 1990; Kapur and Lamberson, 1977; Maes et al, 1993). Figure 2.5 illustrates the concept, with the load and resistance effects being shown as random variables. The shaded region shows the interference area, which is indicative of the probability of failure. Thus, in quantitative risk assessment, the probability of failure of a casing design can be estimated directly, given an appropriate limit state equation, estimated magnitude and uncertainty of each basic variable, and a reliability analysis tool such as Monte Carlo simulation.

Although simple in concept, the QRA method usually presents some difficulties to implement in practice. Firstly, the limit state equation is not always a manageable equation, which needs a complementary understanding of the mechanism between load and resistance. Secondly, the uncertainties in the load and resistance parameters have to be estimated each time, when a design is attempted. Thirdly, the density distributions of each variable in the limit state equation are not normally ready. The probability distributions and occurrence frequencies have to be determined after statistical analysis under a large collection of field load and casing material data. Finally, an appropriate reliability analysis tool is needed to estimate the probability of failure. It is suggested that the variables and parameters be treated as normal variants, and a first order reliability method (FORM) use to calculate the propagation of uncertainty (Walpole and Myers, 1993). However, the probability distributions are usually not all normal, and FORM propagation is not always appropriate because it only gives reliable information on the central tendencies of the resultant distributions while erroneous on estimating the tail probabilities. From Fig. 2.5, it is very clear that the tail probability plays a vital role in QRA. Therefore, it is important to obtain a detailed investigation of the efficiency and accuracy of a number of reliability techniques, including the first/second order reliability method (FORM/SORM), Monte Carlo, Monte Carlo with tail improvement etc. It is believed that the asymptotic importance sampling (AIS) technique can improve tail probability estimation (Maes et al, 1993). It is possible to determine an optimised reliability method to use in the QRA design process. Because the inherent variability of each parameter is considered directly, applying a full QRA in the limit state design of casing can really give how safe a design will be. Therefore, this project focuses on the development of a methodology of using full QRA in the limit state design of casing in cooperation with another researcher at the University of Wolverhampton. This thesis will mainly contribute to the mechanical aspects of limit state casing design for the derivation of the limit state design equations, while the other will focus on the evaluation of the reliability analysis techniques to give a full quantitative risk assessment of casing design by employing the limit state design equations developed in this thesis.

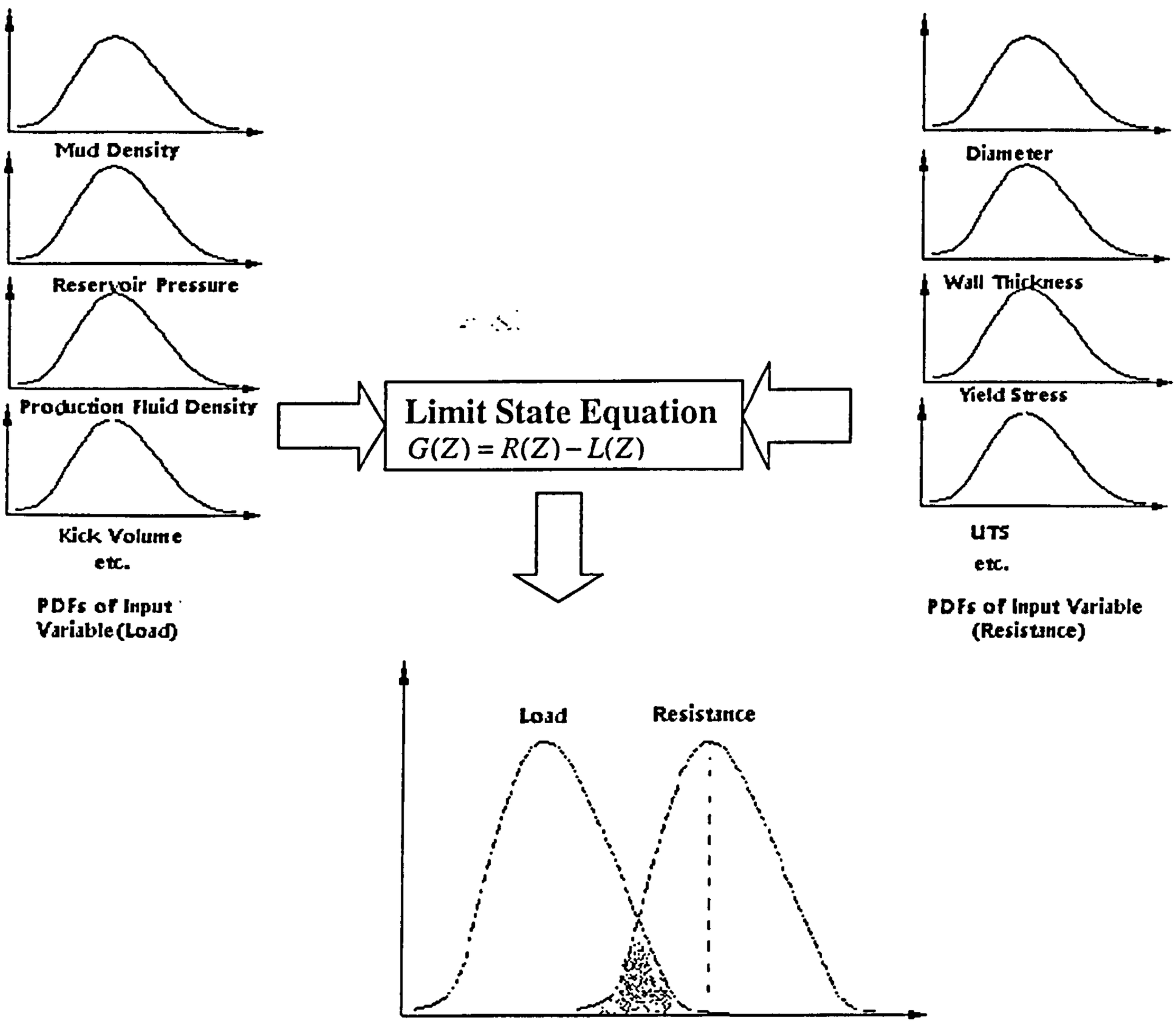

Fig. 2.5 A full QRA methodology

2.4.4 Comparison Of WSD And Reliability Based Design

First of all, it is noted that the working stress design (WSD) and reliability-based limit state design are essentially two different approaches. In traditional working stress design, safety factors are relentlessly used without any idea of the inherent reliability or risk associated with any design. It is intuitively obvious that lower factors of safety lead to higher risk design. Therefore, it is of great interest to investigate the relationship of the use of the traditional safety factor to the reliability of a design, as ascertained from a QRA or LRFD approach. However, safety factors have no reliability information explicitly associated with them. If a WSD design is executed correctly, the resistance will exceed the load, and the relative magnitude of the difference between the two values will represent the safety factor as shown in Fig. 2.6. The conclusion that can be drawn from the WSD is that designs made to the recommended safety factor are generally safe. Viewing the safety factor from a reliability perspective will give a useful insight into the reliability of traditional WSD designs. Therefore, comparisons are made on how to determine the load and resistance, for both WSD and reliability based designs.

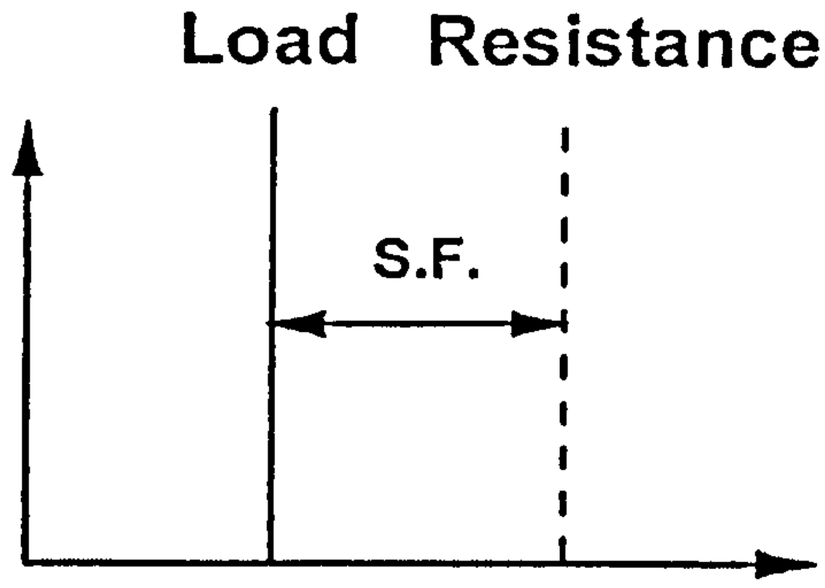

Fig. 2.6 Standard deterministic design (Working Stress Design)

2.4.4.1 Load Calculation

In working stress design (WSD), the load calculation is different from company to company and sometimes different within the same company. However, the designer attempts to estimate the worst case load that can possibly occur on the casing during its service life. In load and resistance factor design (LRFD), load calculation must be done in accordance with a pre-set methodology. The reason for this is that the load factors have been calibrated from a set load methodology and the uncertainty is estimated on the basis of that load methodology. Any methodology can be used as long as it is consistently applied in practice. The closer the methodology is to the actual load, the lower the uncertainty, and hence closer the load factor to unity. In quantitative risk assessment (QRA), load calculation can be done in any way the designer wants. The designer attempts to define the load as close to reality as possible. The only criterion in load definition is that the error or uncertainty of the primary variables must be known or defined. In other words, the distributions of each load variables must be known first. It is noted that such information is available after an initial study of QRA through a joint industry project DEA-64 (1994).

2.4.4.2 Resistance Calculation

The resistance calculation in working stress design (WSD) is almost universally based on the equations from the American Petroleum Institution (API). The API Spec 5C3 (1992) outlines the collapse, burst and tensile ratings for API tubular goods. Although these strength values have been used by the industry for decades, many casing designers recognize that API values are often conservative. This is for two reasons: 1) API uses the thin wall pressure vessel theory that is conservative; and 2) API uses the minimum values for wall thickness and yield strength. In reliability based limit state design, resistance calculation is based on the actual distribution of the parameters that determine resistance (such as wall thickness, yield etc.), and upon the limit state equations.

2.4.5 Design Examples

Optimizing the design of casings cannot only directly impact the well cost, but can also impact on the deliver ability of the well. The following examples are intended to demonstrate the advantages of using a reliability-based design (LRFD) for the casing by comparing the examples with the original working stress design (WSD) for the same load combinations. As the full QRA design of casings is still under development, the design examples are compared between the LRFD and WSD only. For comparison purposes, Tables 2.2 and 2.3 describe the definition of loads and the minimum safety factor required by the WSD in the following examples (Brand and Lewis, 1995; Lewis et al, 1995). For the LRFD casing design, the definitions of loads remain consistent with those used in the WSD. These loads are multiplied by the appropriate load factors for the designed probability of failure. The acceptability of LRFD design is described by the design factor, which is defined as the factored load divided by the factored resistance. The design factor describes the percentage of the available strength utilized for a given probability of failure, giving the engineer an indication of the allowable load to retain the desired probability of failure.

Table 2.2 Load and safety factor for drilling casing

Load combination	Description of load	Safety Factor
Burst	Minimum of fracture at shoe and methane gas to surface	1.0
Collapse	Above top of inside fluid, mud weight. Below top of inside fluid, weight of mud minus internal pressure.	1.0
Tension	Buoyed weight of casing plus tension required to set slips.	1.6

Table 2.3 Load and safety factor for production casing

Load combination	Description of load	Safety Factor
Burst	Bottom formation pressure minus gas gradient to surface on top of packer fluid.	1.25
Collapse	Above top of inside fluid, mud weight. Below top of inside fluid, weight of mud minus internal pressure.	1.0
Tension	Buoyed weight of casing plus tension required to set slips.	1.6

2.4.5.1 Design Example 1

The first example is a deep, sour (H_2S), high temperature well (Brand and Lewis, 1995). The pore pressure, mud weight, and fracture gradient curves for the area are shown in Fig. 2.7. As the well is planned for a single well field, maximizing flow is a primary design objective. Figure 2.8 illustrates the original design using WSD. In this design, an intermediate casing string is set prior to drilling into the over pressurised salt water sands. Table 2.4 shows the design loads and the safety factors for the selected 13 3/8" casing. It is noted that the selected material does not meet the minimum design requirements for burst and collapse, and other options have significant problems. Increasing the wall thickness of the selected casing will pose a problem in drill bit selection, availability and cause restrictions for running the next string of casing. Increasing the casing grade may result in a brittle fracture due to the high hydrogen sulphide (H_2S) in the area. The design engineer is forced to choose between options and subjectively select the best alternative. The decision to run the 13 3/8" N80 casing is rationalized due to the low flow potential for the formations that are open below the string. The engineer knows that the design guidelines have been violated and risk is being taken, but there are no options for quantifying the risk in this WSD design.

Table 2.4 Design data for 13 3/8" intermediate casing (WSD)

Case	Resultant Load		API Strength		Safety Factor
	(psi)	(MPa)	(psi)	(MPa)	
Burst	5454	37.60	5380	37.09	0.99
Collapse	4130	28.47	2761	19.03	0.67
Tension	1000367	6896.53	1661000	11450.93	1.66

The WSD loads and safety factors for the 10 3/4" tie back and 9 5/8" liner are shown in Tables 2.5 and 2.6. It is shown again that the design guidelines must be violated. The design is justified due to the fact that flow at the casing shoe is not possible. Therefore the casing is designed for a specific kick size. The production casing string is designed using a maximum estimated surface pressure of 8100 psi (55.8 MPa). The design loads and safety factors for 7 5/8" and 7" production casings are given in Table 2.7 and Table 2.8.

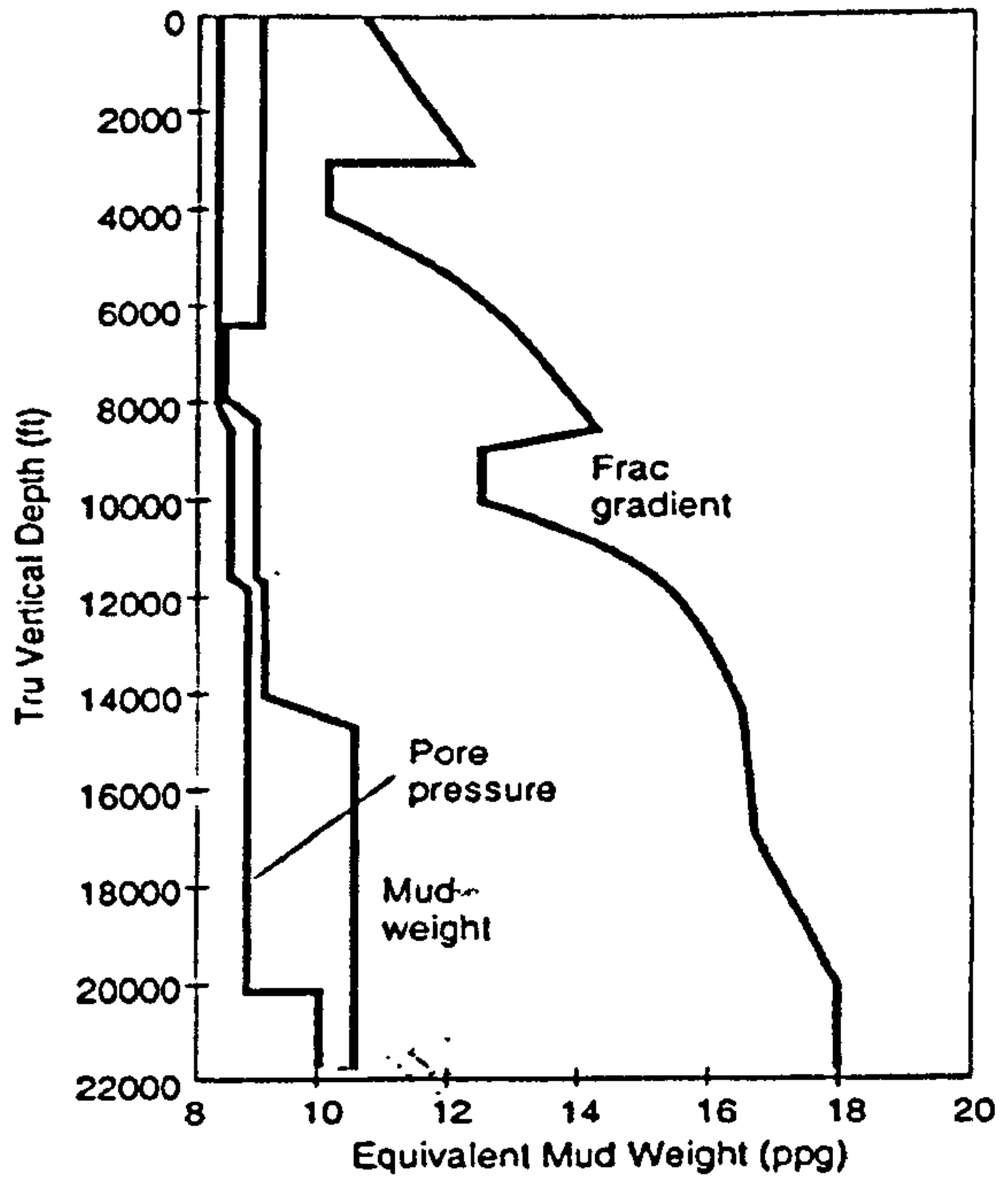

Fig. 2.7 Design data of example 1

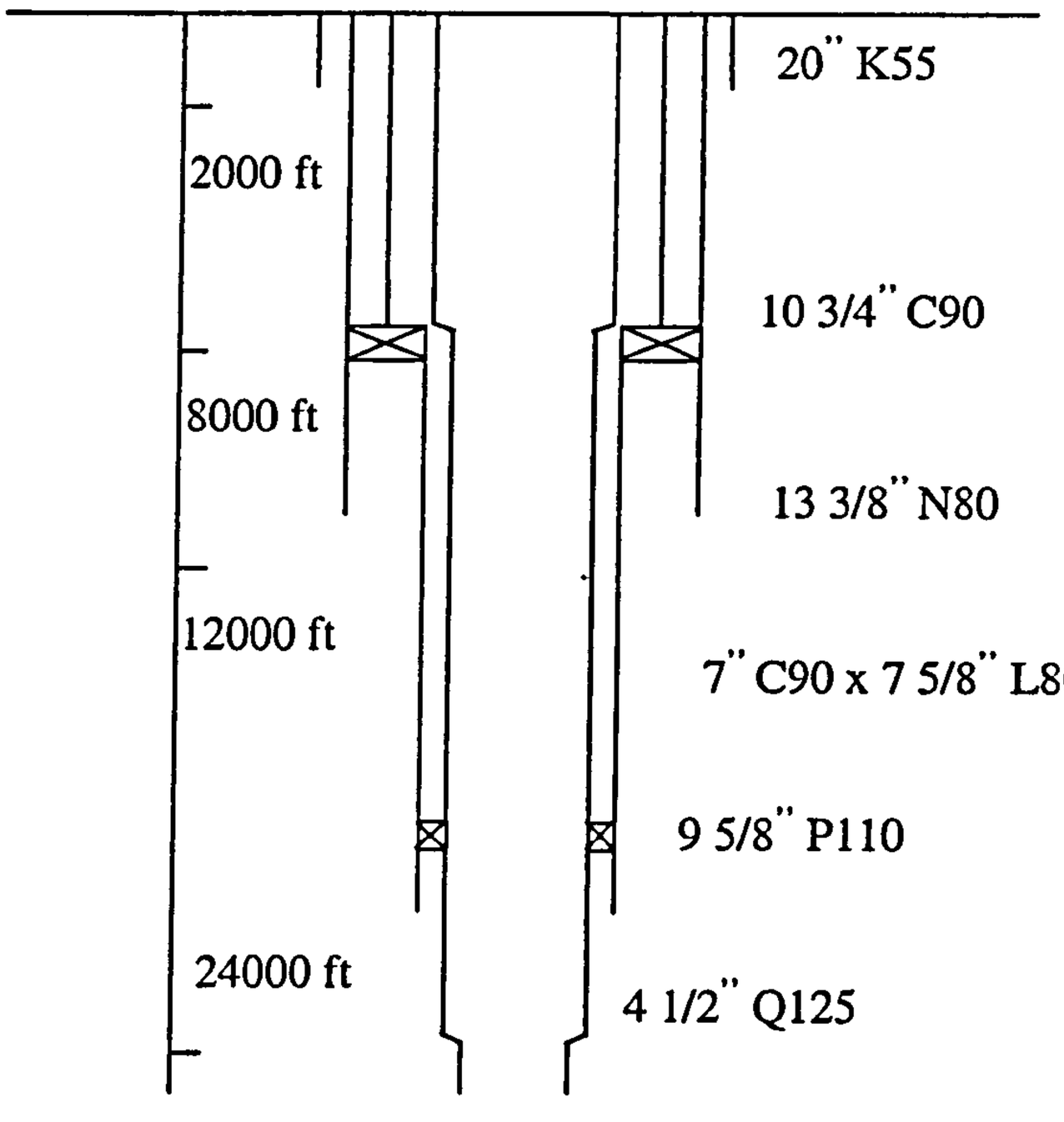

Fig. 2.8 Casing design from WSD (example 1)

Table 2.5 Design data of 10 3/4" tie-back (WSD)

Case	Resultant Load		API Strength		Safety Factor
	(psi)	(MPa)	(psi)	(MPa)	
Burst	9332	64.33	8720	60.12	0.93
Collapse	5896	40.65	6760	46.60	1.15
Tension	633246	4365.60	1708000	11774.95	2.70

Table 2.6 Design data of 9 5/8" liner (WSD)

Case	Resultant Load		API Strength		Safety Factor
	(psi)	(MPa)	(psi)	(MPa)	
Burst	6608	45.56	9410	64.87	1.43
Collapse	5261	36.27	7340	50.60	1.40
Tension	556603	3837.22	1477000	10182.44	2.65

Table 2.7 Design data of 7 5/8" production casing (WSD)

Case	Resultant Load		API Strength		Safety Factor
	(psi)	(MPa)	(psi)	(MPa)	
Burst	8142	56.13	10920	75.28	1.34
Collapse	5896	40.65	11510	79.35	1.95
Tension	463528	3195.56	1051000	7245.60	2.27

Table 2.8 Design data of 7" production casing (WSD)

Case	Resultant Load		API Strength		Safety Factor
	(psi)	(MPa)	(psi)	(MPa)	
Burst	8159	56.25	13280	91.55	1.63
Collapse	10761	74.19	13900	95.83	1.29
Tension	107740	742.76	1069000	7369.69	9.92

The well is redesigned in an attempt to increase deliver-ability due to the competitive nature of the field using the LRFD. The 13 3/8" casing is analyzed again by LRFD with probability specifications as shown in Table 2.9. Although the casing string design is not modified from WSD, LRFD allowed the risk of using this particular string under the described well conditions. This casing string is acceptable for the designed probability of failure. The probability of failure for the kick load combination is selected due to the risk to the health and safety of the personnel and the environment. Considering the depth of the next string, the cost is estimated at medium. The probabilities of failure for the running and cementing load combination and the lost circulation load combination are selected due to the minimal risk to safety and the environment and the cost impact for a collapse or tensile failure in this string.

Table 2.9 Design data of 13 3/8" intermediate casing (LRFD)

Load Combination	Probability of failure	Design Factor
Kick	$10^{-6.5}$	0.73
Running and Cementing	$10^{-3.5}$	0.62
Lost Circulation	$10^{-3.5}$	0.54

To meet the design requirement of increased deliver-ability, the 9 5/8'' by 10 3/4" casing string is redesigned as both intermediate and production casing in LRFD. This allows an enlarged tubing size from 4 1/2" (designed in WSD) to 5 1/2". Although the savings in the 7" by 7 5/8" production casing will be offset by the increased cost of the tubing, this design will increase the deliver-ability. The design probabilities of failure are selected at 10^{-8} for the kick and the tubing leak load combinations, due to the high risk to life caused by the high concentrations of H_2S. The probability for a deep failure in the 9 5/8" liner is selected at $10^{-6.5}$ due to the decreased cost and consequence of failure. The failure probability for the accidental collapse load combination for the 9 5/8" liner is selected at 10^{-2}, as this is an accidental condition that possibly will not occur until the end of casing service life. The LRFD design probabilities of failure and design factors are shown in Table 2.10 and Table 2.11.

As the design factors for all load combinations are below 1.0, the 9 5/8" by 10 3/4" casing is acceptable for the design probability of failure. A diagram of the resulting LRFD design is shown in Figure 2.9. This design allows for usage of a 5 1/2" casing at virtually the same well cost as the original WSD utilizing 4 1/2" casing.

Table 2.10 Design data of 10 3/4" tie-back (LRFD)

Load Combination	Probability of Failure	Design Factor
Kick	10^{-8}	0.83
Tubing Leak	10^{-8}	0.92
Running and Cementing	$10^{-3.5}$	0.64
Lost Circulation	$10^{-3.5}$	0.38
Accidental Evacuation	$10^{-3.5}$	0.99

Table 2.11 Design data of 9 5/8" liner (LRFD)

Load Combination	Probability of Failure	Design Factor
Kick	10^{-8}	0.46
Tubing Leak	10^{-8} Open $10^{-6.5}$ Case	0.73
Running and Cementing	$10^{-3.5}$	0.33
Lost Returns	$10^{-3.5}$	0.25
Accidental Evacuation	10^{-2}	0.82

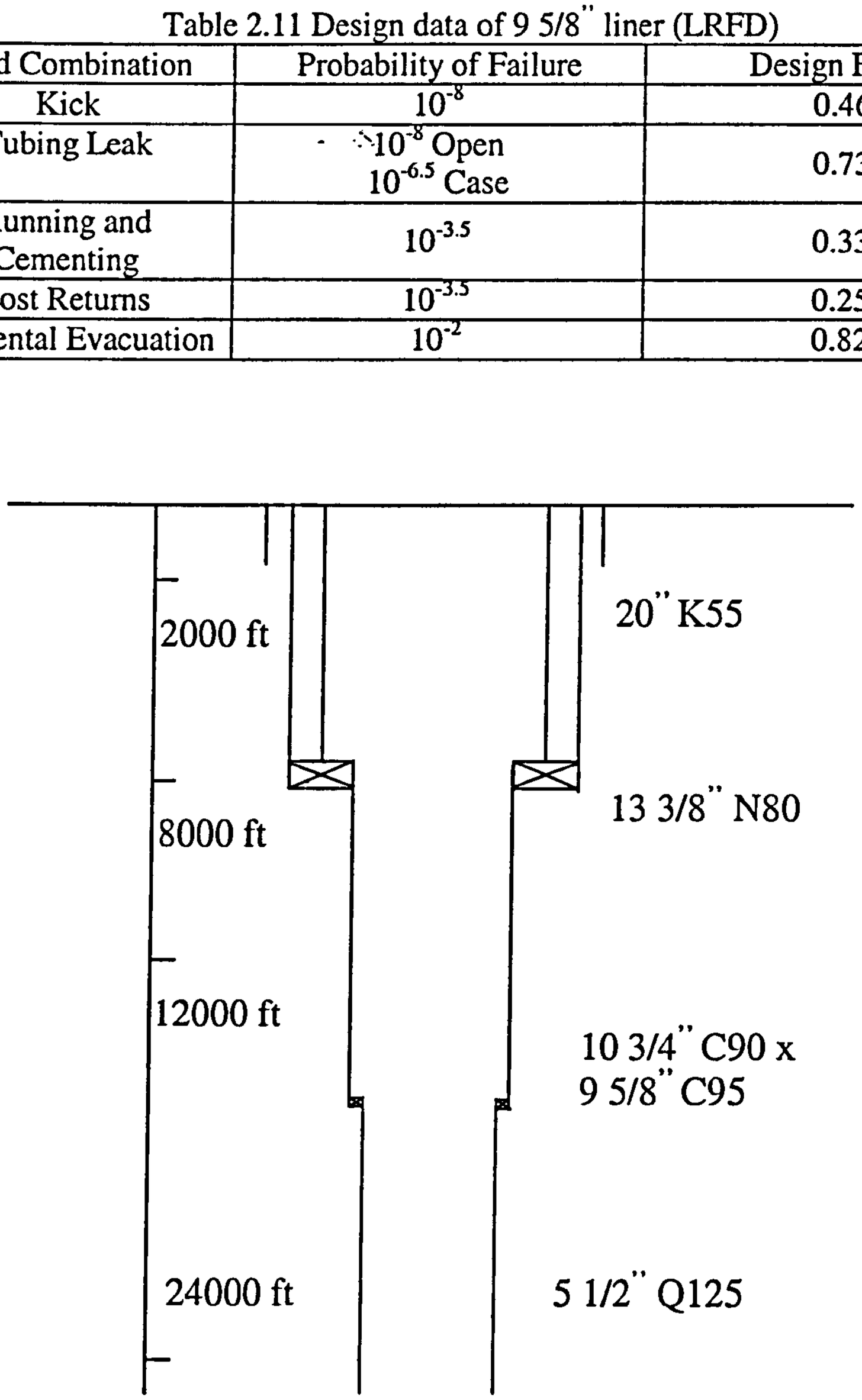

Fig. 2.9 Casing design from LRFD (example 1)

2.4.5.2 Design Example 2

The second example describes a well drilled from a platform. The pore pressure, mud weight and the fracture gradient curves are shown in Fig. 2.10. The well design sketch from the WSD is shown in Fig. 2.11. The calculated loads for the proposed 9 5/8" intermediate casing in WSD are shown in Table 2.12, with the loads for the 7" production casing shown in Table 2.13.

Table 2.12 Design loads for 9 5/8" intermediate casing (WSD)

Case	Resultant Load		API Strength		Safety Factor
	(psi)	(MPa)	(psi)	(MPa)	
Burst	6868	47.35	7930	54.67	1.15
Collapse	3251	22.41	6620	45.64	2.04
Tension	583350	4021.61	1086000	7486.88	1.86

Table 2.13 Design loads for 7" production casing (WSD)

Case	Resultant Load		API Strength		Safety Factor
	(psi)	(MPa)	(psi)	(MPa)	
Burst	7492	51.65	9960	68.66	1.33
Collapse	8479	58.45	10180	70.18	1.20
Tension	482330	3325.18	814000	5611.72	1.69

The well is redesigned by LRFD in an effort to determine if the 9 5/8" casing can be used as a combination of production and intermediate casing for cost saving as shown in Fig. 2.12. An LRFD design for the drilling and production load combinations including the design probabilities are shown in Table 2.14. The design probability of failure for the kick and tubing leak load combinations are selected due to the fact that this well is drilled off a platform. As the platform is designed for a probability of failure of 10^{-6}, and a burst failure open to the production zone can damage the platform, the probability of failure is set slightly lower than that of the platform. As shown, the 9 5/8" casing is acceptable for production casing for the design probability of failure. The design is found to be acceptable, and the well is successfully drilled and completed. The total cost saving is estimated at US$ 450,000 (Brand et al, 1995).

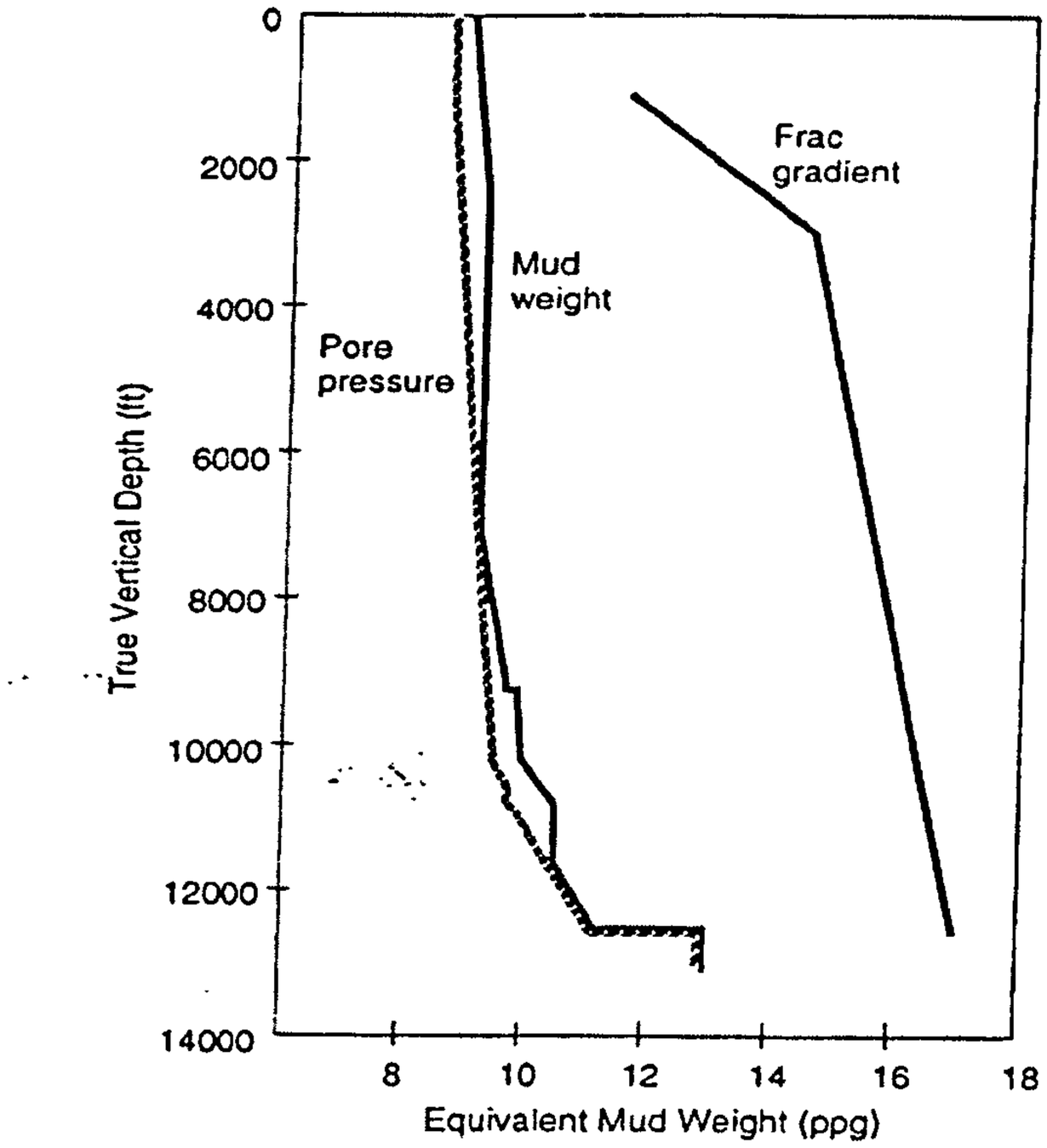

Fig. 2.10 Design data for example 2

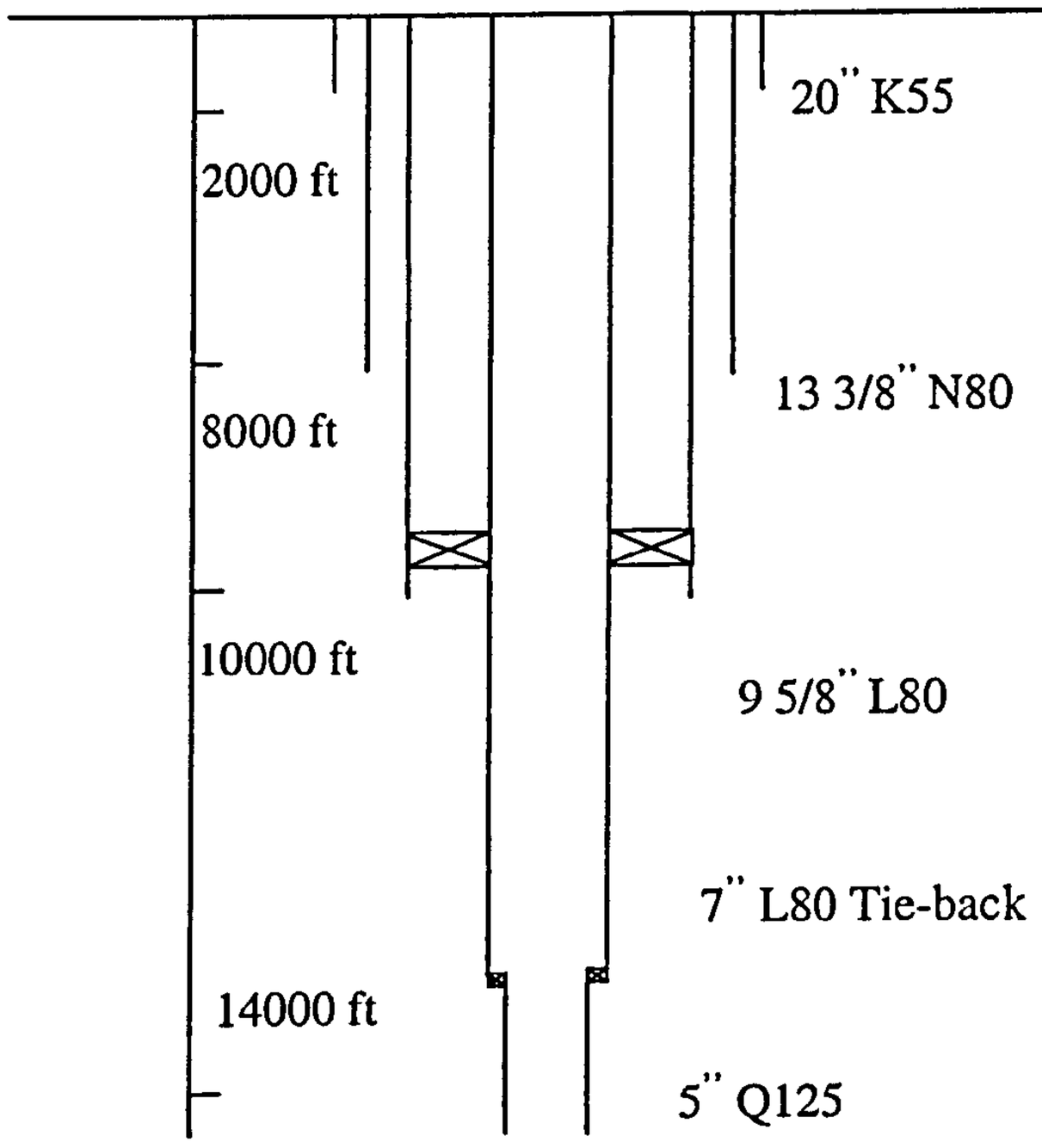

Fig. 2.11 Casing design from WSD (example 2)

Table 2.14 Design loads for 9 5/8" production casing (LRFD)

Load Combination	Probability of Failure	Design Factor
Kick	$10^{-6.5}$	0.60
Tubing Leak	$10^{-6.5}$	0.82
Running and Cementing	$10^{=3.5}$	0.47
Lost Returns	$10^{-3.5}$	0.17
Accidental Evacuation	$10^{-3.5}$	0.74

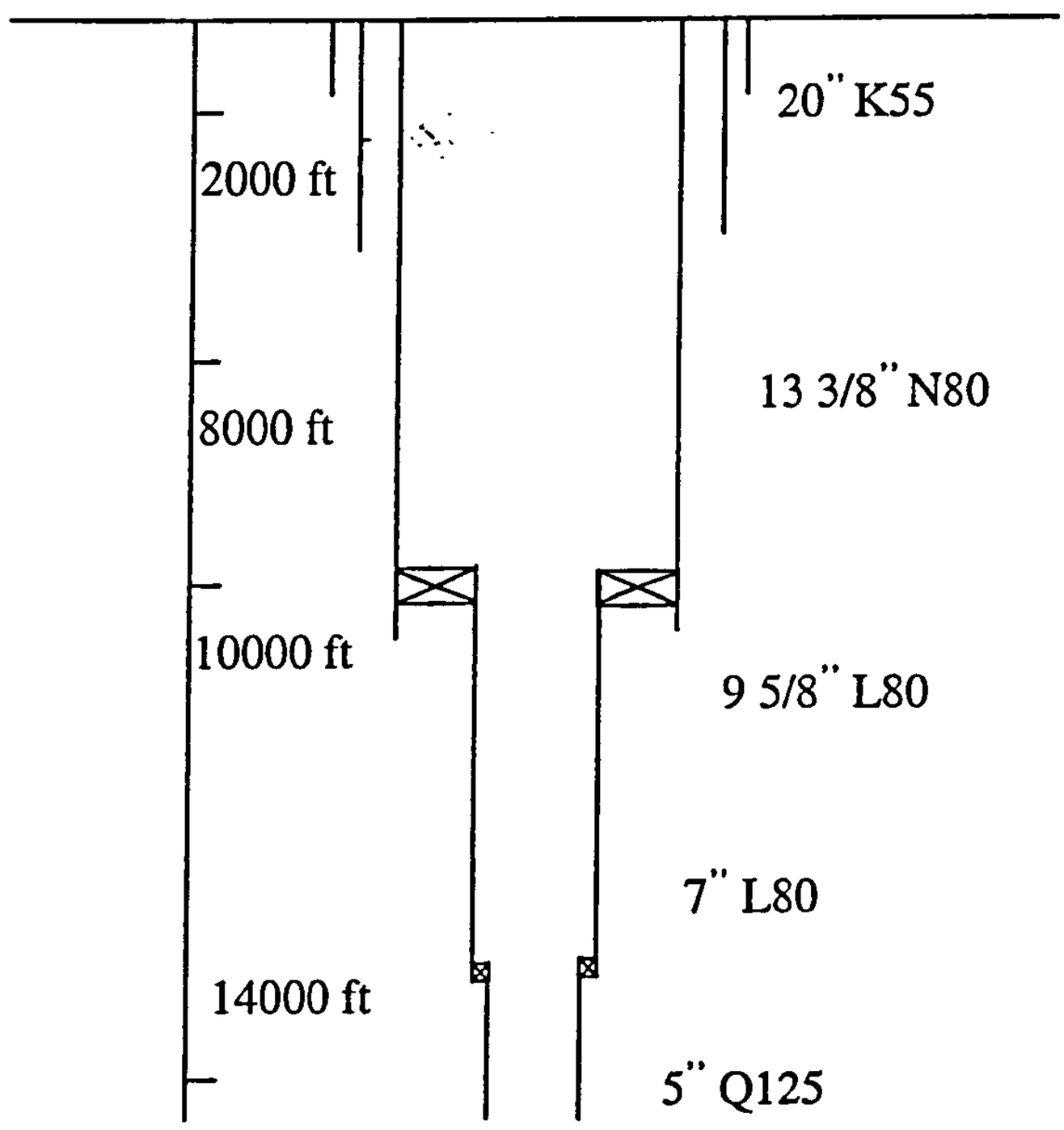

Fig. 2.12 Casing design from LRFD (example 2)

2.5 Applying QRA In The Limit State Design Of Casing

From the comparison of examples designed by LRFD and WSD respectively, it has been shown that design from LRFD can achieve an acceptable probability of failure as well as possible cost savings. However, the probability of failure from LRFD design is for a pre-set load condition. For a different load combination, the pre-set

probability of failure is not applicable. However, a full QRA design can provide the casing engineer with a real probability of failure for any load condition. In addition, it is anticipated that a full QRA can achieve even more cost savings. Therefore, the next stage of development of casing design is to consider a full QRA implementation for every well design, or at least to have the capability of doing so. The benefits of a full QRA are twofold. It is a tool by which the designer can quickly and objectively evaluate casing design on a risk basis. It is also useful in that it allows the regular revalidation of the design, maintaining accuracy in the light of fresh information or changes in conditions. There are a number of issues for implementing a full QRA casing design, which are briefly described in the following sections.

2.5.1 Randomly Distributed Variables

Quantitative risk assessment (QRA) uses randomly distributed variables. The real case of many variables is one whereby there is no absolute and simple way of predicting the outcome in any single case. Taking yield stress as an example, if a tensile test is performed on one steel sample, a single value for yield strength is produced. However, if the same test is performed on an identical specimen, it will yield at a different value. If this process is repeated, a large range of values will be obtained. This will produce a distribution of possible yield strength, each one having a different frequency of occurrence. This behaviour characterises an underlying normal distribution as shown in Fig. 2.13. A probability density function shows which values are more likely to occur by representing higher probability through a larger area under the graph over that range.

Each of the input variables in a casing design has a probability density function associated with it. For example, on the load side, there is a pore pressure distribution, a kick size and intensity distribution. When predicting casing resistance, diameter, thickness and yield strength are not single-value quantities, but also have distributions associated with them. The spread of the values for a probability density function can be measured by the standard deviation, showing how far the values deviate from the mean. Another method of expressing the spread is through the use of the coefficient

of variance (COV), which combines the mean and standard deviation into a single dimensionless coefficient, often useful where only limited or generic data is available, or as a comparative indicator of dispersion as expressed below,

$$COV = \frac{\phi}{\mu} \tag{2.8}$$

where ϕ is the standard deviation, and μ is the mean value of a variable.

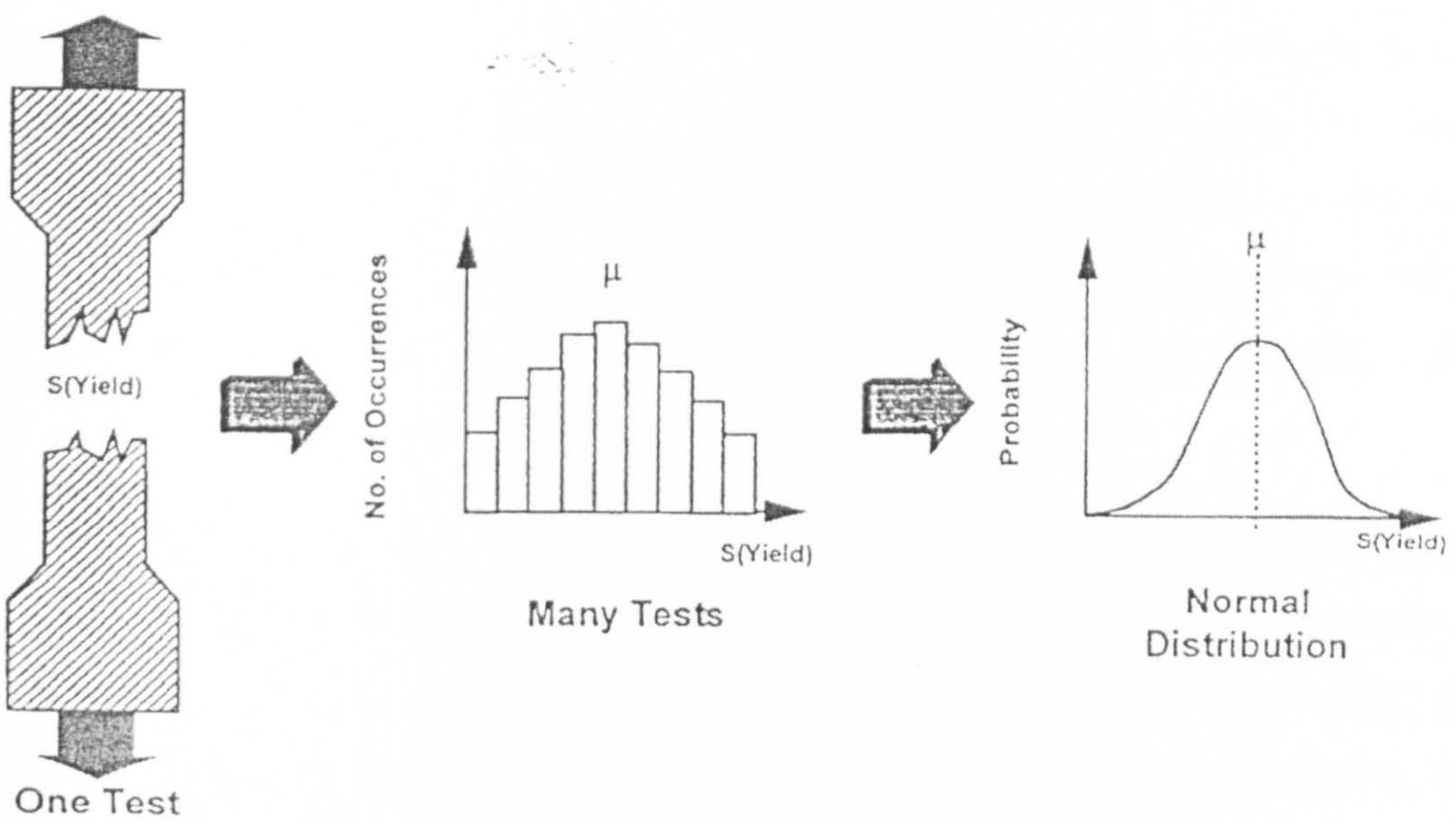

Fig. 2.13 An example of how a probability distribution is formed

After the input probability density functions are defined, the design process begins. Quantitative risk assessment uses probabilistic mathematics and statistics to factor together the load and resistance variables into two distributions. The first defines all the possible values that a load case can have. The second distribution will govern casing resistance. Despite a safety factor and good design practices in WSD, there will be a few times in a large number of applications of a particular design, in which load exceeds resistance. This is almost inevitable. Rather than ignoring the possibility, it is far more sensible for a design engineer to ensure that this failure rate is reduced to an economic level.

2.5.2 Tolerable Risk Levels (TRLs)

A tolerable risk level is defined as the maximum acceptable failure probability level for a particular casing design. In general, tolerable risk level depends on the consequence and nature of failure (i.e., the hazard to human health and safety, damage to the environment economic lost, and the amount of expense and effort required to reduce such a potential hazard). Many researchers have addressed how to determine the tolerable risk level for the purpose of developing an optimal limit state based design code (Turkstra, 1970; Ravindra and Lind, 1973; Allen, 1981; Ellingwood et al, 1982; Keilty and Rabia, 1996; Maes et al, 1993; Adams et al, 1993; Jiao et al, 1997). In general, risk level is determined by cost and safety. The appropriate risk level depends on an analysis and an evaluation of the consequences of a limit state failure with respect to each of these attributes. It is noted that the economic and the safety aspects of a well risk analysis are interrelated.

Each failure event has a consequence. Consequence of failure is defined as both the risk to life and the environment and the cost, given a failure occurs. The failure mode and the resulting cost of a failure are the primary drivers in determining the appropriate design probability of failure. For different load combinations, the probability of failure may vary in a particular string for a given well, depending on the failure consequence. In general, only failures during drilling and production will potentially lead to a blowout, failure during the remainder of the well operations (cementing, pressure test etc) will in general lead to a casing repair. The severity of each event consequence depends on the conditions that, whether a repair is necessary, whether a repair is possible, whether hydrocarbons are released to the environment. The consequence levels are chosen as follows: 1) surface blow-out; 2) deep surface blow-out; 3) major repair; 4) repair; 5) no repair necessary. The consequence of each failure event is determined and allocated to one of the above consequence levels. The next step is to select the acceptable probability of failure for each level, which is achieved by calibration against historical data, sensitivity checking and reference to established industry standards.

The optimum risk level is not the same for all load combinations and failure modes because the consequences are much different. As the consequential failure cost is hard to quantify, a guideline for selecting the appropriate probability of failure values as shown in Table 2.15 is proposed for casing design (Brand and Lewis, 1995; Lewis et al, 1995). Thus, quantitative risk assessment involves not only an assessment of the likely probability of failure, but also consideration of the effect of each type of failure.

Table 2.15 An example of a set of guidelines for tolerable risk levels

COST				
High	Medium	Low		
10^{-8}	$10^{-6.5}$	10^{-5}	Severe	Consequence
10^{-5}	$10^{-3.5}$	10^{-2}	Low	

2.5.3 Reliability Techniques For Full QRA

There are a number of reliability techniques available when implementing a quantitative risk assessment (QRA) approach in the limit state design of casing. A brief description of each is given in the following sections.

2.5.3.1 Convolution Integral

This method is highly abstract and mathematically elegant, which requires reformulation for each failure case. Mathematical expression of each probability density function is integrated, and the relative size of the failure area is determined. Finally a failure rate can be determined on the basis of limit state design equations.

2.5.3.2 Gaussian Linearisation

This procedure takes the mathematical formulation for the various input probability density functions, and converts each to an expanded series of terms, which can be linearly combined to produce the desired formulation. Therefore, a failure rate can be produced. This process is relatively simple, although it requires a new formulation for every design case. It introduces some degree of error when the series are truncated. It is noted that the conventional integrals and Gaussian linearisation are implemented in commercial MathCAD spreadsheets.

2.5.3.3 FORM/SORM

The first/second order reliability method (FORM/SORM) converts the probabilistic density functions into a standard form, performing a transformation on each one. The normalised probabilistic density functions are then substituted into the equation (for example, a limit state equation), and a failure probability can be determined. This method is advantageous in that it is accurate, quick, repeatable, and requires very little rearranging for each different case. It is reported that the FORM/SORM technique has been implemented as a computer program, by integrating a global finite element program for casing and tubing analysis (MacEachran and Adams, 1991) within a proprietary package for FORM/SORM calculation.

2.5.3.4 Monte Carlo Simulation

Monte Carlo simulation randomly selects a value for each input variable in the probability density function. In this way, a single value for each input variable is obtained, and input into the standard equations. If this process is carried out repeatedly, a picture of system response for all combinations of inputs (or at least a

representative sample) is obtained. Thus the proportion of failures can be directly read from the results. This process is conceptually simple, requiring very little additional formulation and effort. However, due to the very large number of calculation repetitions required (often of the order of several million), a powerful computer is required to perform the task in an acceptable time. In addition, the time consuming procedure must be repeated for every assessment.

2.5.4 Implementation Of QRA In Casing Design

In order to make the most of a quantitative risk assessment implementation in casing design, a number of issues will need to pay attention. First of all, companies should be willing to do more than simply re-jig their safety factors. A change in design procedures presents a number of potentially valuable opportunities to improve the whole design process, but also a number of challenges that must be met. Secondly, the acquisition, quality control and subsequent use of all types of data are central for the adequate execution of a quantitative risk assessment. To enable a QRA based limit state design, the casing collapse and burst are determined by combining mechanical models with a large statistical database of casing mechanical properties. These casing data may come from cooperating mills, or indirectly through mill test reports (MTRs). The load combination data (pore pressure, fracture gradients, temperature etc) will come from real field data supplied by the drilling data centre (Lewis et al, 1995). These data are provided in sufficient quantity to give statistical significance. The mean value and distribution of each variable can be identified by reliability analysis.

The next step is to identify the possible failure modes under the load combinations. A mechanical model can be constructed for each failure model, and a limit state equation can be derived, or assessed from existing equations. The quantitative risk assessment can be implemented by employing reliability techniques. Therefore, probability of failure of the casing design can be obtained and compared to the pre-set tolerable risk level (TRL). If the calculated probability of failure is less than the pre-set TRL, the limit state design is accepted. Otherwise, the design process can be performed repeatedly until the calculated probability of failure is less than the TRL.

The above design process of applying full QRA in the limit state design of casing is further illustrated in Fig. 2.14.

2.6 Summary

The traditional deterministic casing design method (WSD) has a number of shortcomings such as poor economics, inflexibility and uneven risk. The fundamental criticism is that the deterministic design cannot tell how safe a design will be. On the contrary, reliability based limit state design can give an answer to that question. A full QRA design can give the actual probability of failure of a casing design, while an LRFD can only give the minimum reliability.

Reliability based design of well casing/tubing system has undergone rapid development in recent years. However, nearly all the work to date has been limited on the load and resistance factor design. In comparison with LRFD, the full implementation of QRA design can provide maximum benefits. However, little work is found on the implementation of a full QRA design methodology, partly because of the relatively more complicated technical background and the conservatism of the industry when facing new technology. Therefore, a full QRA methodology is proposed to be applied in the limit state design of casing in this project in collaboration with BG Technology at Loughborough.

Two catalogues of limit states are usually considered in the limit state design. As a first step of this investigation of applying a full QRA methodology in the limit state design of casing, only the ultimate limit states are considered in this thesis. Before a limit state equation can be built, a set of failure modes under different load conditions need to be identified and are described in the next chapter.

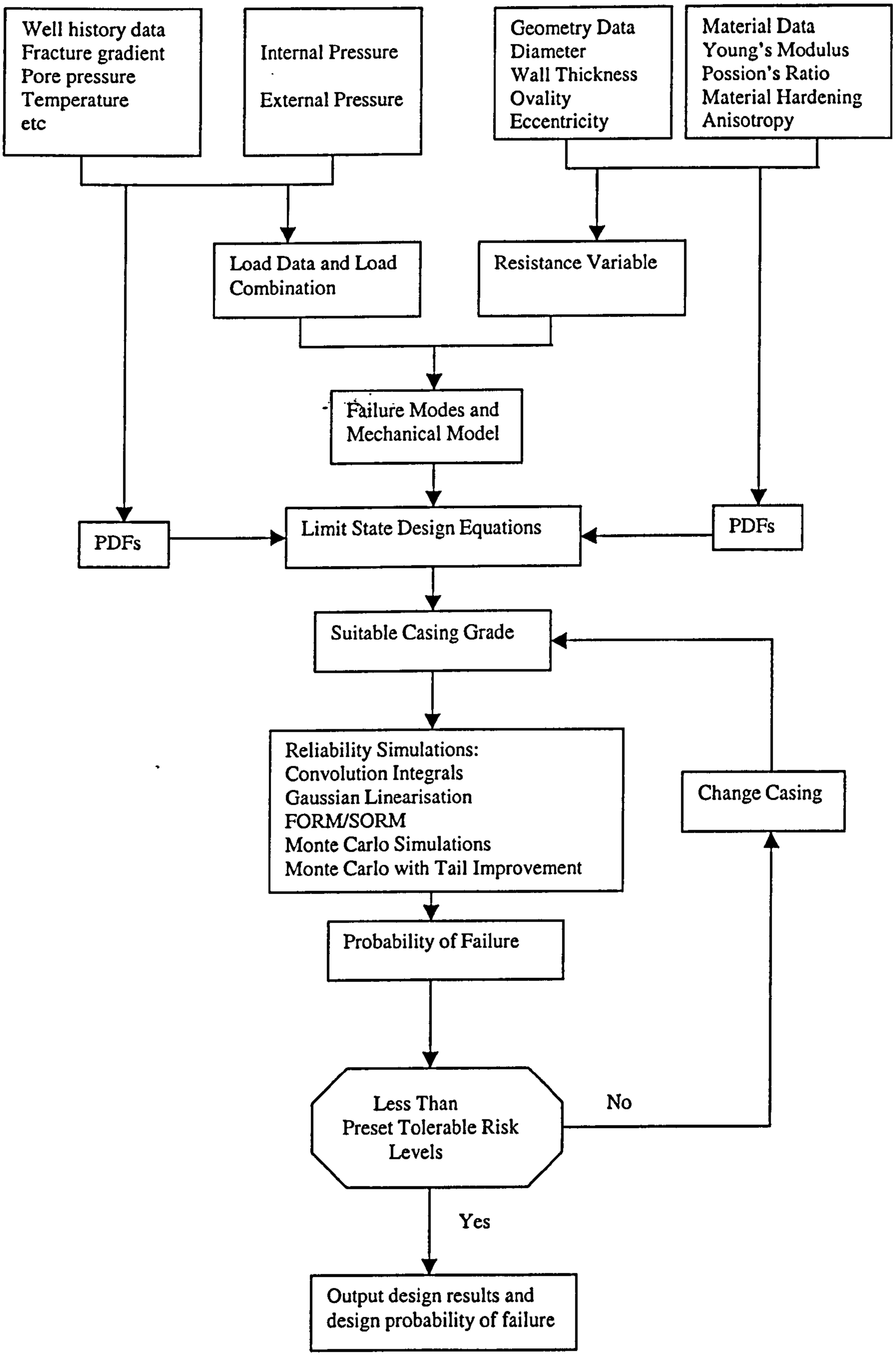

Fig. 2.14 Implementation of full QRA in limit state design of casing

Chapter 3

Identification Of Casing Failure Modes

3.1 Introduction

A fundamental principle in drilling is to maintain equilibrium with the natural formation pressure along the entire length of an open hole, which is achieved by filling the hole with weighted fluids (mud) of requisite density. When formation pore pressure is monotonically increasing with depth of penetration, the equilibrium can be readily achieved. However, an anomalous change in pressure gradient, e.g., a high-pressure formation underlain by a low-pressure formation, can be encountered, which causes a local imbalance in pressure. Drastic imbalance of pressure in either direction caused by incorrect mud weight, can cause an accident that can load the casing with large internal or external pressure. Therefore, the casings in a well are subjected to forces due to self-weight and end restraint, pressure loads induced by the contained moving fluids within and outside a given casing, plus the accidental loads caused by the loss of drilling fluids. In addition, variation of temperature along the length of a pipe during installation and subsequently as hot fluids are produced, or when hot or cold fluids invade or are injected into a pipe, induce additional loads. In general, all loads described above can be reduced to a few fundamental forces consisting of the internal and external pressures as well as the axial tension and compression of the casing body. Depending on the predominance of a particular loading, and the environmental conditions affecting the casing material behaviour, a number of failure mechanisms that define ultimate casing capacity can thus be identified. Failure analysis in the oil and gas industry shows that the principal failure mechanisms, which must be assured in the design process as intended casing performance, include collapse failure under excessive external pressure, burst failure under excessive internal pressure, and casing tensile failure under axial forces. Therefore, casing should be initially designed for collapse, burst and tension. A more detailed

description of these principal failure modes in the casing design is presented in the following sections.

3.2 Casing Collapse

The casing collapse failure mode models the conditions in which either a high-permeable zone (thief zone) is encountered during well drilling; the mud weight exceeds the formation fracture strength; the mud pumps become unavailable; or a combination of these. Casing collapse failure is assumed to occur once the external pressure exceeds the ultimate casing collapse strength. Usually the primary collapse load is supplied by the fluids on the outside of a casing, which are usually the mud and possibly the cement in which the casing is set. The backup fluids are generally considered either negligible or partially supportive in the casing collapse design, as shown in Fig. 3.1. The former results from complete loss or evacuation of the mud inside the casing, while the latter results from partial loss of internal mud. In practice, complete evacuation is assumed for surface casing, and partial evacuation for intermediate and production casings. Therefore, the ultimate collapse limit state is caused by the excessive formation pore pressure when the casing is accidentally evacuated of internal fluids. In the partial loss of internal mud, it is assumed that the fluid column drops to balance the pore pressure at the lost circulation depth. In practice, this is an extreme situation, as it requires that one drills into a high permeability zone at the same time as all mud pumps become unavailable.

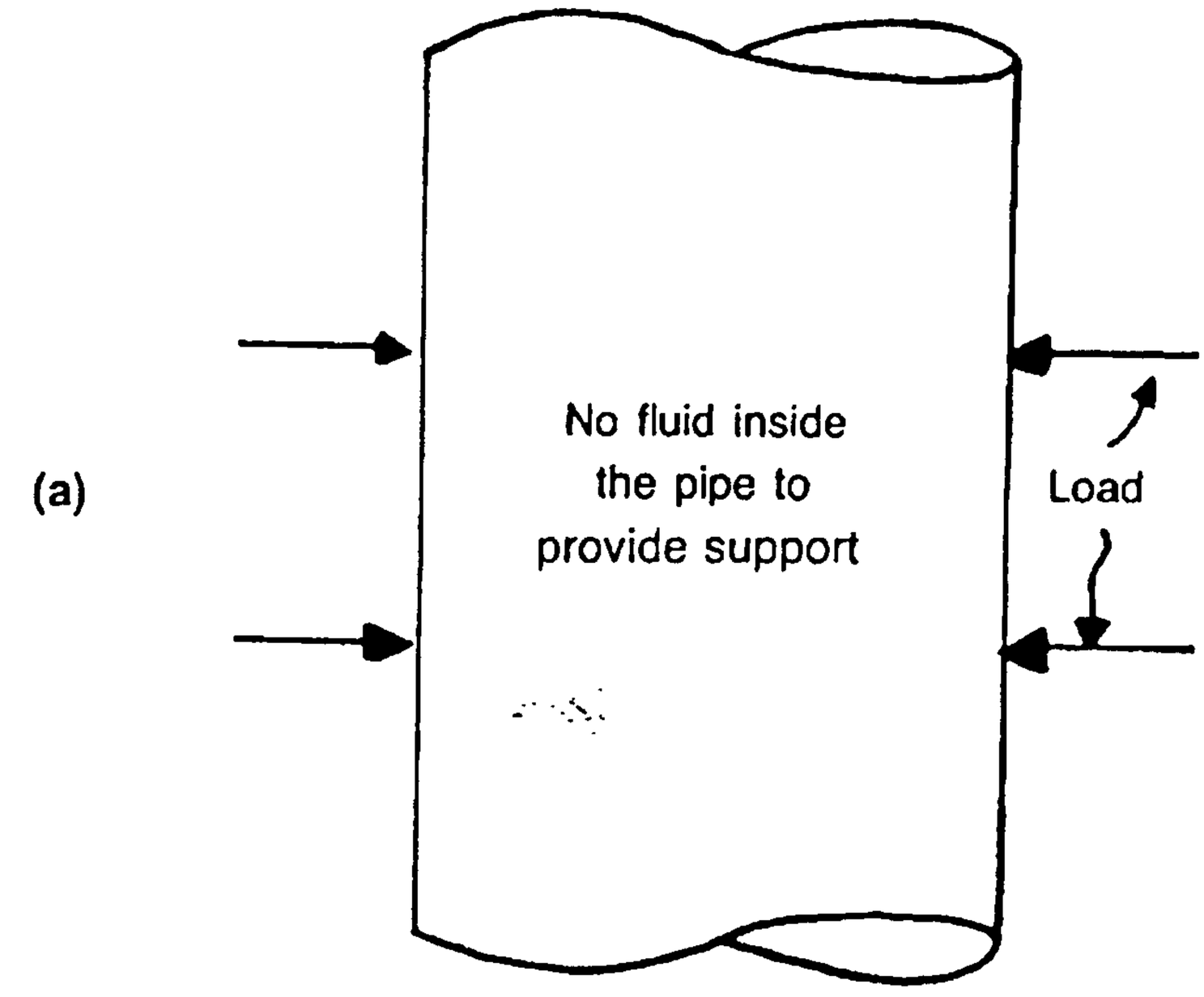

Fig. 3.1 Collapse failure mechanism

3.2.1 Collapse Load Calculation

External pressure acting on the outside of the casing originates from the column of mud used to drill the hole. Since the hydrostatic load of a column of mud increases with depth, collapse pressure is the highest at the bottom and zero at the top.

For conductor casing, the collapse pressure at the casing shoe is equal to the superposition of external pressure due to a column of seawater from sea level to the casing set depth and the pressure caused by the mud inside the casing.

Surface casings are normally designed with no collapse backup fluid inside the pipe. In other words, complete evacuation is assumed. As the internal pressure is zero, the external pressure is caused by the mud in which the casing is set. Therefore, the collapse load is calculated as follows,

$$P_{cs} = \rho_m H_{CSD} g \tag{3.1}$$

where, P_{cs} is the collapse load of surface casing at casing seat, ρ_m is the mud density, H_{CSD} is the vertical casing setting depth, and g is the gravity acceleration.

For intermediate and production casing, complete evacuation is virtually impossible. During lost circulation, the fluid column inside the casing will drop to a height such that the remaining fluid inside the casing just balances the formation pressure of the thief zone as shown in Fig. 3.2. When the mud pressure exactly balances the formation pressure of the thief zone, the fluid loss into the formation will cease. Assuming that the thief zone is at the casing seat, the following relationship should hold during lost circulation,

$$H_{CSD} \rho_f g = l \rho_{mi} g \tag{3.2}$$

where, l is the length of mud column inside the casing, ρ_{mi} is the mud density inside the casing, ρ_f is the formation density of the thief zone. Thus,

$$l = \frac{H_{CSD} \rho_f}{\rho_{mi}} \tag{3.3}$$

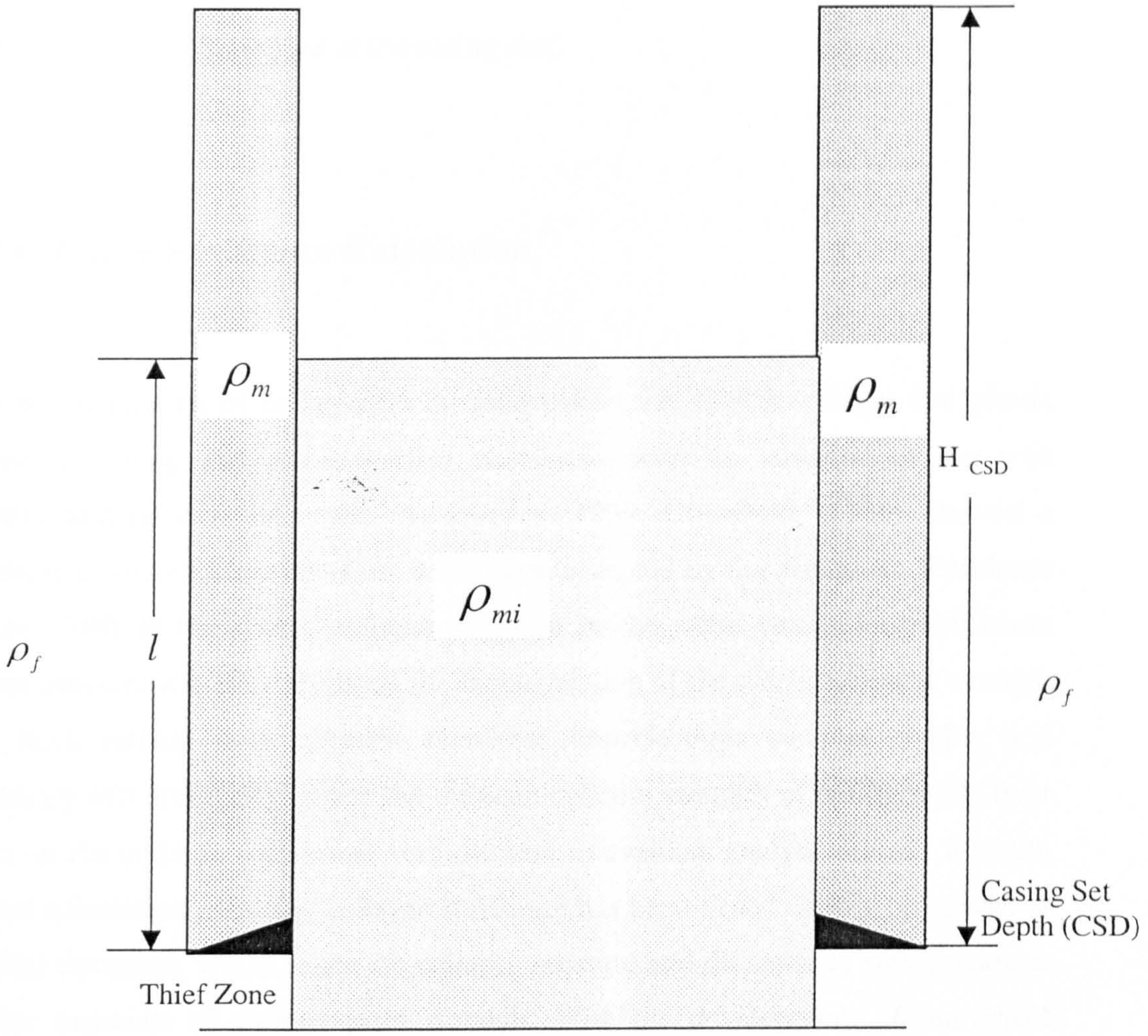

Fig. 3.2 Design consideration of casing collapse

Therefore, the collapse load is still zero at the surface. At depth ($H_{CSD} - l$), the collapse load is provided by the hydrostatic pressure of the same column of external mud, which is expressed by,

$$P_{CSD-L} = \rho_m \, g \, (H_{CSD} - l) \tag{3.4}$$

In addition, the collapse load of intermediate and production casings at the casing seat is calculated as follows,

$$P_{Cl} = (H_{CSD}\,\rho_m\,g) - (l\,\rho_{mi}\,g) \tag{3.5}$$

where, P_{Cl} is the collapse load at the casing seat.

3.2.2 Collapse Resistance Calculation

There are two modes of collapse for an ideal casing, i.e. elastic collapse and plastic collapse, assuming that it has perfect roundness, with no variation of the wall thickness and no residual stress. As early as 1939, Clinedinst (1939) derived a theoretical elastic collapse equation, which was accepted by the American Petroleum Institute (API) as the elastic collapse equation in the same year. The yield onset collapse pressure was later proposed for the calculation of the plastic collapse strength for a thick infinite long cylinder. However, imperfections such as ovality and eccentricity will drastically reduce the ultimate collapse strength of casing while their impact on the collapse strength is very difficult to evaluate analytically. As a result, practical calculation of casing collapse resistance has been based mainly on curves or empirical equations, which relate the collapse pressure and diameter to wall thickness ratio for materials of various yield strength. With the development of numerical analysis, it is now possible to accurately simulate the whole collapse process of casing with imperfections. Therefore, the ultimate collapse resistance term in a limit state equation will be determined in Chapter 5 on the basis of numerical analysis. For brevity, it is omitted here.

3.3 Casing Burst

Large internal pressure in a casing can arise either as a result of pressure testing, a kick or tubing leak. It may also arise from injection of a fluid, or shutting in of a well during production. Therefore, the load calculation of casing burst is divided into three cases, i.e., tubing leak, gas kick and pressure test. Under these conditions, the casing

body is simultaneously subjected to pressures on its internal and external surfaces and an axial load. However, the internal pressure makes the largest contribution to the casing stresses and determines the dominant failure mode. The backup fluid on the outside of the casing will supply a hydrostatic pressure that helps resist casing burst as shown in Fig. 3.3. Thus the effective burst pressure is the differential pressure of the internal load minus any outside pressure. Casing burst is assumed to occur once the differential pressure exceeds the ultimate burst strength. Two distinct failure modes, consisting respectively of ductile and brittle failure, can be identified corresponding to casing failure under excessive internal pressure (Maes et al, 1995; Gulati et al, 1994).

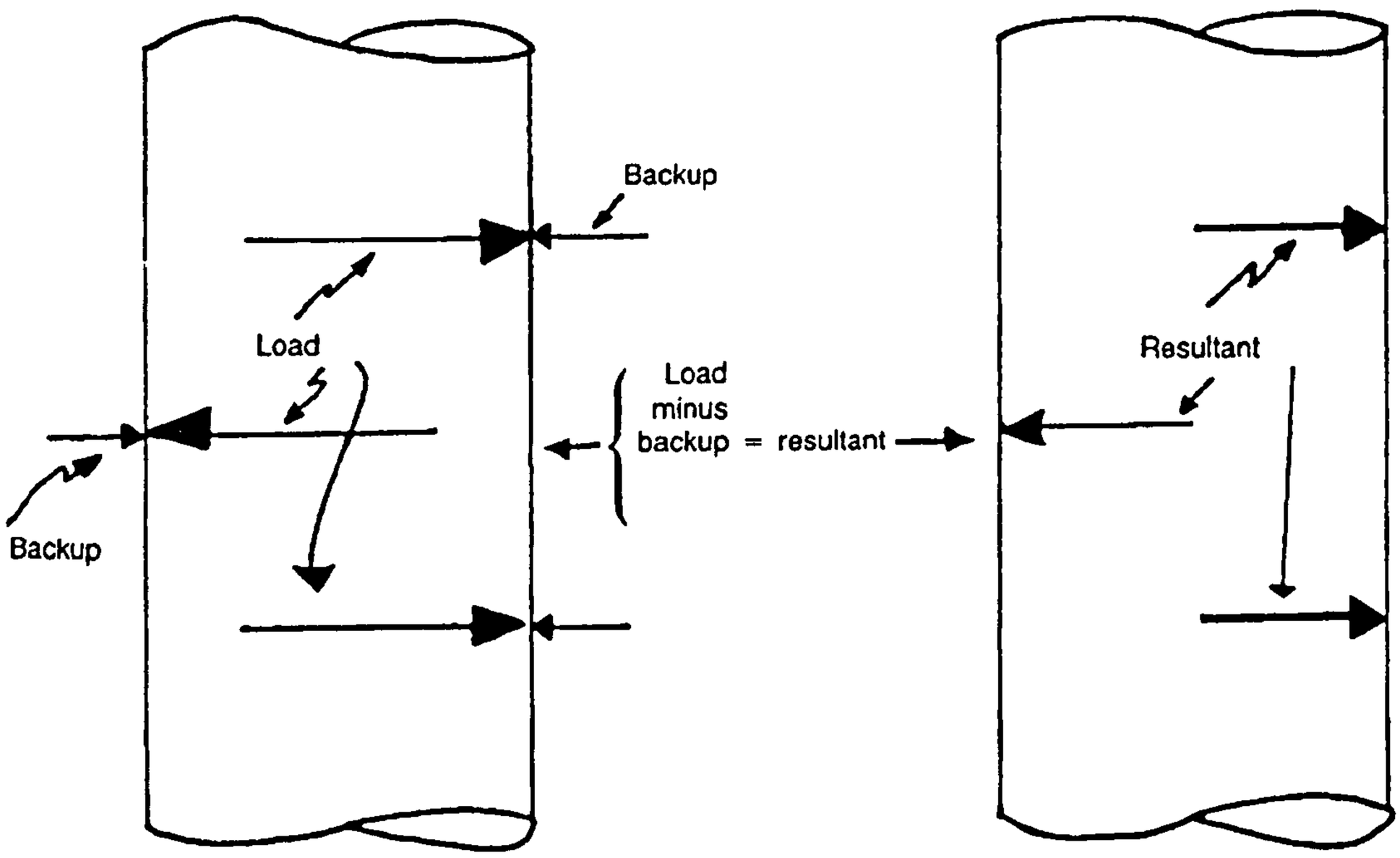

Fig. 3.3 Typical relationship between burst load, backup and resultant

Under internal pressure, ductile casing burst is achieved when the yielding of the entire pipe cross-section precedes the pipe failure. Ductile burst requires a limit state model based on a fully plastic section of a thick casing. With the casing loads dominated by internal pressure increasing, yielding of the pipe body starts first at the inner fibre (Johnson and Mellor, 1973; Harvey, 1986). The ultimate casing burst strength is attained as the plastic zone spreads under increasing loads until the outside

fibre of the casing yields. Well-executed experiments show that the ultimate burst capacity of casing is only slightly larger (typically 2 to 3%) than that corresponding to the yielding of the outside fibre of casing under excessive internal pressure (Brand and Lewis, 1995). Therefore, yielding of the outside fibre can be considered to represent the ultimate limit state of the ductile casing burst.

In some oil and gas well applications, casings are subjected to an aggressive environment containing compounds such as hydrogen sulphide (H_2S). Such environment induces brittle burst behaviour in casing material. In addition to the concentration of compounds such as H_2S, other parameters that influence brittle behaviour include material toughness properties, service temperature, magnitude of the tensile stress and flaw or discontinuity size and distribution. Ideally, the casing ultimate burst capacity in brittle behaviour should be determined by the critical mode I stress intensity factor value K_{Ic}, where this value is determined by proper experiments (Gulati et al, 1994). However, these critical stress intensity factors under corrosive environment for the steels used in casing design are currently not available. Therefore, it was proposed by Gulati et al (1994) that the ultimate casing burst capacity in brittle behaviour be determined by comparing the maximum principal tensile stress with an experimentally determined threshold value below which brittle failure is precluded. It should be pointed out that those threshold values show a pronounced dependence on the service temperature, grade, and H_2S concentration. As more and more high strength materials are used for casings, as well as a high temperature existing in the real well, it is reasonable to assume a more ductile burst failure for a real casing under excessive internal pressure. Therefore, emphasis is placed on ductile casing burst rather than a brittle casing burst. A simple criterion for identifying the ductile burst failure is given in Chapter 6.

3.3.1 Burst Load Calculation

There are three load cases, which will cause casing burst failure to occur. For each load case, the calculation of ultimate burst load is different. However, calculation of the ultimate burst resistance is the same for the three load cases.

3.3.1.1 Casing Burst Due To Tube leak

This load case models the condition in which the tubing develops a leak during the produced oil and gas flow. In this case, the tubing pressure at the leak point is exerted on the fluid in the production casing, resulting in casing burst failure, as shown in Fig. 3.4. The physical mechanisms, which transfer excessive pressure to the production casings, are very complicated and have not been clearly understood yet. The analysis strategy in this thesis, therefore, uses an extreme rather than an expected load condition. It is assumed that, the tubing leak always occurs at the production start-up

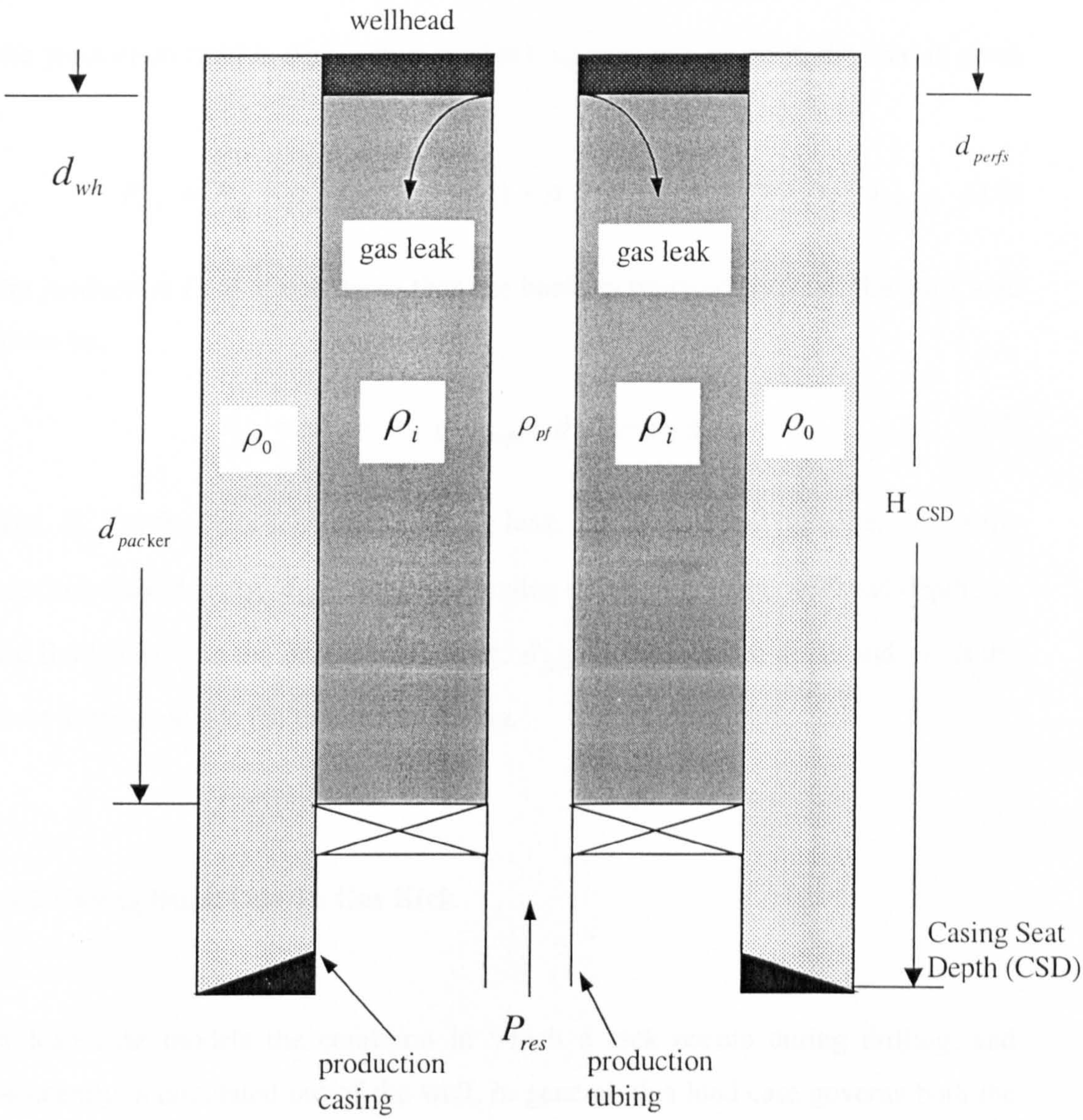

Fig. 3.4 Casing burst design consideration

and develops just below the wellhead. This is a conservative assumption, because the field data shows that a significant proportion of tubing leak events occur late in the well life (DEA 64, 1994).

There are two cases for the calculation of this ultimate burst limit state load term, depending on the production fluid density. If the production fluid is denser than the back-up pressure gradient, the highest stressed point is just above the production packer, with cemented section back-up pressure. If the production fluid is less dense than the back-up pressure gradient, the highest stressed point is at the wellhead, with drill mud in the outer annulus. Therefore the ultimate burst limit state load can be calculated as follows:

If the production fluid is denser than the back-up pressure gradient, the load is given by,

$$P_{b-tl} = [P_{res} - \rho_{pf}\, g\,(d_{perfs} - d_{wh}) + \rho_i\, g\,(d_{packer} - d_{wh})] - \rho_0\, g\, d_{packer} \quad (3.6)$$

If the production fluid is less dense than the back-up pressure gradient, the burst load is given by,

$$P_{b-tl} = [P_{res} - \rho_{pf}\, g\,(d_{perfs} - d_{wh})] - \rho_0\, g\, d_{wh} \quad (3.7)$$

where, P_{b-tl} is the burst load due to tubing leak, P_{res} is reservoir pressure, ρ_{pf} is the production fluid density, d_{perfs} is the perforation depth, d_{wh} is the wellhead depth, ρ_i is the fluid density in the production casing, d_{packer} is the packer depth and ρ_o is the cement density outside the production casing.

3.3.1.2 Casing Burst Due To Gas Kick

This load case models the condition in which a kick occurs during drilling, and subsequently is circulated out of the well. In general, this load case governs both the casing size and the casing setting depth. As the kick circulation is fairly complex in the real situation, several methods, including Kastor's method, the Driller's method

and the Wait-and-Weight method, are proposed for the calculation of an annulus pressure profile during a well kick (Rabia, 1987). It is proposed by the Drilling Engineer Association (DEA) that casing burst load calculation can be based on a fairly simple single bubble model, with the bottom-hole pressure held constant during circulation. In fact, this roughly equates to the use of the Driller's method for well control. A brief description of a single gas bubble circulating up the annulus during a kick is shown in Fig. 3.5 to help understand pressure variation in the annulus. Initially after a kick is detected, the well is shut-in. After the well is shut-in, formation fluids continue to enter the wellbore until the hydrostatic pressures exerted by mud inside the drill-pipe and the drill-pipe shut-in pressure (DPSIP), and by the invading fluid (assumed here as gas), mud in annulus and casing shut-in pressure, are equal to the formation pressure. When it happens, further entry of formation fluids will cease, and the shut-in pressures on the casing are assumed to be constant values. Figure 3.5(a) shows the situation when the gas bubble is still at bottom hole giving an annulus surface pressure of P_a. As the gas bubble rises up the hole, it expands slightly due to loss of pressure and its length increases. The casing shut-in pressure is now the

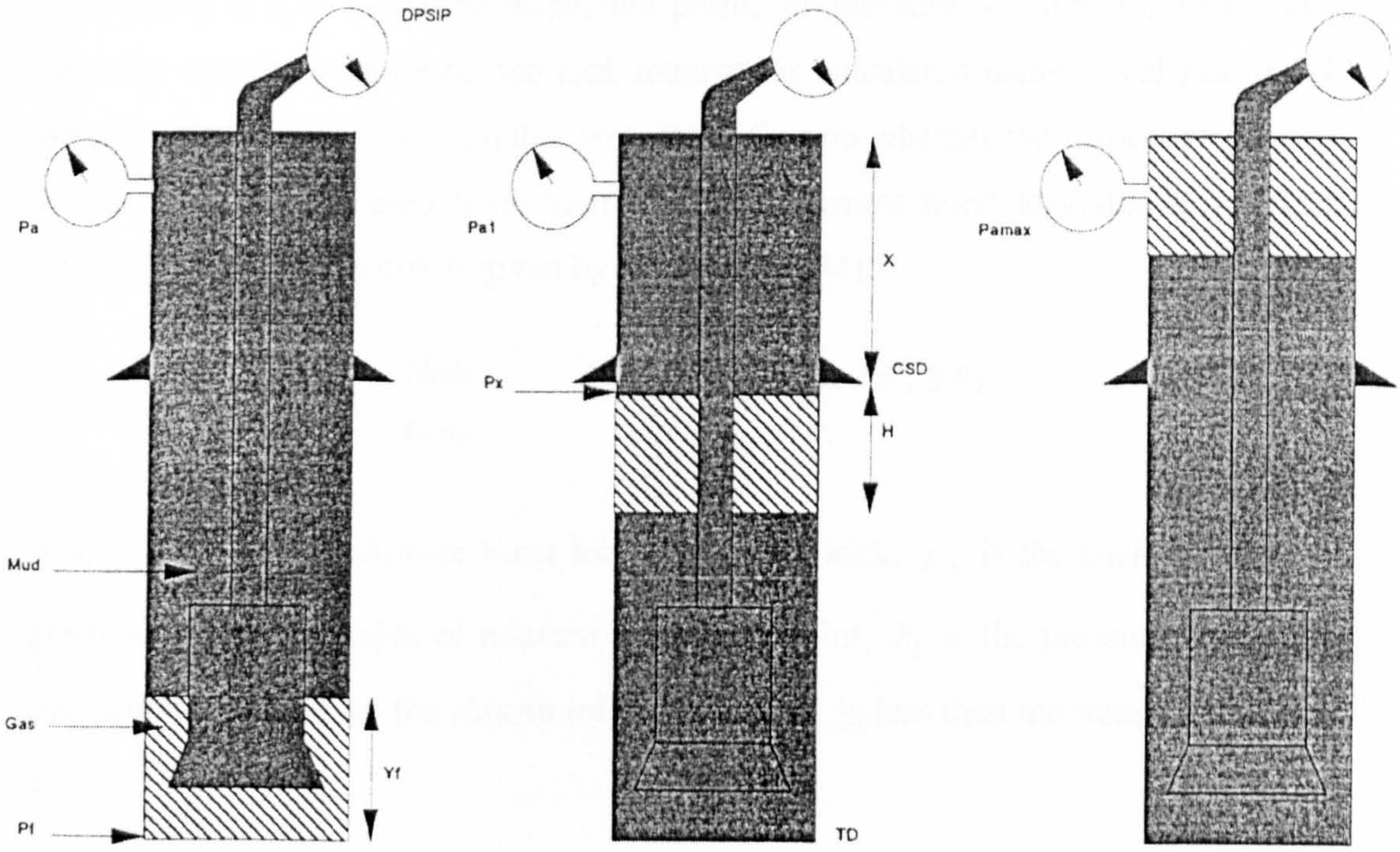

(a) Before circulation (b) Gas halfway up (c) Gas at surface

Fig. 3.5 Diagram of the single bubble method for casing burst design (Rabia, 1987)

difference between the reduced pressure at the top of the gas bubble and the hydrostatic head of a smaller mud column. Consequently, the surface shut-in pressure is now higher than when the gas bubble is at bottom, which is shown in Fig. 3.5(b) as P_{a1}. Eventually the bubble arrives at the surface exerting a maximum surface annulus pressure $P_{a\max}$ as seen in Fig. 3.5(c).

In general, the kick influx volume is a function of the rate of penetration, the hole diameter, the response time and the formation permeability (DEA 64, 1994). There are two possible cases for this ultimate burst limit state model. If the formation does not fracture during kick circulation, the limit state loads of casing burst due to gas kick are giving by kick circulation. However, if the formation fractures during circulation and underground flow develops, the casing ultimate burst limit state loads are given by a hydrocarbon column from the minimum fracture strength in the open hole section.

In the ultimate burst limit state kick circulation model, there are two possible cases, i.e. the initial top-of-bubble height may be below or above the inspection point. If it is below the inspection point, the pressure is a function of the kick volume and intensity. Conversely, if it is above the inspection point, the pressure is a function of the kick intensity only. In both cases, the kick intensity is calculated using a real gas model, which assumes a constant annulus area depending on whether the inspection point is within the open or cased hole. Therefore, the ultimate burst load due to gas kick without formation fracture is given by (DEA 64, 1994),

$$\begin{aligned} &Cased\ \ Hole && P_{b-gk} = P_2 - \rho_o\, g\, d_2 \\ &Open\ \ Hole && P_{b-gk} = P_2 \end{aligned} \qquad (3.8)$$

where, P_{b-gk} is the ultimate burst load due to gas kick, ρ_o is the back up pressure gradient, d_2 is the depth of relevant inspection point, P_2 is the pressure at relevant inspection point. When the shut-in influx volume V_i is less than the transition volume V_t,

$$P_2 = \frac{1}{2}\left[c + \sqrt{\left[c^2 + 4(\rho_m - \rho_{in})P_{in}\, g \frac{T_2}{T_1}\frac{V_i}{A_{ann}}\right]}\right] \qquad (3.9)$$

When the shut-in influx volume V_i is greater than the transition volume V_t,

$$P_2 = P_{in} - \rho_{in}\, g\,(d_1 - d_2) \tag{3.10}$$

$$V_t = (d_1 - d_2)A_{ann}\left(\frac{T_1}{T_2}\right)\left[\frac{P_{in} - \rho_{in}\, g\,(d_1 - d_2)}{P_{in}}\right] \tag{3.11 a}$$

$$c = (K_i - O_b)\, g\, d_1 + \rho_m\, g\, d_2 \tag{3.11b}$$

$$\rho_{in} = \left(\frac{P_{in}}{P_o}\right)\left(\frac{T_o}{T_1}\right)\left(\frac{Z_o}{Z_1}\right)\rho_o \tag{3.11c}$$

$$P_{in} = (\rho_m + K_i - O_b)\, g\, d_1 \tag{3.11d}$$

$$\rho_o = g_r\, \rho_{air} \tag{3.11e}$$

where, ρ_{in} is the influx density, P_{in} is the influx pressure, T_2 is the absolute temperature at the relevant inspection point, T_1 is the absolute temperature at influx depth, A_{ann} is the annulus area, d_1 is the influx depth, K_i is the kick intensity, O_b is the overbalance, ρ_{air} is air density at standard temperature and pressure, g_r is the kick gas gravity at standard temperature and pressure, and,

Z_o and Z_1 are calculated from the ideal gas state equation,

$$PV = ZRT \tag{3.12}$$

where, R is real gas factor and T is the temperature at inspection point.

If the formation fractures during kick circulation, the casing ultimate burst limit state load is given as follows,

$$P_{b-ff} = \{P_{frac} - \rho_{in}\, g\,(d_{shoe} - d_2)\} - \rho_o\, g\, d_2 \tag{3.13}$$

where, P_{frac} is the formation fracture pressure and d_{shoe} is shoe depth.

3.3.1.3 Casing Burst Due To Pressure Test

This load case models the condition in which a test pressure is applied to the casing to verify its integrity prior to drilling ahead. Because pressure tests are almost invariably performed with balanced inner and outer fluid densities, their hydrostatic contributions to the burst load term are cancelled. Therefore, the ultimate burst limit state load for the un-cemented section is the test pressure only. The ULS load term for a cemented casing section, on the other hand, contains both top pressure and hydrostatic contributions. In summary, the ultimate burst load for this limit state is given by

$$\begin{aligned} &\textit{Uncemented} && P_{b-pt} = P_{test} \\ &\textit{Cemented} && P_{b-pt} = \left[P_{test} + \rho_m\, g\,(d_{shoe} - d_{toc})\right] - \rho_{cement}\, g\,(d_{shoe} - d_{toc}) \end{aligned} \tag{3.14}$$

where, P_{b-pt} is the ultimate burst limit state load, P_{test} is the test pressure, d_{toc} is the top of cement depth, ρ_{cement} is the cement density.

3.3.2 Burst Resistance Calculation

The resistance calculation of the ultimate casing burst limit state is relatively simple compared to the burst load calculation, since it is simplified as an infinite long cylinder under excessive internal pressure. Analysis and experiments have been performed in order to develop a predictive model for the ultimate burst limit state. Assuming the casing material to be ductile, a notable analytical model based upon Von Mises's yield criterion for a thin walled casing is proposed for casing burst ULS (Klever et al, 1993). The model is further developed to predict the ultimate burst strength of a thick walled casing (Stewart and Klever, 1998). For the purpose of developing a quantitative risk assessment for casing design, an evaluation of these casing burst models is necessary. Therefore, the existing predictive equations for the casing burst will be carefully assessed on the basis of numerical analysis and experiments. The most accurate predictive equation will be selected for this ultimate

limit state design. How to determine the most accurate burst equation will be discussed in detail in the Chapter 6.

3.4 Casing Tension

In the general case, axial loads on the casing arise due to buoyancy, bending, drag, shock and pressure test. Most axial tension loads on the casing arise from the weight of the casing itself. In a casing design for axial tension, a load case is assumed to model the condition in which the over-pull pull force is applied by the drill rig to attempt to free the pipe when the casing becomes stuck during operating. The failure is assumed to occur once the extreme fibre stress exceeds the temperature degraded ultimate tensile stress. It is noted that, casing tensile failure is an assumed failure mode, rather than one determined from field data such as casing collapse and burst. Tensile loads are defined by computing the buoyancy forces acting on the casing and the casing weight. The buoyancy forces are defined as the product of wellbore pressures acting on the horizontal cross sectional area. In this failure mode, forces acting on the vertical sections of the casing are considered negligible since the inside and outside forces approximately cancel each other. Therefore, the ultimate load of casing tension is given by,

$$L_{at} = (\rho_s A_s g d - \rho_m A_s g d + P_{op})\left(\frac{1}{A_s}\right) \tag{3.15}$$

where L_{at} represents the ultimate load of axial tension, ρ_s is the density of steel, A_s is the cross sectional area, d is the casing shoe depth at stuck point and P_{op} is the over-pull force.

It is assumed that the resistance term of the ultimate axial tension limit state contains the ultimate tensile stress (UTS) and the degradation due to temperature, which will be further investigated in Chapter 7. In general, casing axial tension failure is the least important failure mode compared to casing collapse and burst. However, casing collapse and burst resistance will be altered if the casing is loaded in tension

simultaneously. It is very important that these effects, termed biaxial effects, must be analyzed to ensure they do not reduce the casing ratings below the required burst or collapse requirements.

3.5 Summary

Three fundamental failure modes, (i.e. casing collapse, casing burst and casing axial tension), have been identified according to the predominance of a particular loading. On the basis of the casing operating conditions, a set of equations for the calculation of ultimate load of each failure mode has been proposed. It is noted that the load is an ultimate limit state load rather than a real load condition, since the real casing running condition is very complex and is still the subject of debate. Only a brief review of the determinations of the ultimate material resistance for each failure mode is given in this chapter, as they are fully investigated and discussed in the following chapters.

Chapter 4

Numerical Analysis Of Casing Failure

4.1 Introduction

The problem of casing failure is complicated because of the large deformation and material non-linearity involved in the process. In addition, an actual problem of casing failure often presents difficulties because there are many important factors, which strongly influence the ultimate strength of casings. These important geometrical factors are the ratio of outside diameter to wall thickness (D/t), the initial ovality and eccentricity. The important mechanical properties are Young's modulus, Poisson's ratio, the yield strength and the stress-strain curve. Residual stress and applied axial stress may be listed as other important factors.

The effects of mechanical properties on the casing ultimate strength have long been studied using classical theories. For example, the earliest work on casing collapse can be traced back as early as 1884 when Levy first developed a rational expression for the elastic collapse of a long cylinder under external pressure. Later in 1939, Clinedinst (1939) examined the assumptions implicit in the elastic failure of a pipe under external pressure and developed an elastic collapse equation. In particular, Holmquist and Nadai (1939) developed the theory of plastic collapse, and pointed out that out-of-roundness (ovality) and variation of wall thickness (eccentricity) were important geometrical factors influencing the material resistance of casing to collapse. Timonshenko (1960) investigated the effect of ovality on the casing strength under external pressure and proposed a collapse equation including the ovality parameter. The investigations on the effects of the geometrical imperfection were further continued (Donnell, 1956; Arbocz and Babcock, 1969; Heise and Esztergar, 1970; Small, 1978). Due to the limitations of theoretical analysis, numerical methods, including finite difference method, finite element method (FEM) and boundary

element method (BEM), were gradually introduced and many advances have been made since then.

4.2 The Finite Difference Method

The finite difference method is a direct mathematical tool. Starting with the partial differential equations governing equilibrium, it is possible to derive a system of a set of ordinary differential equations that describe the stress field in the material on the basis of Von-Mises or Tresca yield criterion. Compared to FEM and BEM, it depends more on mathematical derivation since it directly solves the differential equations. The use of this method needs a good understanding of the problem, which somehow limits its popularity in the numerical analysis of casing failure. Huang and Pattillo (1980) used this finite difference method to directly solve the equilibrium equations in a theoretical analysis of casing collapse on the basis of J_2 incremental theory and J_2 deformation theory. The numerical results agreed well with those from the empirical formulae proposed by the American Petroleum Institute (API) for casing design. Yeh and Kyriakides (1986) studied the problem of casing collapse by using a two-dimensional finite difference formulation with both geometrical and material non-linearity.

4.3 The Boundary Element Method

The boundary element method was proposed as early as the finite element method (Brebbia, 1978). It involves the numerical solution of a set of integral equations that connect the boundary, or surface traction to boundary displacements. Unlike FEM, the BEM is based on the solution of integral rather than differential equations and consists of discretization of only the boundary or the surface of the body into a number of elements. Therefore, the number of dimensions in the problem is reduced by one (e.g. from 3D to 2D or 2D to 1D), and the computational effort is greatly

reduced. However, it is extremely important for BEM to obtain the fundamental solution for the corresponding integral equations. For casing failure, it is usually very difficult to find such a fundamental solution as it is governed by high material and geometrical non-linearities. The application of the boundary element method for casing failure problems is thus limited.

4.4 The Finite Element Method

In the last quarter century, the finite element method has experienced enormous growth in both theoretical development and applications (Zienkiewicz, 1977; Zienkiewicz and Taylor, 1989 and 1991). Having been used since the early 1960s, it is certainly the most popular, flexible and powerful tool for casing strength research. Especially with the rapid development of powerful computers, large commercial finite element analysis packages have been developed. Examples are ABAQUS, ANSYS and NASTRAN. Because of its high efficiency and accuracy, finite element analysis is becoming more and more popular to design engineers. As the finite element method has been developed for many years and there are many books (Zienkiewicz, 1977; Owen and Hinton, 1980; Cook et al, 1989; Rao, 1989; Cheung, 1996) that give a detailed description of the method, only a brief review of FEM is presented here for discussion.

4.4.1 General Description Of The Finite Element Method

While looking for a mathematical description of a physical phenomenon, the engineer derives a set of partial differential equations valid in a certain region and places boundary conditions on this system. For practical applications, only one solution for a particular set of numerical data is required. However, only the simplest forms of equations are capable of being solved exactly with the available mathematical methods. Therefore, numerical techniques, such as finite element method, are

considered for an approximate solution by changing the differential equations to a system of algebraic equations. The basic methodology of the finite element method is very simple. It requires a discretization of a region or body into an assembly of elements as shown in Fig. 4.1. Each element is connected together at points referred to as nodes. A field variable, such as displacement, is assumed to act over each element in a predefined manner. The variable is often incorporated in the solution through a polynomial equation referred to as a shape function, which is defined in terms of the values of the field variable at the nodes.

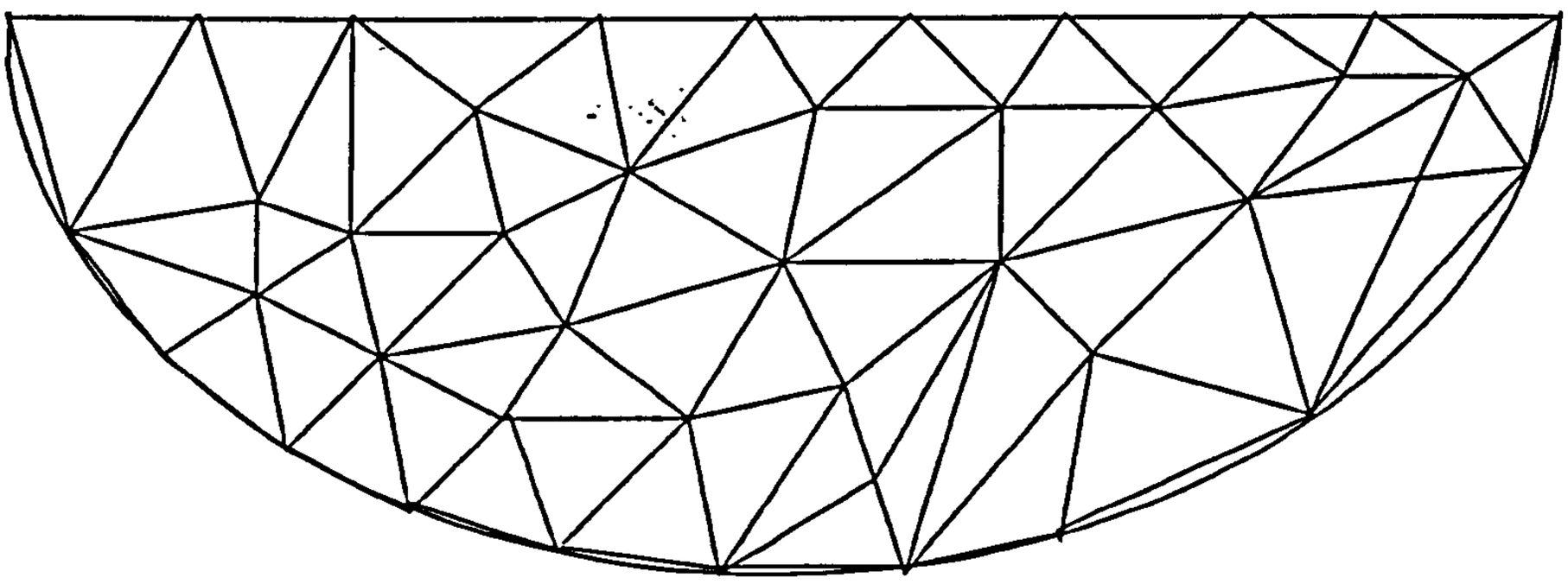

Fig. 4.1 Discretization of a region into a number of finite elements

Once the problem has been discretized, the governing equations for each element are calculated and assembled to give the system equations, which describe the behaviour of the whole body. Usually it takes the following form,

$$[K]\{d\} = \{f\} \tag{4.1}$$

where, $[K]$ is a square matrix, known as the stiffness matrix, $\{d\}$ is the vector of unknown nodal displacements and $\{f\}$ is the vector of applied nodal forces. Equation (4.1) is analogous to the equilibrium of load-displacement relationship for a one-dimensional spring. To find the displacements developed by a given force, the equation is inverted and solved for $\{d\}$, provided boundary conditions are applied. It is noted that the solution to Equation (4.1) is not trivial in practice because the number of equations involved tends to be very large. Fortunately, the stiffness matrix is usually banded, and many techniques have been developed to store and solve the equations efficiently. After solving the unknown nodal values, it is straightforward to calculate the strain and stress from the prescribed displacements.

4.4.2 Performing A Finite Element Analysis

A finite element analysis can be considered to be a four-stage process for any type of problem, whether it is linear or non-linear, and is described as follows:

1. Description of operation – Obtain a complete mathematical description of the process or object in numerical form.

2. Pre-processing – Input data of geometry, mesh, material properties, boundary conditions and initial state parameters.

3. Finite element calculation – Stiffness-matrix equation formulation, assemblage and computational algorithm to obtain the values of state parameters (i.e., displacement, strain and stress) and updated mesh geometry, state parameters and boundary conditions.

4. Post-processing – Output the results from the calculation in a format which can be easily interpreted.

4.5 Key Features Of FE Modelling In ABAQUS

Finite element modelling of casing failure process is a key component of this research. As all the finite element analyses carried out in this thesis are performed using the general finite element code, ABAQUS/Standard (1998), an introduction to ABAQUS is presented. Several key techniques in modelling the casing failure using ABAQUS are described briefly.

4.5.1 About ABAQUS

ABAQUS is a suite of powerful engineering simulation programs capable of solving problems ranging from relatively simple linear analysis to the most challenging non-linear simulation. ABAQUS contains an extensive library of elements that can virtually model any geometry. In addition, it has an equally extensive list of material models that can simulate the behaviour of most engineering materials.

In general, ABAQUS consists of two main analysis modules, i.e. ABAQUS/Standard and ABAQUS/Explicit. Because ABAQUS/Explicit is a special purpose analysis module that uses an explicit dynamic integration FE formulation, it is only suitable for short, transient dynamic problems such as impact, and for some non-linear problems involving changing contact conditions such as metal forming simulations. Different from ABAQUS/Explicit, ABAQUS/Standard is a general purpose FE analysis module designed for advanced analysis applications. It uses an implicit integration scheme, which provides a wide range of linear and non-linear solutions involving the static, dynamic, thermal and other kind of responses of a structure. An important aspect of flexibility within ABAQUS is that, it allows the user to step through the history to be analyzed. This is accomplished by defining the analysis procedures. In general, analysis procedures are divided into two classes, i.e. general analysis and linear perturbation analysis. User-defined material and user subroutines are also available to give users more flexibility.

4.5.2 Non-linear Solution Methods

Let V denote a volume occupied by a part of the solid body, and let S be the surface bounding this volume. Let the surface traction at any point on S be the force t per unit of current area, and let the body force at any point within the volume of material under consideration be f per unit of current volume. The force equilibrium for the volume can be expressed,

$$\int_S t dS + \int_V f dV = 0 \tag{4.2}$$

The "true" or Cauchy stress matrix σ at a point of S is defined by,

$$t = n_1 \sigma \tag{4.3}$$

where, n_1 is the unit outward normal to S at the point. Using these definitions, equation (4.2) can be rewritten as,

$$\int_S n_1 \sigma dS + \int_V f \, dV = 0 \tag{4.4}$$

Gauss's theorem allows a surface integral to be rewritten as a volume integral according to,

$$\int_S n_1 ( ) dS = \int_V \left(\frac{\partial}{\partial x}\right) ( ) dV \tag{4.5}$$

where ( ) is any continuous tensor function. Applying the Gauss theorem to the surface integral in the equilibrium equation gives,

$$\int_S n_1 \sigma dS = \int_V \left(\frac{\partial}{\partial x}\right) \sigma dV \tag{4.6}$$

Since the volume is arbitrarily, this equation must apply point-wise in the body. Thus the differential equation of translational equilibrium is given,

$$\left(\frac{\partial}{\partial x}\right) \sigma + f = 0 \tag{4.7}$$

These are the three familiar differential equations of force equilibrium. In deriving them, no approximation has been made with respect to the magnitude of the deformation or rotation. That is, the equations are an exact statement of equilibrium so long as it is precise about the definitions of surface traction, body forces, Cauchy stress, volume and the area.

The basis for the development of a displacement interpolation finite element model is the introduction of some locally based spatial approximations to parts of the solution. To develop such an approximation, the three equilibrium equations represented by Equation (4.7) need to be replaced by an equivalent equation using virtual work principle. If taking the dot product of Equation (4.7) with the virtual velocity field δv, it results in a single scale equation at each material point. Integrating over the entire body gives,

$$\int_V \left[\left(\frac{\partial}{\partial x}\right) \sigma + f\right] \delta v dV = 0 \tag{4.8}$$

By using the chain rule and Gauss theorem, the virtual work statement, Equation (4.8) may be rewritten as,

$$\int_S t\,\delta v\,dS + \int_V f\,\delta v\,dV = \int \sigma \cdot \left(\frac{\partial \delta v}{\partial x}\right) dV \tag{4.9}$$

It is noted that, $(\cdot)$ represents the dot product. The virtual velocity gradient $\frac{\partial \delta v}{\partial x}$ can be decomposed into a symmetric and an anti-symmetric part,

$$\frac{\partial \delta v}{\partial x} = \frac{1}{2}\left(\frac{\partial \delta v}{\partial x} + \left[\frac{\partial \delta v}{\partial x}\right]^T\right) + \frac{1}{2}\left(\frac{\partial \delta v}{\partial x} - \left[\frac{\partial \delta v}{\partial x}\right]^T\right) = \partial D + \partial \Omega \tag{4.10}$$

Finally, the virtual work equation in the classical form can be obtained,

$$\int_V \sigma \cdot \delta D\,dV = \int_S \delta v\,t\,dS + \int_V \delta v\,f\,dV \tag{4.11}$$

where, t, f, and σ are an equilibrium set and,

$$\sigma = \sigma^T \tag{4.12}$$

The left hand side of Equation (4.11), the internal virtual work rate term, can be replaced with the integral over the reference volume of the virtual work rate per reference volume defined by any conjugate pairing of stress and strain. Written as the virtual work principle, it gives,

$$\int_{V_0} \tau^c \cdot \delta\,\varepsilon dV^0 = \int_S t^T\,\delta v\,dS + \int_V f^T\,\delta v\,dV \tag{4.13}$$

where, τ^c and ε are any conjugate pairing of material stress and strain measures. In general, the finite element interpolator is expressed,

$$U = N_N u^N \tag{4.14}$$

where, N_N are interpolation functions which depend on some material coordinate system, u^N are nodal variables. The virtual field, δv, must be compatible with all kinematic constraints. Introducing the above interpolation constrains the displacement to have a certain spatial variation, so that δv must also have the same spatial form

$$\delta v = N_N \delta v^N \tag{4.15}$$

Therefore, the continuum variational statement Equation (4.13) can be approximated by a finite variation over the finite set δv. Now, $\delta\varepsilon$ is the virtual rate of material strain associated with δv, and because it is a rate form, it must be linear in δv. Hence, the interpolation assumption gives,

$$\delta\varepsilon = \beta_N \delta v^N \tag{4.16}$$

where, β_N is a matrix which depends, in general, on the current position, x, of the material point being considered. The matrix β_N that defines the strain variation from the variations of the kinematic variables is derivable immediately from the interpolation functions once the particular strain measure to be used is defined.

Without loss of generality, the matrix β_N can be written as

$$\beta_N = \beta_N(x, N_N) \tag{4.17}$$

Since the δv^N are independent variables, if each one is chosen to be nonzero and all others zero in turn, a system of non-linear equilibrium equations can be derived,

$$\int_{V^0} \beta_N \cdot \tau^c \, dV^0 = \int N_N^T \, t \, dS + \int N_N^T \, f \, dV \tag{4.18}$$

This system of equations is the basic finite element stiffness (assumed displacement interpolation) model, and is of the form,

$$F^N(u^M) = 0 \tag{4.19}$$

where, F^N is the force component conjugate to the N^{th} variable in the problem, and u^M is the value of the M^{th} variable. The basic problem in an FE analysis is to solve Equation (4.19) for u^M throughout the history of interest.

ABAQUS generally uses Newton-Raphson's method as a numerical technique for solving the non-linear equilibrium equations. The basic formalism of Newton-Raphson's method is as follows (ABAQUS manual, 1998):

Assuming that, after an iteration i, an approximation u_i^M to the solution has been obtained. Let c_{i+1}^M be the difference between this solution and the exact solution to the discrete equilibrium Equation (4.19). This gives,

$$F^N(u_i^M + c_{i+1}^M) = 0 \tag{4.20}$$

Expanding the left-hand side of this equation in a Taylor series about the approximate solution u_i^M gives,

$$F^N(u_i^M) + \frac{\partial F^N}{\partial u^P}(u_i^M)c_{i+1}^P + \frac{\partial^2 F^N}{\partial u^P \partial u^Q}(u_i^M)c_{i+1}^P c_{i+1}^Q + \ldots = 0 \tag{4.21}$$

If u_i^M is a close approximation to the solution, the magnitude of each c_{i+1}^M will be small, and so all but the first two terms above can be neglected. Thus it gives a linear system of equations,

$$K_i^{NP} c_{i+1}^P = -F_i^N \tag{4.22}$$

where, $K_i^{NP} = \frac{\partial F^N}{\partial u^P}(u_i^M)$, is the Jacobian matrix, and,

$$F_i^N = F^N(u_i^M) \tag{4.23}$$

The next approximation to the solution is,

$$u_{i+1}^M = u_i^M + c_{i+1}^M \tag{4.24}$$

The iteration continues until the difference c_{i+1}^M is sufficiently small.

In most cases, ABAQUS uses Newton-Raphson's method to solve the non-linear equations as described above. However, the method has disadvantages. At each iteration, the complete Jacobian matrix has to be calculated and solved. The calculation of the Jacobian matrix may be a problem because, in many important cases, it is difficult to derive the form of matrix algebraically. The solution of the Jacobian matrix may be difficult because of the computational effort involved. As the problem size increases, the direct solution of the linear equations can dominate the entire computation effort.

The most commonly used alternative to the Newton method is the modified Newton-Raphson method, in which the Jacobian matrix in Equation (4.22) is only recalculated occasionally. Therefore, this method is attractive for mildly non-linear problems involving softening behaviour, but it is not suitable for more severe non-linear cases. Another alternative is the quasi-Newton method. The basis of quasi-Newton method is to obtain a series of improved approximations to the Jacobian matrix, $\tilde{K}_i^{NM}$, that satisfy the secant condition,

$$F^N(u_i^M) - F^N(u_{i-1}^M) = \tilde{K}_i^{NM}(u_i^M - u_{i-1}^M) \tag{4.25}$$

which can be symbolically rewritten as

$$c_{i+1}^P = -\left[K_i^{NP}\right]^{-1} F_i^N \tag{4.26}$$

where, the inverse of the Jacobian matrix can be obtained by an iterative process.

4.5.3 Modified Riks Algorithm

Casing failure is a case of instability type of failure and may involve geometrical non-linearity. During the period of load-displacement response, the load and the displacement may decrease as the solution evolves. After the ultimate load, the load-displacement response shows a negative stiffness, the structure must release some strain energy to remain in equilibrium. Therefore, it is necessary to obtain non-linear static equilibrium solutions for unstable problems such as casing failure, where the load-displacement response may exhibit the type of behaviour sketched in Fig. 4.2. The modified Riks method is an algorithm, which allows an effective solution of static equilibrium state during the unstable phase of the response. It is assumed that the loading is proportional. All load magnitudes vary with a single scalar parameter. It is further assumed that the response is reasonably smooth, which means sudden bifurcation does not occur. The essence of the Riks method is that it solves simultaneously for the loads and displacements (ABAQUS theory manual, 1998). ABAQUS uses another quantity, the arc length along the static equilibrium path in load-displacement space, to control the progress of the solution.

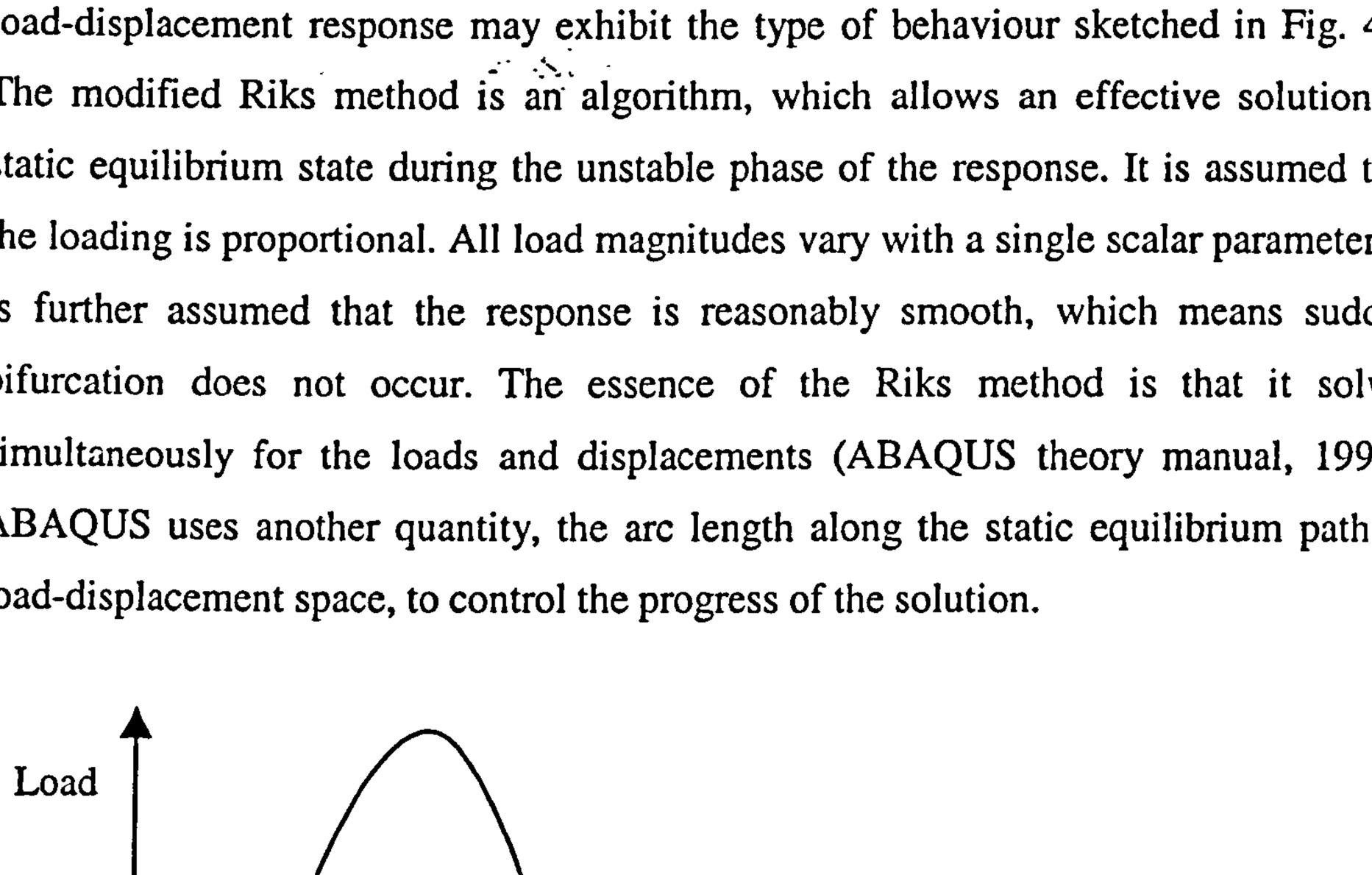

Fig. 4.2 Typical load-displacement response of an unstable problem

Let $\tilde{P}^N$ be the vector of reference loads, as defined in the *CLOAD and *DLOAD options in an ABAQUS input file. Assuming a load magnitude parameter λ, the current configuration of load vector may be expressed using $\lambda \tilde{P}^N$ for proportional loadings. Assume $\tilde{u}^N$ to be the displacement vector at that time. In ABAQUS, the solution space is scaled to make dimensions approximately the same magnitude on each axis by default. This is done by measuring the maximum absolute value of all displacement variables, $\bar{u}$, in the initial linear iteration. Therefore, the scaled space is spanned by:

$$Load = \lambda P^N, \quad P^N = \tilde{P}^N / \bar{P} \tag{4.27a}$$

$$Displacements = u^N = (\tilde{u}^N / \bar{u}) \tag{4.27b}$$

where $\bar{P} = (\tilde{P}^N \tilde{P}^N)^{\frac{1}{2}}$. The solution path is thus the continuous set of equilibrium points described by the vector $(u^N;\lambda)$ in the scaled space (ABAQUS theory manual, 1998). All components of this vector will be of order unity. Without loss of generality, it is supposed that the solution has been developed to the point $A^0 = (u_0{}^N;\lambda_0)$ as shown in Fig. 4.3. The tangent stiffness, K_0^{NM}, can be formed, and we solve:

$$K_0^{NM} \tilde{v}_0^M = \tilde{P}^N \tag{4.28}$$

Denote v_0^N to be the displacement increment $\tilde{v}_0^N$ scaled by $\bar{u}$. The current increment size of magnitude parameter, $\Delta\lambda_0$, (A^0 to A^1 in Fig. 4.3) is chosen from a prescribed arc length, Δl, in the solution space, such that,

$$\Delta\lambda_0^2 (v_0^N;1)\cdot(v_0^N;1) = \Delta l^2 \tag{4.29}$$

where $(\cdot)$ denotes dot product. Hence,

$$\Delta\lambda_0 = \frac{\pm \Delta l}{\left(v_0^N v_0^N + 1\right)^{\frac{1}{2}}} \tag{4.30}$$

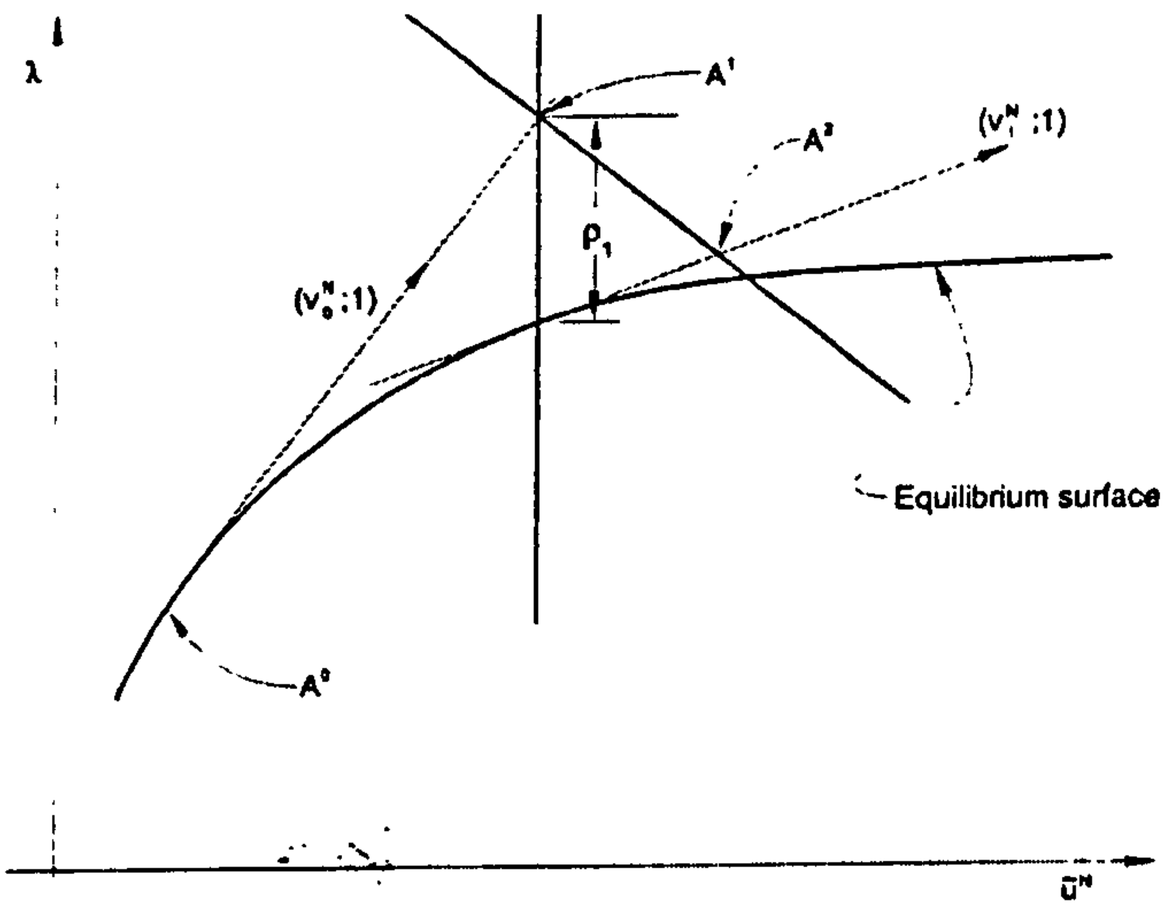

Fig. 4.3 The modified Riks algorithm

The value of Δl is initially suggested by the user in an ABAQUS input file and adjusted by the ABAQUS automatic load incrementation algorithm (ABAQUS theory manual, 1998). The sign of $\Delta\lambda_0$, the direction of response along the tangent line, is chosen so that the dot product of $\Delta\lambda_0\left(v_0^N;1\right)$ on the solution to the previous increment, $\left(\Delta u_{-1}^N;\Delta\lambda_{-1}\right)$, is positive,

$$\Delta\lambda_0\left(v_0^N;1\right)\cdot\left(\Delta u_{-1}^N;\Delta\lambda_{-1}\right)>0 \tag{4.31}$$

That is,

$$\Delta\lambda_0\left(\bar{v}_0^N\,\Delta\bar{u}_{-1}^N+\Delta\lambda_{-1}\right)>0 \tag{4.31}$$

In this way, the point $A^1(u_0^N+\Delta\lambda_0 v_0^N;\lambda_0+\Delta\lambda_0)$ can be found. Thus, the solution is now corrected onto the equilibrium path in the plane passing through A^1 and orthogonal to $\left(v_0^N;1\right)$, by the following iterative algorithm:

Initialize $\Delta\lambda_i=\Delta\lambda_0$, $\Delta u_i^n=\Delta\lambda_0 v_0^N$, for the i th iteration (i=1, 2, 3, etc.),

a) Form I^N, K^{NM}, the internal forces (stress) at the nodes at the state $(u_0^N+\Delta u_i^N;\lambda_0+\Delta\lambda_i)$,

$$I^N=\int\beta^N$$
$$K^{NM}=\frac{\partial I^N}{\partial u^M} \tag{4.32}$$

b) Check the equilibrium,

$$R_i^N = (\lambda_0 + \Delta\lambda_i)P^N - I^N \tag{4.33}$$

If all the entries in R_i^N are very sufficiently small, the increment has converged. If not, the following step proceeds.

c) Solve equation

$$K^{NM}\{v_i^M; c_i^M\} = \{P^N; R_i^N\} \tag{4.34}$$

It is noted that two load vectors, P^N and R^N, are solved simultaneously and two displacement vectors, v_i^N and c_i^N, are obtained.

d) Scale the vector $(v_i^N;1)$ and add it to $(c_i^N;\rho_i)$, where $\rho_i = R_i^N P^N / \overline{P}^2$ is the projection of the scaled residuals onto P^N, so that the solution can move from A^i to A^{i+1} in the plane orthogonal to $(v_0^N;1)$. This gives the following equation,

$$\{(0;-\rho_i) + (c_i^N;\rho_i) + \mu(v_i^N;1)\} \cdot (v_0^N;1) = 0 \tag{4.35}$$

Simplification of equation (4.35) gives,

$$\mu = -\frac{c_i^N v_0^N}{v_i^N v_0^N + 1} \tag{4.36}$$

Now, the solution point is $A^i(u_0^N + \Delta u_i^N + c_i^N + \mu v_i^N; \lambda_0 + \Delta\lambda_i + \mu)$.

e) Update for the next iteration,

$$\begin{aligned} \Delta u_{i+1}^N &= \Delta u_i^N + c_i^N + \mu v_i^N \\ \Delta\lambda_{i+1} &= \Delta\lambda_i + \mu \\ i &= i+1 \end{aligned} \tag{4.37}$$

and return to step a) above for the next iteration.

It is noted that the implementation of Riks algorithm in ABAQUS also includes the additional update, $v_0^N = v_i^N$, after each iteration. This causes the equilibrium search to be orthogonal to the last tangent, rather than to the tangent at the beginning of the increment. The main motivation for this additional modification comes from the use of the method in plasticity problems, where the first iteration of each increment uses the elastic material stiffness to establish the direction of straining. The total path length traversed is determined by the load magnitudes supplied by the user in the loading options, while the number of increments is determined by the data card supplied with the *STATIC option, assisted by ABAQUS automatic incrementation scheme if chosen.

4.5.4 Material Plasticity Modelling

4.5.4.1 General Introduction

Casing failure nowadays occurs with excessive plastic deformation. As a result, a better understanding of the material plasticity behaviour is very important to accurately determine the ultimate strength of a casing. However, it is neither possible nor necessary to have a complete treatment of the classical mathematical theory of plasticity within the confines of a single section. The history of plasticity theory dates back to 1864 when Tresca published his yield criterion. Tremendous progresses have been made by many researchers since then (Hill, 1950; Johnson and Mellor, 1973; Khan and Huang, 1995).

4.5.4.2 True Stress-Strain Curve

Nominal stress and strain are defined on the original dimensions. In particular, nominal stress, σ_{nom}, is defined as the load divided by the original cross-sectional area, while nominal strain, ε_{nom}, is defined as the deformed length divided by the original length, i.e.,

$$\varepsilon_{nom} = \frac{\Delta l}{l_0}$$
$$\sigma_{nom} = \frac{F}{A_0} \tag{4.38}$$

where, Δl is the deformed length, l_0 is the original length, A_0 is the original cross sectional area and F is the force in the material. As an alternative, true stress, σ, and strain, ε, are defined on the current dimensions,

$$\varepsilon = \int_{l_0}^{l_c} d\varepsilon = \int_{l_0}^{l_c} \frac{dl}{l_0} = \ln\left(\frac{l_c}{l_0}\right)$$
$$\sigma = \frac{F}{A} \tag{4.39}$$

where, l_c is the current length and A is the current area.

In plasticity theory, the material is usually assumed to be incompressible based on experimental evidence. Therefore, the relationship between the true and nominal stresses is formed by considering the incompressible nature of plastic deformation,

$$l_0 A_0 = l_c A \tag{4.40}$$

Thus, an expression relating the current area to the original area is formed,

$$A = A_0 \frac{l_0}{l_c} \tag{4.41}$$

Substituting this definition of current area into the definition of true stress gives,

$$\sigma = \frac{F}{A} = \frac{F}{A_0}\frac{l_c}{l_0} = \sigma_{nom}\left(\frac{l_c}{l_0}\right) \tag{4.42}$$

with $\frac{l_c}{l_0} = \frac{\Delta l + l_0}{l_0} = 1 + \varepsilon_{nom}$, and,

$$\sigma = \sigma_{nom}(1 + \varepsilon_{nom}) \tag{4.43}$$

The nominal strain can be expressed as,

$$\varepsilon_{nom} = \frac{\Delta l}{l_0} = \frac{l - l_0}{l_0} = \frac{l_c}{l_0} - 1 \tag{4.44}$$

Adding unity to both sides of this expression and taking the natural log of both sides provides the relationship between the true strain and the nominal strain,

$$\varepsilon = \ln(1 + \varepsilon_{nom}) \tag{4.45}$$

4.5.4.3 Defining Material Plasticity In ABAQUS

When defining elastic-plastic material data in ABAQUS, true strain and true stress are used. ABAQUS expects these values and interprets the data in the input file accordingly. The *PLASTIC option defines the true yield stress of the material as a function of true strain. In particular, it approximates the smooth stress-strain

behaviour of the material with a series of straight lines joining the given data points in the *PLASTIC option. Any number of points can be used to approximate the actual material behaviour, therefore, it is quite simple to generate a very close approximation of the actual stress-strain curve.

However, the strains provided in material test data used to define the plastic behaviour are not likely to be the plastic strains in the material. Instead, they will probably be the total strains in the material. Therefore, the total strain values will need to be decomposed into the elastic and plastic strain components. The plastic strain is obtained by subtracting the elastic strain, defined as the value of true stress divided by the Young's modulus, from the total strain value. This relationship is expressed,

$$\varepsilon^{pl} = \varepsilon^{t} - \varepsilon^{el} = \varepsilon^{t} - \frac{\sigma}{E} \tag{4.46}$$

where, ε^{pl} is true plastic strain, ε^{t} is total true strain, ε^{el} is true elastic strain, σ is true stress and E is Young's modulus.

An example of a stress-strain curve is shown in Fig. 4.4 to demonstrate how to convert the test data defining a plastic material behaviour into the appropriate input format for ABAQUS. The six points shown on the nominal stress-strain curve are used as the data for the *PLASTIC option. The first step is to use Equations (4.43) and (4.45) to convert the nominal stress and nominal strain to true stress and true strain. Once these values are known, Equation (4.46) is used to determine the plastic strains associated with each yield stress value. The converted data are shown in Table 4.1. It is noted that there is little difference between nominal and true values at small strains, while there are very significant difference at larger strain values. Therefore, it is extremely important to provide the proper stress-strain data to ABAQUS if analysis

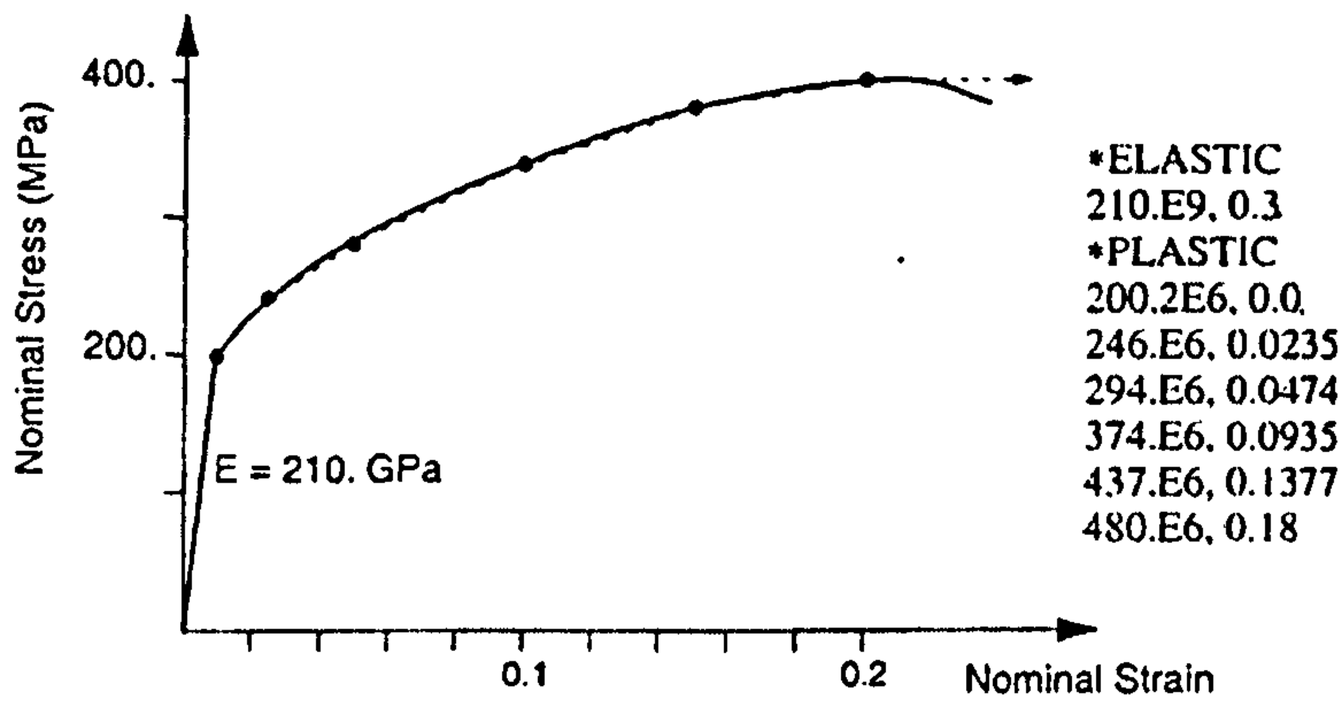

Fig. 4.4 An elastic-plastic material behaviour and corresponding ABAQUS input data

involves large deformation. The format of the input data defining the material behaviour is also shown in Fig. 4.4. ABAQUS interpolates linearly between the data points provided to obtain the material's response and assumes that the response is constant outside the range defined by the input data.

Table 4.1 An example of converting data for ABAQUS

Nominal Stress (MPa)	Nominal Strain	True Stress (MPa)	True Strain	Plastic Strain
200E6	0.00095	200.2E6	0.00095	0.0
240E6	0.025	246E6	0.0247	0.0235
280E6	0.050	294E6	0.0488	0.0474
340E6	0.100	374E6	0.0953	0.0935
380E6	0.150	437E6	0.1398	0.1377
400E6	0.200	480E6	0.1823	0.1800

4.6 Summary

Numerical analysis techniques including boundary element and finite element methods were reviewed in this chapter. Due to its efficiency and accuracy, the finite element method is dominant in the field of casing failure analysis. Therefore, the fundamentals of finite element analysis are briefly reviewed. A general introduction of this commercial FE package has been given. Several key features of the proposed FE analysis, including the non-linear equilibrium equation solution, Riks algorithm and material plasticity modelling, are described in this chapter.

Chapter 5

Casing Collapse

5.1 Introduction

The steadily increasing demand for energy and the necessity of ensuring an adequate energy supply has led to a situation, in which boreholes are being drilled to ever greater depths worldwide in the search for oil and gas reservoirs and for subsequent production. As a result, exploration of offshore areas with water depths between 1000 ft (300 m) and 7000 ft (2100 m) is on the increase (Verner et al, 1983; Langner, 1984). Such enormous depths, as well as the penetration of difficult geological formations (plastic clays and plastic salt), imposes stringent demands on the load-bearing capability of casing strings, while the limitations on technical feasibility are frequently attained. Therefore, tubular structures such as well casings will have to withstand the high loads dictated by the extreme depth.

During installation and depending on the laying method used, casing sections can experience a combination of external pressure, internal pressure, bending and tension loads. However, when eventually the casing reaches the sea floor and depending on the terrain, it can be considered, in most cases, to be relatively free of other loads but the external pressure. Excessive external pressure will lead to catastrophic collapse of well casings. As a result, one of the most important and decisive factors in the design of casing strings is thereby the collapse strength.

Deep-water application of casing implies use of tubulars with low diameter to thickness ratios (D/t) and, when possible, use of high strength materials. If a casing under consideration collapses in the elastic state, an improvement of the collapse strength for a large ratio of D/t can no longer be achieved by the use of a steel grade with higher strength. Selection of a casing with thicker wall thickness is the only way

to improve the collapse strength to withstand the external pressure. However, limitations are imposed on the casing geometry too, as a result of the given clearance conditions. Externally, restrictions are governed by the internal diameter of the previously landed casing. Internally, allowance must be made for the drift diameter corresponding to the next drill bit size. Moreover, casing with a D/t ratio as low as 10 has been considered in the feasibility studies for deep-water applications (Yeh and Kyriakides, 1986). For this value of D/t, the collapse strength is determined by the inelastic behaviour of the casing material. As a result, any serious attempt at predicting the collapse strength must involve a careful modelling of the inelastic material characteristic. The importance of the inelastic material effect was recognized very early by Southwell (1915). Other factors, such as geometric imperfections and residual stress, must be re-examined in the light of the strong dependence on the inelastic material properties. Hence, it is vital that an accurate method be established for the calculation of collapse strength, in order to permit a better utilisation of the available casing grades without safety compromise.

5.2 Review Of Casing Collapse

Casing collapse is an instability type of failure. The elastic collapse is one in which failure occurs under elastic deformation, while the plastic case is one in which failure is preceded by permanent plastic deformation. The collapse strength of a casing under external pressure depends, in general, on a number of factors. The length, diameter and wall thickness of a casing, as well as the physical properties of the casing material, the yield point, elastic limit and Poisson's ratio, are especially decisive. These parameters also determine whether a plastic or elastic failure occurs under the action of external pressure. Moreover, there are additional factors, which more or less strongly influence the ability of a casing to withstand external pressure. These include the lobe number of casing collapse pattern, geometrical imperfections and residual stress.

5.2.1 Elastic Collapse Equation Review

For a perfect infinitely long cylinder under external pressure, Levy developed a rational expression for elastic collapse strength as early as 1884,

$$P = \frac{2E}{1-\upsilon^2}\frac{1}{(D/t-1)^3} \tag{5.1}$$

where, P is the elastic collapse strength, E is Young's modulus, υ is Poisson's ratio, D is outside diameter and t is wall thickness. It is noted that in deriving Equation (5.1), the external pressure is assumed to act on the mean diameter instead of the outside diameter of the casing. For large ratios of D/t, Equation (5.1) is approximated closely by

$$P = \frac{2E}{1-\upsilon^2}\frac{1}{(D/t)^3} \tag{5.2}$$

Stewart (1906) developed an empirical equation for elastic collapse in connection with his experiments on welded steel tubes, which was written in a similar form to Equation (5.2) as

$$P = \frac{2CE}{(1-\upsilon^2)}\frac{1}{(D/t)^3} \tag{5.3}$$

where, C is an experimental constant with a value of 0.761. Apart from the fundamental assumptions made by the general theory of elasticity, Equation (5.3) assumes that a linear distribution of stress occurs along the wall thickness. Clinedinst (1939) investigated the critical collapse strength by assuming both linear and hyperbolic distributions of stress along the wall thickness of casings. For a hyperbolic stress distribution, elastic collapse strength was calculated by:

$$P = \frac{2E}{(1-\upsilon^2)}\frac{3\chi}{\left(\frac{D}{t}\right)} \tag{5.4}$$

where,

$$\chi = -1 + \frac{(D/t-1)}{2}\ln\left(\frac{D/t}{D/t-2}\right) \tag{5.5}$$

For a linear stress distribution,

$$P = \frac{2E}{(1-\upsilon^2)} \frac{1}{D/t\,(D/t-1)^2} \tag{5.6}$$

Equations (5.1), (5.2), (5.4) and (5.6) can be used without any serious error in the elastic range. If taking Equation (5.4) as the comparison base (because it has the most logical assumption made in the derivation), it was shown (Clinedinst, 1939) that Equations (5.4) and (5.6) gave practically identical results, whereas Equations (5.1) and (5.2) deviated considerately for a casing with relatively low values of D/t. However, an assumption of linear distribution was relatively safer. Therefore, Equation (5.6) is recommended for the calculation of the elastic collapse strength of a perfect round long casing.

In summary, the elastic collapse strength of a perfect casing depends only on the D/t ratio and on the material constants, i.e. Young's modulus and Poisson's ratio. It is noted that, an axial stress has no influence on the elastic collapse strength (Holmquist and Nadai, 1939).

5.2.2 Plastic Collapse Equation Review

For casings exhibiting ideally plastic material behaviour, damage due to external pressure occurs because the material begins to yield. A yield onset pressure is often used as an approximate estimate of the plastic collapse strength, which is given by the API Bulletin 5C3 (1992) as

$$P = 2\sigma_y \frac{D/t-1}{(D/t)^2} \tag{5.7}$$

where, σ_y is the yield strength. It is noted that the state, in which the tangential stresses induced at the inner surface of the casing body by the external pressure attain the yield strength, is assumed as the plastic collapse load limit in this Equation. However, the inception of plastic deformation of the material at the inner surface of the casing does not imply that the casing has already failed. Instead, an elastic-plastic boundary is formed with augmenting loads, which shifts from the inner surface of the

casing toward the outside. Thus, the casing body is subdivided into an interior, plastically deformed zone and exterior, as yet elastic material zone as shown in Fig. 5.1.

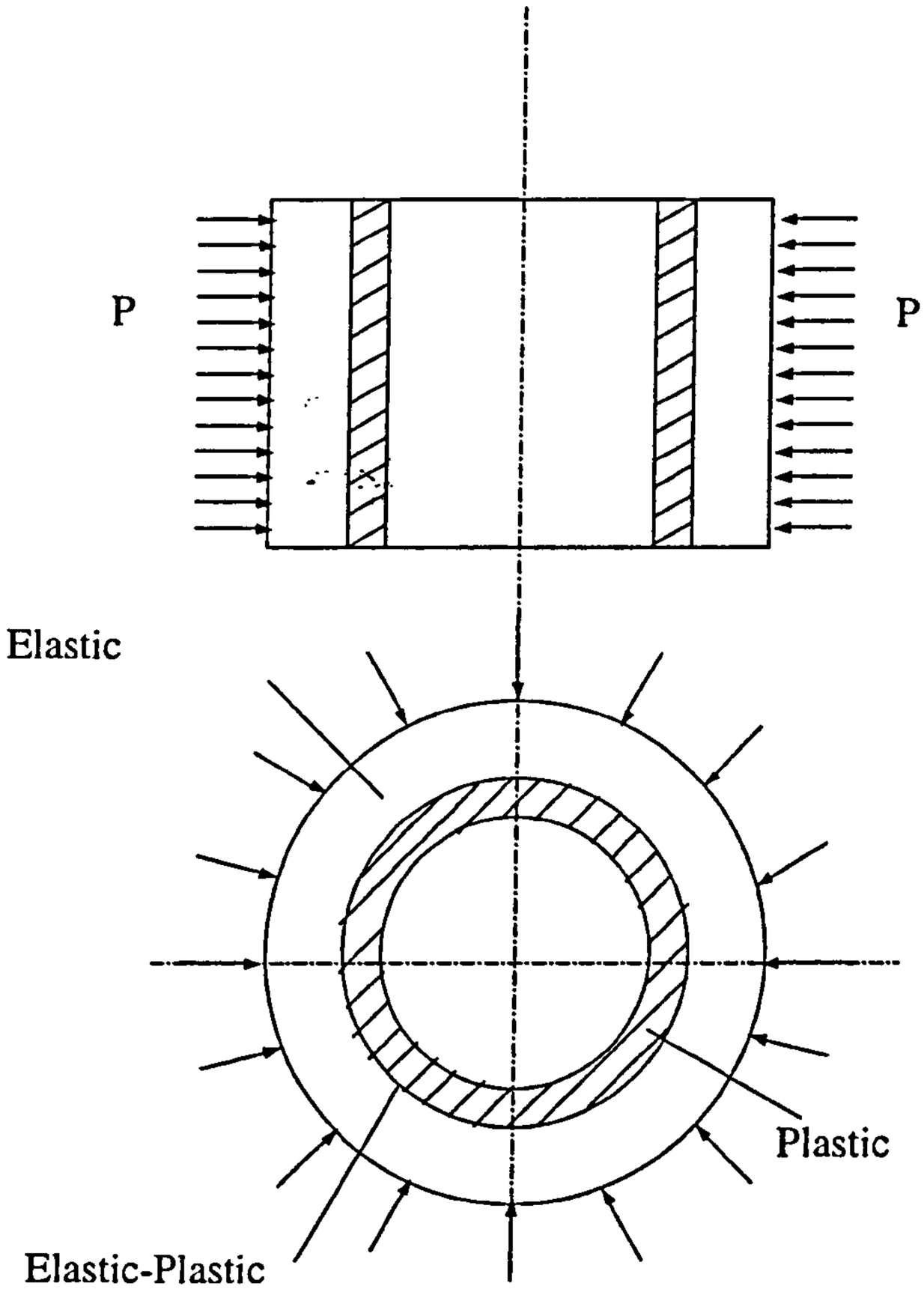

Fig. 5.1 Elastic and plastic material zones under external pressure

A partially plastic transition occurs for a realistic casing between the range of elastic behaviour and the yield strength. The collapse behaviour of casings, which fail in the transition range, represents a problem of instability, as does that of elastic collapse behaviour. However, prediction of the critical collapse strength can no longer be found based on Young's modulus only. A tangent modulus, E_t, which represents the local slope in the stress-strain material curve of casings, is used to replace Young's modulus. Thus Equation (5.2) may be rewritten for an approximate prediction of collapse strength in the transition range,

$$P = \frac{2E_t}{(1-\upsilon^2)} \frac{1}{(D/t)^3} \tag{5.8}$$

However, the calculation of the collapse strength from Equation (5.8) yields a value, which is rather low in comparison with that obtained from experiment. Timoshenko (1933) proposed that the critical plastic collapse strength in the transition range be calculated by replacing Young's modulus in the elastic collapse equation by a reduced modulus, which was given by

$$E_r = \frac{4E\dfrac{d\sigma}{d\varepsilon}}{\left(\sqrt{E}+\sqrt{\dfrac{d\sigma}{d\varepsilon}}\right)^2} \tag{5.9}$$

where, $\frac{d\sigma}{d\varepsilon}$ is the local slope in the stress-strain curve of the casing material. It is noted that $E_r = E$ when $\frac{d\sigma}{d\varepsilon} = E$.

Considering the analogy between casing collapse and buckling of a straight bar, Holmquist and Nadai (1939) proposed the following equation for the calculation of plastic collapse strength

$$P = \frac{2E_r}{(1-\upsilon^2)}\frac{1}{\left(\dfrac{D}{t}-1\right)^3} \tag{5.10}$$

Another equation proposed by Clinedinst (1939) had the following expression,

$$P = \frac{2E_r}{(1-\upsilon^2)}\frac{1}{\dfrac{D}{t}\left(\dfrac{D}{t}-1\right)^2} \tag{5.11}$$

In as much as the plastic collapse strength depends on the shape of the stress-strain curve, casings made from materials having the same conventional yield strength can have considerably different plastic collapse strength if their material curves have different shapes. In contrast to Young's modulus, the reduced modulus, E_r, is not a constant, but rather depends on the particular value of the stress. Exact knowledge of the stress-strain behaviour of the material is necessary for the determination of the plastic collapse strength. Therefore, it is extremely important to carefully model the actual material of casings as accurately as possible in solving the casing plastic collapse problem.

The axial stress has no effect on the elastic collapse strength, whereas the presence of axial stress greatly affects the plastic collapse strength. On the basis of Von Mises yield criterion, Holmquist and Nadai (1939) derived a calculation for the plastic collapse strength under a combination of external pressure and axial loading,

$$P_A = P_0\left[\sqrt{1-\frac{3}{4}(\sigma_A/\sigma_y)^2}-\frac{1}{2}(\sigma_A/\sigma_y)\right] \qquad (5.12)$$

where, P_A is the plastic collapse strength under axial stress, P_0 is the plastic collapse pressure without axial stress and σ_A is the applied axial stress respectively.

In summary, for the calculation of the collapse strength in the elastic-plastic range, an accurate knowledge of the stress-strain relationship of casing material is extremely important. Imperfections may occur in the casing body, and can influence the collapse strength dramatically. For these reasons, it appears both sensible and expedient to describe the collapse strength of casings exhibiting elastic-plastic collapse behaviour with the use of simple empirical formulae from the start. The elastic-plastic collapse behaviour of casings is also extremely important in the practice simply for the fact that, standardised dimensions of oil field tubular goods lie for the most part in this range.

5.3 Factors Influencing The Collapse Strength

The collapse strength of casing is governed by the D/t ratio or by a power thereof. If the damage is caused by yield of the material, the collapse strength is directly proportional to the yield strength of the casing. If, on the contrary, the collapse is controlled by the geometrically determined instability of the casing body, the collapse strength is dependent on Young's modulus and Poisson's ratio. In addition, the collapse strength of a casing is influenced by other factors, of which the most important ones are described in the following sections.

5.3.1 Number Of Lobes

One of the important quantities for appraising the stability behaviour of a casing subjected to external pressure is the number of lobes, as shown in Fig. 5.2. The number of lobes depends on the casing length and the D/t ratio. Southwell (1915) developed a formula, which took into account the influence of the length and lobe number on the elastic collapse behaviour of short cylinders

$$P = \frac{1}{3}(n_l^{\,2} - 1)\frac{2E}{(1-\upsilon^2)}(t/D)^3 + \frac{2Et}{D}\frac{Z_b}{(n_l^{\,2}-1)n_l^{\,4}(2L/D)^4} \qquad (5.13)$$

where, n_l denotes the lobe number, L denotes the length and Z_b is a parameter for the boundary conditions.

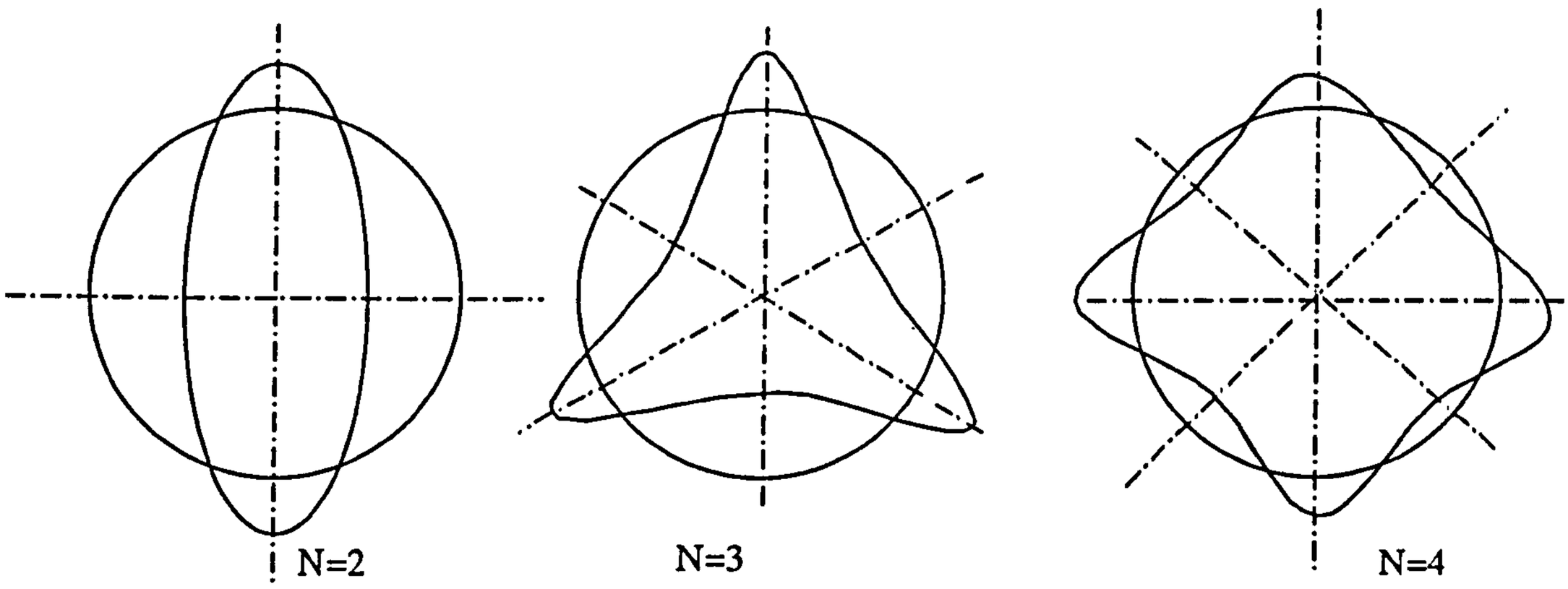

Fig. 5.2 Lobe number and shape for plastic collapse

Sturm (1941) made a correction term of the effect of lobe number to Equation (5.2) for the calculation of elastic collapse strength,

$$P = \frac{2E}{(1-\upsilon^2)}\frac{1}{(D/t)^3}\left\{\frac{n_l^{\,4} - n_l^{\,2} + \left(\frac{\pi}{2}Z_b\frac{D}{L}\right)^4 + \left(\frac{\pi}{2}Z_b\frac{D}{L}\right)^2(2n_l^{\,2}-\upsilon)}{3n_l^{\,2}}\right\} \qquad (5.14)$$

Equation (5.13) was simplified subsequently by substitution of an enveloping curve for the family of n_l-curve for each D/t ratio, which was approximately described by (Saunders and Winderburg, 1931) as

$$P = \frac{32}{9} E \frac{t^2}{LD} \sqrt[4]{\frac{Z_b}{36} \left(\frac{1}{1-\upsilon^2} \right)^3 (t/D)^2} \tag{5.15}$$

Equation (5.15) was further simplified (Saunders and Winderburg, 1931) by substituting the value of $\pi^4/16$ for Z_b, and by performing the calculation with $\upsilon = 0.3$. Thus,

$$P = 1.11 \frac{2E}{(1-\upsilon^2)} \frac{t^2}{LD} (t/D)^{0.5} \tag{5.16}$$

According to Saunders and Windenburg (1931), the lobe number itself can be calculated by means of the following formula:

$$n_l = \sqrt[4]{7.06 \, (D/L)^2 (D/t)} \tag{5.17}$$

The validity of Equation (5.17) was confirmed by performing tests on specimens made of steel and aluminium (Krokel, 1965). In particular, a comparison of the theoretical lobe numbers from Equation (5.17) with those obtained from the tests, was performed by Krug (1983). Jasper and Sullivan (1931) obtained an important conclusion that, for a value of L/D greater than 8, only the lobe number $n_l = 2$ occurs regardless of the diameter or wall thickness, which is basically in agreement with Equation (5.17). As the L/D ratio of a casing is usually greater than 8, the lobe number can be taken as two without inducing any significant error. Therefore, the effect of lobe number on the collapse strength can be neglected for well casings and will not be included in the following numerical investigation.

5.3.2 Critical Casing Length

Oil field tubular goods are usually manufactured in lengths corresponding practically to infinitely long cylinders. In the case of collapse failure due to external pressure, therefore, only a lobe number of $n_l = 2$ occurs. In order to determine accurately the actual collapse strength of a casing, however, it is necessary to employ sufficiently long specimens during the test. In this thesis, the critical casing length is defined as

the length for which only a lobe number of 2 occurs, and for which the clamping of ends exerts no influence on the test result.

After transformation of Equation (5.16) and insertion of the critical collapse strength P_c according to the classical Equation (5.2), the following relationship is obtained (Saunders and Windenburg, 1931),

$$P = 1.11 P_c \frac{D}{L} (D/t)^{0.5} \tag{5.18}$$

For the condition $P = P_c$, it yields the critical casing length,

$$\therefore L_c = 1.11 D (D/t)^{0.5} \tag{5.19}$$

A number of other means of calculations can be found in the literature, which differ only in the modified values of the constants in the equations. Those equations are summarised below (Krokel 1965):

$$\begin{aligned} &Kantorowitch: && L_c = 1.73 L_0 \\ &Domaschnew: && L_c = 1.17 L_0 \\ &Brounwell \quad : && L_c = 1.11 L_0 \\ &Ebner \quad\quad : && L_c = 0.66 L_0 \\ &Cook \quad\quad\ : && L_c = 1.73 L_0 \end{aligned} \tag{5.20}$$

where, L_0 denotes the expression $D(D/t)^{0.5}$.

Independent of the wall thickness, Karman (1965) gave a multiple of 6 to 8 times the diameter as the critical casing length. The test results performed on casing specimens, steel grade J55 with 2 inches (50.8 mm) outside diameter by Jurgens (1973), provided evidence that the effect of the specimen length on the ultimate collapse strength became negligible at a multiple of 8 to 10 times the diameter. Krug (1983) conducted a large number of experiments to study the effect of casing length to diameter ratio on the collapse strength, which fully supported the aforementioned conclusion as shown in Fig. 5.3.

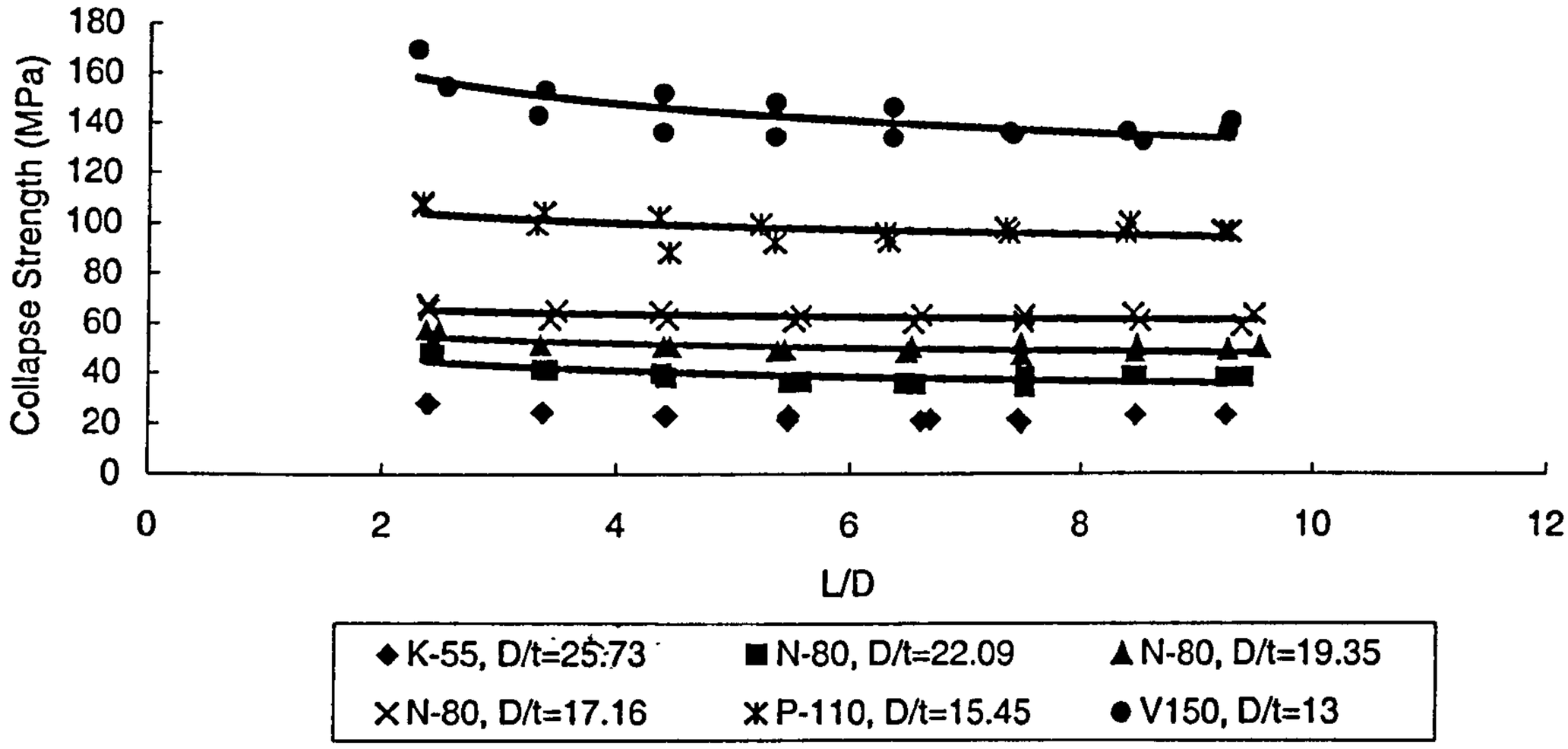

Fig. 5.3 Influence of casing length on the collapse strength (Krug, 1983)

In contrast to the methods described here for determining the critical length in the elastic range, Clinedinst (1977) came to the conclusion after evaluating the API test results that the L/D ratio exerts no influence on the elastic collapse, but does affect the collapse strength in the plastic transition range. For the yield range, sufficient test results were not available at that time. The influence of the length on the collapse strength in the transition range is shown in Fig. 5.4. The resulting multiple for the critical casing length is 8 times the specimen diameter. An empirical equation for conversion of the collapse strength of short specimens was thus given by Clinedinst (1977)

$$P_{(L/D)} = P_{(L/D=8)} \left(\frac{8D}{L}\right)^{0.0708} \tag{5.21}$$

For the yield range, Jurgens (1973) proposed the following approximation:

$$P = P_c \left(1 + \frac{0.1D}{L}\right) \tag{5.22}$$

where, P_c denotes the critical collapse strength for an infinitely long specimen as calculated from Equation (5.2).

In summary, it can be safely concluded that casing length exerts a negligible small effect, on the ultimate collapse strength as long as the length of practical casing is greater than 8 times of its outside diameter.

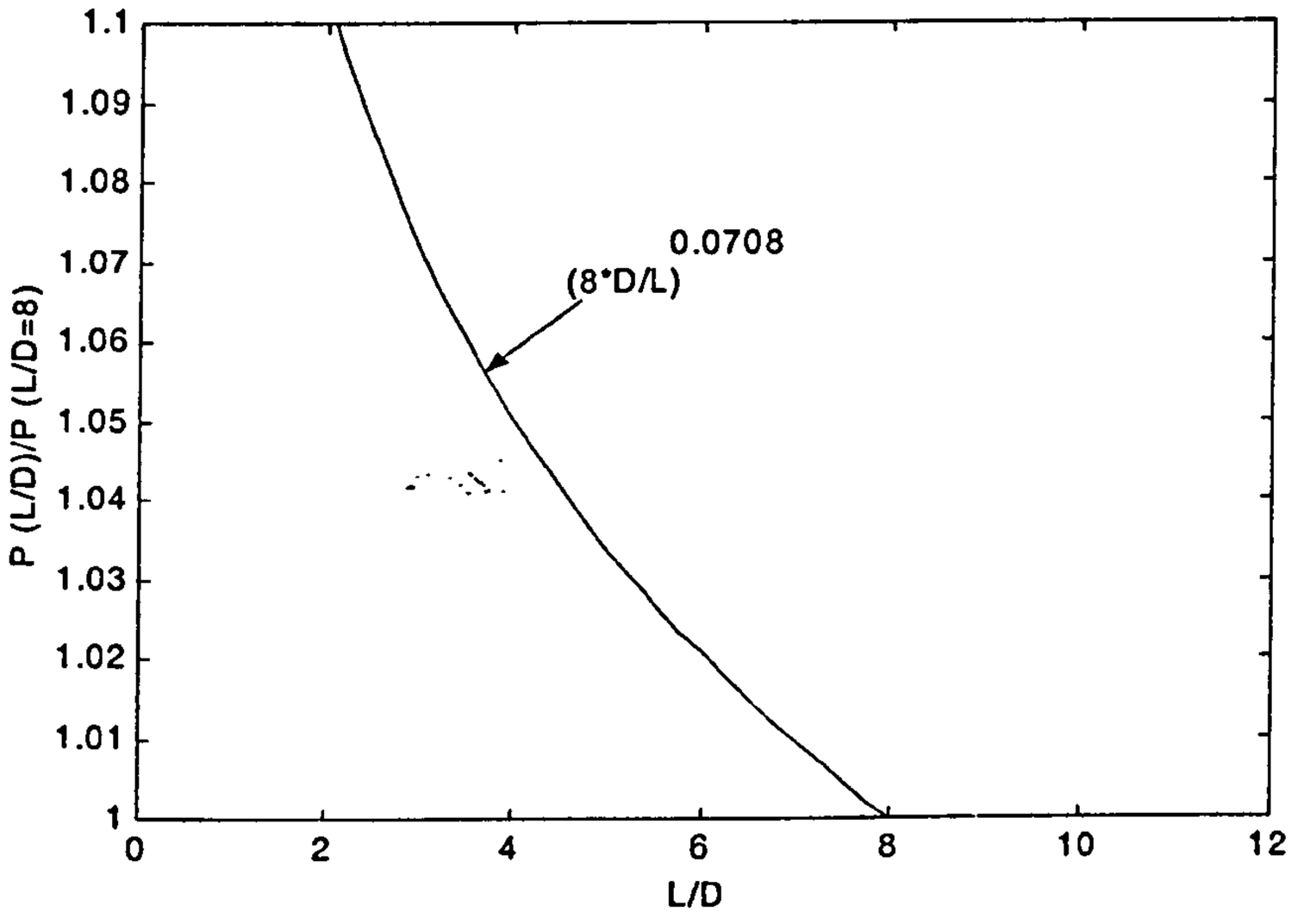

Fig. 5.4 Influence of casing length on the collapse strength (Clinedinst, 1977)

5.3.3 Ovality

It is a well known fact that the actual collapse strength deviates significantly from the theoretical prediction determined by classical equations. This discrepancy is usually attributed to a variety of imperfections in the materials and/or geometry of a real casing, of which the ovality (out of roundness) appears to be the leading offender (Small, 1978). In general, ovality and eccentricity (non-uniform wall thickness) are always presented in seamless and even welded casings. In the particular case of seamless casing, ovality depends on several operational factors, but generally the manufacture can produce a casing of high collapse strength with a maximum ovality of 0.5% (Assanelli et al, 1999). As a result, predictions of casing ultimate collapse strength are usually made by applying a substantial safety factor to the applicable classical theories.

The effect of ovality on the collapse strength has long been studied in order to quantify the safety factors. Among them, a very common procedure is to assume that the initial cross shape is the same as the appropriate elastic buckling mode for the round casing as shown in Fig. 5.5. It is noted that the lobe number of two is assumed for the infinitely long cylinder as discussed before. Therefore, the initial pattern of ovality, $w_i(\theta)$, is expressed by,

$$w_i(\theta) = w_o \cos(2\theta) \tag{5.23}$$

where w_o and θ are depicted in Fig. 5.5.

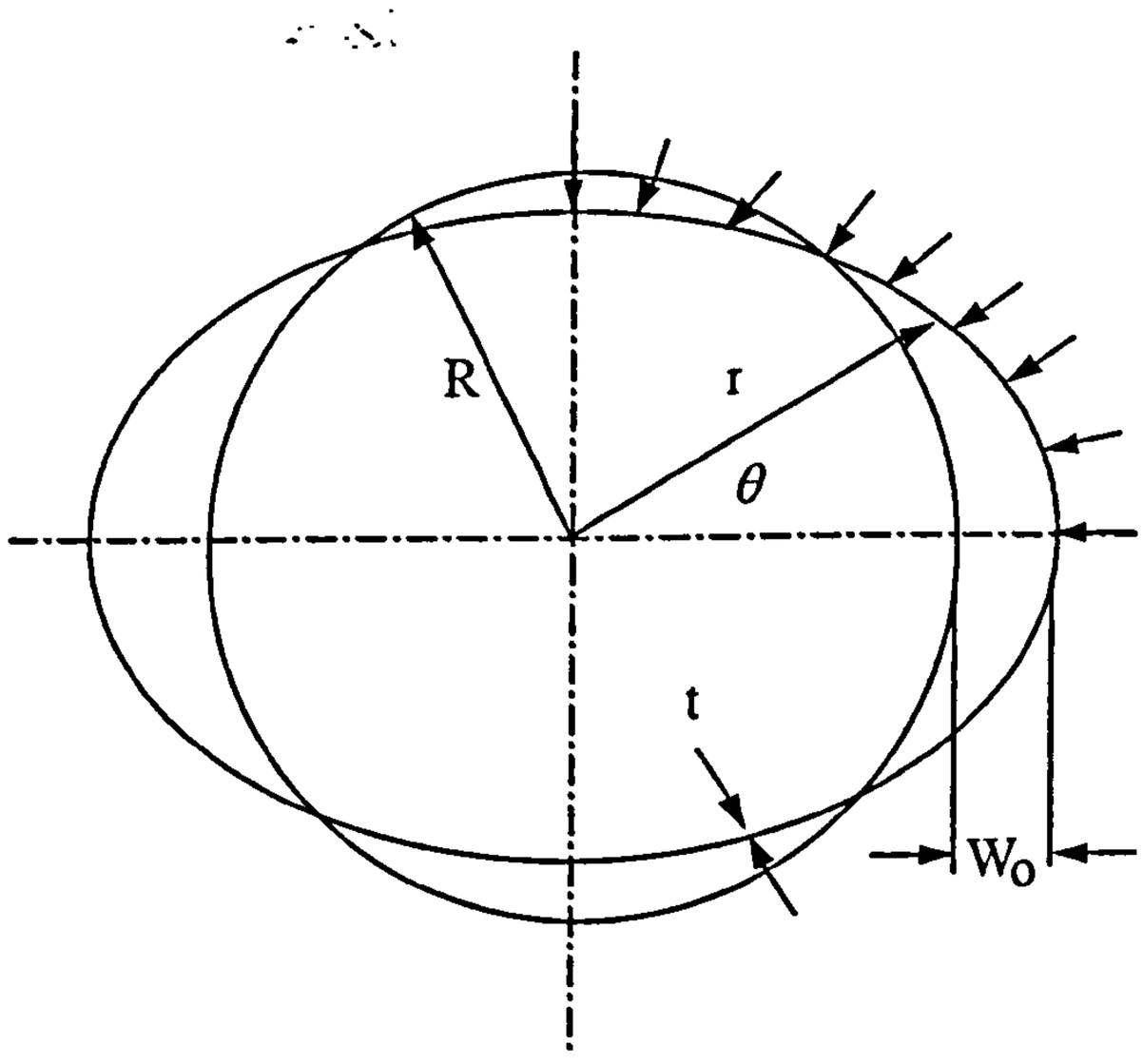

Fig. 5.5 Buckling pattern of an infinitely long casing

The ovality serves as a measure of the fluctuation in outside diameter over the cross section of a casing. In this thesis, ovality is defined by,

$$u = 2\frac{(D_{\max} - D_{\min})}{(D_{\max} + D_{\min})} \tag{5.24}$$

where u is the ovality parameter, while $D_{\max}$ and $D_{\min}$ are the maximum and minimum outside diameters respectively.

According to the API specification, the outside diameter of a casing is indicated to a tolerance of ± 0.75 percent, that is, the maximum permissible ovality amounts to 1.5 percent. Jasper and Sullivan (1931) presented a study on the effect of ovality on the collapse strength based on theoretical derivations. Their research concluded that, the

decrease in collapse strength does not depend only on the respective magnitude of the ovality itself, but also increases with augmenting D/t ratio.

Timoshenko and Gere (1961) recognised the importance of the initial ovality and derived an elastic collapse strength formula to include the effect of initial ovality as follows:

$$P_{ov} = \frac{4\sigma_y (t/D)}{\left(A + \sqrt{A^2 - 4B}\right)} \tag{5.25}$$

where P_{ov} is the collapse strength of a casing with initial ovality, and,

$$\begin{aligned} A &= 1 + 1.5u(t/D) + 2\sigma_y (t/D)/P_E \\ B &= 2\sigma_y (t/D)/P_E \\ P_E &= \frac{2E}{(1-\upsilon^2)}(t/D)^3 \end{aligned} \tag{5.26}$$

It is proposed (Nishioko et al, 1978, Hirakawa et al, 1980) that Equation (5.25) can be used to evaluate the plastic collapse strength of a casing with initial ovality.

On the basis of Timoshenko theory, Heise and Esztergar (1970) presented an equation for the calculation of the collapse strength of an oval casing as follows:

$$P = P_E \left(\frac{(A_1 + B_1)}{2} - \sqrt{\left(\frac{A_1 + B_1}{2}\right)^2 - B_1} \right) \tag{5.27}$$

with

$$\begin{aligned} A_1 &= 1 + 1.5u\frac{D}{t} \\ B_1 &= \frac{2\sigma_y}{P_E}\frac{t}{D} \end{aligned} \tag{5.28}$$

It is clearly evident (Timoshenko and Gere, 1961; Jurgens, 1973) that the collapse strength is most strongly influenced by the ovality in the elastic-plastic range. By means of a detailed comparison between nearly round casings with those exhibiting more pronounced ovality in the tests, Jurgens (1973) presented the following equation for assessing ovality:

$$P_{ov} = 1.1K\left\{(\sigma_y + EK^2 B_2) - \sqrt{(\sigma_y + EK^2 B_2) - 4EK^2 \sigma_y C_2}\right\} \tag{5.29}$$

where $K = \frac{t_{nom}}{D_{nom}}\psi$ and ψ denotes the fluctuation in wall thickness (eccentricity).

If the initial ovality is less than 0.005,

$$B_2 = 1 + \frac{2u}{3K}0.8065 - 0.0182$$
$$C_2 = 0.9818 \qquad (5.30a)$$

If the initial ovality is larger than 0.005,

$$B_2 = 1 + \frac{2u}{3K}0.4585 - 0.1404$$
$$C_2 = 0.8596 \qquad (5.30b)$$

For simplicity, the fluctuations in wall thickness are neglected here. That is, the coefficient ψ is set to unity. Except for values of the D/t-ratio at which the maximum reduction in collapse strength, depending on the material, calculations from Equation (5.29) exhibit a point of discontinuity in correspondence with the conditions expressed by (5.30a) and (5.30b) at an ovality value of 0.005. This gives rise to considerable differences in the collapse strength reduction. Hence, the application of Equation (5.30) is not advisable, especially since this range of ovality is relevant within the vast majority of commonly used casings.

In summary, many efforts have been conducted to investigate the effect of initial ovality and as a result, a number of equations have been proposed to quantify the reduced casing collapse strength due to initial ovality. However, care should be taken as some may give predictions with considerable error. Detailed review shows that it is possible to quantify the effect of initial ovality on the casing collapse strength by assessing those proposed equations and validation from the experimental data.

5.3.4 Eccentricity

Depending on the conditions prevailing during manufacture, casing can exhibit different values of the wall thickness over a cross sectional plane. This kind of imperfection is termed eccentricity, i.e. non-uniform wall thickness. The variation in

wall thickness usually depends on temperature distribution before piercing, piercing method, and to a lesser extent on the rolling operation (Assanelli et al, 1999). Eccentricity also varies with the ratio of outside diameter to wall thickness, decreasing as the ratio decreases. Experimental observations suggest that, the casing section consists of two eccentric circles as a result of piercing displacement during the manufacturing process as shown in Fig. 5.6. It can be clearly seen that the centres of inner and outside circles are not at the same point. The variation in wall thickness proceeds continuously from a minimum to a maximum on the opposite side. Therefore, the eccentricity parameter ψ is defined in this thesis as,

$$\psi = \frac{2(t_{max} - t_{min})}{(t_{max} + t_{min})} \tag{5.31}$$

where t_{max} and t_{min} denote the maximum and minimum wall thickness respectively.

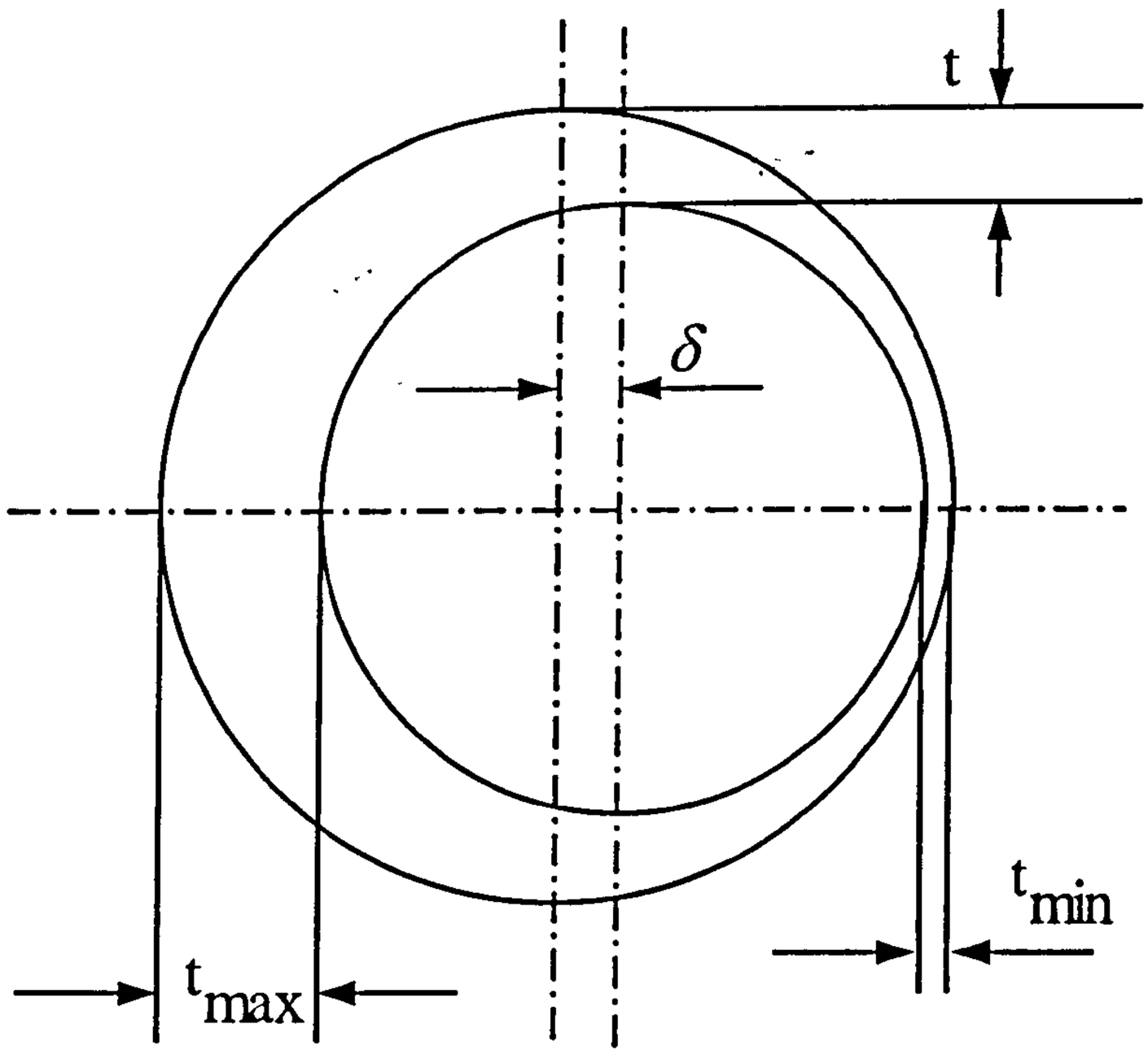

Fig. 5.6 Eccentricity of a casing

In contrast to burst failure due to excessive internal pressure, casing collapse is not governed by the weakest spot in the casing wall. Instead, the whole cross section of casing must be taken into consideration during collapse failure analysis (Geller, 1931). Thus, under some circumstances, a casing specimen whose wall thickness is locally below the permissible limit, but whose average wall thickness exceeds the

nominal thickness, is able to withstand a higher external pressure than the one with constant nominal wall thickness over the circumference. According to the API specifications, the permissible variation in the wall thickness of a casing is specified only by a negative tolerance of –12.5 percent.

On the basis of a theoretical investigation for determining the extent to which eccentricity influenced the collapse strength, Geller (1931) found that the decrease in collapse strength amounted to less than 2 percent for casing with a tolerance of –12.5 percent in the wall thickness. Another calculation leads to a very close result to Geller's, which has the following expression (Jurgens, 1973):

$$\Delta P = 210\xi^2 \tag{5.32}$$

where ξ denotes the relative deviation of the smallest wall thickness from the nominal value, $\xi = \frac{t_n - t_{\min}}{t_n}$ and ΔP is the reduction in collapse strength due to eccentricity. For a tolerance of –12.5 percent for the wall thickness ($\xi = 0.125$), a reduction of the collapse strength by 3.3 percent can be obtained from Equation (5.32).

For the calculation of plastic collapse strength of a casing with initial eccentricity, the following equation was proposed (Tokimasa and Tanaka, 1986):

$$P_{ec} = P_p\left(1 - \frac{\psi}{2}\right) \tag{5.33}$$

where P_{ec} is the collapse strength with eccentricity. It is noted that

$$P_p = Min\left(\frac{2\sigma_y t}{D}, 2\sigma_y \frac{D/t - 1}{(D/t)^2}\right) \tag{5.34}$$

According to the investigations conducted by Kanda et al (1983) and Mimura et al (1987), the effect of variation in wall thickness could be calculated with the use of the following equation:

$$P_{ec} = P_{cr0}\left\{1 - \left(1 - \frac{1}{2(1 - t/D)}\right)\psi\right\} \tag{5.35}$$

Here P_{cr0} represents the collapse strength of the perfect round casing without eccentricity.

In practice, however, it is difficult to separate the effect of eccentricity on the collapse strength from the considerably greater influence of the ovality. Therefore, efforts will focus on accurately understanding the effect of eccentricity. As a result, the numerical simulation of casing with eccentricity alone will be performed for this purpose.

5.3.5 Residual Stress

In the course of the manufacturing processes, residual stress may remain in the casing body as a result of non-uniform, mechanically or thermally induced deformations during individual production steps such as rolling, quenching, tempering and straightening. Such residual stresses may occur as tensile or compressive stresses over the whole or part cross section. If the stresses induced by external forces are superimposed on the residual stresses, the presence of the latter can be either favourable or detrimental with respect to the overall load bearing capability of the casing, depending on the imposed stresses. In general, it is believed that, compressive residual stresses in the casing decrease the collapse strength, while tensile residual stresses give rise to an increase of collapse strength. The opposite is true of the resistance to the internal pressure. Since casing must be optimally manufactured to withstand all kinds of loads in practice, it is expected that the residual stress be kept as low as possible, and usually this can be accomplished by keeping the eccentricity small, by hot straightening, and possibly by stress-relief heat treatment, or a combination of the latter (Kanda et al, 1983; Mimura et al, 1987).

Frame (1938) examined the residual stresses on 122 collapse test specimens by means of the slit-ring method. For this purpose, rings of 1 to 1.5 inches (25.4 mm to 38.1 mm) in length were cut in the axial direction after the designation of measuring points in each casing, and the gap width due to the opening or closing of the slit was measured. For the calculation of the residual stress, $\sigma_{\theta R}$, the following equation was employed, under the assumption of a linear distribution of stress over the wall thickness,

$$\sigma_{\theta R} = \frac{a}{4}\frac{tE}{\pi R^2} \tag{5.36}$$

where, a and R were measured as shown in Fig. 5.7.

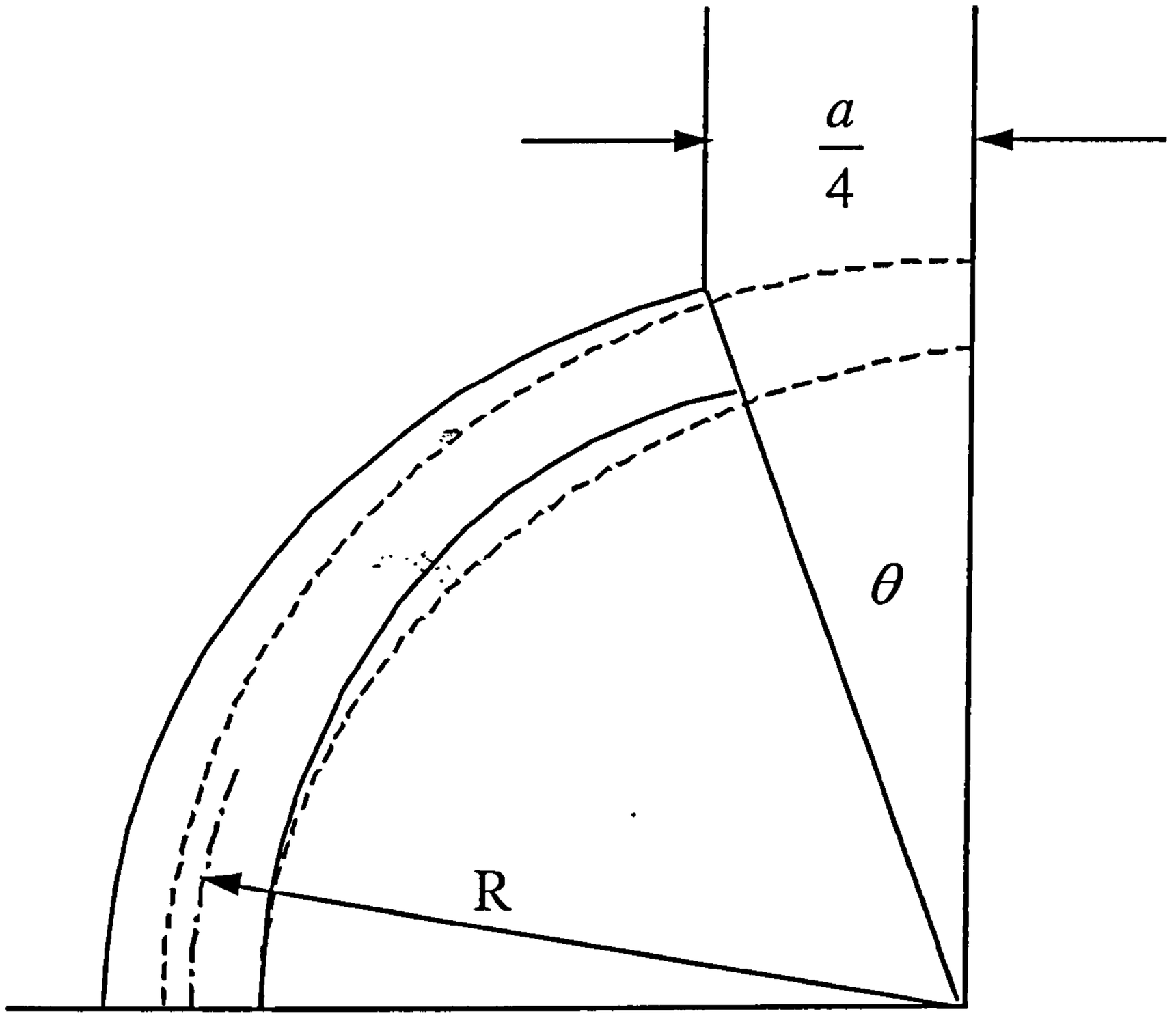

Fig. 5.7 Determination of residual stress (Frame, 1938)

Tamano (1982) provided another calculation for the circumferential residual stress at the inside surface of test casings as

$$\sigma_{\theta R} = \frac{E}{1-\upsilon^2} \frac{t(D_b - D_f)}{(D_b - t)(D_f - t)} \tag{5.37}$$

The suffixes b and f here correspond to before and after longitudinal slit cutting, respectively. It is noted that the length of the specimen in the test is predetermined at 2.5 times the casing outside diameter.

A better method of determining the residual stress is shown in Fig. 5.8 (Nippon Steel Corporation report, 1979). The annular cross sectional area of a ring specimen is continuously decreased by means of stepwise reaming of the internal diameter. The deformations, ε_a and ε_t, which thereby occur in the axial and tangential directions, are measured. In particular, the residual tangential stress is determined by:

$$\sigma_{\theta R} = \frac{E}{1-\upsilon^2}\left[(A_0 - A_2)\frac{d\varpi}{dA_2} - \frac{A_2 + A_0}{2A_2}\varpi\right] \tag{5.38}$$

where d_b is the drilled internal diameter, d is the inner diameter, and

$$A_0 = d^2(\frac{\pi}{4})$$

$$A_2 = d_b^2(\frac{\pi}{4}) \tag{5.39}$$

$$\varpi = \varepsilon_t + \upsilon\varepsilon_a$$

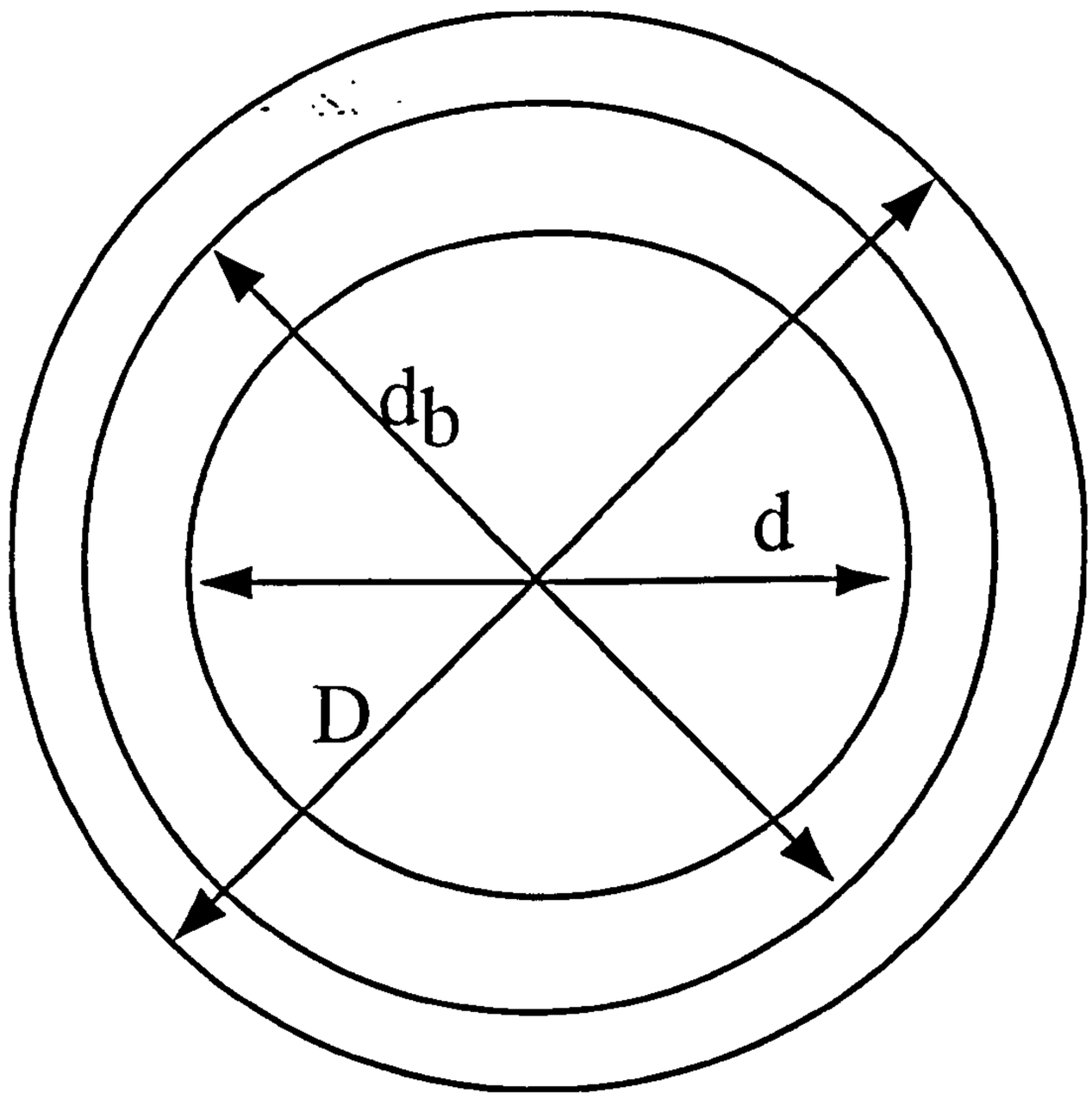

Fig. 5.8 Determination of the residual stress (Nippon Steel, 1977)

The residual stresses remaining in the casing section have been investigated by Nippon Steel after manufacturing processes such as quenching, tempering, straightening with different degrees of deformation and subsequent stress relief. This is a notable contribution to the problem as the distributions of residual stress over the casing wall thickness for variously treated casing specimens are obtained as shown in Fig. 5.9 (Nippon Steel Corporation report, 1979). It is found that, locally high residual compressive stress generated by extreme cold straightening is detrimental to the collapse strength.

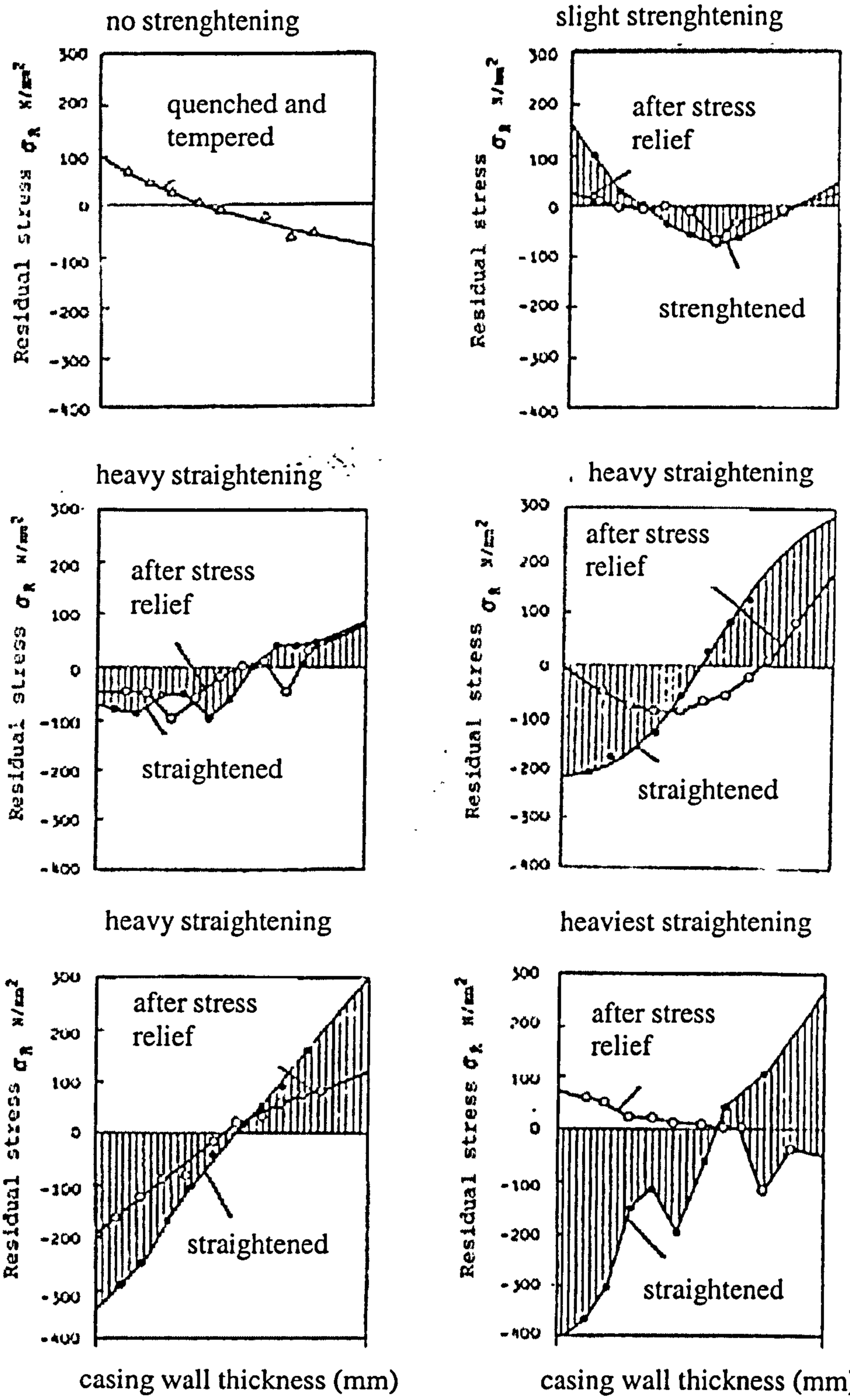

Fig. 5.9 Distribution of residual stresses over the casing wall (Nippon Steel, 1977)

In contrast to Nippon Steel's investigation, it is reported in the literature (Yeh and Kyriakides, 1986; Bai et al, 1993; Issa et al, 1993) that the residual stress has no effect at all on the casing strength in the fully elastic collapse region and the fully plastic region. Even in the elastic plastic transition region, the effect of residual stress is very small and could normally be neglected.

The mechanism of how residual stress affects the collapse strength of casings may be described as follows. The stress that is caused in the casing by the loading of external pressure is mainly compressive in the circumferential direction. It is at a maximum at the inside surface and decreases toward the outside surface. The equivalent stress becomes a maximum at the inside surface when there is no residual stress, therefore, yielding first starts at the inside surface. When there is a compressive residual stress in the inside surface, the equivalent stress in the inside surface further increases and yielding originates at a lower external pressure. When there is a tensile residual stress, it can offset the difference in equivalent stress between the inside and outside surface. Therefore, yielding may start simultaneously at both inside and outside surfaces at a higher external pressure.

In summary, manufacturing processes, which do not involve annealing, will leave residual stresses in the casings. For example, all of the specimens tested by Yeh and Kyriakides (1988) were found to have residual stresses. The amount and the distributions of residual stress depend on the type of manufacturing process involved. It is widely believed that the residual stress will weaken the casing. The question as to what extent the residual stress may reduce the collapse strength is still debatable. Therefore, it is necessary to clarify the effect of residual stress on the casing collapse strength.

5.3.6 Material Work Hardening

It is generally known from experimental evidence that during the process of incremental plastic deformation, the loading surface changes size, shape, and location. A rule governing this aspect of behaviour, that defining the manner of constructing the subsequent loading surface, is called the hardening rule. Mathematically,

hardening is characterized by parameters, which vary with the plastic load history. The hardening parameter may vary in form from material to material. The choice of a specific hardening rule depends primarily on the case with which it can be applied and its ability to represent the hardening behaviour of a particular material. Work hardening defines the way the yield surface changes with plastic straining (Johnson and Mellor, 1972).

In general, three possible hardening rules are commonly used in the analysis of casing collapse. These are perfect plasticity, isotropic hardening and kinematic hardening. Perfect hardening means that the yield stress does not change with plastic strain. For an elastic-perfectly-plastic material, deformation can increase unboundedly without any additional load after the yield stress is reached. Tamano (1983) assumed an elastic-perfectly-plastic material model in the investigation of casing collapse. The elastic perfectly plastic material behaviour is expressed by,

$$\begin{aligned} \varepsilon &= \frac{\sigma}{E} && for \quad \sigma < \sigma_E \\ \varepsilon &= \frac{\sigma}{E} + \gamma && for \quad \sigma = \sigma_E \end{aligned} \tag{5.40}$$

where γ is a positive scalar and σ_E is the elastic proportional limit.

However, as a perfect plastic material is an idealised material, it is only a very rough approximation to the actual casing material behaviour. Two improved hardening models have been proposed to evaluate the effect of hardening behaviour of a casing material on the plastic collapse strength by Tokimasa and Tanaka (1986). These are the elastic-linear hardening and elastic-exponential hardening models. In mathematical form, the elastic-linear hardening model can be expressed as,

$$\begin{aligned} \varepsilon &= \frac{\sigma}{E} && for \quad \sigma \le \sigma_E \\ \varepsilon &= \frac{\sigma_E}{E} + \frac{(\sigma - \sigma_E)}{E_l} && for \quad \sigma > \sigma_E \end{aligned} \tag{5.41}$$

where E_l is the slope of the idealized manner of the hardening range, the value of which is normally smaller than the Young's modulus, E. As an extension to this model, a piecewise-linear model consisting of several line segments may be constructed. The elastic-exponential hardening model is given by,

$$\begin{aligned} \sigma &= E\varepsilon \qquad for \quad \sigma \le \sigma_E \\ \sigma &= k\varepsilon^n \qquad for \quad \sigma > \sigma_E \end{aligned} \tag{5.42}$$

where k and n are material constants determined by best fit of an experimentally obtained stress-strain relationship. It is noted that these two material constants are not independent because the stress-strain curve must be continuous at $\sigma = \sigma_E$, thus the condition $\sigma_E = k(\sigma_E / E)^n$ must be satisfied.

Tokimasa and Tanaka (1986) assumed that, the effects of the coefficient E_l of the linear-hardening law and the exponent n of the exponential hardening on the plastic collapse strength were as follows:

$$P_{sh} = 2\sigma_E \frac{D/t - 1}{(D/t)^2} f(E_l) \tag{5.43}$$

$$P_{sh} = 2\sigma_E \frac{D/t - 1}{(D/t)^2} g(n) \tag{5.44}$$

Detailed finite element analysis gave:

$$f(E_l) = 1 + 7.7 \times 10^{-5} E_l \tag{5.45}$$

$$g(n) = 1 + 0.231\, n^{1.3} \tag{5.46}$$

The ranges of E_l and n for the above equations were given (Tokimasa and Tanaka, 1986),

$$\begin{aligned} &5000 \le E_l \le 12000 MPa \\ &40000 \le E_l \le 80000 MPa \\ &0.05 \le n \le 0.12 \\ &0.3 \le n \le 0.4 \end{aligned} \tag{5.47}$$

Different to Tokimasa and Tanaka (1986), Assanelli et al (1998) assumed a bilinear material hardening model by considering the yield stress σ_y to be independent of E_l. In order to explore different hardening ranges, three values for the constant tangential modulus were considered by Assanelli et al (1998), i.e. E_l equal to 0.0 (perfect plasticity), $E_l = 0.057E$, and $E_l = 0.10E$. The numerical results are summarized in Table 5.1. Assanelli et al (1998), therefore, concluded that the strain hardening of the

casing material did not play an important role in the determination of casing collapse strength.

Isotropic hardening material behaviour is used very commonly for metal plasticity calculations because of its particular simple form. Isotropic hardening means that the yield surface changes size uniformly in all directions, so that the yield stress increases (or decreases) in all stress directions as plastic straining occurs. This hardening model was used in the derivation of the Issa equation for casing collapse (Issa and Crawford, 1993). As a result, the effect of the isotropic strain hardening on the collapse strength was taken into account implicitly in the derivation.

Table 5.1 Work hardening effect on casing collapse strength (Assanelli et al,1998)

D/t	Ovality (%)	Collapse Strength (Mpa)		
		E_t=0.0	E_t=0.057E	E_t=0.10E
17.66	0.75	611	614	616
17.66	0.35	684	686	688
24.37	0.75	272	272	272
24.37	0.35	296	297	297

Furthermore, Bai et al (1993,1995 and 1997) employed an isotropic hardening rule in the analysis of casing collapse, which has the particular stress-strain relationship of

$$\begin{aligned} \sigma &= E\varepsilon && \varepsilon \le \varepsilon_{ly} \\ \sigma &= \sigma_{ly}\left(\frac{nE\varepsilon}{\sigma_{ly}} + 1 - n\right)^{\frac{1}{n}} && \varepsilon > \varepsilon_{ly} \end{aligned} \tag{5.48}$$

where σ_{ly}, ε_{ly} and n are linear stress limit, linear strain limit and strain-hardening parameter respectively.

If many strain reversals take place, the modelling of the Baushinger effect associated with these reversals is important. Therefore, the kinematic hardening rule may be used. In this model, the yield surface stays the same size in stress space, but moves around, thus modelling the strain induced anisotropy in the material to a limited extent. Assuming a large deflection-large strain class of kinematics, which incorporates the "plane sections remain plane" assumption, Yeh and Kyriakides (1986) investigated the material hardening parameter on the collapse strength of

casings. It is noted that in this analysis, the constitutive material behaviour is fitted to a three-parameter, Ramberg-Osgood model from the experimental tests as follows:

$$\varepsilon = \frac{\sigma}{E}\left[1+\alpha\left(\frac{\sigma}{\beta}\right)^{n-1}\right] \tag{5.49}$$

where α and β are material constants.

In summary, the material hardening behaviour will effect the collapse strength of casings. The question of how much the effect of the material hardening parameter has on the collapse strength remains unsolved. It is proposed by Assanelli et al (1998) that the effect of material hardening may be neglected. However, his conclusion is based on the assumption of an elastic linear hardening rule, which is too simple to represent the actual material hardening behaviour of a casing. Besides, the effect of ovality is not excluded from the analysis as seen from Table 5.1. It is quite possible that the effect of the material hardening parameter on the collapse strength may be cancelled by the effect of the initial ovality. Therefore, further investigations are necessary to clarify the effect of material hardening on the casing collapse strength. As the stress-strain relationship is very crucial for an accurate prediction of the collapse strength of a casing under external pressure, it is important that a general form of material hardening behaviour can be found to represent the actual casing material behaviour. A possible method is to find the best-fit curve of the experimental stress-strain relations for the majority of casings.

5.3.7 Material Anisotropy

Many of the thick walled casings are drawn, and many of the plates used for welded casings are rolled. These manufacturing processes tend to induce material anisotropy. The presence of material anisotropy was well proved by experiments (Yeh and Kyriakides, 1988). Generally, the effect of material anisotropy is more pronounced in the plastic range (Hill, 1950). However, the influence of material anisotropy is ignored by most of the researchers in this field.

Theories describing the anisotropic material behaviour were proposed a long time ago (Hill, 1950). All metals exhibit anisotropy to a greater or lesser degree when deformed at room temperature. The mechanical properties of the metal vary in different directions, the amount and type of anisotropy are characteristic of the mechanical and heat treatments applied in manufacturing processes. Hill's anisotropic plasticity potential is simply defined in ABAQUS, consisting of ratios of yield stress in different directions with respect to a reference stress. The purpose of this review is to provide the mathematical relationship necessary to convert the strain ratios to stress ratios that can be input into ABAQUS. In general, Hill's potential function is a simple extension of the von Mises function to allow anisotropic behaviour, which is expressed as

$$f(\sigma)=\sqrt{F(\sigma_y-\sigma_z)^2+G(\sigma_z-\sigma_x)^2+H(\sigma_x-\sigma_y)^2+2Q\tau_{yz}^{\ 2}+2M\tau_{zx}^{\ 2}+2N\tau_{xy}^{\ 2}} \quad (5.50)$$

In terms of rectangular Cartesian stress components, where F, G, H, Q, M, N are constants obtained by tests of the material in different directions. They are defined as:

$$\begin{aligned}
F &= \frac{\sigma_0^{\ 2}}{2}\left(\frac{1}{\sigma_{22}^2}+\frac{1}{\sigma_{33}^2}-\frac{1}{\sigma_{11}^2}\right)=\frac{1}{2}\left(\frac{1}{R_{22}^2}+\frac{1}{R_{33}^2}-\frac{1}{R_{11}^2}\right)\\
G &= \frac{\sigma_0^{\ 2}}{2}\left(\frac{1}{\sigma_{33}^2}+\frac{1}{\sigma_{11}^2}-\frac{1}{\sigma_{22}^2}\right)=\frac{1}{2}\left(\frac{1}{R_{33}^2}+\frac{1}{R_{11}^2}-\frac{1}{R_{22}^2}\right) \qquad (5.51a)\\
H &= \frac{\sigma_0^{\ 2}}{2}\left(\frac{1}{\sigma_{11}^2}+\frac{1}{\sigma_{22}^2}-\frac{1}{\sigma_{33}^2}\right)=\frac{1}{2}\left(\frac{1}{R_{11}^2}+\frac{1}{R_{22}^2}-\frac{1}{R_{33}^2}\right)
\end{aligned}$$

and

$$\begin{aligned}
Q &= \frac{3}{2}\left(\frac{\tau_0}{\tau_{23}}\right)^2=\frac{3}{2R_{23}^2}\\
M &= \frac{3}{2}\left(\frac{\tau_0}{\tau_{13}}\right)^2=\frac{3}{2R_{13}^2} \qquad (5.51b)\\
N &= \frac{3}{2}\left(\frac{\tau_0}{\tau_{12}}\right)^2=\frac{3}{2R_{12}^2}
\end{aligned}$$

Where σ_0 is the reference yield stress specified in the *PLASTIC option in an input file, R_{11}, R_{22}, R_{33}, R_{12}, R_{13}, and R_{23} are anisotropy yield stress ratios

($R_{11} = \frac{\sigma_{11}}{\sigma_0}, R_{22} = \frac{\sigma_{22}}{\sigma_0}$, and so on), which are specified in the *POTENTIAL option, and $\tau_0 = \sigma_0/\sqrt{3}$.

From the experiment conducted by Yeh and Kyriakids (1986 and 1988), the casing material was found to have a lower yield stress in the circumferential direction than the one measured in the axial direction. This characteristic of the anisotropy distinguishes it from the normal anisotropy, which is known to exist in rolled metal sheets and to affect sheet metal forming. An experimental method was developed for establishing the parameters, which sufficiently described the anisotropy present in metal casings (Kyriakids and Yeh, 1988). Therefore, the degree of material anisotropy can be quantified if Hill's definitions of equivalent stress and yield function for anisotropic materials are adopted. It is assumed that the yield stresses of the material in the circumferential and thickness directions are the same but different from the yield stress in the axial direction. Under these conditions, the material anisotropy parameter λ can be quantified (Yeh and Kyriakids, 1986 and 1988) by:

$$\frac{\lambda+1}{2} = \left(\frac{\sigma_x}{\sigma_s}\right)^2 \tag{5.52}$$

where σ_x and σ_s are the yield stresses in the axial and circumferential directions respectively.

Once the appropriate value of material anisotropy is established, it can be used in the FE analysis for a more accurate estimate of the collapse strength of casings. Limited initial studies of the material anisotropy on the casing collapse strength performed by Yeh and Kyriakids (1988) showed that, $\lambda > 1$ leads to a reduction of the collapse strength, while $\lambda < 1$ leads to an increase of the collapse strength. Another work (Bai et al, 1997) investigated the material anisotropy on the collapse strength envelope, and concluded that a higher material anisotropy led to a higher collapse envelope.

In summary, material anisotropy will directly affect the collapse strength of a casing. However, current research on this factor is insufficient. It is therefore, necessary to quantitatively clarify the effect of material anisotropy since most of casings have varying amounts of material anisotropy.

5.4 Casing Collapse Test Database

As pointed out in the previous sections, the collapse strength of steel casings is affected by a number of parameters. One of the main objectives of this research is to accurately predict the collapse strength of a given casing if these parameters are carefully measured and provided in the numerical simulation. As a result, along with the physical testing, accurate measurement must be performed to document the test itself as well as to feed numerical models. In application, the accuracy and reliability of any proposed numerical model must be validated by the experimental data. Therefore, a casing collapse test database is necessary before any numerical simulation can be discussed. In order to provide such a database, test data from available literature were collected and selected for this study.

All of the data was obtained from full-scale casing collapse testing. The first source reported is from Clindinst (1977), for 2488 collapse tests on three grades of casing, K55, N80 and P110, conducted in the early 1960's. The majority of casing specimens in these tests had D/t ratios between 12 and 25, common values for oil field tubular goods. Although the diameter, wall thickness, specimen length, yield stress, and ultimate tensile stress of tested casings were reported, the ovality was not measured. It is important to note that, the test specimens (Clindinst, 1977) have a small length to diameter ratio of 2. Therefore, those data were discounted as unrepresentative and were not selected in the final collapse test database for the validation of the finite element analysis in this study.

A significant number (2083) of collapse tests (Ju et al, 1998; Adams et al, 1998) have been conducted over the years since the Clindinst (1977) data were reported. The tests provided a fairly good representative basis for casing collapse. However, they are not available because of company confidential policy. The database constructed to validate the FE analysis in current study is based on the following sources:

- Full scale casing collapse tests conducted by Nishioko et al (1978), Hirakawa and Tokimasa (1980).
- Full scale casing collapse tests conducted by Krug (1983).

- Full scale casing collapse tests conducted by Yeh and Kyriakides (1986 and 1988).

Krug (1983) performed over 400 tests of steel casing grades with various dimensions, of which 97 long specimens ($L/D>8$) were subjected to external pressure only. Another 80 tests were provided by Nishioka et al (1978), Hirakawa and Tokimasa (1980), of which 28 long specimens were selected. In addition, 8 long specimen tests were provided by Yeh and Kyriakides (1986 and 1988). The D/t ratios of these selected test specimens in the database cover from 10 to 40, with casing grades from H40 to V150. The outside diameters of the selected test specimens range from 1 inch (25.4 mm) to $13\frac{3}{8}$ inches ($339.\dot{7}$ mm). Furthermore, the ovality parameter ranges from 4×10^{-4} to 1.18×10^{-2}, while eccentricity varies between 1.7×10^{-2} and 23.4×10^{-2}. From the variations of these important parameters, the selected test data have a very good representative basis for the real casings. Therefore, these 133 tests comprise the collapse test database for this study to validate the finite element analysis. They have been used to evaluate and calibrate the potential collapse design equations used in the limit state casing design analysis of this study. The detailed collapse test data are listed in Appendix 1.

5.5 Numerical Analysis Of Casing Collapse

The problem of casing collapse is a complicated system governed by highly non-linear equations for the stress, strain and displacement because of the large deformation and material non-linearity. To make it worse, casing collapse strength is sensitive to geometrical imperfections. In this study, finite element analysis is performed using ABAQUS (1998), which allows accurate modelling of material non-linearity (plasticity) and geometric non-linearity (large deformation). To obtain an accurate modelling of material plasticity and large deformation, a Newton-Raphson solution technique is used to solve the non-linear equations. To prevent possible artificial locking in the calculation of stiffness matrices, a reduced integration

technique is employed in the FE program. During the simulation, a uniform pressure is applied to the faces of the elements on the outside diameter of the casing section. The line direction of the applied pressure changes as the casing section deforms and the pressure is increased incrementally. A modified Riks algorithm is employed to carefully control the external pressure to the ultimate load. Following the maximum external pressure, the program automatically reduces the external pressure so that the collapse simulation can be continued. In this way, the post collapse behaviour of a casing can be investigated, and the ultimate collapse strength can be obtained.

It is noted that true stress and true strain, instead of engineering stress and strain, are used in the simulation and no approximation is made in formulating the non-linear equations of the casing collapse problem. As normally the ratio of casing length to outside diameter is greater than 8, the effect of end restraint can be neglected. Therefore, the problem of casing collapse is dramatically simplified to a case of a plane strain problem and only one element is necessary in the longitudinal direction. The above procedures enable the FE programs to accurately model the collapse behaviour of a casing under external pressure.

5.5.1 Modelling Of Geometric Imperfections

The importance of initial imperfections, such as ovality and eccentricity, was well recognized long before (Timoshenko, 1933). In fact, casing collapse is an instability type of failure and sensitive to these imperfections. Casing collapse strength can be dramatically reduced even when only small imperfections are present. The Riks method is developed to solve this type of instability problem, and a modified Riks method is implemented in ABAQUS. However, the exact post collapse behaviour usually cannot be analyzed directly due to the discontinuous response (bifurcation) occurring at the point of collapse. In order to investigate completely the casing collapse behaviour in the simulation, it must be transformed into a problem with a continuous response instead of a bifurcation. This is accomplished by introducing a very small (in reference to a magnitude of imperfection presented in an ordinary casing) geometric imperfection pattern to the perfect geometry so that there is some

response in the collapse mode just before the critical collapse load is reached. Without this imperfection, the collapse process would not occur and the casing section would deform uniformly in the simulation. Kyriakides and Babcock (1981) clearly demonstrated that, the presence of initial geometric imperfections transformed the problem of casing collapse from one governed by bifurcation instability to one which exhibited a limit load instability. Thus, the ultimate casing collapse strength can be determined accurately and uniquely because no bifurcation occurs with the presence of a small initial imperfection. As a result, the problem left is to solve how to superimpose the geometric imperfection pattern into the finite element program.

For the casing with a ratio of length to outside diameter greater than 8, a lobe number of 2 is assured. For this particular case of lobe number of 2, the casing collapse shape pattern is assumed (refer to Fig. 5.5)

$$w_i(\theta) = w_0 \cos 2\theta \tag{5.53}$$

According to the definition of initial ovality,

$$u = \frac{2(D_{\max} - D_{\min})}{D_{\max} + D_{\min}} = \frac{2(D_0 + 2w_0 - D_0 + 2w_0)}{2D_0} = \frac{4w_0}{D_0} = \frac{2w_0}{R} \tag{5.54}$$

Therefore, the initial ovality u can be constructed by the following expression,

$$r = R + w(\theta) = R\left[1 + \frac{u}{2}\cos(2\theta)\right] \tag{5.55}$$

where r is the imperfect casing radius, R is the nominal perfect casing radius, u is the initial ovality and θ is the angular coordinate measured from the centre of the casing as shown in Fig. 5.5.

Actual wall thickness of a casing varies along the circumference. Experimental observations suggest that the casing section be idealised as two eccentric circles as shown in Fig. 5.6. The maximum and minimum wall thickness can be determined, with $t_{\max} = t + \delta$ and $t_{\min} = t - \delta$ respectively. Therefore, the eccentricity parameter ψ is introduced into the FE simulation of casing collapse by:

$$\psi = \frac{2(t_{\max} - t_{\min})}{t_{\max} + t_{\min}} = \frac{2(t + \delta - t + \delta)}{(t + \delta + t - \delta)} = \frac{2\delta}{t} \tag{5.56}$$

where δ is the distance between the centres of inner and outside circles and t is the nominal wall thickness as shown in Fig. 5.6.

It is assumed that all of the geometrical variables involved in the analysis are uniform as it is found that the geometric variables and imperfections do not substantially vary along the casing length (Yeh and Kyriakides, 1988). The imperfections are introduced to allow the collapse to occur, although they may not be plainly visible.

In general, ABAQUS introduces the imperfections by perturbations in the geometry. Possible ways to define an imperfection in ABAQUS are available either as a linear superposition of buckling eigen-modes, from the displacements of a *STATIC analysis, or by specifying the node number and imperfection values directly on the data lines. ABAQUS will then calculate the normals using the standard algorithm based on the perturbed coordinates. Unless the precise shape of an imperfection is known, an imperfection consisting of multiple superimposed buckling modes can be introduced in this way. Usually the approach involves a two-stage-analysis run with the same model definition. In the first analysis, an eigen-value buckling analysis is performed on the perfect structure to establish probable collapse modes and to verify that the mesh discretizes those modes accurately. The eigen-modes are written in the default global system to the result file using the *NODE FILE option with the GLOBAL=YES (default) parameter.

In the second analysis, an imperfection in the geometry is introduced by adding these buckling modes to the perfect geometry using option *IMPERFECTION in an ABAQUS input file. The lowest buckling modes are assumed to provide the most critical imperfections, so that usually these are scaled and added to the perfect geometry to create the perturbed mesh. The imperfection thus has the following form,

$$\Delta w_i = \sum_{i=1}^{M} Q_i \Phi_i \tag{5.57}$$

where Φ_i is the i^{th} mode shape and Q_i is the associated scale factor. Usually the lowest buckling mode has the largest factor. In addition, magnitudes of the perturbation used are typically a few percent of a relative structural dimension such as a beam cross section or a shell thickness.

After some imperfections are introduced, collapse analysis of a structure can be performed using the Riks method. However, the eccentricity and ovality imperfection

cannot be modelled simultaneously using the imperfection generation options within ABAQUS. It can be easily seen that there is an analogy relationship between Equations (5.53) and (5.57), because Equation (5.53) comes directly from critical collapse mode shape. Thus, the ovality can be easily implemented using option *IMPERFECTION in ABAQUS. However, the eccentricity assumption comes from experimental observation, which is hardly linked with the collapse mode shape. It is thus, impossible to model both ovality and eccentricity imperfections simultaneously using option *IMPERFECTION in ABAQUS. Fortunately, ABAQUS provides another option, which enables the ABAQUS input file to read node coordinates directly from an external file. Therefore, a Fortran program was written to construct the finite element model with the desired geometrical imperfections using Equations (5.55) and (5.56). The code is listed in Appendix 2. The generated data with imperfections are read directly into the input file. In this way, the casing section can be modelled with outside diameter D, wall thickness t, initial ovality u and eccentricity ψ simultaneously.

5.5.2 Element And Mesh Studies

A right element and a suitable mesh density are extremely important for a finite element analysis. The correct choice of elements for a particular problem is vital because the formulation and order of integration used in a particular element can have a very significant effect on the accuracy and cost of the analysis, especially for a highly non-linear casing collapse problem. In addition, the numerical accuracy of the FE result depends on the mesh used. A suitable mesh density can be important in computational efficiency as well as convergence. Generally, element type and mesh density studies are necessary to ensure that the proposed FE model provides an accurate but unique solution to a problem. However, a converged mesh does not necessarily ensure that the result from a finite element analysis will match the actual behaviour of the physical problem, which also depends on other approximations and idealizations made in the FE model. For casing collapse in this study, detailed element type and mesh density studies are performed to eliminate the element type and mesh

density dependencies in the finite element simulation. Practical criteria for selecting a right element and a suitable mesh density are accuracy and computational efficiency as well as convergence on the basis of a series of comparisons with casing collapse test data.

Several element types for a finite element analysis have been proposed for casing collapse in the literature. For example, Assanelli et al (1998) used a 9-node shell element within the FE package ADINA. Bai et al (1993, 1995 and 1997) studied casing collapse problems by an 8-node isotropic shell element in ABAQUS. Issa and Crawford (1993) employed a second order, isotropic, generalized plane strain continuum element in the derivation of a new collapse design equation. In addition to these elements available in different finite element codes, new elements have also been developed for the modelling of casing collapse. An example is the 4-node quadrilateral QMITC shell element, which was developed and used in the modelling of casing collapse by Assanelli et al (1999).

The element type used in the current study focuses on the shell and continuum element in the ABAQUS element library. According to the guidelines within ABAQUS, a 10-node biquadratic quadrilateral generalized plain strain element CGPE10R, an 8-node biquadratic plain strain element CPE8R, an 8-node biquadratic plain stress element CPS8R, and an 8-node doubly curved thick shell element S8R are chosen as candidate elements in this element study. As reported by Assanelli et al (1999), for a 2D simulation of casing collapse, the actual collapse test is dominated neither by a case of plane strain nor by a plane stress model. The absence of longitudinal restraint imposes a plane stress situation at the sample edge, while the length of the test sample ($L/D > 8$) approximates a plane strain situation at its centre. Therefore, the general plane stress element CPS8R is included in the element study to determine, which assumption, either plane strain or plane stress, better describes the actual behaviour of casing collapse. In addition, different mesh densities are employed to determine a suitable mesh generation pattern in terms of accuracy and efficiency.

Because of the crucial effect of the material inelasticity on the accurate prediction of casing collapse strength, this element study should be able to eliminate its influence in the comparisons. An assumption of an elastic-perfectly-plastic material in the element study will help to eliminate the material inelasticity effect. Thus, test samples with an almost perfect plastic material response are required. For this purpose, one of the test

specimens (Yeh and Kyriakides, 1988) was specially chosen for the validation data. It was reported that the material property of this test specimen exhibited an upper and lower yield point followed by an almost perfectly plastic response. The measured material and geometric parameters of the specimen are summarised in Table 5.2. These parameters are used to generate the imperfect geometry of the specimen in the element type study. Different numbers of layer across the thickness of the casing are generated, and different numbers of element around the casing circumference are designed for each candidate element. Predictions from the element type and mesh studies are compared and summarized in Table 5.3.

Table 5.2 Specification of test specimen in the element study

Material	D_{nom} (mm)	t_{nom} (mm)	D_{actual} (mm)	t_{actual} (mm.)	D/t	E (MPa)	σ_{API} (MPa)	λ	P_{test} (MPa)
X-42	101.6	3.556	101.6	3.645	27.87	204.06	330.91	1.3	18.75

From the element study, the best prediction is obtained using the generalized plane strain element CGE10R in comparison with the experimental collapse strength. If the prediction error is defined by,

$$\text{Prediction Error} = \frac{(P_{FEM} - P_{test})}{P_{test}} \tag{5.58}$$

The element type and mesh studies have found that, predictions from the ordinary plane strain element are higher than the test results (with a maximum error of 4.7%), while predictions from the ordinary plane stress element are smaller than the test collapse strengths (with a maximum error of –6.1%). A very conservative prediction can be obtained if using a shell element. The results predicted from the normal plane strain and plane stress elements in this element study are basically in accordance with the output from the literature (Assanelli et al, 1999), where a general error level between–20% to +5% was reported for a prediction from the plane strain element, and a error level of –25% to –5% for the plane stress circumstance. This may be explained as follows.

The imperfection measurement for the test specimen, such as ovality and eccentricity, are usually reported for the middle section in the experiments, while the imperfection patterns of the middle section may not be fully representative of the sample geometry.

As a result, disagreement exists between numerical and experimental results. In particular, the numerical prediction may be greater or smaller than the experimental collapse strength, if the imperfections of the middle section are more severe or less than the weakest section in the test sample.

Table 5.3 Summary of element type and mesh studies

Element Type	Element number Per layer	Predicted collapse pressure P_{FEM} (MPa)		
		Layer Numbers		
		3	5	7
CGPE10R	100	18.86	18.86	18.87
	50	18.85	18.85	18.86
	20	18.84	18.90	18.86
	10	18.95	18.90	18.88
CPE8R	100	19.54	19.57	19.57
	50	19.54	19.57	19.54
	20	19.59	19.59	19.59
	10	19.72	19.76	19.75
CPS8R	100	17.76	17.73	17.73
	50	17.76	17.73	17.74
	20	17.78	17.75	17.75
	10	17.95	17.87	17.86
S8R	100	16.49	16.51	16.52
	50	16.53	16.51	16.52
	20	16.55	16.59	16.55
	10	16.62	16.63	16.63

A prerequisite in using a shell element is that, the thickness dimension of the structure is assumed to be significantly smaller than the other two dimensions and the stresses normal to the thickness direction are negligible. As a result, the shell thickness can only be defined by either option *SHELL SECTION or *SHELL GENERAL SECTION in ABAQUS, which uses numerical integration to calculate the stresses and strain independently at each section point through the thickness direction. However, these assumptions are not valid for thick casings with a D/t value as low

as 10. Especially, the circumferential deformation and stress are very important in the casing collapse problem and thus cannot be neglected in the analysis. Therefore, the above assumptions are the origins of its conservatism in predicting the casing collapse strength.

The experimental setup may impose on the test specimen unilateral radial restraints at both ends (Assanelli et al, 1999). Those restraints cannot be described by the ordinary two-dimensional elements such as plane strain and plane stress elements. The difference in boundary conditions between a numerical analysis and an actual test partially accounts for the fact that, the collapse strength of a casing predicted from a 2D plane strain or plane stress model, deviates from the test result. For a more accurate prediction, Assanelli (1999) proposed to use a 3-dimensional finite element model for casing collapse. However, a prediction error of 1.7% was still reported even using the 3D simulation, leading to greatly increased computational time and very slow convergence. The requirement of computational economics demands other options.

It should be noted that the 2D plane strain element gives better predictions than those from the 2D plane stress element, and it is quite possible to give an accurate, while fast prediction using a modified plane strain element. Therefore, a generalized plane strain element is proposed in the simulation of casing collapse. In general, generalized plane strain theory (ABAQUS theory manual, 1998) provides for the modelling of cases where the structure has constant curvature with respect to one material direction, i.e. the axial direction. The theory involves a model that lies between two planes, each orthogonal to the axial material direction of the model. These planes may move as rigid bodies with respect to each other. A 10-node generalized plane strain element is basically similar to an 8-node plane strain element, while the former has two extra nodes to account for the relative movement of the bounding planes. The strain components in the cross section of the generalized plane strain model are computed from the displacements of the regular nodes of the element in the usual way as in the ordinary plane strain element. Although the generalized plane strain element is a 2D element, its initial length between the two bounding planes can be defined using the option *SOLID SECTION in ABAQUS. Therefore, the generalized plane strain element combines the advantages of an ordinary plane strain element and a 3D continuum element. With a 2D element, less computational effort is anticipated. The

above description explains the conclusion why the best prediction is obtained from a genearlized plane strain element. As seen from Table 5.3, the prediction from a generalized plane strain element with a finer mesh gives the most accurate collapse strength.

Different mesh densities of 100, 50, 20 and 10 elements per layer in the circumference of the casing have been studied and the comparison is shown in Table 5.3. The convergence rate depends on the element type. It is obvious that the mesh with 10 elements in the circumference is too coarse for a problem of casing collapse. With the mesh refined, the predictions from different elements converge to a stable value with 100 elements in the circumference. It is easily seen that, 3 layers with 100 elements in each layer in the circumference is enough for an accurate prediction of casing collapse strength as well as good computational efficiency. Therefore, the conclusion is made that the 10-node quadrilateral generalized plain strain element CGPE10R is capable of an accurate prediction for casing collapse strength. It is noted that element CGPE10R is preferred according to the guidelines from the ABAQUS User Manual (1998). The mesh is designed to be 3 layers in the thickness direction with 100 elements along the circumferential direction, which is shown in a typical mesh plot Fig. 5.10.

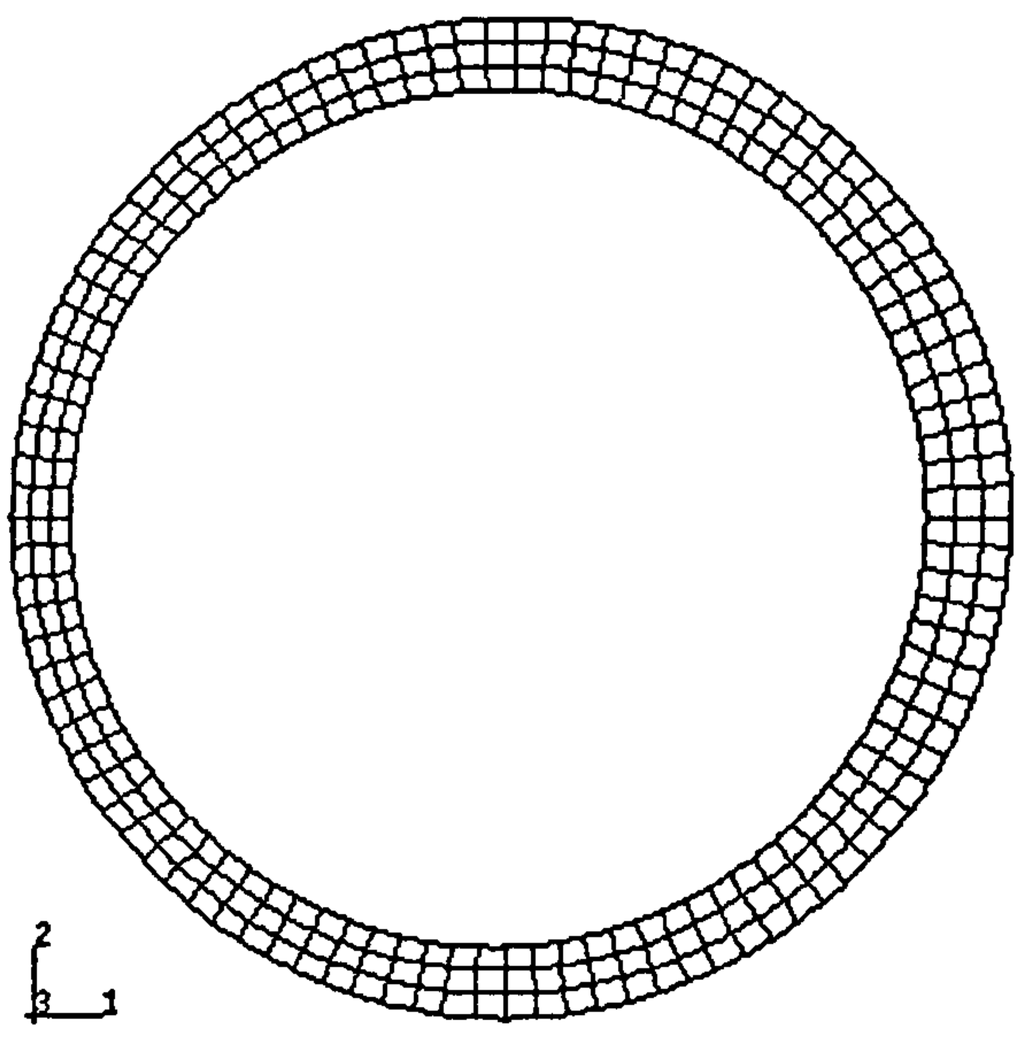

Fig. 5.10 An FE model with imperfections

5.5.3 Validation With Experimental Data

Finite element analysis in this research has been validated through an extensive comparison with a series of full-scale experimental tests of commercial steel casings (Nishioka et al, 1978; Hirakawa and Tokimasa, 1980; Krug, 1983; Yeh and Kyriakides, 1986 and 1988). The steel casings used in the experimental programs were manufactured according to the API specifications (1992). As the casings are often designed to withstand many severe operating conditions, the test data of casing collapse are collected to accommodate a wide variation in yield strength to meet the potential requirements in the casing design process. An important principle in collecting such collapse test data is that, the ratios of length to outside diameter (L/D) of the casings tested must be assured to be larger than 8. Usually, the test specimens are cut from approximately the middle of the sections provided. Care is taken to avoid permanently deforming the casings during the cutting. Additional sections are cut adjacent to the test specimens, which are used for mechanical material property measurements.

The dimensions of the test specimens are first measured manually using micrometers. Usually six diametral measurements are made at approximate eight axial positions. The value of the ovality parameter can then be calculated from these measured maximum and minimum outside diameter values. The casing wall thickness is also measured with a micrometer at approximately 12 circumferential positions at each end of the test specimen. The actual radial imperfection and wall thickness variation are measured through a specially deigned imperfection scanning system (Yeh and Kyriakides, 1988). Normally the imperfections are measured over the middle 6 diameters in the test. Typical accuracy of the measured data is reported as follows. The wall thickness is within $\pm 0.5\times10^{-3}$ inch (0.01 mm), the radial imperfections are within $\pm 0.5\times10^{-3}$ inch (0.01 mm), the axial position is within $\pm 2\times10^{-3}$ inch (0.5 mm), and the angular position is within ± 0.1 degree.

The material properties of the test specimens are measured individually. First, a uniaxial test coupon is cut along the axis of the casing, which is used to obtain the stress-strain behaviour of the casing material. Substantial inelastic anisotropy is found to present in drawn, seamless casings. Because of the inherent difficulties in

measuring the material properties in the circumferential direction, a special biaxial test is developed for measuring such anisotropy (Yeh and Kyriakides, 1986).

Following the imperfection measurements, the test specimens are sealed at both ends and placed in a high pressure test facility. The collapse experiments are then carried out under volume controlled loading conditions, where the pressurization rate is kept low enough to avoid strain rate effects. During the test, the applied external pressure is continuously monitored by a calibrated pressure transducer and analog time-based recording equipment.

The geometry data as well as the material behaviour measured from experiments are carefully coded into the FE programs. The external pressure-strain response of the casing is recorded in the simulation to determine the collapse strength. A typical pressure strain plot is shown in Fig. 5.11. With the increment of external pressure, the measured pressure increases until the maximum pressure is reached and then a decrease in the pressure can be observed with a relatively large increase of deformation. The maximum pressure is then taken as the collapse strength of a casing. In the experiment, collapse of the test specimen is observed when a sudden drop of

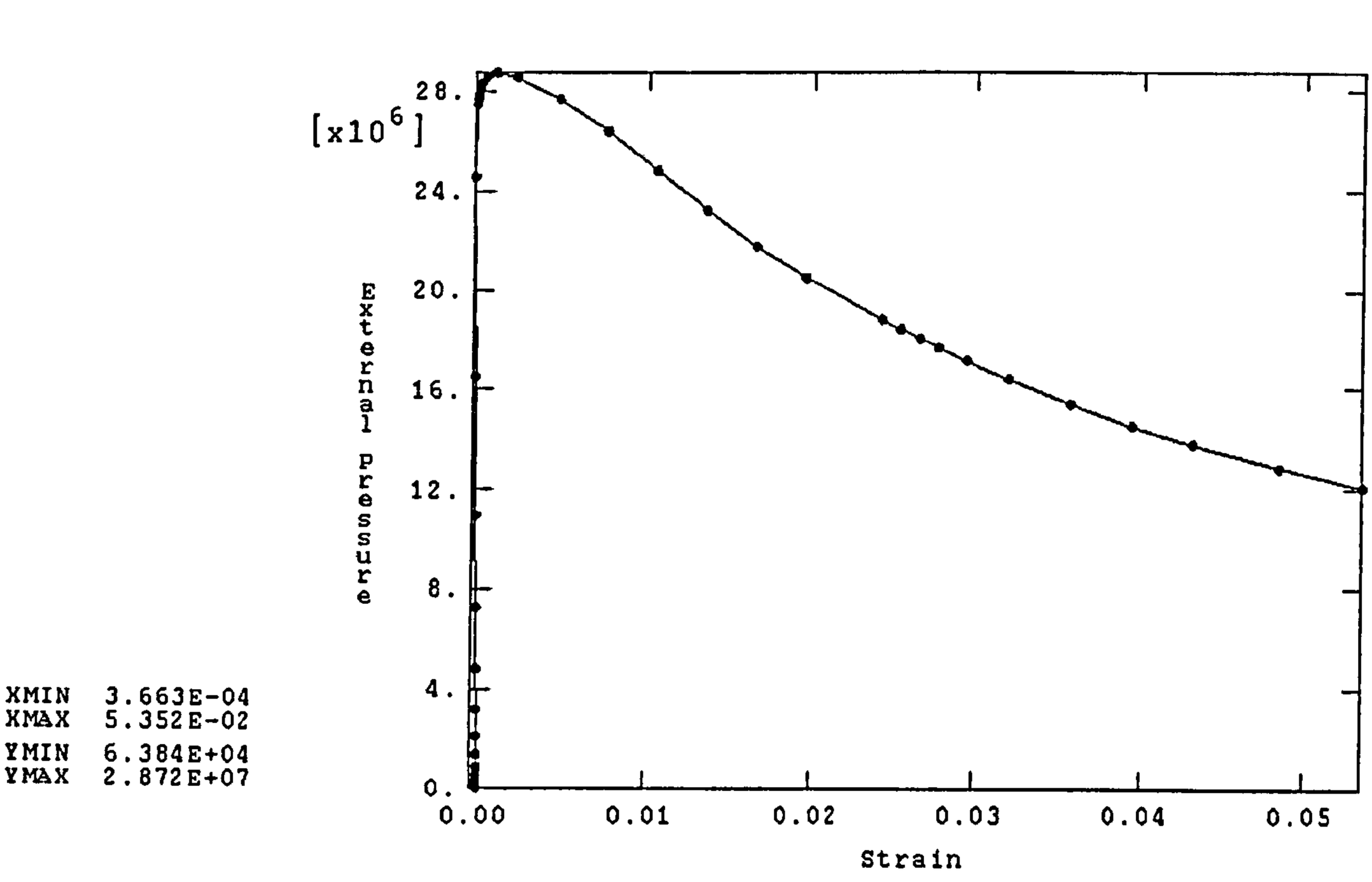

Fig. 5.11 Typical predicted relationship between external pressure and strain

the pressure is recorded in the test facility. With the determination of the collapse strength as above, the comparison between the FEM and experiments is shown in Fig. 5.12, with the biggest deviation less than 8-percent. Such an error level can be acceptable because of assumptions regarding material properties. It is crucial for any FE simulation to simulate the circumferential material properties as accurately as possible because material anisotropy might be induced in the manufacturing processes. However, anisotropy data are only available for Yeh's tests (Yeh and Kyriakides, 1986 and 1988), while the others do not include any information on material anisotropy. As a result, the axial material properties have to be used for those tests without any anisotropy data reported in the current validation. Some errors may also be introduced by the fact that the geometric imperfections are idealized, such as a uniform ovality. The current validation does, however, clearly demonstrate that the collapse strength of a casing can be predicted to a satisfactory degree of accuracy using the finite element analysis developed in this study.

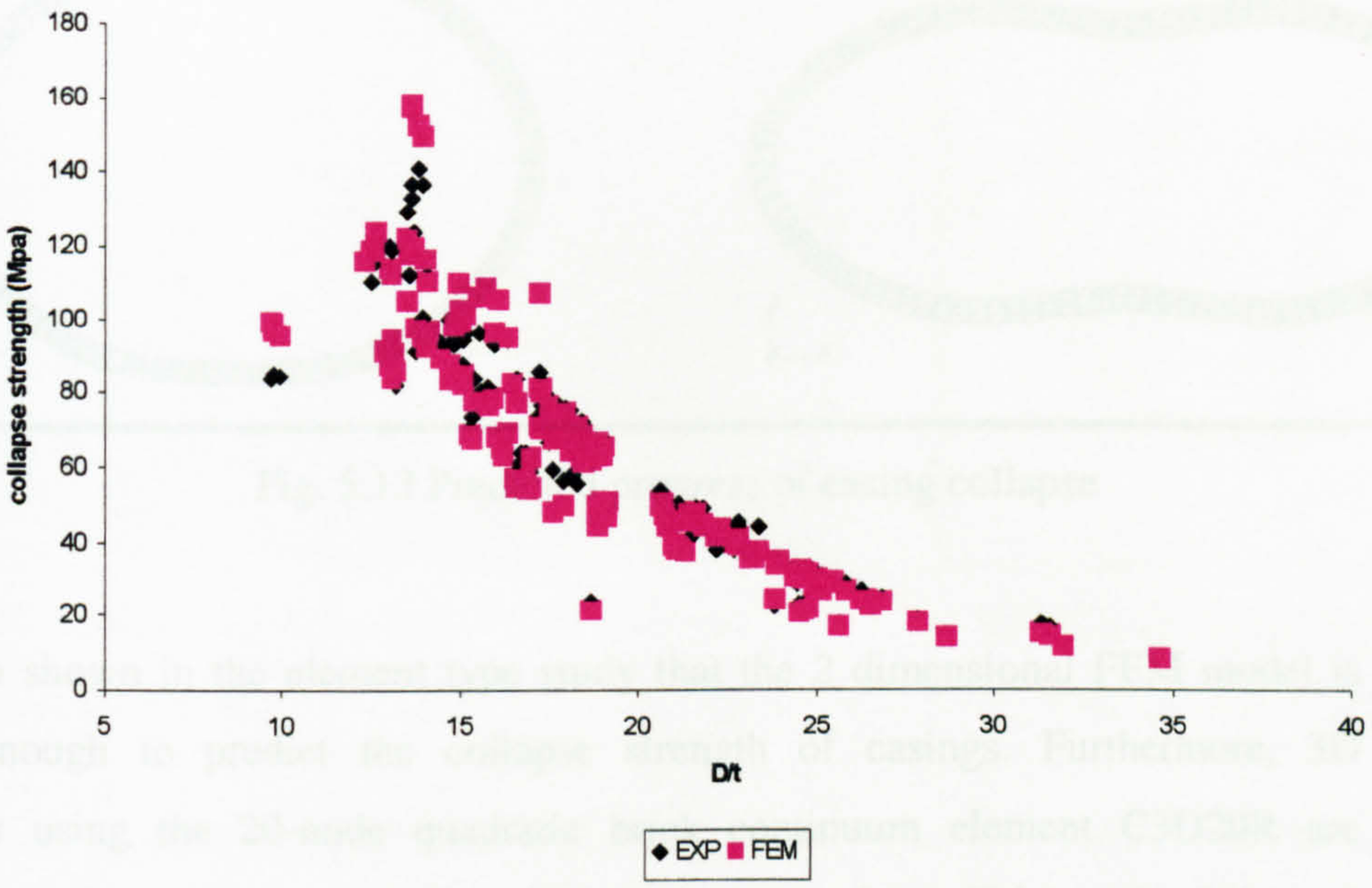

Fig. 5.12 Collapse strength comparisons between experiment and FEM

In addition to predicting the collapse strength, it is important that a good FEM model is capable of predicting the post collapse behaviour of a casing under external pressure. A typical casing collapse process from FEM is shown in Fig. 5.13. In addition, for one of the test specimens (Yeh and Kyrikides, 1986), pictures of the

casing after collapse are used in comparison with the predicted deformation profiles from FEM as shown in Fig. 5.14. It is noted that in Fig. 5.14c, only half of the casing is modelled because of symmetry. The excellent agreement between the collapse test data and the predictions from the FEM model as well as the post collapse behaviour justify a very satisfactory degree of confidence in using the finite element model developed in this thesis to investigate the problem of casing collapse.

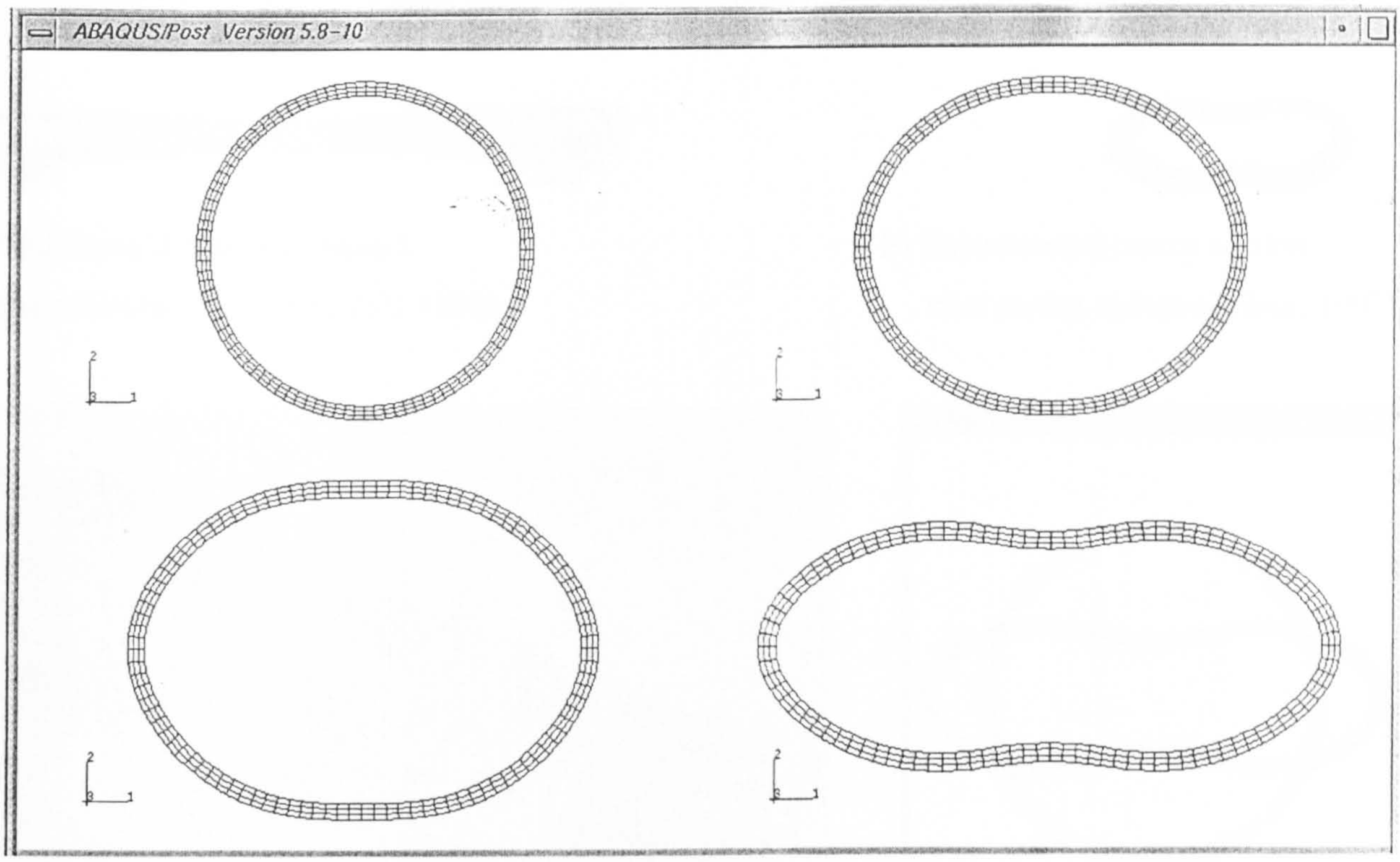

Fig. 5.13 Predicted progress of casing collapse

It has been shown in the element type study that the 2 dimensional FEM model is accurate enough to predict the collapse strength of casings. Furthermore, 3D simulations using the 20-node quadratic brick continuum element C3D20R are performed in this validation for altogether 8 specimens from Yeh's tests (Yeh and Kyriakides, 1986 and 1988). There are 3 layers in the thickness direction of each casing section plane as well as 15 layers in the axial direction. Each section is constructed with 60 elements in the circumference of the casing as seen in Fig. 5.14c. The geometry and initial imperfections, including ovality and eccentricity, are assumed uniform along the axial direction of the casing in the 3D simulation. The above assumptions are proved to be reasonable from experimental observations. In the

imperfection measuring process, the imperfections in wall thickness were found to retain their shapes and orientations along the length of casings for all test specimens (Yeh and Kyridkides, 1986 and 1988). As to ovality, almost all but one specimen retained their radial imperfection shapes and orientations along the casing length. Since the wall thickness is measured from the outside surface and the thickness variation does not exhibit axial variation, a conclusion can be made that, the inside surface of a casing must have similar imperfections as those in the outside surface.

a) Experimental casing collapsed under External Pressure (Yeh, 1988)

b) Experimental casing section after casing collapsed (Issa, 1993)

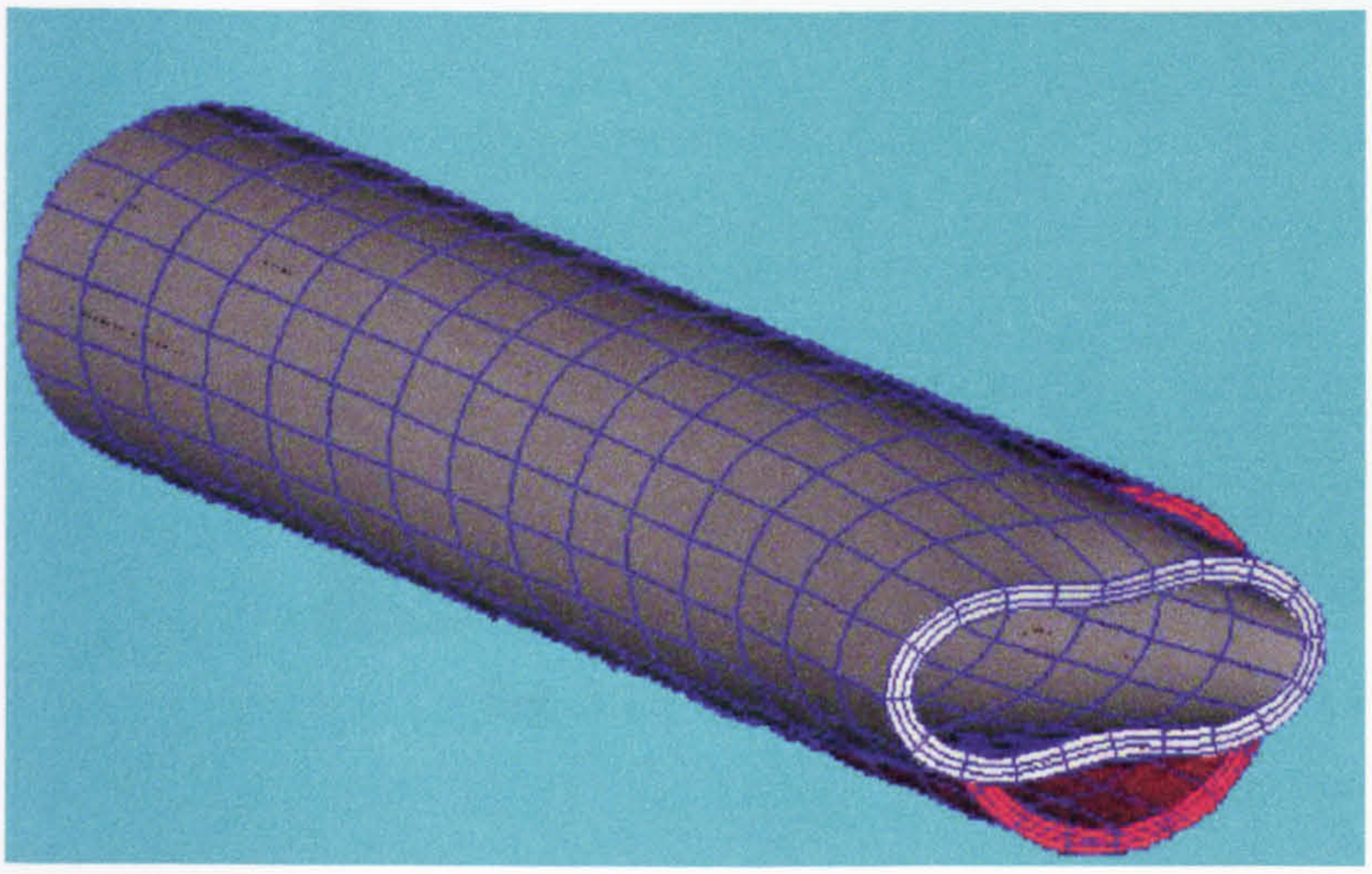

c) FEM predicted casing collapsed under external pressure (half casing)

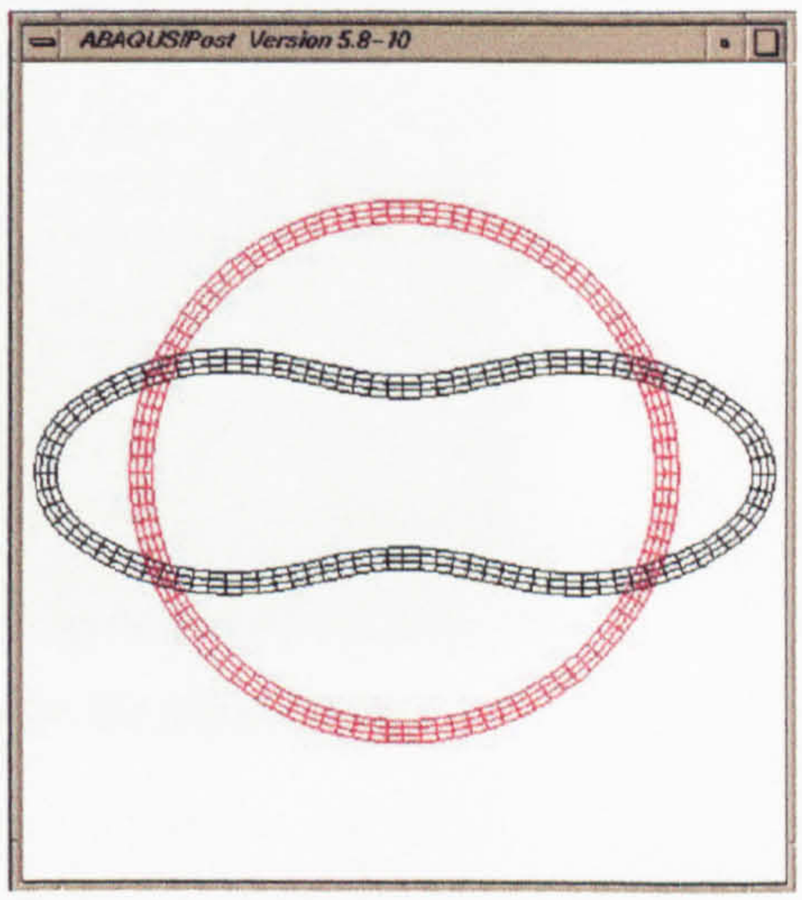

d) FEM predicted casing section after casing collapsed

Fig. 5.14 Predicted post collapse behaviour in comparison with experiment

Similar to a 2D simulation, the external pressure is exerted in the normal direction of the outside surfaces in a 3D simulation, which is kept normal to the surface during the casing deformation. A typical stress distribution from a 3D simulation is shown in Fig. 5.15. Finally, it is found that the predicted collapse strength from a 3D simulation is exactly the same as that from a 2D model using the CGPE10R element. From this 3D validation process, it further proves that the collapse strength of an infinitely long

casing can be predicted accurately using the 2D modelling of the severest casing section.

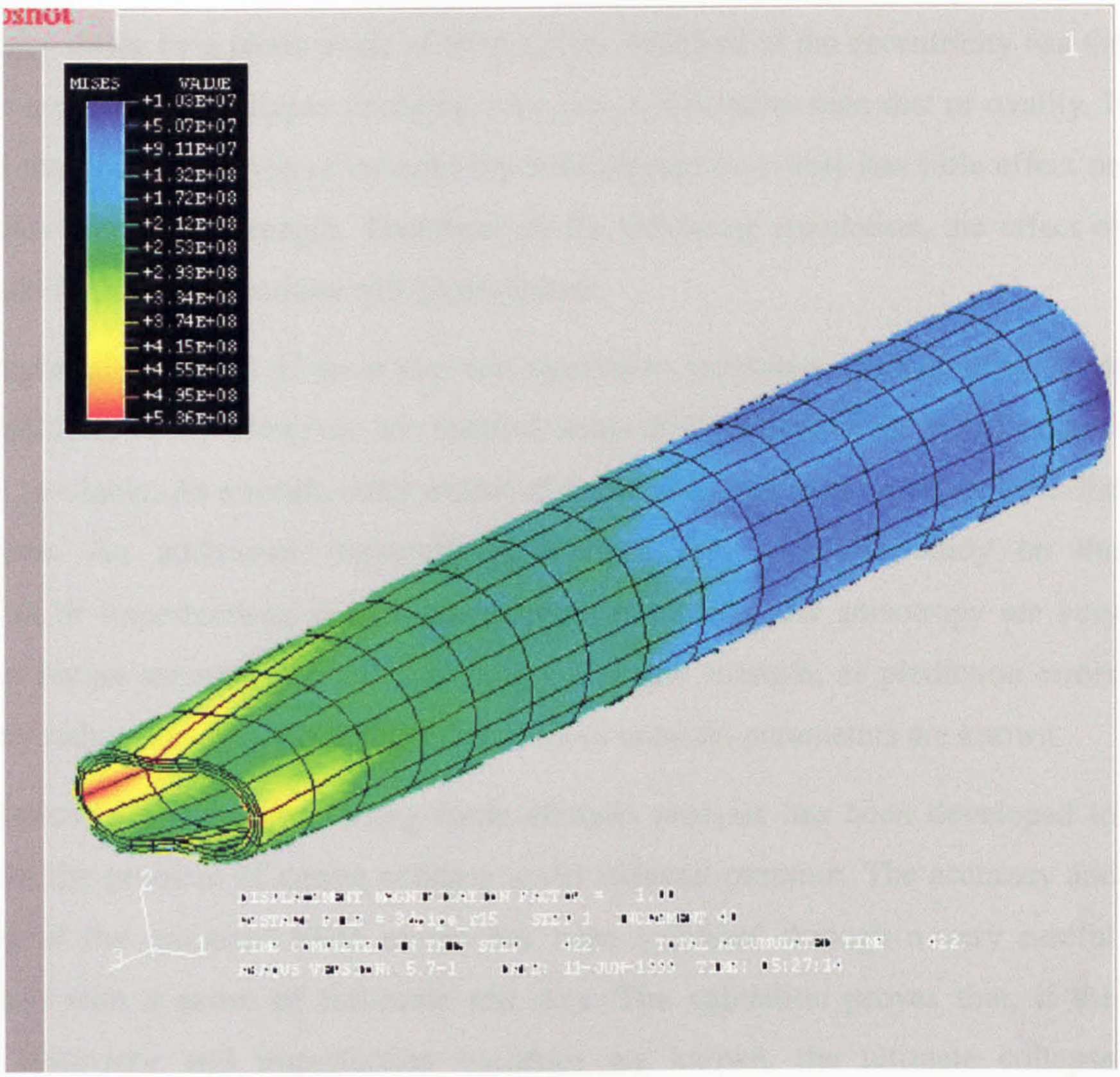

Fig. 5.15 Typical stress distribution of a casing in 3D simulation

Little is given in the literature on the effect of orientation of eccentricity with respect to ovalization on the collapse strength. For simplicity, two specimens have been selected for this particular purpose with specifications shown in Table 5.4. A number of different representations of the initial imperfections are considered and final comparisons are summarised in Table 5.5. The first case is the perfectly circular one. The minimum values of elastic collapse strength (from Equation 5.6) and the plastic collapse strength (from Equation 5.7) are calculated as the collapse strength of a perfect casing. As expected, if the geometric imperfections are neglected, the predicted collapse strengths are unconservative in comparison with the corresponding experimental values. In the next case a uniform ovality with a constant wall thickness are assumed, and collapse strengths are obtained from FEM with an elastic-perfect-

plastic material behaviour. They are lower than those for perfectly circular case, and higher than those from experiments. In the third and fourth cases the wall thickness are assumed to be eccentric in addition to the initial ovality. The two orientations of eccentricity differ by a phase angle of 90 degrees. Addition of the eccentricity has the effect of reducing the collapse strengths, however, it is smaller than that of ovality. It is found that the orientation of eccentricity with respect to ovality has little effect on the predicted collapse strength. Therefore, in the following simulation, the effect of orientation of the imperfections will be neglected.

It was reported that both of these two test specimens exhibited residual stress (Yeh and Kyridkides, 1986). However, the residual stress distributions of the tested casings were not available. As a result, some extent of prediction error may be expected in the comparison. An additional important point from this particular study on the orientation of imperfections is that, the material hardening and anisotropy are very important for an accurate prediction of casing collapse strength, as prediction errors are greatly reduced as seen from Table 5.5, if these material parameters are known.

In conclusion, a methodology using finite element analysis has been developed to investigate the problem of casing collapse under external pressure. The accuracy and reliability of the proposed FEM model has been validated through a very careful comparison with a series of full-scale test data. The validation proves that, if the material behaviour and imperfection variables are known, the ultimate collapse strength can be predicted to a satisfactory degree of accuracy. There is a high degree of confidence in using the method to accurately model the problem of casing collapse.

Table 5.4 Casing specification

Spec. No	1	2
Material	X-42	X-65
D (in.) (mm)	4.0 101.6	4.012 101.91
D/t	27.87	31.97
E (ksi) (GPa)	29.6×10^3 204.1	29.7×10^3 204.8
σ_y (ksi) (MPa)	48.0 330.9	75.0 517.1
σ_0 (ksi) (MPa)	-	65.0 448.1
n^*	-	6.5
λ^*	1.3	1.0

* n is the material hardening parameter and λ is the anisotropy parameter.

Table 5.5 Imperfection orientation study

FEM Model	Specimen No.	1	2
Perfect Geometry	D (in.) (mm)	4.0 101.6	4.012 101.91
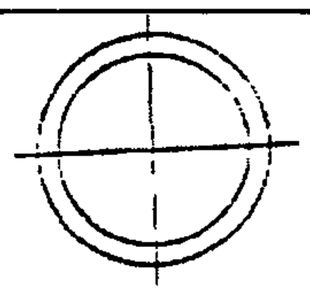	t (in.) (mm)	0.1435 3.645	0.1255 3.1877
	D/t	27.87	31.97
	P_{co} (MPa)	22.29	14.68
Idealized Imperfection	Ovality ($u\ x10^{-4}$)	5	27.4
Pure ovality 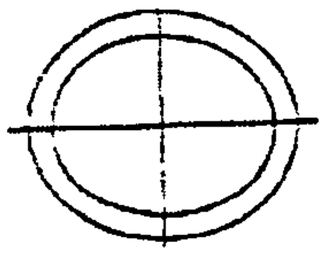	Eccentricity (ψ)	0	0
	P_{FEM} (MPa)	20.23	13.28
Both ovality Eccentricity	Ovality ($u\ x10^{-4}$)	5	27.4
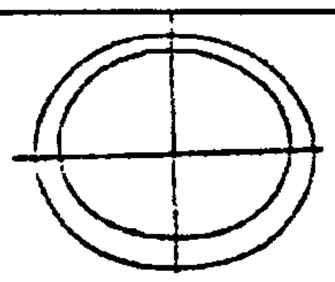	Eccentricity ($\psi\ x10^{-2}$)	3.83	3.58
	P_{FEM} (MPa)	19.62	13.12
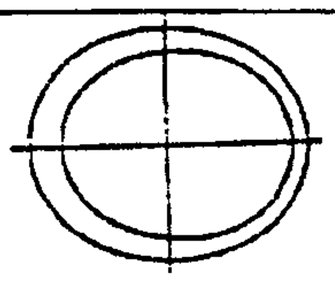	Ovality ($u\ x10^{-4}$)	5	27.4
	Eccentricity ($\psi\ x10^{-2}$)	3.83	3.58
	P_{FEM} (MPa)	19.62	13.12
Experimental Collapse Pressure (psi) (MPa)		2720 18.75	1764 12.16
FEM with hardening	P_{FEM} (MPa)	19.62	11.78
	$Error_{FEM}$	4.64%	-3.2%
FEM with anisotropy	P_{FEM} (MPa)	18.87	11.78
	$Error_{FEM}$	0.7%	-3.2%

5.5.4 Generalized Material Behaviour

A detailed literature review on casing material behaviour suggests several forms of material behaviour may be suitable for a generalized material behaviour for casing collapse, which are listed below:

- Elastic-linear hardening material model, Equation (5.41) (Tokimasa and Tanaka, 1986; Assanelli et al, 1999)
- Elastic-exponential hardening material model, Equation (5.42) (Tokimasa and Tanaka, 1986)
- Isotropic material hardening model, Equation (5.48) (Bai et al, 1993; 1995 and 1997)
- Ramberg-Osgood material model, Equation (5.49) (Yeh and Kyriadies, 1986 and 1988)

The only way to determine the most suitable material behaviour is to evaluate the predictive accuracy of all four candidate material behaviours against full scale test data. The process to determine a generalized material behaviour is very time consuming. A huge number of computational efforts have been spent in the comparison to select the best material behaviour as well as to determine the value of the associate variables. Considering the large number of test data available, it is neither necessary nor possible to perform all the simulations of each test on the basis of these candidate material behaviours. Therefore, six representative test data selected from the test database, which are shown in Table 5.6. It is noted that the principle to select the test data is to enable those points varying in the whole interested D/t range (10 to 40), their yield stress varying between 267 MPa (40 ksi) to 862 MPa (125 ksi), with different extents of material hardening and anisotropy. The above criterion enables the selected data be a suitable representation of the whole test data. The generalized material behaviour is determined such that it gives the best predictive collapse strength in comparison with actual test results.

For the representative data, simulations are performed for all forms of candidate material behaviours. Compared with tested collapse strengths, typical results are shown in Fig. 5.16 to 5.19 with respect to different material behaviour. It is therefore

concluded that the best predictions are from the three-parameter Ramberg-Osgood material behaviour, which has the following expression:

$$\varepsilon = \frac{\sigma}{E}\left[1+\frac{3}{7}\left(\frac{\sigma}{\sigma_m}\right)^{n-1}\right] \tag{5.59}$$

where σ_m is a material parameter determined by the material yield strength.

It is clear that the generalized material behaviour above has the ability to simulate different casing materials with desired yield strength. To further validate the representation of the generalized material behaviour, simulations have been performed for more data in the collapse database. Again, the predictions are very close to the actual collapse strength as shown in Fig. 5.20. It is clearly demonstrated that, the proposed generalized material behaviour can represent for the realistic material behaviour of casings in this research. Thus, the determined generalized material behaviour is used in the forthcoming parametric studies as well as in the derivation of collapse design equations.

Table 5.6 Typical test data for the determination of a generalized material behaviour

No	1	2	3	4	5	6
D/t	18.66	25.66	27.87	28.65	31.97	34.67
u	.0008	.0012	.0005	.0015	.00274	.0005
ψ	.030	.0505	.0383	.0208	.0358	.0278
σ_y (ksi)	38.7	49.8	48.0	50.1	75.	43.5
(MPa)	266.8	341.9	330.9	345.4	517.1	299.9
E (10^6 psi)	28.5	27.6	29.6	28.7	29.7	26.6
(GPa)	196.5	190.3	204.1	197.9	204.8	183.4
n	13.0	14.5	0.0	14.0	6.5	12.0
λ	2.0	1.6	1.3	1.6	1.0	1.8
Exp. (psi)	3427	2563	2720	2092	1764	1300
(MPa)	23.6	17.7	18.8	14.4	12.2	8.9

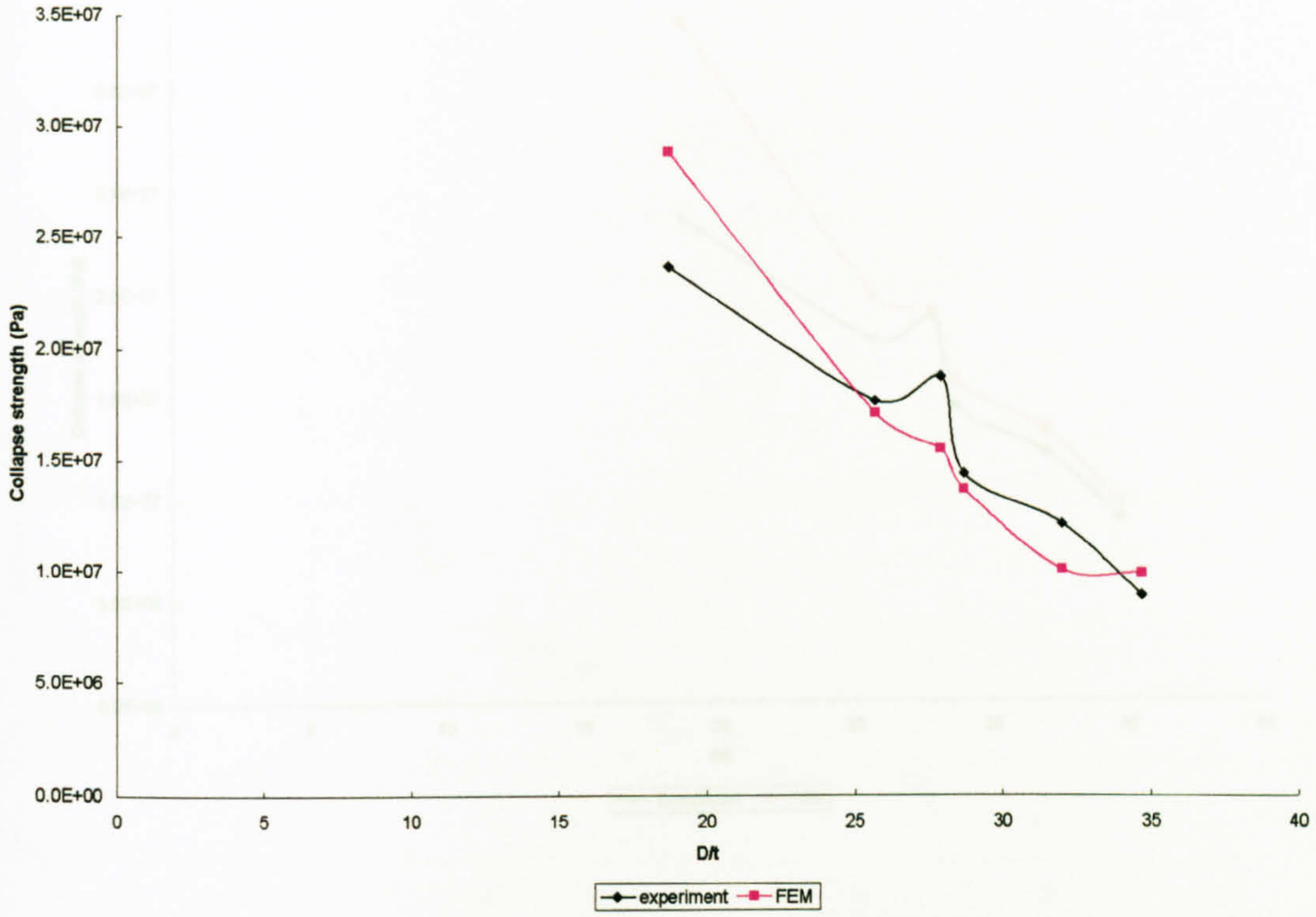

Fig. 5.16 Predicted collapse strength from an elastic-linear hardening material model in comparison with experiments

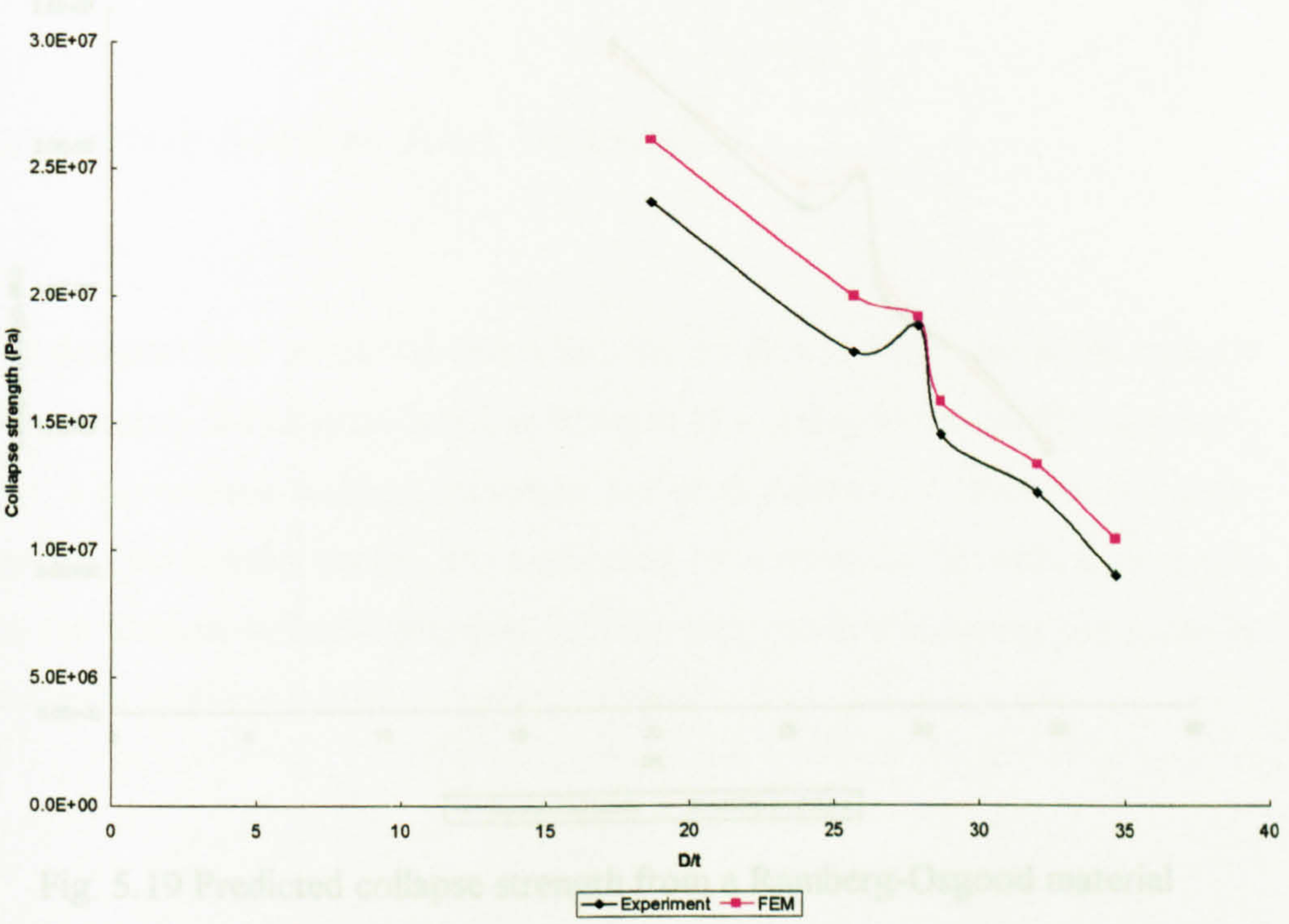

Fig. 5.17 Predicted collapse strength from an elastic- exponential hardening material

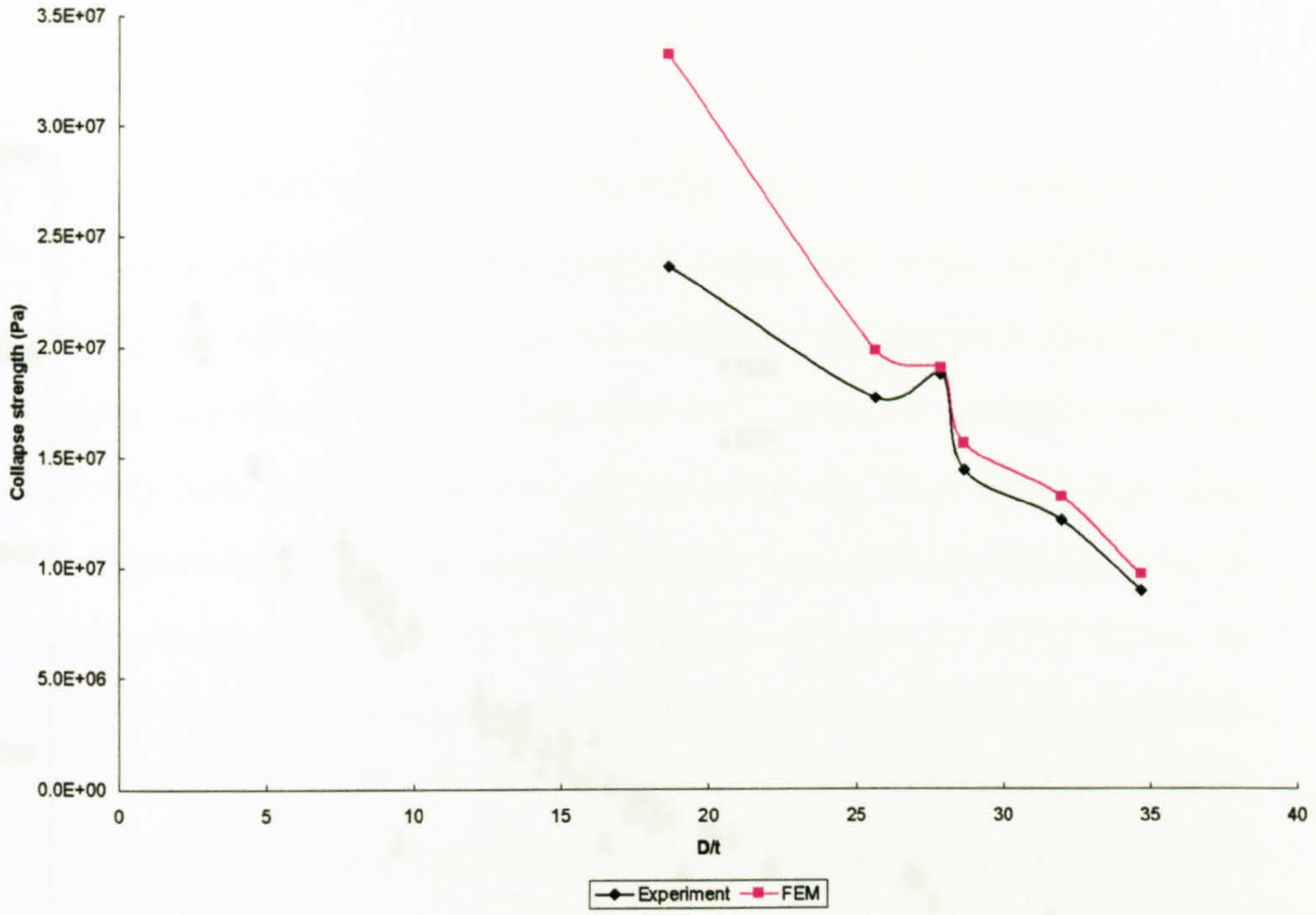

Fig. 5.18 Predicted collapse strength from an isotropic material hardening material

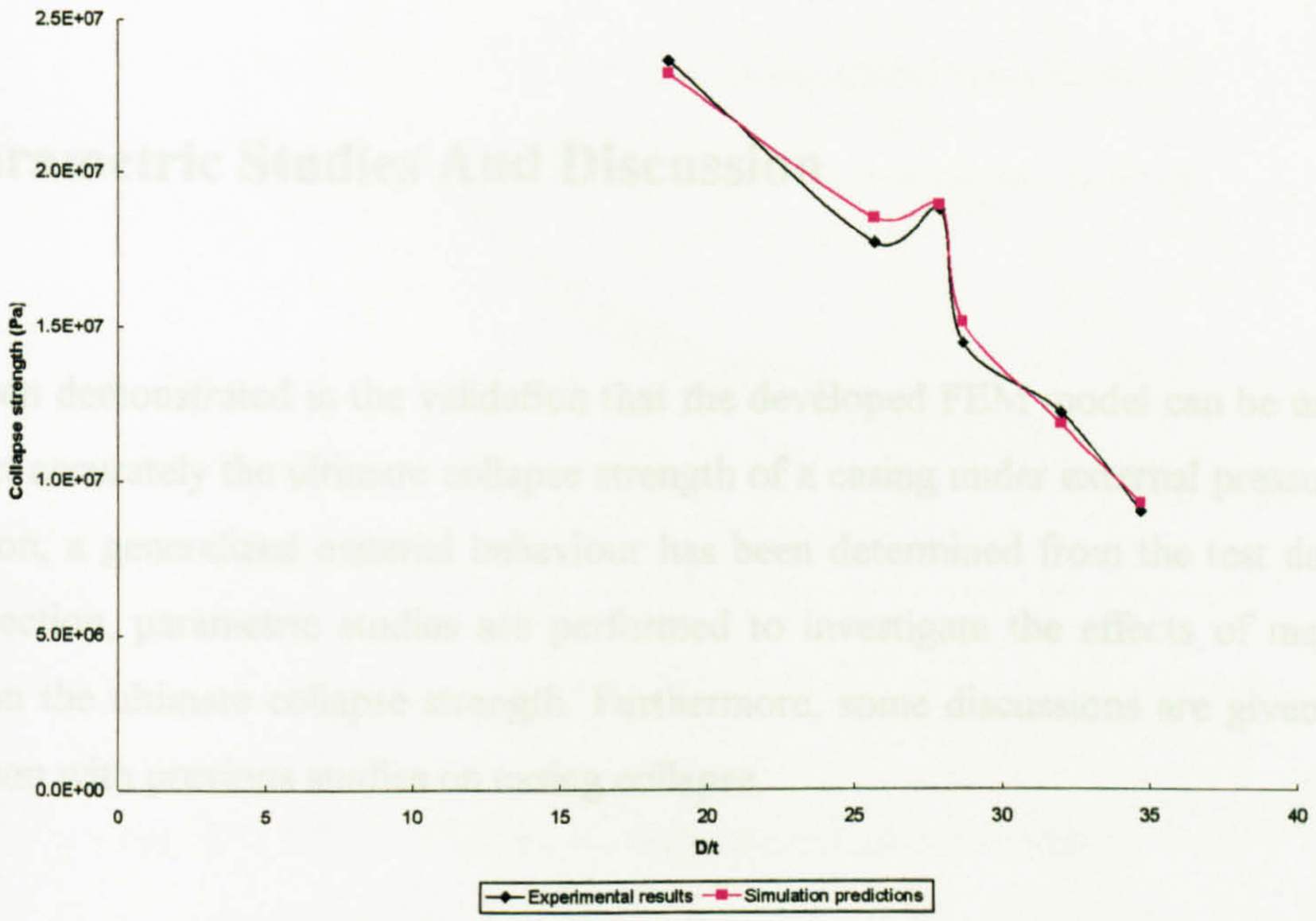

Fig. 5.19 Predicted collapse strength from a Ramberg-Osgood material

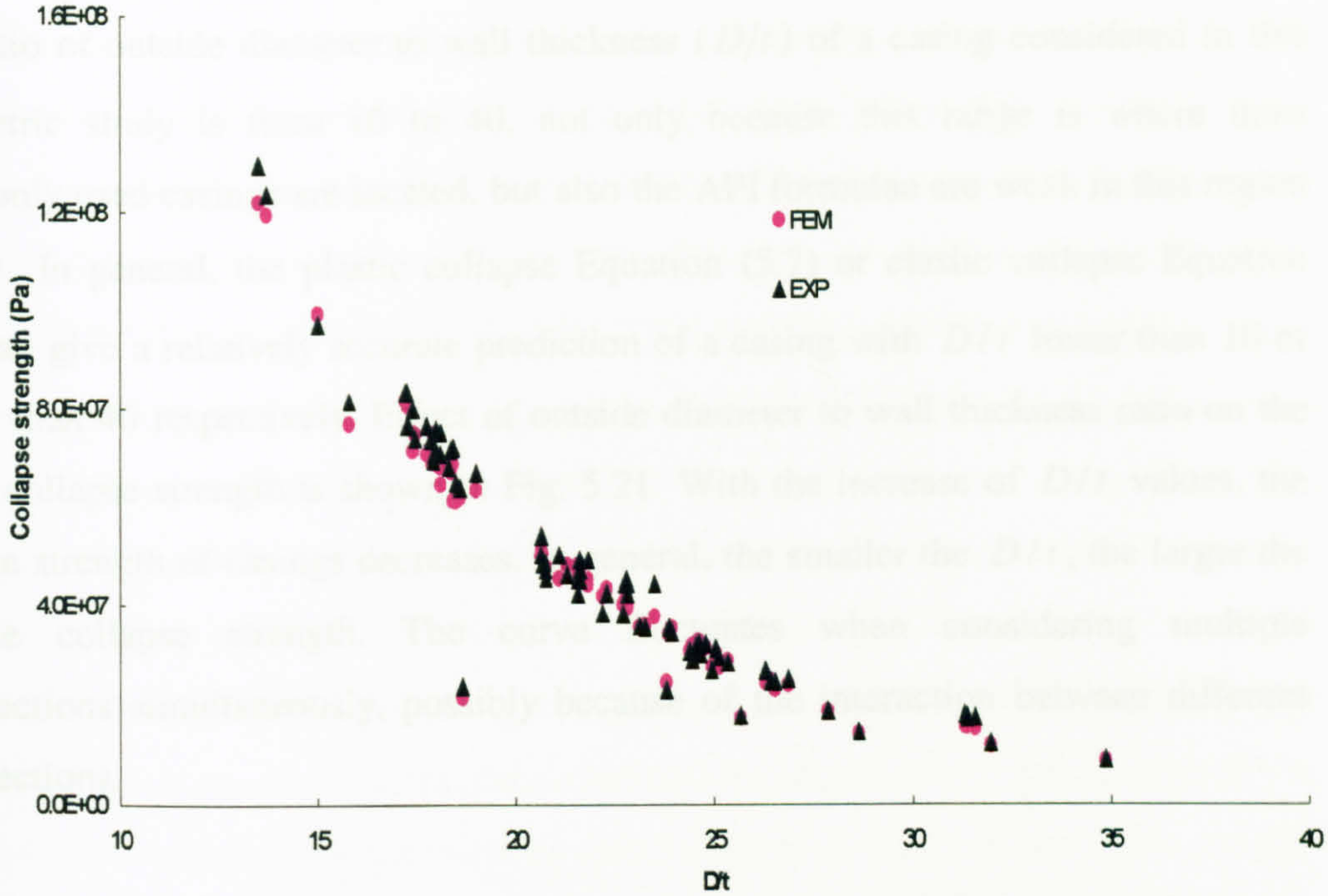

Fig. 5.20 Comparison between FEM and experiments using the generalized material behaviour

5.6 Parametric Studies And Discussion

It has been demonstrated in the validation that the developed FEM model can be used to predict accurately the ultimate collapse strength of a casing under external pressure. In addition, a generalized material behaviour has been determined from the test data. In this section, parametric studies are performed to investigate the effects of major factors on the ultimate collapse strength. Furthermore, some discussions are given in comparison with previous studies on casing collapse.

5.6.1 Effect Of Outside Diameter To Wall Thickness Ratio

The ratio of outside diameter to wall thickness (D/t) of a casing considered in this parametric study is from 10 to 40, not only because this range is where most commonly used casings are located, but also the API formulae are weak in this region of D/t. In general, the plastic collapse Equation (5.7) or elastic collapse Equation (5.6) can give a relatively accurate prediction of a casing with D/t lower than 10 or greater than 40 respectively. Effect of outside diameter to wall thickness ratio on the casing collapse strength is shown in Fig. 5.21. With the increase of D/t values, the collapse strength of casings decreases. In general, the smaller the D/t, the larger the ultimate collapse strength. The curve fluctuates when considering multiple imperfections simultaneously, possibly because of the interaction between different imperfections.

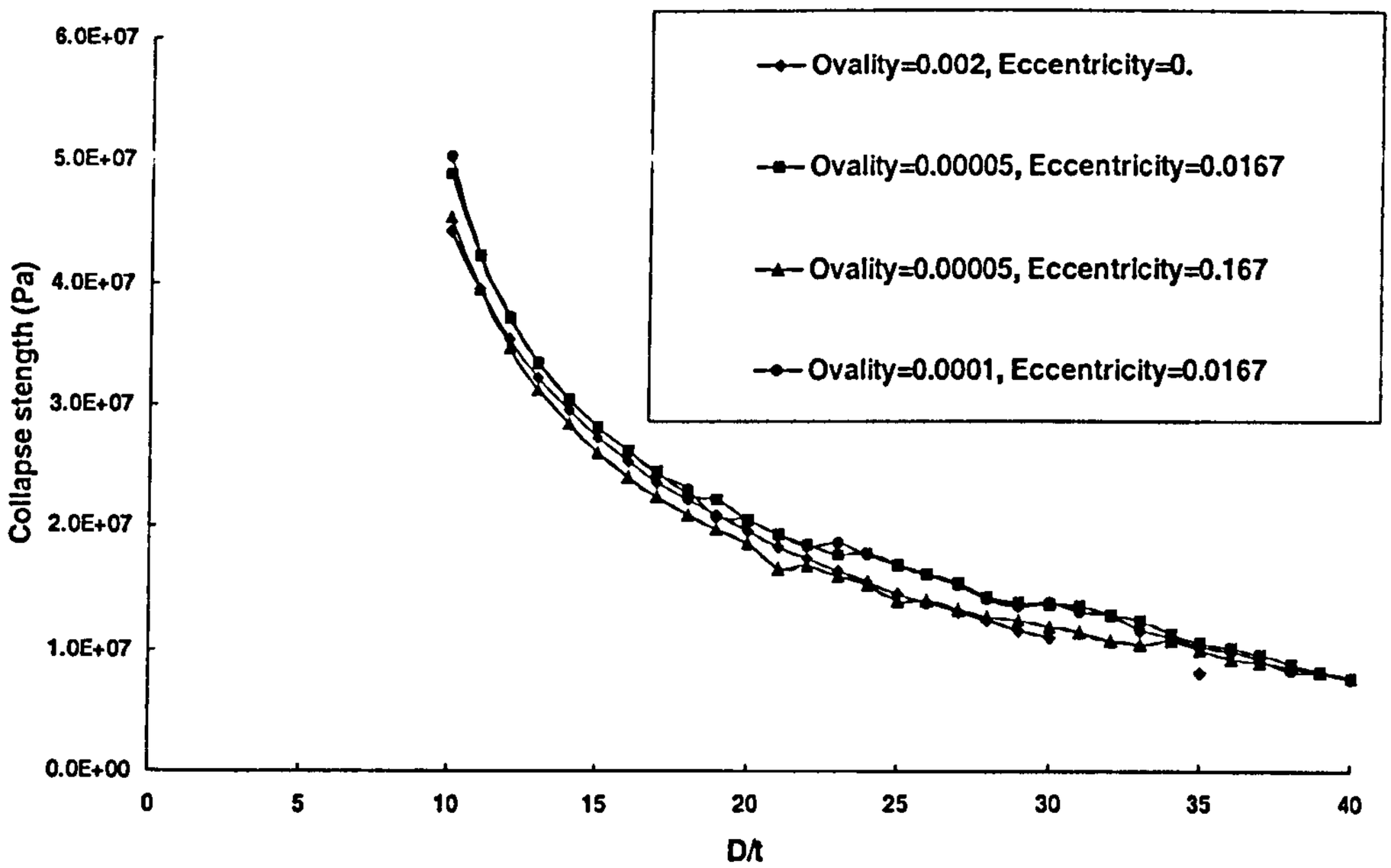

Fig. 5.21 Effect of D/t on the ultimate collapse strength

5.6.2 Effect Of Ovality

The importance of initial ovality on the ultimate casing collapse strength is well demonstrated in the experiments (Yeh and Kyriakides, 1986). For example, in all casings examined by Yeh and Kyriakides (1986), an initial ovality of 5 percent caused more than 50 percent reduction in the collapse strength. The experimental observation is further proved by the prediction from the finite element simulation of current study.

Bai et al (1997) presented an investigation to study the effect of initial ovality on the collapse strength of casings under external pressure, where the magnitude was required to be greater than 0.005. However, common values of initial ovality as measured from experiments are much smaller than 0.005. For example, an initial ovality with a magnitude as small as 4×10^{-4} is reported in the experimental data in Appendix 1. As a result, an extrapolation method was employed by Bai et al (1997) to transform the collapse strength with an initial ovality of 0.005 to that with a much smaller magnitude of ovality. Such an approximation will bring extra prediction errors inevitably. It is also noted that a shell element is employed in Bai's program, which is unable to provide an accurate prediction for the problem of casing collapse as already pointed out in the element study of this thesis. The use of an unsuitable element may explain why Bai's program requires a big initial ovality value as input, which makes the result unconvincing. The smaller the initial ovality that can be simulated, the more convincing the results. The finite element program in the present study extends the initial ovality modelling capability, and can accurately simulate an initial ovality as small as 10^{-5} by using a generaized plane strain continuum element. This in turn implies that the choice of the generaized plane strain element for casing collapse is suitable.

The effect of initial ovality on the ultimate collapse strength of casings under external pressure is shown in Fig. 5.22 with ovality varying from 10^{-5} to 10^{-2}. It is noted here that, the magnitude of 10^{-2} is not the upper limit of initial ovality modelling capability, but because a casing seldom has a greater initial ovality in practice. In fact, the program can model any magnitude of ovality between 10^{-5} and 1. With the increase of ovality, the collapse strength decreases greatly. In addition, the effect of ovality on the collapse strength is greater for a casing with a relatively high D/t value than that

with a low D/t. It is clearly demonstrated in Fig. 5.22 that, a 1-percent initial ovality causes an approximate 50 percent reduction in the ultimate collapse strength for a casing with a relatively high D/t value. Therefore, initial ovality has a dramatically detrimental effect on the ultimate collapse strength.

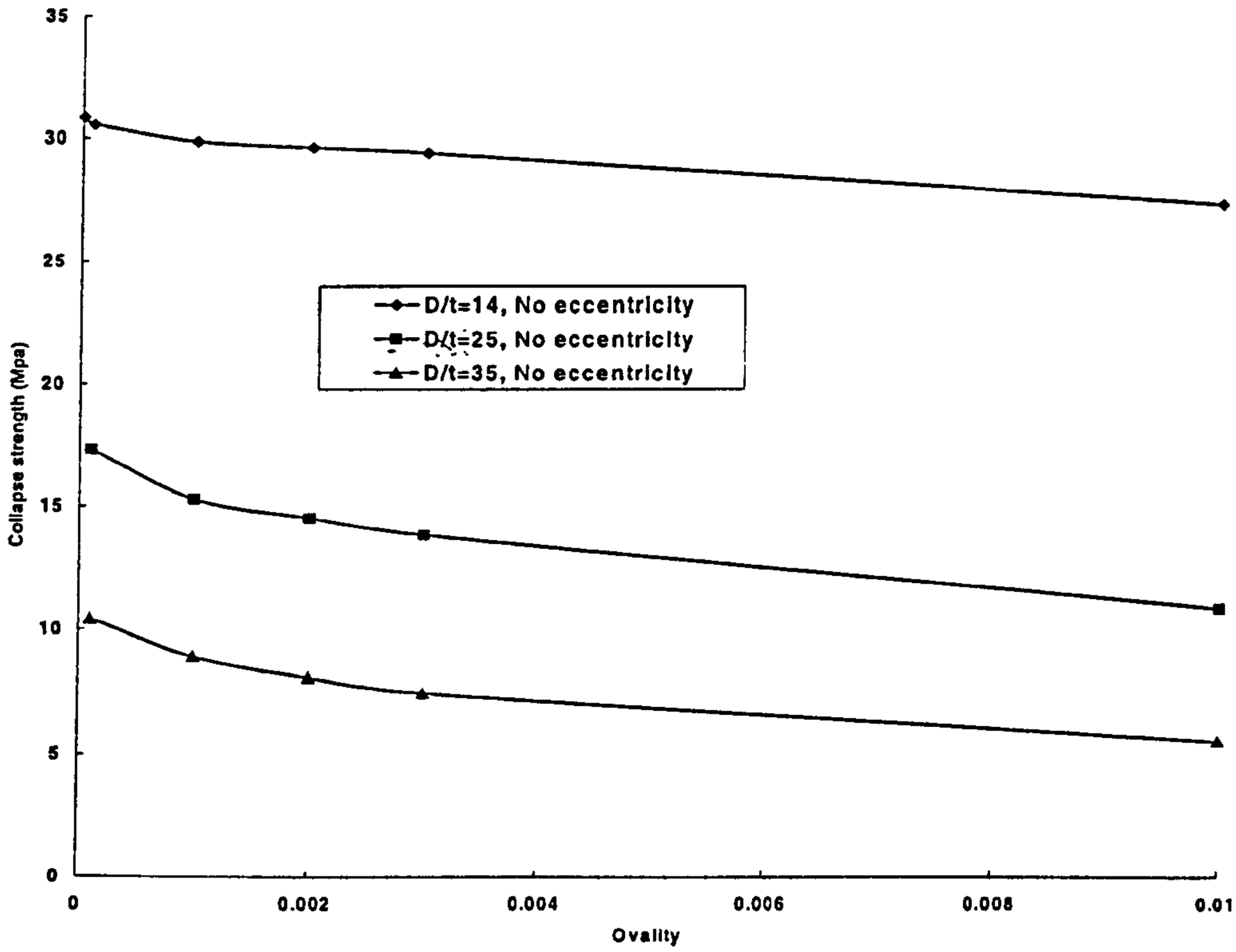

Fig. 5.22 Effect of initial ovality on the ultimate collapse strength

5.6.3 Effect Of Eccentricity

Eccentricity is the second most important parameter affecting the ultimate collapse strength. The importance of eccentricity is recognized in the literature (Kennedy and Venard, 1962; Nordgren and Murphey, 1968; Tokimasa and Tanaka, 1986; Yeh and Kyriadies, 1986). However, an apparent lack of dependable measurement of how the thickness varies along the casing length still exists. A fundamental limitation in using a shell element in the finite element analysis is that, it cannot model the variation of wall thickness of a casing. As a result, the effect of initial eccentricity on the collapse

strength has not been studied when employing shell elements (Bai et al, 1993; 1995 and 1997).

In general, initial ovality and eccentricity coexist. For the idealized geometry assumed in this study, the oval section has two planes of symmetry and the section with non-uniform thickness one. Theoretically, an infinite number of geometric combinations of the two imperfection patterns are possible. For two particular casings, two extreme combinations of both imperfections have been studied in the validation process. A conclusion has been drawn that the orientation of imperfections with respect to one another has a negligible effect on the casing collapse strength. In this section, it is noted that ovality is not considered in the analysis, as the aim is to find out the sole effect of eccentricity on the ultimate casing collapse strength.

The effect of eccentricity on the ultimate casing collapse strength is shown in Fig. 5.23. With the increase of eccentricity, the collapse strength decreases. The effect of initial eccentricity on the collapse strength is greater for a casing with a relatively lower D/t value than that with a higher D/t. It is clearly demonstrated that 30 percent of initial eccentricity causes about 15 percent reduction in collapse strength for a casing with a relatively low D/t value. In general, both the ultimate collapse

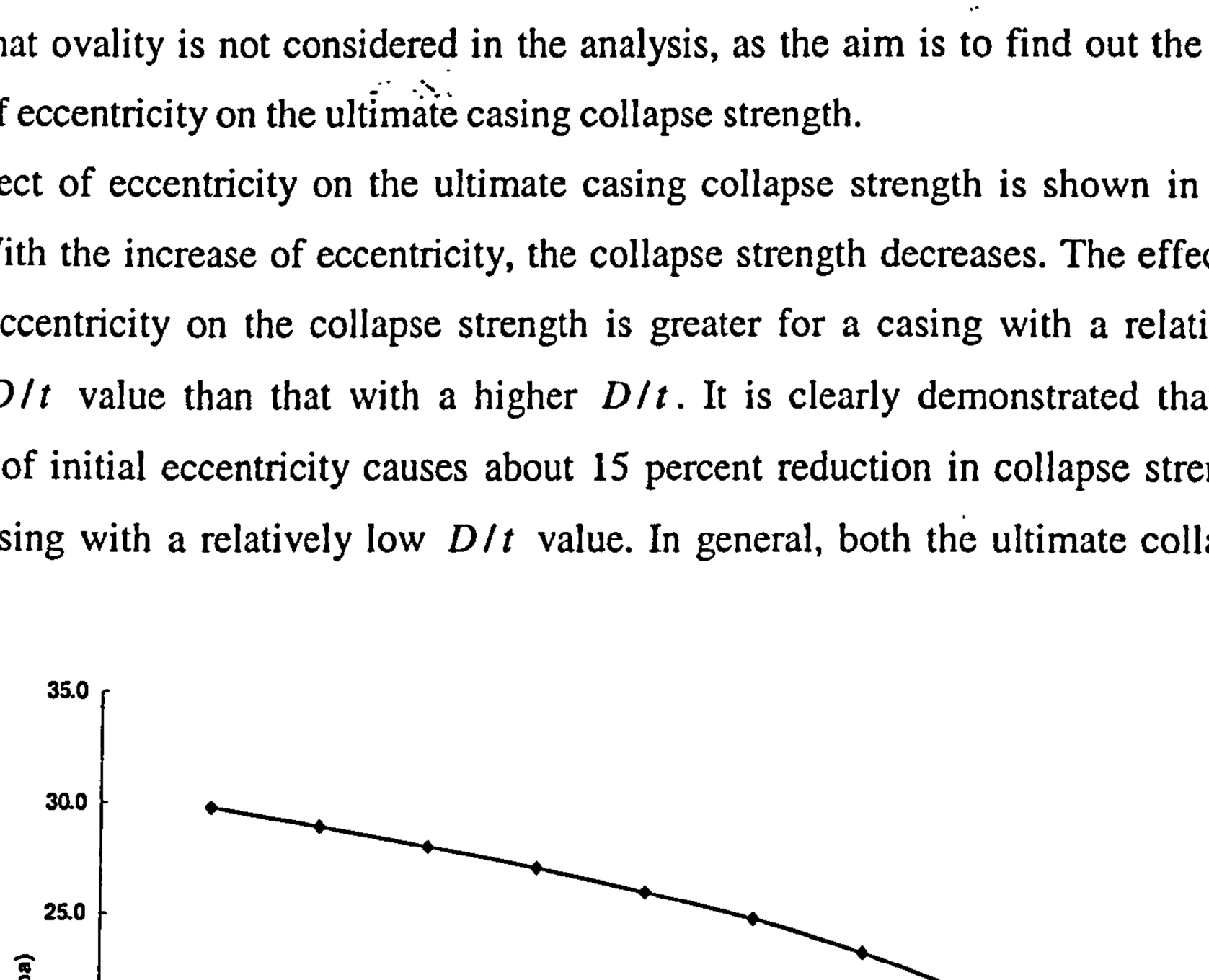

Fig. 5.23 Effect of initial eccentricity on the ultimate collapse strength

strength and the slope of the casing response to external pressure are affected by the value of initial eccentricity. The wall thickness variation causes a non-uniform membrane stress distribution around the circumference so that it leads to the development of a limit load, which is lower than the bifurcation load of the perfect casing.

In summary, the presence of initial eccentricity reduces the ultimate casing collapse strength. Its effect is more pronounced for casings with relatively low values of D/t. However, its effect on the ultimate collapse strength is relatively minor than that of initial ovality. This conclusion is in agreement with similar observations from the experiments (Tokimasa and Kanata, 1986; Yeh and Kyriadies, 1986).

5.6.4 Effect Of Residual Stress

Manufacturing processes usually leave residual stress in the casing. The amount and distribution of residual stress depend on the type of manufacturing process involved. It is widely believed that the residual stress weakens the casing. However, the question as to what extent the residual stress may reduce the ultimate collapse strength is still a subject of debate. Tamano et al (1983), as well as Tokimasa and Tanaka (1986), claimed that the circumferential residual stress greatly reduced the collapse strength, while Issa and Crawford (1993) thought that its effect was very small and the effect of residual stress was neglected in the Issa equation. Therefore, it is necessary to clarify to what extent the residual stress may affect the ultimate collapse strength of a casing.

Based on the experimental measurements, a linear solution of pure bending of a curved bar (Timoshenko and Gere, 1961) is assumed to model the approximate linear distribution of residual stress in the casing wall thickness (Yeh and Kyriadies, 1986; Bai et al, 1993). To model the induced stress distribution, a more accurate solution of the axisymmetric two-dimensional problem is expressed by,

$$\sigma_r = -4kR_i^2\left[\left(\frac{R}{R_i}\right)^2 - 2\left(\frac{R}{R_i}\right)^2 \ln\left(\frac{R}{R_i}\right) - 1\right] \tag{5.60}$$

$$\sigma_s = -4k\left[-\left(\frac{R_i^2 R^2}{r^2}\right)\ln\left(\frac{R}{R_i}\right) + R^2\ln\left(\frac{r}{R}\right) + R_i^2\ln\left(\frac{R_i}{r}\right) + R^2 - R_i^2\right] \quad (5.61)$$

where, r is a polar coordinate and $R_i \le r \le R$, with internal radius $R_i = R - t$. It is noted that k is a mathematical constant (Pa m^{-2}). σ_r is prescribed and can be determined from the boundary condition. Thus, k can be evaluated from Equation (5.60). In this way, the residual stress is evaluated from Equation (5.61) and modelled approximately in the finite element analysis.

In the current study, initial residual stress is introduced into the FE program as initial stress by an option of *INITIAL STRESS in ABAQUS. It is noted that the distribution of initial stress must be assumed to be in equilibrium with the applied load and the boundary conditions or at least close to an equilibrium state in ABAQUS. The effect of residual stress on the ultimate collapse strength is shown in Fig. 5.24, assuming the maximum magnitude of circumferential residual stress to vary from 0 to $0.4\sigma_y$. It is clearly shown that the effect of residual stress is very small on the ultimate collapse strength.

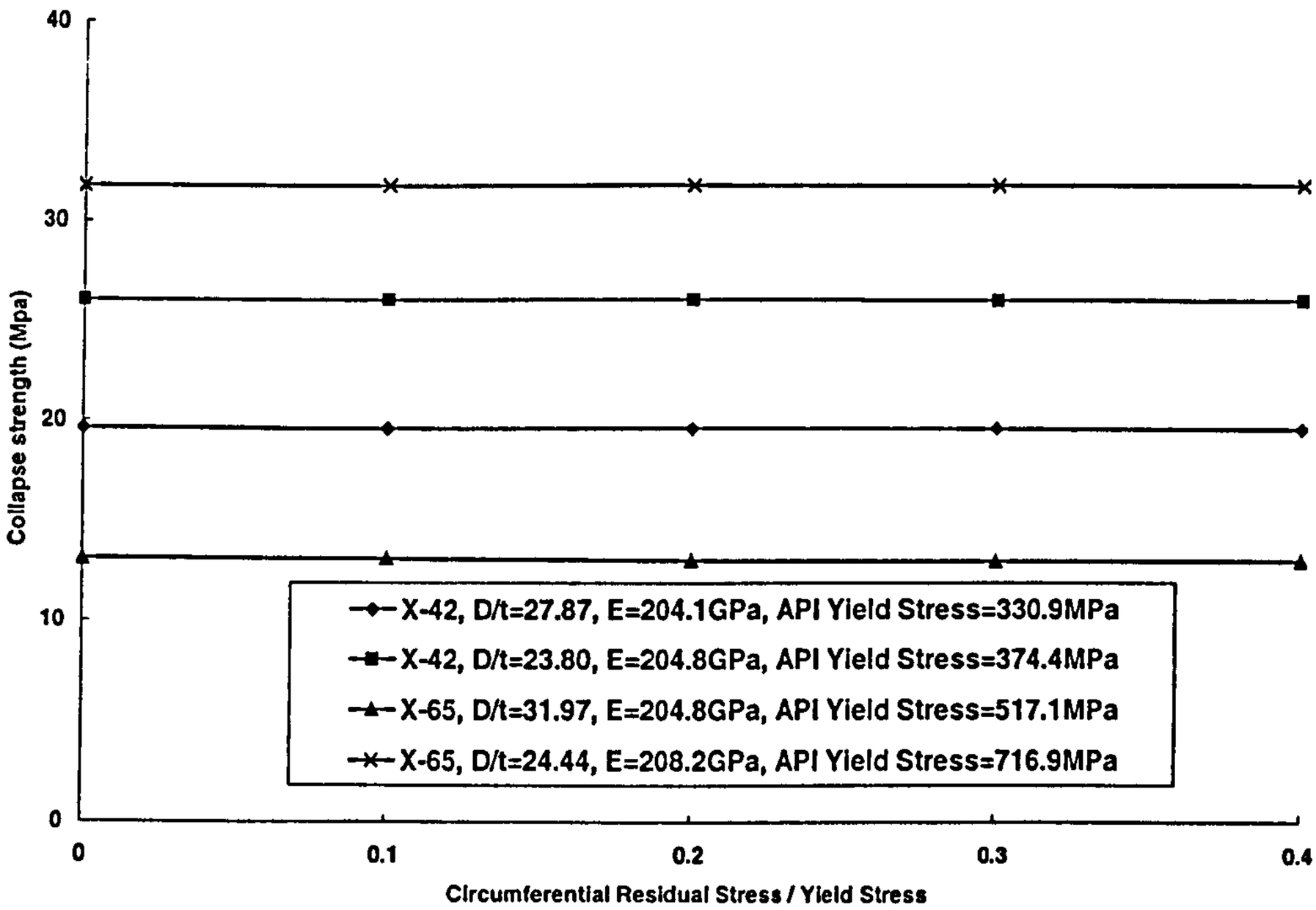

Fig. 5.24 Effect of residual stress on the ultimate collapse strength

5.6.5 Effect Of Material Hardening

The stress-strain relationship used in FEM is crucial for an accurate prediction of the collapse strength of a casing under external pressure. In view of this importance, a Ramberg-Osgood type of generalized material behaviour is determined to be representative of the realistic casing material behaviour, and has been adopted in the current study. Therefore, the stress-strain behaviour of the material has been calculated according to Equation (5.59) and converted to true stress and strain format as required by ABAQUS. For the particular case of test specimen 2 as listed in Table 5.5, though its material behaviour just presents a smooth hardening, the predicted ultimate collapse strength will be 7.9% higher than the experimental collapse strength if adopting an elastic-perfect-plastic material model. The predicted deviation is reduced to –3.2% by adopting the generalized material model as described in the validation process. Furthermore, the effect of material hardening on the ultimate collapse strength is shown in Fig. 5.25. It is seen that the predicted collapse strength of a casing with a relatively low value of D/t decreases dramatically as the hardening parameter increases. However, the predicted collapse strength of a

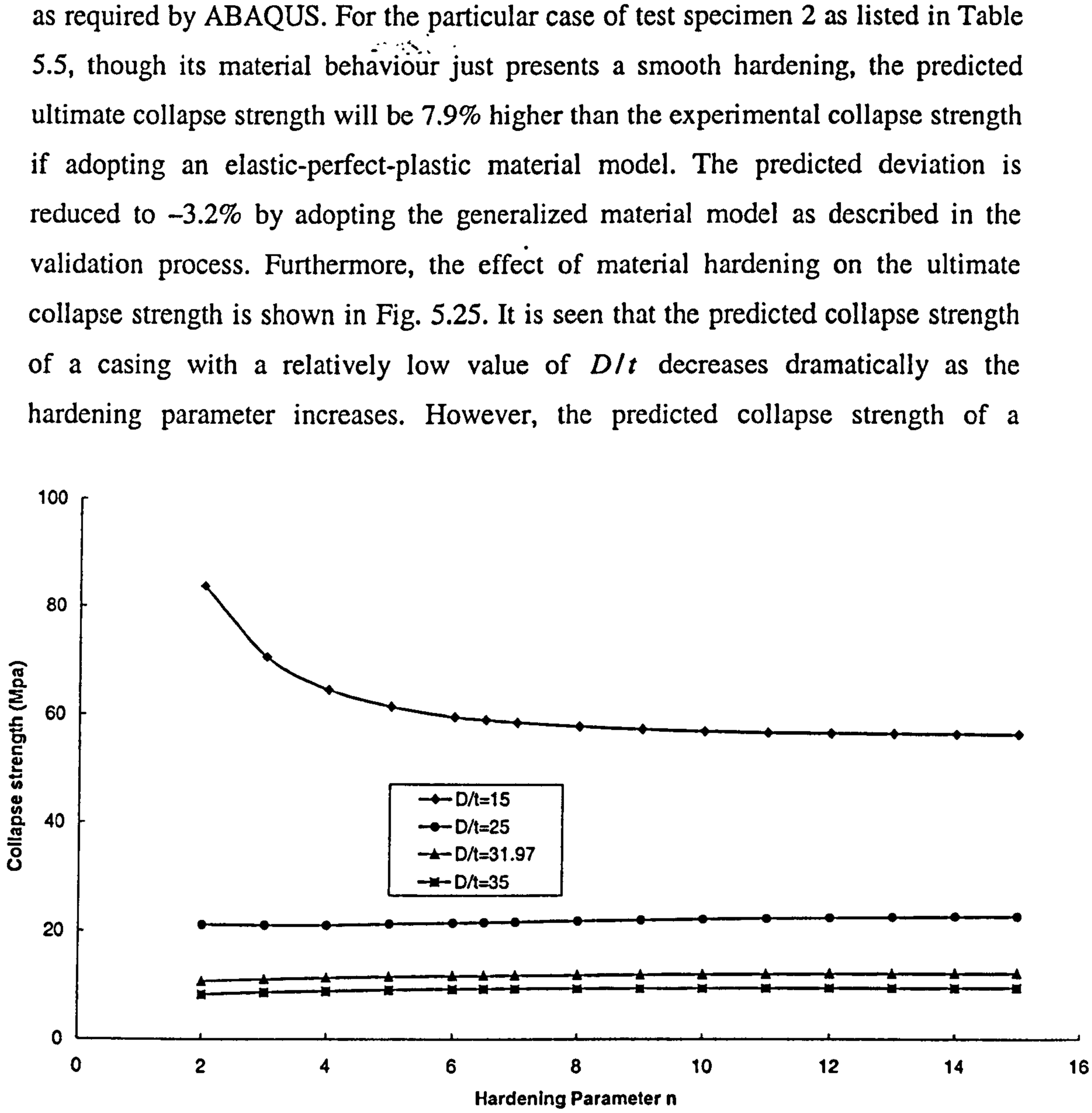

Fig. 5.25 Effect of material hardening on the ultimate collapse strength

relatively high D/t casing increases with the increase of the hardening parameter, though the effect of material hardening is relatively small for high D/t casings.

5.6.6 Effect Of Material Anisotropy

Manufacturing processes, such as drawing and rolling, tend to induce material anisotropy, which is more pronounced for casings with D/t values between 10 to 40. However, none of the previously published design equations for casing collapse so far is derived with the effect of anisotropy considered. For a majority of cases, experiments proved that, material anisotropy occurred in the form of a difference in the measured yield stress in the hoop and axial directions (Yeh and Kyriadies, 1988). In general, the yield stress in the axial direction is larger than that in the hoop direction. For a relatively thick walled casing, which does not collapse in the pure elastic collapse range, such an anisotropy directly affects the ultimate collapse strength. An anisotropy parameter λ is introduced to model the effect of material anisotropy, as expressed in Equation (5.52).

In the current FEM analysis, the effect of material anisotropy is carefully modelled by means of the parameter λ. In ABAQUS, anisotropy yield can be introduced by user-defined stress ratios that are described in Hill's potential function. In particular, an option of *POTENTIAL in connection with *PLASTIC is used to define an anisotropy yield model within ABAQUS. Therefore, the effect of material anisotropy on the ultimate collapse strength is obtained and shown in Fig. 5.26. It is clearly shown that material anisotropy directly affects the collapse strength. The presence of material anisotropy in general tends to reduce the collapse strength when $\lambda > 1$. Its effect is greater for casings with relatively low D/t values. However, it is interesting to note that for a D/t value of 22, the presence of material anisotropy is somehow beneficial. In addition, the prediction deviation between the experiment and FEM can be reduced greatly when the anisotropy parameter is considered in the program (Huang and Mihsein, 2000). It also proves that material anisotropy is a very important factor for casing failure in the plastic range. Thus, it is obvious that the best prediction

will be obtained if a stress-strain curve obtained from a circumferential test is used in the analysis.

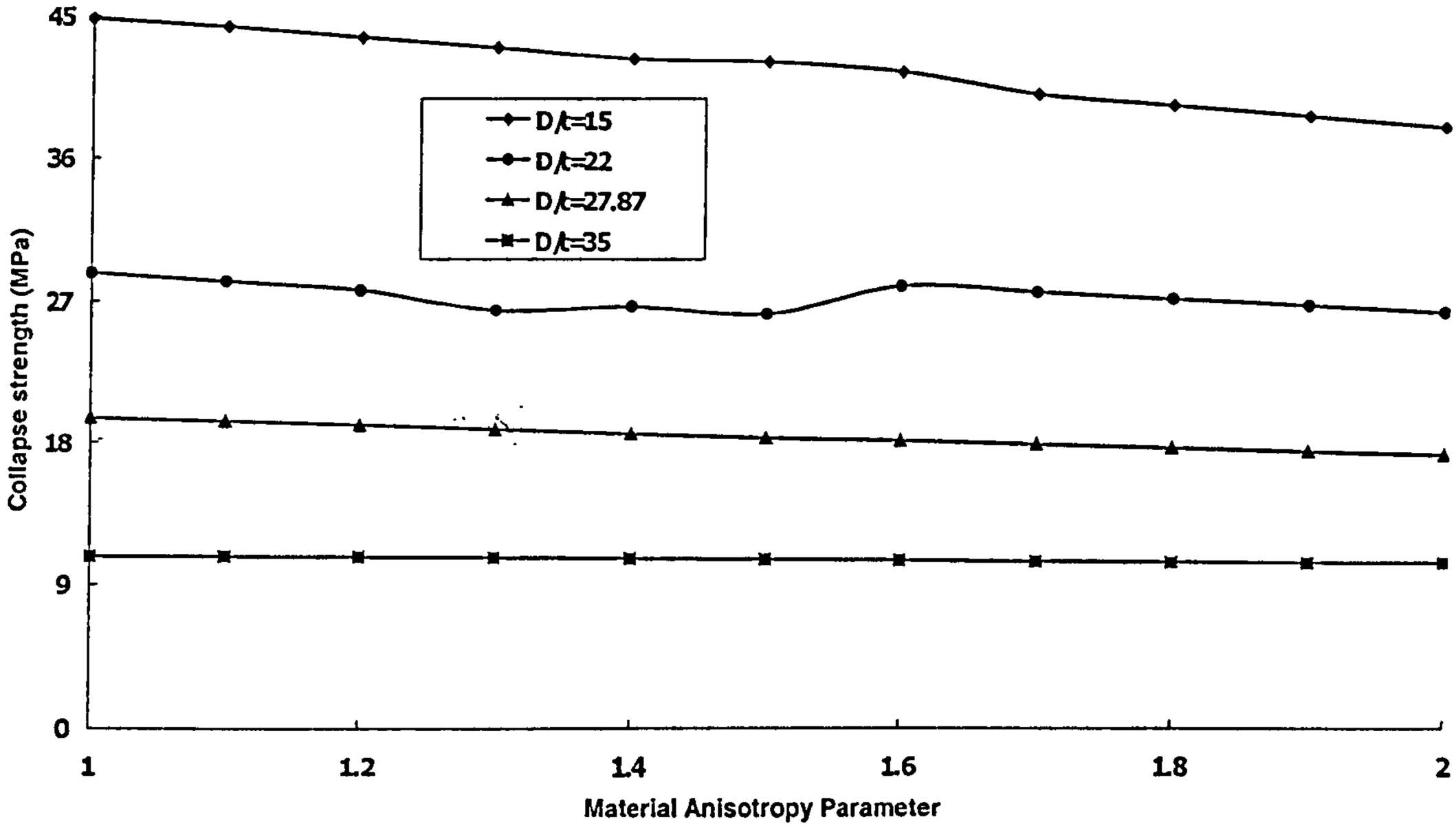

Fig. 5.26 Effect of material anisotropy on the ultimate collapse strength

5.7 Development Of A New Design Equation For Casing Collapse

In general, the collapse strength of a casing is calculated in accordance with the API equations given in the API Bulletin 5C3 (1992) in the casing design process for the oil and gas industry. During practical application, it is found that the API design equations for casing collapse design give widely varying failure probabilities over the D/t region of 10 to 40 for casings (Adams et al, 1998a and 1998b). For casings with relatively low D/t values, they give unconservative design (excessive risk); while for casings with relatively high D/t values, over-conservative designs are obtained (excessive safety). Under design leads to potential severe failure while over design leads to extra amount of high grade casing purchase. It is therefore, necessary to

develop more advanced design methods, in order to remedy the limitations of the widely used API design equations. On the basis of the elastic and plastic collapse theories, several design equations have been proposed for the collapse strength calculation in the casing design process, which are listed below for the purpose of evaluating a most suitable design equation in the limit state design of casing,

- Tamano et al (1983)
- Tokimasa and Tanaka (1986)
- Issa and Crawford (1993)

In the current study, detailed development of an advanced design equation for the limit state design of casing is described by evaluating the candidate equations. A fundamental selective principle is that the most suitable predictive equation gives the most accurate prediction from the conservative side in comparison with experimental data.

5.7.1 Review Of Collapse Design Equations

In four sets of predictive equations for casing collapse, the API collapse equation is the most complicated using the nominal rather than the actual dimensions. In particular, the API formulation is based on the equations of theoretical elastic collapse strength and yield onset strength, with a specially fitted expression for the plastic (actually elastic-plastic) collapse from a statistical analysis. The other three design equations all employ the theoretical elastic and yield onset equations within a global expression allowing for the effect of strength decrement. The coefficients for the decrement terms are generally obtained from an elastic-plastic finite element analysis. It is noted that Tamano et al (1983) also modifies the yield strength term to allow for the fact that the yield onset strength underestimates the actual collapse strength.

5.7.1.1 Calculation According To The API Equation

Four equations, i.e. elastic collapse, yield strength collapse, plastic collapse, and transition collapse, are proposed by the API for calculating the collapse strength of casings. The API recommends the use of a minimum elastic collapse strength value, which is equal to 71.25% (safety factor) of the theoretical values obtained from Equation (5.6) (Clinedinst, 1939). Given a Young's modulus of $E = 207$ GPa and a Poisson's ratio $\upsilon = 0.3$, the API elastic collapse strength, P_E, is calculated by,

$$P_E = \frac{3.237 \times 10^6}{(D/t)[(D/t)-1]^2} \tag{5.62}$$

The yield strength collapse pressure, P_Y, refers to the external pressure that generates the minimum yield stress on the inside wall of a casing, and is calculated using Equation (5.7). Although tests have indicated that the actual values of the collapse strength are in fact higher, the incipient yield of the material in the casing has been considered to be the decisive criterion by the API. No further correction factor has been introduced to take into account the geometrical deviations from the nominal dimensions.

The equation for the plastic collapse strength is found empirically, and is given by,

$$P_p = \sigma_y \left(\frac{A_{API}}{D/t} - B_{API} \right) - C_{API} \tag{5.62}$$

where the two parameters, A_{API} and B_{API}, are dependent on the respective yield points. A constant pressure, C_{API}, has been calculated statistically for each steel grade, in order to take into account the effect of tolerance limits of dimensions.

However, the introductions of the parameter C_{API} and the associated generalized decrease of the critical external pressure give rise to an anomaly. The curve corresponding to the plastic collapse strength, which depends on the respective value of the yield strength, no longer intersects the curve for the elastic collapse strength. Consequently, it is no longer possible to take the elastic collapse behaviour into consideration. This problem has been mathematically solved by the creation of an

artificial collapse type, i.e. transition collapse. The transition collapse strength, P_T, is calculated by:

$$P_T = \sigma_y \left(\frac{F_{API}}{D/t} - G_{API} \right) \tag{5.63}$$

where the constants F_{API} and G_{API} are dependent on the respective parameters A_{API} and B_{API}. The constants involved in the API equations are summarized below:

$$\begin{aligned}
A_{API} &= 28.762 + 1.5488\times10^{-3}\sigma_y - 1.6209\times10^{-9}\sigma_y{}^3 \\
B_{API} &= 0.26233 + 7.3400\times10^{-4}\sigma_y \\
C_{API} &= -32.13 + 0.30867\sigma_y - 1.5204\times10^{-5}\sigma_y{}^2 + 7.7804\times10^{-9}\sigma_y{}^3 \qquad (5.64)
\end{aligned}$$

$$F_{API} = \frac{3.237\times10^5 \left[\dfrac{3B_{API}/A_{API}}{2 + B_{API}/A_{API}} \right]^3}{\sigma_y \left[\dfrac{3B_{API}/A_{API}}{2 + B_{API}/A_{API}} - (B_{API}/A_{API}) \right] \left[1 - \dfrac{3B_{API}/A_{API}}{2 + B_{API}/A_{API}} \right]^2}$$

$$G_{API} = \frac{F_{API} B_{API}}{A_{API}}$$

It is noted that the above formulae for calculating the individual parameters have been converted for the use of SI units.

5.7.1.2 Calculation According To The Tamano Equation

Similar to the API calculation, Tamano et al (1983) adopts the theoretical elastic collapse Equation (5.6) for the calculation of elastic collapse strength. However, the customarily used yield onset collapse Equation (5.7) for an ideal thick walled casing is re-examined. A general yield strength is developed for the plastic collapse strength of an ideal casing as the yield onset collapse strength underestimates the actual collapse strength. The general yield strength means the critical external pressure needed when the whole section of a casing area turns into the plastic stress state. The general yield collapse strength under external pressure alone is derived from a finite element analysis:

$$P_{G0} = 2\sigma_y \frac{D/t-1}{(D/t)^2}\left[1+\frac{1.47}{D/t-1}\right] \tag{5.65}$$

The effects of the initial ovality, eccentricity and residual stress have been evaluated by regression analysis, and the following empirical formula for the determination of the collapse strength of a casings is obtained (Tamano et al, 1983):

$$P_T = \left[\frac{P_E + P_{G0}}{2} - \sqrt{\left[\frac{(P_E - P_{G0})^2}{4} + P_E P_{G0} H_T\right]}\right] \tag{5.66}$$

where, P_E and P_{G0} are the elastic collapse strength and the general yield collapse strength calculated from Equation (5.6) and Equation (5.65) and

$$H_T = 0.0808u + 0.00114\psi - 0.1412\frac{\sigma_{R\theta}}{\sigma_y} \tag{5.66}$$

where u, ψ and $\sigma_{R\theta}$ are ovality, eccentricity and residual stress.

5.7.1.3 Calculation According To The Issa Equation

The elastic collapse strength is calculated by the theoretical elastic collapse Equation (5.6) according to Issa and Crawford (1993). However, in contrast to an elastic-perfectly-plastic material assumed in the derivation of the Tamano equation, a strain hardening elastic-plastic material is employed in the derivation of the Issa equation. Similar to applying a general yield collapse strength in the derivation of Tamano equation, an elastic-plastic collapse strength, P_{EP}, is proposed to replace the yield onset collapse strength calculated from Equation (5.7), which is:

$$P_{EP} = \frac{\sigma_y (D/t-1)}{(D/t)^2}\left[\frac{A_{I1}}{1+\left[A_{I2}+A_{I3}(\sigma_y/E)\right](D/t)}\right] \tag{5.67}$$

with

$$A_{I1} = 7.0333$$
$$A_{I2} = 0.1295 \qquad (5.68)$$
$$A_{I3} = 12.3298$$

Finite element analyses were performed to obtain a collapse equation for the nearly perfect casings. Its name originates from the fact that a limit load type of collapse strength is obtained with a small initial imperfection. After regression analysis, the best function to describe the collapse strength of a nearly perfect casing is found to have the following expression:

$$P_{IP} = \left[\frac{1}{2}(P_E + P_{EP}) - \frac{1}{2}\sqrt{(P_E - P_{EP})^2}\right] \qquad (5.69)$$

where P_{IP} represents the collapse strength of a nearly perfect casing, P_E is the classical elastic collapse pressure from Equation (5.6) and P_{EP} is the elastic-plastic collapse strength calculated from Equation (5.67).

Reduction functions are constructed due to ovality and eccentricity based on the finite element analyses. The ovality reduction is derived by constructing a series of allowable ovalities in accordance with the API specification (1992), which has the following form:

$$g_I\left(u, \frac{D}{t}\right) = \frac{1}{1 + \left[B_{I1} + B_{I2}\left(\frac{D}{t}\right)\right] u^{B_{I3}}} \qquad (5.70)$$

with $B_{I1} = 0.1648$, $B_{I2} = 0.5972$ and $B_{I3} = 0.7618$.

In addition, the eccentricity reduction function is fitted with a simple polynomial expression by regression analysis, which is expressed as:

$$h_I(\psi) = (1 - \psi)(1 + C_{I1}\psi + C_{I2}\psi^2) \qquad (5.71)$$

with $C_{I1} = 0.8123$ and $C_{I2} = -1.1272$.

Therefore, the ultimate collapse strength of a casing under external pressure is calculated by:

$$P_I = P_{IP} \times g_I\left(u, \frac{D}{t}\right) \times h_I(\psi) \qquad (5.72)$$

5.7.1.4 Calculation According To The Tokimasa Equation

According to Tokimasa and Tanaka (1986), The elastic collapse strength of a perfect round tube is calculated from Equation (5.2), while the plastic collapse strength is obtained by finite element analysis as:

$$P_P = 2\sigma_{0.04}\,(D/t-1)/(D/t)^2 \tag{5.73}$$

where $\sigma_{0.04}$ corresponds to the proof stress of offset strain of 0.04. It is noted that by using $\sigma_{0.04}$, the effect of work hardening has been considered implicitly.

Including the effects of geometric imperfections and residual stress, the Tokimasa equation is expressed as follows:

$$P_{cr} = P_0 \times f(u) \times f(\psi) \times f(\sigma_{R\theta}) \tag{5.74}$$

where P_0 is the minimum value of the elastic and plastic collapse strength. In addition, the reduction functions $f(u)$, $f(\psi)$ and $f(\sigma_{R\theta})$ are listed in Table 5.7.

Table 5.7 Summary of the Tokimasa equation (1986)

Factors	Elastic Collapse	Plastic Collapse
D/t	$P_E = \dfrac{2E}{1-\upsilon^2}(t/D)^3$	$P_P = 2\sigma_{0.04}\dfrac{D/t-1}{(D/t)^2}$
Ovality	$f(u) = \dfrac{A-\sqrt{A^2-4B}}{2}$ $A = 1+1.5u(D/t-1)+B$ $B = P_p/P_E$	$f(u) = \{1-r(1-P_C/P_P)\}$ $r = 0.0856D/t-1.14$ $P_C = 2P_P/\left(A+\sqrt{A^2-4B}\right)$
Eccentricity	$f(\psi) = 1$	$f(\psi) = 1-\xi/2$
Residual stress	$f(\sigma_{R\theta}) = 1$	$(a)\ \sigma_{R\theta} < 0 \qquad f(\sigma_{R\theta}) = d_1$ $(a)\ \sigma_{R\theta} > 0 \qquad f(\sigma_{R\theta}) = \min(d_1, d_2)$ $d_1 = 1+0.8\dfrac{\sigma_{R\theta}}{\sigma_y}$ $d_2 = \left[2(1-0.8\sigma_{R\theta}/\sigma_y\right]/\left\{1+(1-2t/D)^2\right\}$

5.7.2 Evaluation Of Collapse Design Equations

Although the above collapse design equations have been proposed for the calculation of collapse strength by considering the influences of the dimensional imperfections and residual stress, the question as to whether it is safe to use these equations for a specific casing design is still uncertain. An evaluation of these empirical equations using available experimental casing collapse data can give a confident answer. Therefore, detailed comparisons have been conducted between these predictions from different design equations and the full scale experimental data.

It is found that almost all of the predictions from the Tamano equation are unconservative as shown in Fig. 5.27. The potential risk in using the Tamano equation for casing design is unacceptably high. The possible reason for its high risk arises from the fact that the material model is assumed to be isotropic, elastic-perfectly-plastic without material hardening. To make it worse, the yield stress in the circumferential direction is assumed to be 5% larger than that in the axial direction, which gives rise to the collapse strength. Another reason may come from the assumption that a general yield collapse strength is taken when the whole casing

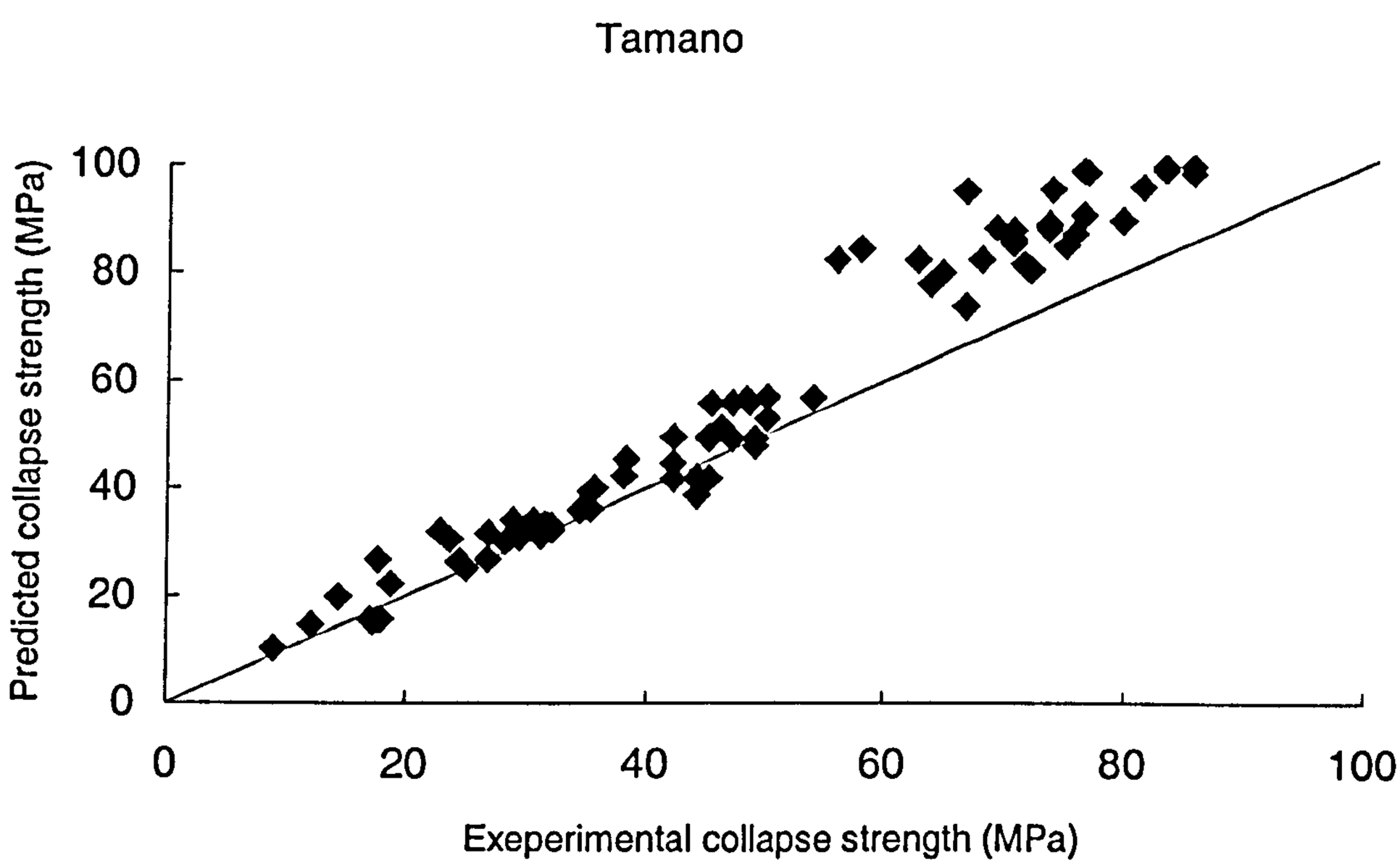

Fig. 5.27 Comparison between experiments and predictions (the Tamano equation, 1983)

section begins to yield. However, these assumptions may not be valid for the problem of actual casing collapse. Therefore, the Tamano equation overestimates the collapse strength of a realistic casing.

The predictions from the Issa and Tokimasa equations are relatively closer to the experimental data with approximately half the predictions conservative and half unconservative as shown in Fig. 5.28 and Fig. 5.29, compared with those of the Tamano equation. It is observed that the Issa equation is better than the Tokimasa equation with a smaller deviation from the experiments. Though an elastic-perfectly-plastic material model is used in the derivation of the Tokimasa equation, the effect of material hardening on the collapse strength is considered implicitly using a proof stress of $\sigma_{0.04}$, which may be the reason why its predictions are more conservative than the Tamano equation. Different from the Tamano and Tokimasa equations, the Issa equation is developed on the basis of a strain hardening elastic-plastic material model fitted from tensile tests of the axial properties of commercial casing, which makes its predictions closer to the experimental data than those of the Tamano and Tokimasa equations. However, its material model is still assumed to be isotropic and the axial material properties are used to derive the Issa equation rather than the circumferential material properties.

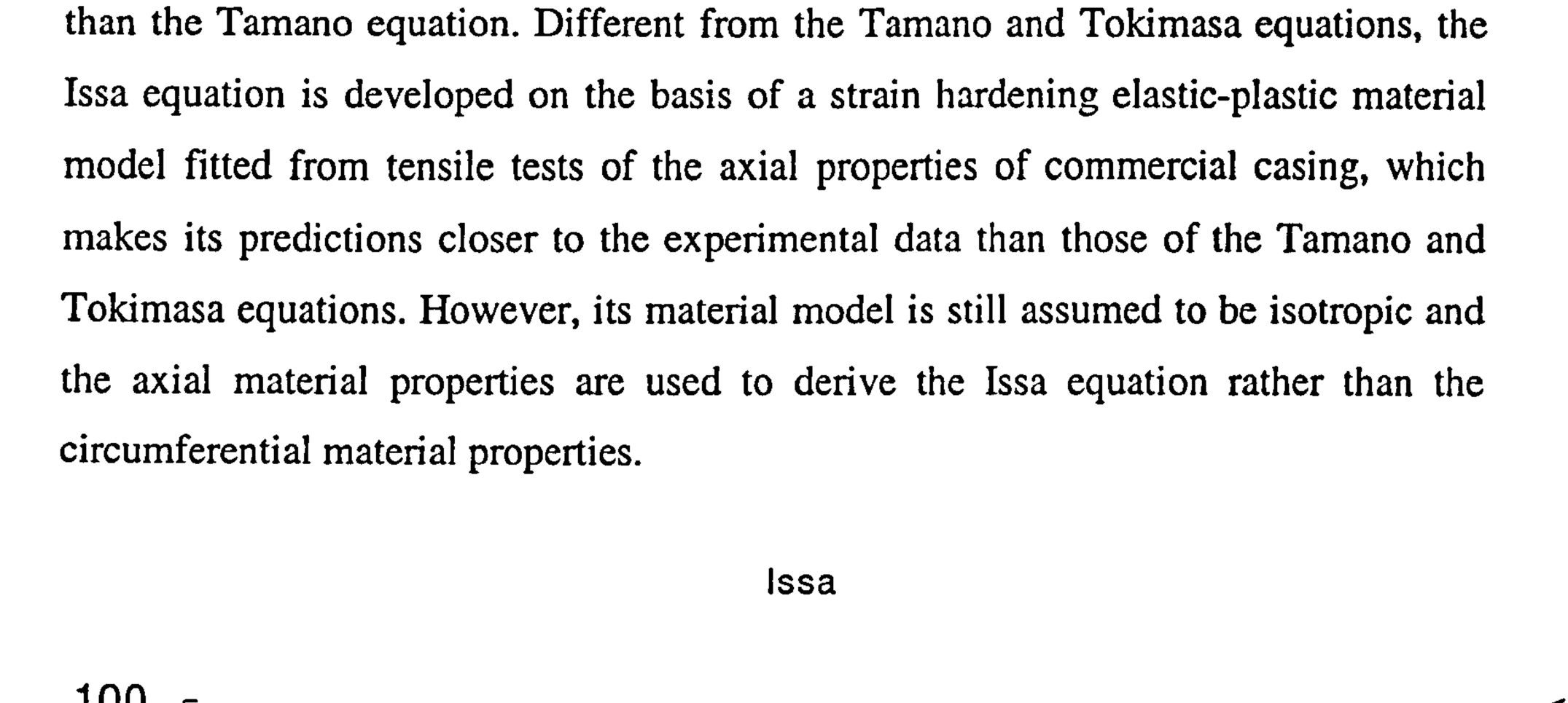

Fig. 5.28 Comparison between experiments and predictions (the Issa equation, 1993)

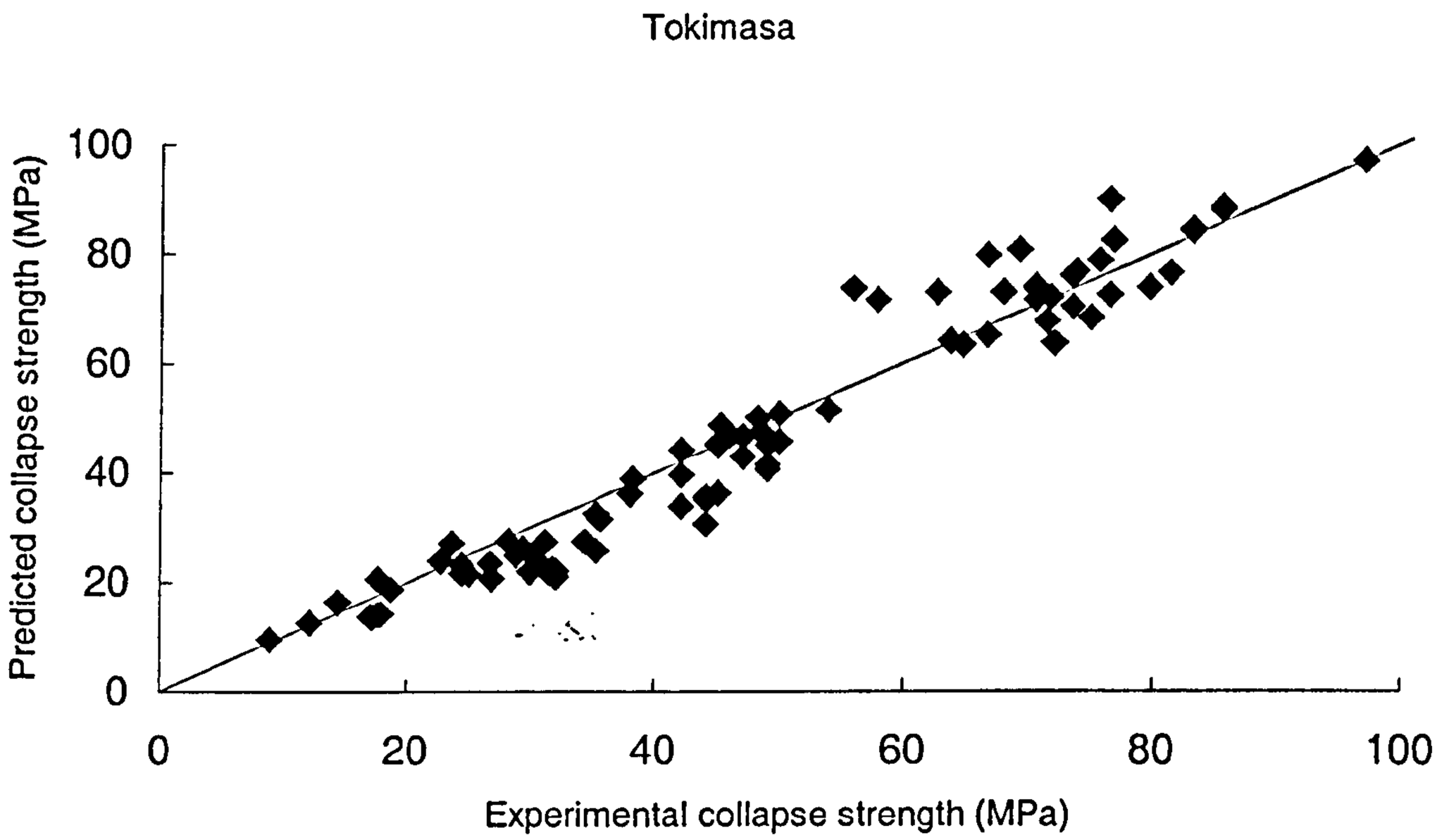

Fig. 5.29 Comparison between experiments and predictions (the Tokimasa equation, 1986)

The predictions from the API equations for the collapse casing are compared with experimental data as shown in Fig. 5.30. It is found that it is conservative in the high collapse strength region, while unconservative in the relatively low collapse strength region. In addition, the API equation is the most complicated system among the predictive equations, derived from statistical analysis rather than theoretical deduction.

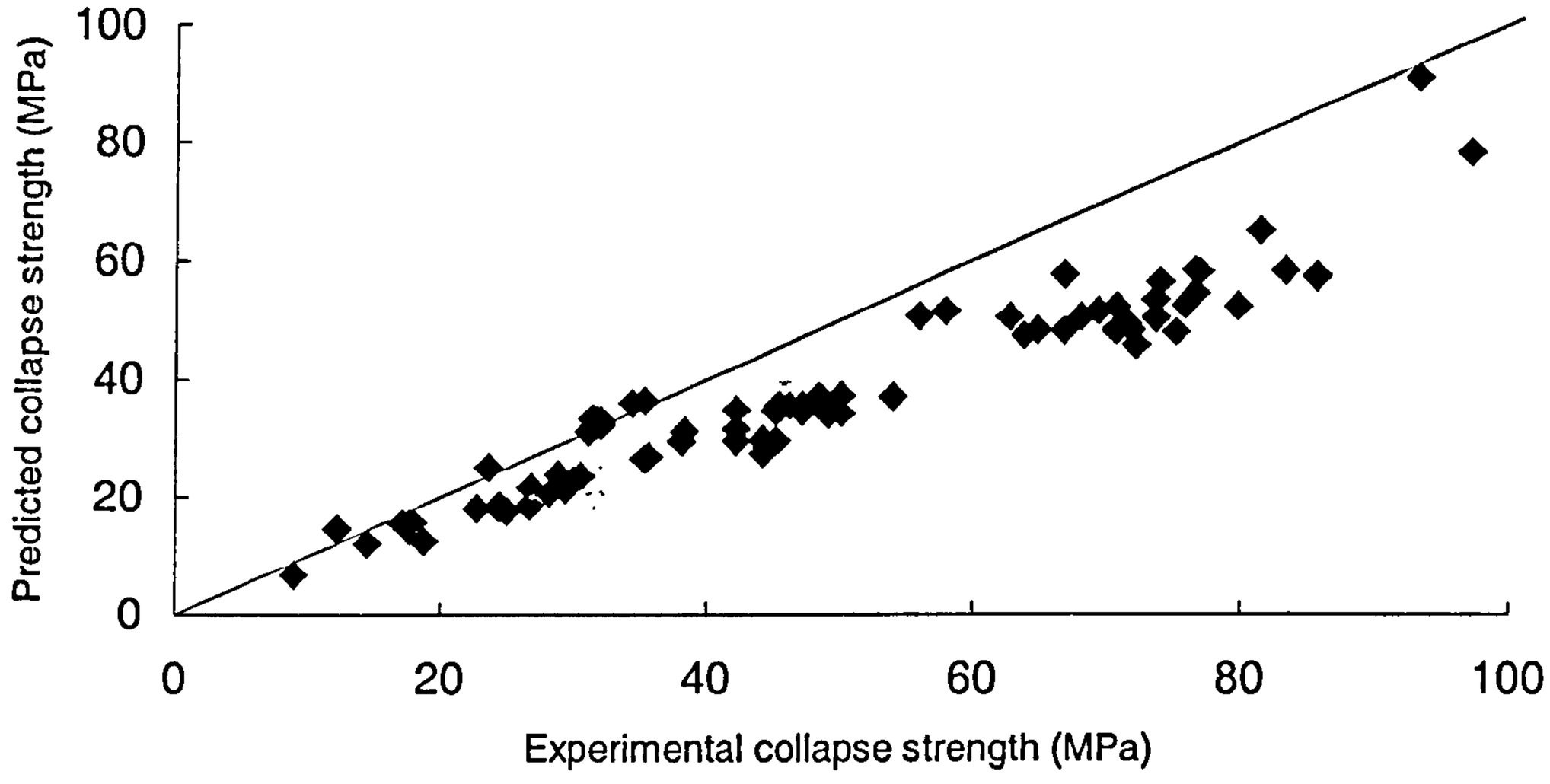

Fig. 5.30 Comparison between experiments and predictions (the API equation, 1992)

5.7.3 Derivation Of Implicit Collapse Design Equation

From the evaluation of the existing design equations for casing collapse, it is necessary to establish a new design equation for casing collapse. Based on the generalized material model developed from experimental data, a large number of finite element analyses have been performed to investigate the casing collapse strength of different grades of casings. The interested yield stress range is from 40 ksi (276 MPa) to 125 ksi (862 MPa), i.e. from grade K40 to grade P125. The D/t range (10 to 40) covered in this study focuses on relatively thick walled casings.

The predictions from simulation are shown in Fig. 5.31. As expected, the predicted collapse strength is independent of material yield stress and corresponds closely to the elastic collapse equation for casings with relatively high D/t values. While for casings with relatively low D/t ratios, the predicted collapse strength depends strongly on the material yield strength. In the region between the elastic collapse and

elastic-plastic collapse, each of the predicted curves undergoes a transition at the onset of plasticity as a sudden change of curve slope. It is reasonable to assume that every curve in Fig. 5.31 has the same mathematical expression. The problem of determining this expression remains a non-linear regression analysis, however, an appropriate transformation of the variables can make the relationship between the transformed variables linear. It is found that the logarithm transformation of the ratio of predictions from FEM to expression $\frac{2\sigma_y(D/t-1)}{D/t}$ is almost linear to the abscissa D/t. Thus, the problem left is to determine the two variables associated with the linear line.

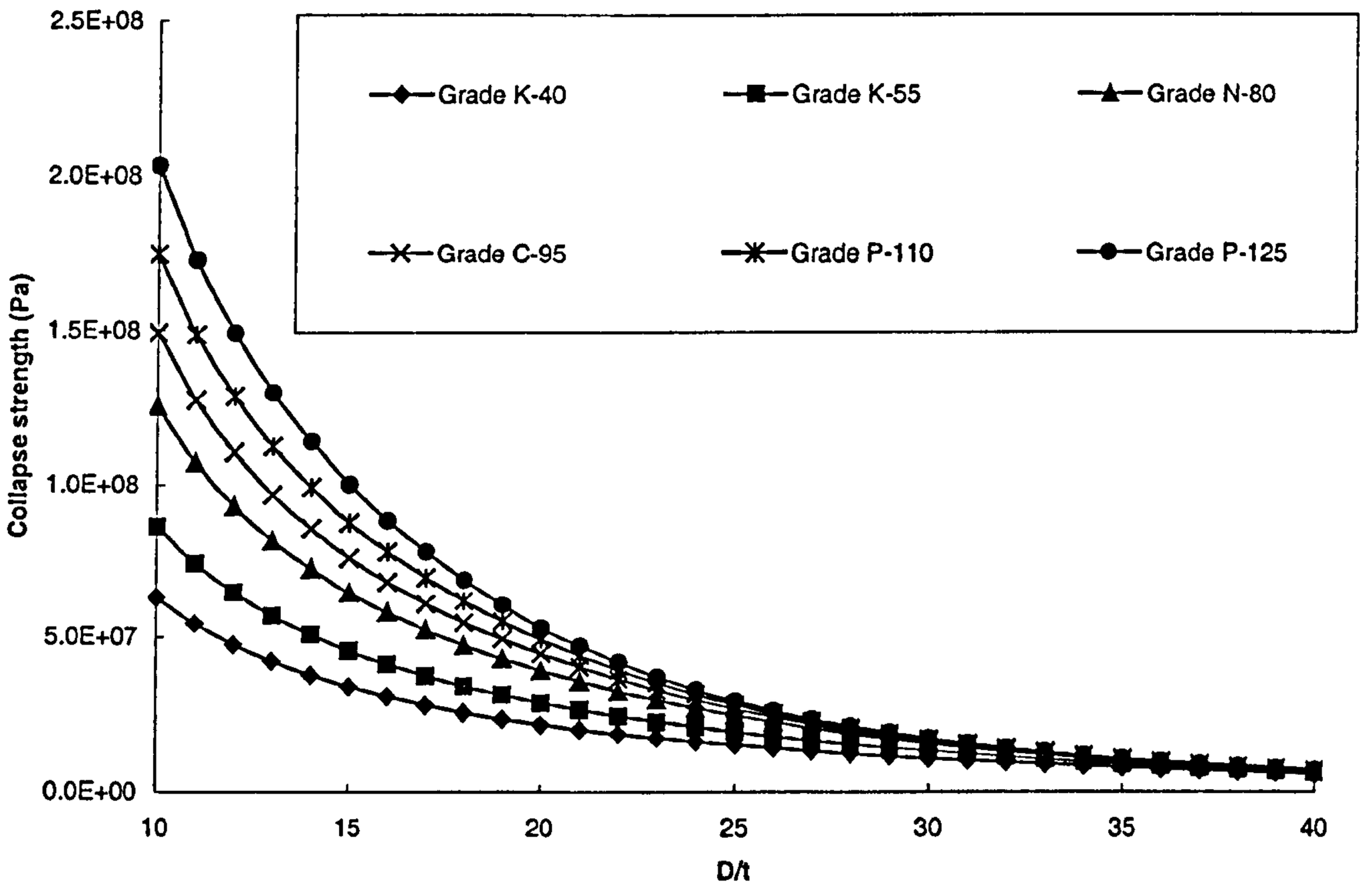

Fig. 5.31 Predicted collapse strength of casing of grade K40 to P125

There are two different methods to determine the expression of a straight line from the sample points, i.e. the least square method and the minimum variance method. Fortunately, both methods yield exactly the same solution for a linear relationship. Therefore, the variables of the linear relationship can be determined. It is not

surprising that the two variables associated with the linear relationship have their own relationship against other parameters. After carefully recalculating the transformation, it is found that the two variables are approximately linear to the variable σ_y / E. Using the least square method, these variables are determined. Therefore, the proposed collapse equation with imperfections implicitly considered is expressed as shown below (Huang et al, 2000):

$$P_{est} = \frac{2\sigma_y (D/t - 1)}{D/t} e^{(h_1 + h_2 D/t)}$$

$$h_1 = 167.6393 \frac{\sigma_y}{E} - 2.25314 \qquad (5.75)$$

$$h_2 = -10.57427 \frac{\sigma_y}{E} - 0.0571617$$

A comparison has been performed against available test data as shown in Fig. 5.32. It is shown that the predictions from the new design Equation (5.75) are wholly conservative as expected. In addition, the predictions are more accurate than the predictions from the API equation in the relatively low collapse strength region as shown in Fig. 5.33. However, the new design equation is relatively too conservative in the very high collapse strength region, corresponding to a casing with an approximate D/t value less than 15, which arises from the approximations made in the derivation. Finally, the ranges of the parameters in the foregoing Equation (5.75) where it can be applied are given,

$$10^{-4} \le u \le 2.74 \times 10^{-3}$$

$$8.5 \times 10^{-3} \le \xi \le 8.4 \times 10^{-2} \qquad (5.76)$$

$$277.8MPa \le \sigma_y \le 861.8MPa$$

In conclusion, this new empirical equation is simple to use, conservatively closer to the experimental data. For those casing design engineers who are familiar with the API design equations, it is particularly useful because they do not have the imperfection data in most circumstances. However, the effects of imperfections are considered implicitly, which make its predictions more conservative for those casings with very small imperfections. Therefore, it is necessary for a further refinement of the empirical design equation by considering the imperfections effect explicitly, which is described in the following section.

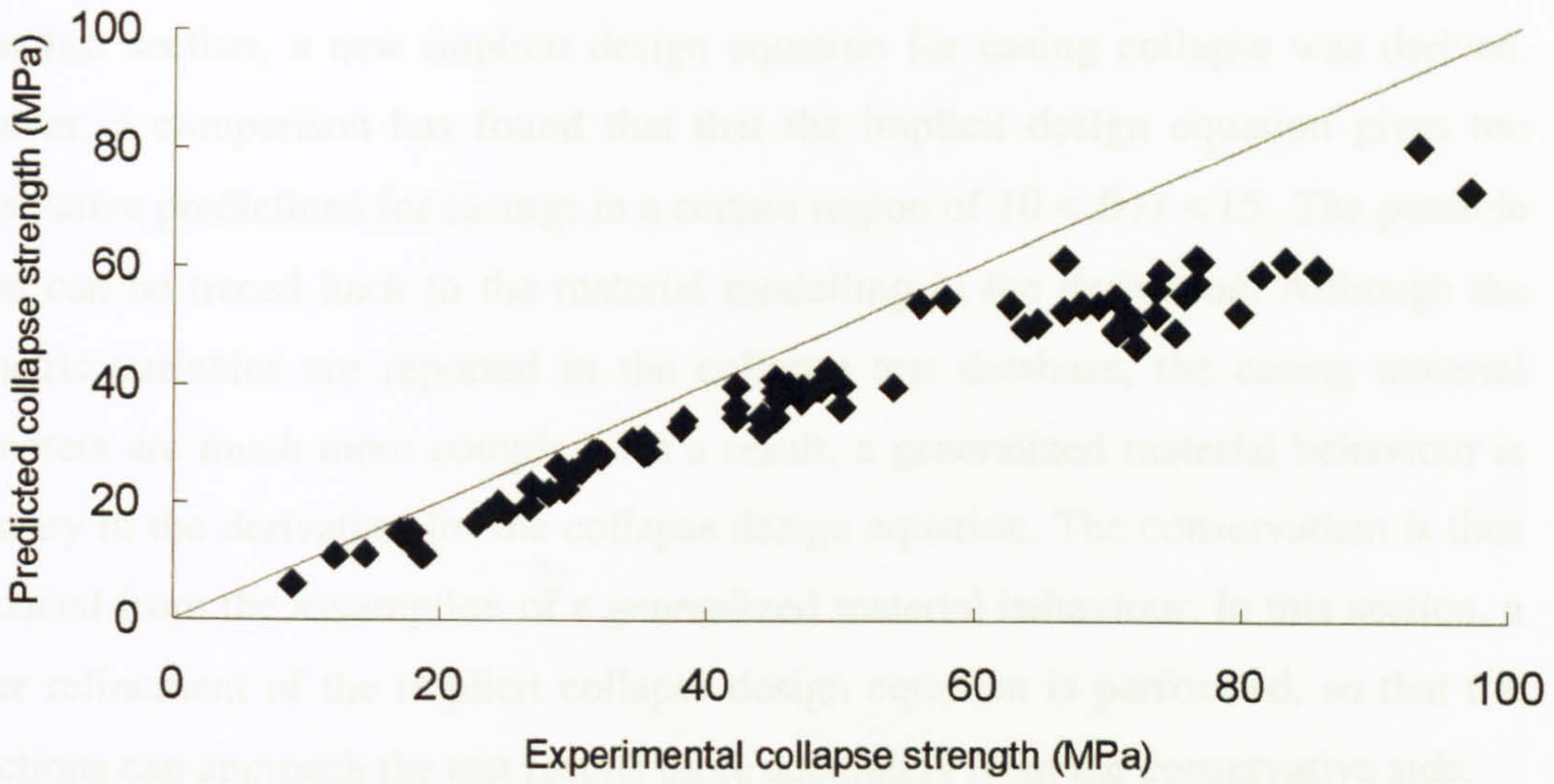

Fig. 5.32 Comparison between experiments and predictions from Equation (5.75)

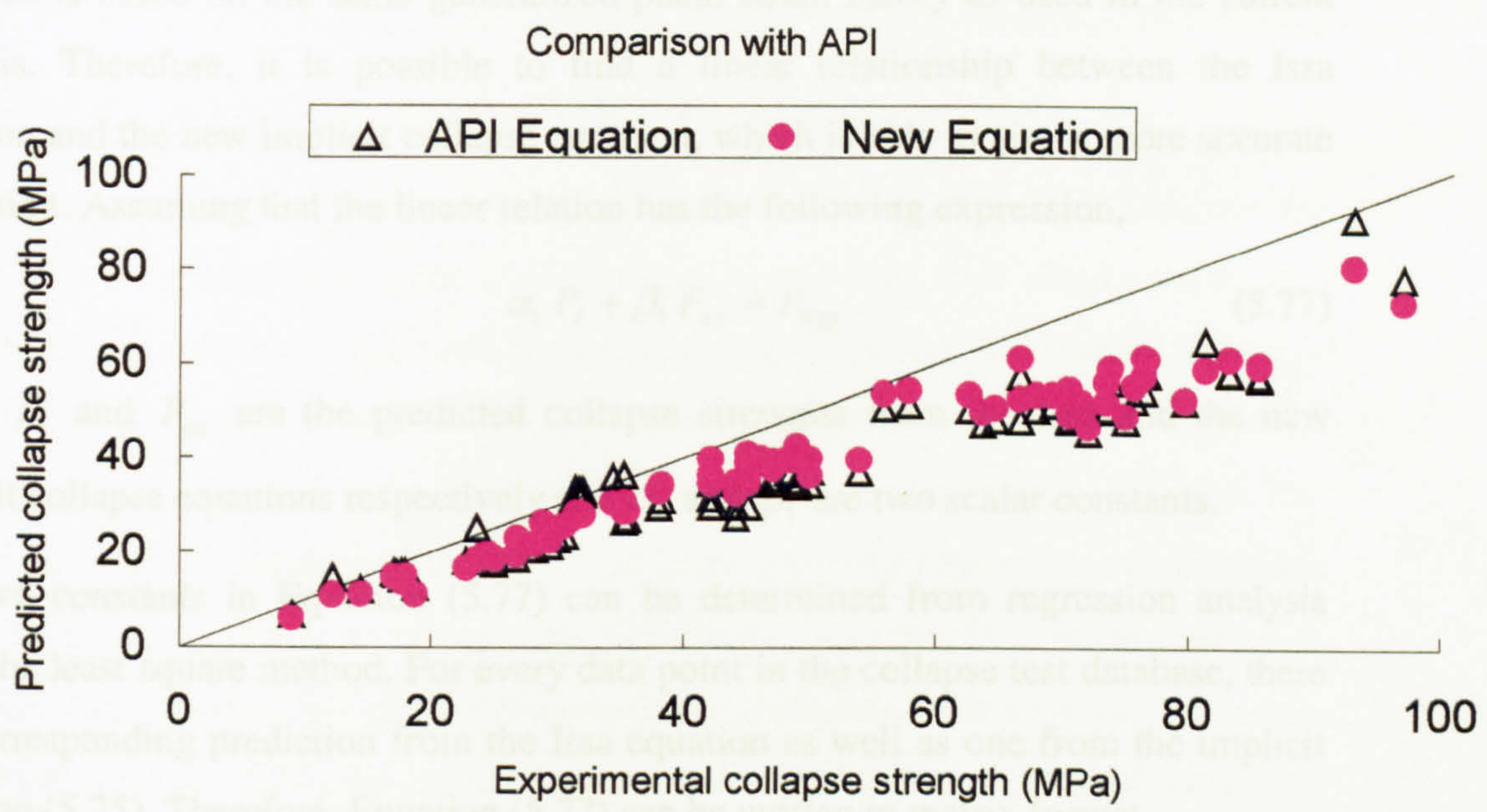

Fig. 5.33 Comparison between the implicit Equation (5.75) and API equation

5.7.4 Refinement Of The Collapse Design Equation

In the last section, a new implicit design equation for casing collapse was derived. However, a comparison has found that that the implicit design equation gives too conservative predictions for casings in a certain region of $10 < D/t < 15$. The possible reason can be traced back to the material modelling in the derivation. Although the geometric variables are reported in the collapse test database, the casing material parameters are much more complex. As a result, a generalized material behaviour is necessary in the derivation for the collapse design equation. The conservatism is thus introduced from the assumption of a generalized material behaviour. In this section, a further refinement of the implicit collapse design equation is performed, so that the predictions can approach the test results more accurately from the conservative side.

It is noted that from the evaluation of existing collapse design equations as described in Section 5.7.2, the Issa Equation (1993) gives the best predictions in all of the 4 previous published predictive equations. In addition, the derivation of the Issa equation is based on the same generalized plane strain theory as used in the current analysis. Therefore, it is possible to find a linear relationship between the Issa equation and the new implicit collapse equation, which is able to give a more accurate prediction. Assuming that the linear relation has the following expression,

$$\alpha_1 P_I + \beta_1 P_{est} = P_{Exp} \tag{5.77}$$

where P_I and P_{est} are the predicted collapse strengths from the Issa and the new implicit collapse equations respectively and α_1 and β_1 are two scalar constants.

The two constants in Equation (5.77) can be determined from regression analysis using the least square method. For every data point in the collapse test database, there is a corresponding prediction from the Issa equation as well as one from the implicit Equation (5.75). Therefore, Equation (5.77) can be written in matrix format,

$$\left[P_{Issa} \quad P_{Huang}\right]_{133x2} \begin{Bmatrix} \alpha_1 \\ \beta_1 \end{Bmatrix}_{2x1} = \left\{P_{Exp}\right\}_{133x1} \tag{5.78}$$

where the dimension length of 133 is after the total number of experimental data points used.

If matrix $[P_I \quad P_{est}]_{133x2}$ is inverted,

$$\begin{Bmatrix} \alpha_1 \\ \beta_1 \end{Bmatrix} = [P_I \quad P_{est}]^{-1} \{P_{Exp}\} \tag{5.79}$$

Because Equation (5.78) is over-determined, the inverse of $[P_I \quad P_{est}]_{133x2}$ cannot be calculated in a conventional way, but has to be obtained from its least square solution to account for measurement errors. According to Hilderbrand (1965), Nobel and Daniel (1988), the inverse can be calculated according to,

$$[P_I \quad P_{est}]^{-1} = \left([P_I \quad P_{est}]^T [P_I \quad P_{est}]\right)^{-1} ([P_I \quad P_{est}]) \tag{5.80}$$

Therefore,

$$\begin{Bmatrix} \alpha_1 \\ \beta_1 \end{Bmatrix} = \begin{Bmatrix} 0.4951 \\ 0.5647 \end{Bmatrix} \tag{5.81}$$

The explicit collapse design equation is expressed as follows,

$$P_c = 0.4951\, P_I + 0.5647\, P_{est} \tag{5.82}$$

where P_c is the predicted collapse strength. P_I is calculated according to Equation (5.72) and P_{est} is calculated according to Equation (5.75).

To validate the refined equation, comparison has been performed between the predictions from Equation (5.82) and the experimental data. It is clearly shown that the predictions accurately approach the experimental data from the conservative side as expected as shown in Fig. 5.34. Furthermore, comparison has been made with predictions from the API equations for the same collapse database as shown in Fig. 5.35. It is clearly demonstrated that all of the predictions from the refined equation are closer to the test data than those from the API equations. In the D/t range of interest, the refined Equation (5.82) gives a more accurate prediction with a smaller deviation. Compared to Fig. 5.32, the conservatism associated with the implicit empirical Equation (5.75) has been greatly reduced. In addition, by including the Issa equation in the refined collapse design equation, the parameters of imperfections are expressed explicitly. Therefore, if the imperfections are known, the refined Equation (5.82) should be used in the design of casing collapse. The implicit empirical Equation (5.75) should be used when those data are not available.

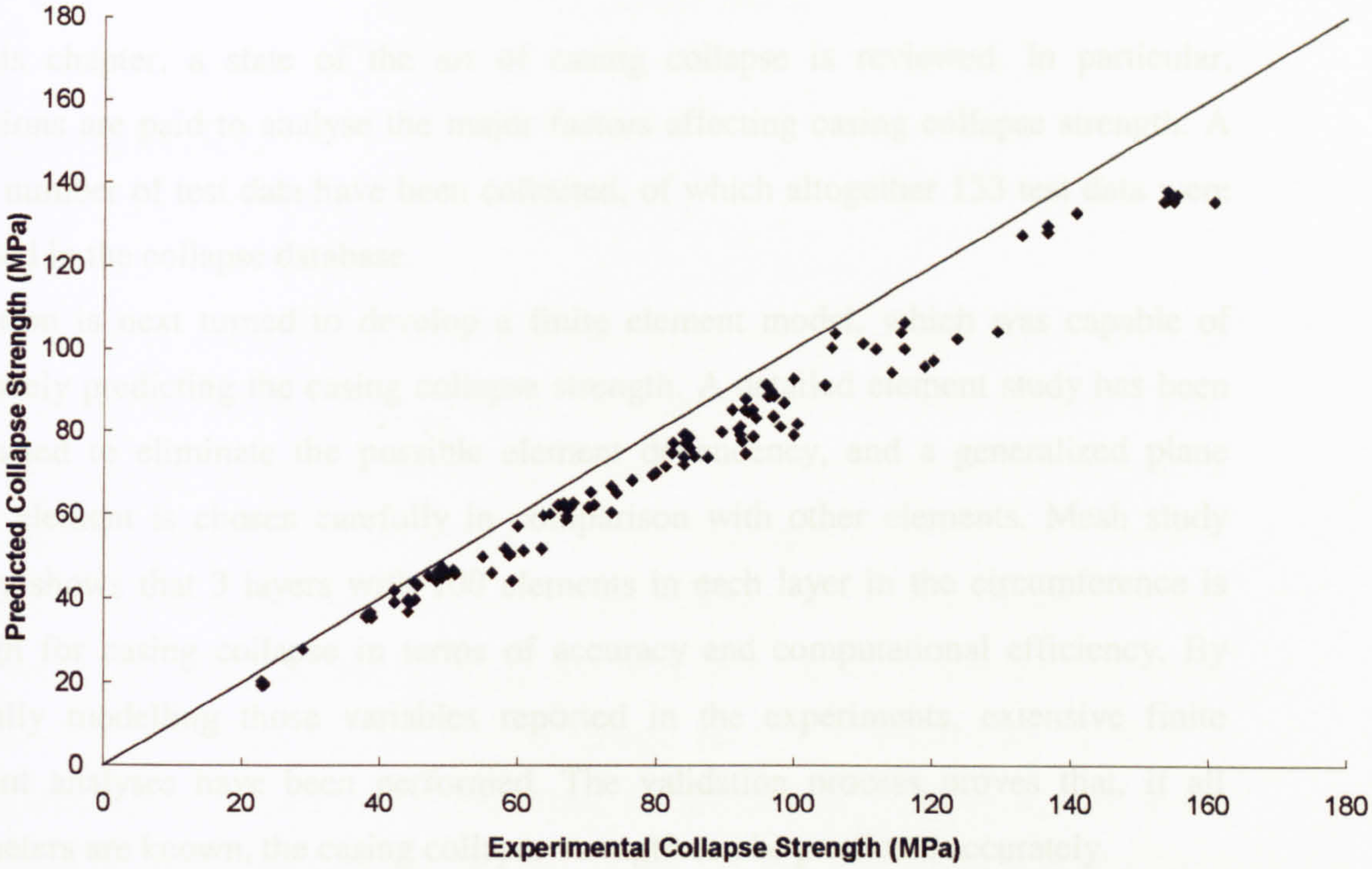

Fig. 5.34 Comparison between experiments and predictions from Equation (5.82)

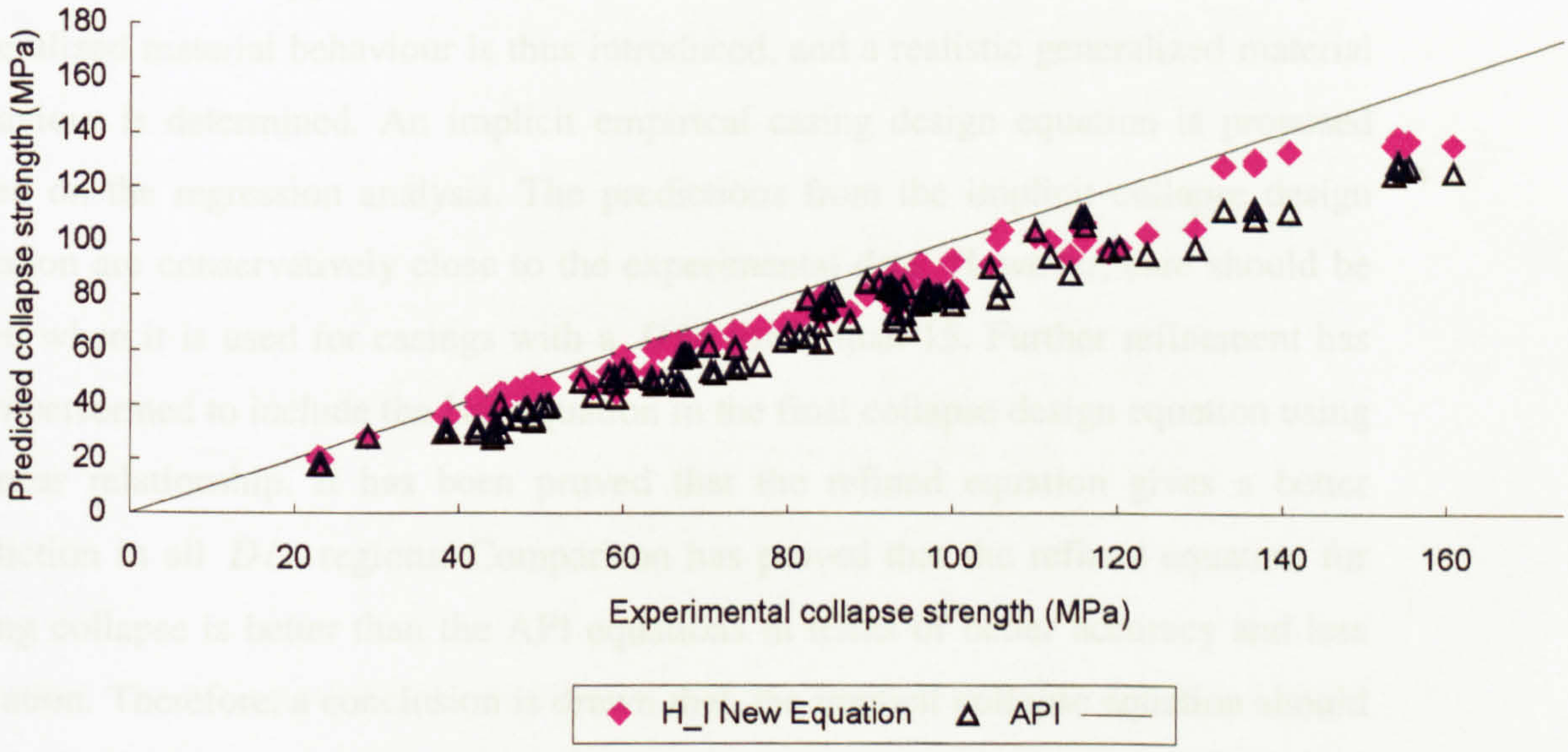

Fig. 5.35 Comparison between the explicit equation and API equation

5.8 Summary

In this chapter, a state of the art of casing collapse is reviewed. In particular, attentions are paid to analyse the major factors affecting casing collapse strength. A large number of test data have been collected, of which altogether 133 test data were selected in the collapse database.

Attention is next turned to develop a finite element model, which was capable of accurately predicting the casing collapse strength. A detailed element study has been conducted to eliminate the possible element dependency, and a generalized plane strain element is chosen carefully in comparison with other elements. Mesh study clearly shows that 3 layers with 100 elements in each layer in the circumference is enough for casing collapse in terms of accuracy and computational efficiency. By carefully modelling those variables reported in the experiments, extensive finite element analyses have been performed. The validation process proves that, if all parameters are known, the casing collapse strength can be predicted accurately.

The capabilities of previously published collapse equations have been assessed using the available test data in terms of an accurate prediction. It is found that the Issa equation gives the best predictions with the least deviation. However, almost half of the Issa predictions approach the experimental data from the unsafe side. A concept of generalized material behaviour is thus introduced, and a realistic generalized material behaviour is determined. An implicit empirical casing design equation is proposed based on the regression analysis. The predictions from the implicit collapse design equation are conservatively close to the experimental data. However, care should be taken when it is used for casings with a D/t lower than 15. Further refinement has been performed to include the Issa equation in the final collapse design equation using a linear relationship. It has been proved that the refined equation gives a better prediction in all D/t regions. Comparison has proved that the refined equation for casing collapse is better than the API equations in terms of better accuracy and less deviation. Therefore, a conclusion is drawn that, the implicit collapse equation should be used when imperfection data are not available; the explicit collapse equation should be used when imperfection data become available.

Chapter 6

Casing Burst

6.1 Introduction

Burst strength is another important consideration in the design of casings, which is defined as the maximum value of internal pressure required to cause the steel casing to fail. Present-day procedures for the burst design of well casings are still based on a deterministic working stress design methodology. This approach is very conservative and, leads to actual safety margins against burst that vary widely over different grades of steels. In this approach, the casing is designed such that the nominal casing burst strength is higher than the worst case design load. The limitations of such a deterministic design have been described in Chapter 2. Improved and novel approaches towards casing design call for models that can accurately predict a burst failure as opposed to a conservative assessment procedure.

Progress has been made towards developing improved burst models for regular casings, considering the initial imperfections. Whereas conventional burst design makes use of a conservative estimate of the casing burst strength, applying limit state design techniques require the availability of a reliable casing burst model, which is capable of predicting the ultimate burst strength. A limit state design equation for casing burst is thus developed on the basis of that casing burst model. There are two modes of burst failure, ductile instability and brittle fracture. In practice, the chance for a brittle fracture is very rare. Therefore, only ductile burst failure will be investigated in this research. In general, the ultimate burst strength is attained as the plastic zone spreads under increasing internal pressure and the outer fibre of the casing yields.

In the next section, a set of simple criteria is described to determine whether a given casing can be designed for ductile burst failure or not. Attention is next turned to the review of the equations used to predict the ultimate casing burst strength of ductile failure, which relates casing geometry and material behaviour to the ultimate burst

strength. Finite element analyses have been performed for casing burst, which is validated by extensive comparisons with experiments. Furthermore, a new burst design equation is proposed for the limit state design of casing burst after an assessment of previously proposed burst design equations.

6.2 Criteria For Ductile Burst Failure

Although the external environment of a casing may impose an important effect, whether a ductile or brittle failure will occur depends basically on the casing material. In a practical design situation, a designer must have a set of simple criteria to decide which design procedure should be used. A brief description of these criteria is presented in this section, which is based on the empirical relationships between Charpy impact energy and the critical stress intensity for a material. The criteria are supported with J_1 integral measurements and calculations for all specimens tested by Paslay et al (1998).

Studies in fracture mechanics have shown that the stress intensity factor, K_{1C}, is a parameter which can be correlated with brittle fracture (Rice, 1968; Roberts and Newton, 1981). Therefore, the development of a ductile/brittle criterion should relate to this measurement. There have been many efforts devoted to establishing a relation between K_{1C} values and the easily and commonly measured Charpy V-notch impact value, CVN. As a result, two criteria are derived below. One is based on a correlation between K_{1C} and CVN in the transition zone of CVN versus temperature plots. The second criterion is based on a correlation between K_{1C} and CVN as well as yield strength σ_y for the upper shelf of CVN versus temperature plots. These correlations are expressed by (Tallin et al,1998) as:

$$K_{IC} = 9.35(CVN^{0.63}) \tag{6.1}$$

$$\left(\frac{K_{IC}}{\sigma_y}\right)^2 = 4.0\left(\frac{CVN}{\sigma_y} - 0.1\right) \tag{6.2}$$

It is noted that Equations (6.1) and (6.2) are empirical and the terms are not dimensionally consistent.

It is important to establish values for K_{IC} corresponding to the above equations, which is accomplished by using the concept of a plastic zone size. The maximum normal stress at the tip of a two dimensional, plane strain crack whose plane is perpendicular to a uniform far field tensile stress is $K_I/\sqrt{2\pi r}$ (Rice, 1968). By setting this stress equal to the yield stress σ_y and K_I to K_{IC}, a value of radius, r_p, may be found, which is a rough estimate of the plastic zone size as follows,

$$r_p = \frac{1}{2\pi}\left(\frac{K_{IC}}{\sigma_y}\right)^2 \tag{6.3}$$

The above result indicates that the plastic zone size estimate is proportional to $\left(\frac{K_{IC}}{\sigma_y}\right)^2$. When a fracture or sharp flaw is in a casing wall, the ratio of the plastic zone size r_p to the wall thickness t, is a determining factor for the nature of fracture growth. Usually a factor, β_0, which is proportional to the r_p/t ratio, is defined as follows:

$$\beta_0 = \frac{1}{t}\left(\frac{K_{IC}}{\sigma_y}\right)^2 = 2\pi\frac{r_p}{t} \tag{6.4}$$

To avoid brittle fracture, the plastic zone size ahead of the fracture-initiating flaw must be greater than that required to maintain plane strain ahead of the flaw. The ASTM standard test (1995) indicates that this condition is satisfied when

$$\beta_0 > 0.5 \tag{6.5}$$

More recent brittle tests indicate that a value of 0.688 in the above inequality is appropriate for casing burst design (Tallin et al, 1998). Using 0.688 in the inequality for β_0 and combining this with Equation (6.4) and the transition Equation (6.1), yields:

$$CVN \geq 0.0179(\sigma_y{}^2 t)^{0.79} \tag{6.6}$$

For a proposed design for casing burst, both yield strength σ_y and wall thickness t will be known so that the minimum required value for CVN can be found to ensure that the material is above the transition condition. If Inequality (6.6) is not satisfied, brittle fracture may occur and will therefore be anticipated. Inequality (6.6) is the first criterion.

The second criterion is now derived using the upper shelf Equation (6.2). The minimum value of β used to establish a K_{IC}/σ_y value from Equation (6.4) is chosen to ensure at least a 50-75% shear fracture. The minimum value of β for this condition is about 1.5 (ASTM, 1995). Using 1.5 for the minimum value of β in Equation (6.4), Equation (6.2) gives:

$$CVN \geq \sigma_y (0.375t + 0.1) \tag{6.7}$$

If this inequality is satisfied, ductile fracture can be anticipated and design can proceed on that base.

In summary, a combination of these two criteria is described as follows to give a specific set of conditions, which should be met before ductile (plastic) instability can be used as the basis for casing burst design,

1. If Inequality (6.7) is satisfied, the casing should be designed on the basis of ductile burst failure.
2. If Inequality (6.6) is not satisfied, the material should be assumed brittle and a brittle fracture burst design procedure should be used for the casing design.
3. If Inequality (6.7) is not satisfied but Inequality (6.6) is satisfied, the casing lies in an area of uncertainty. It is not brittle, but also it is not quite fully ductile. In this case, brittle design is recommended for safety.

The criteria presented above have been applied to the casing burst experiments (Paslay et al, 1998) with the validation shown in Table 6.1. The validation shows that all of the tested casings satisfy Inequality (6.7), therefore, their burst behaviours are controlled by ductile instability. This expectation was borne out in the burst tests. It is noted that, Test No 1 (Paslay et al, 1998) is the closest to not meeting the ductile criterion and it is also the test with the greatest deviation from fully ductile behaviour.

Table 6.1 Criterion validation for ductile instability of casing burst design

Test No.	σ_y		t		Eq. (6.7)		Eq. (6.6)		Test CVN	
	(10^3 psi)	(MPa)	(in.)	(mm)	($ft\,lb$)	(Nm)	($ft\,lb$)	(Nm)	($ft\,lb$)	(Nm)
1	67.6	466.0	.352	8.94	15.7	21.29	6.8	9.22	24	32.54
2	100.9	695.6	.254	6.45	19.7	26.71	9.4	12.75	104	141.0
3	131.4	905.9	.575	14.6	41.5	56.27	28.7	38.92	81	109.8
4	120.7	832.1	.524	13.3	35.8	48.54	23.4	31.73	76	103.1
5	88.6	610.8	.408	10.4	22.4	30.37	11.8	16.00	54	73.2
6	122.6	845.2	.407	10.3	31.0	42.04	19.6	26.58	87	118.0
7	92.9	640.5	.388	9.86	22.8	30.92	12.2	16.54	64	86.78
8	87.5	603.2	.567	14.4	27.4	37.15	15.0	20.34	66	89.50
9	100.3	691.5	.154	3.91	15.8	21.42	6.6	8.95	88	119.3

6.3 Review Of Casing Burst Design Equations

Under excessive internal pressure, ductile burst of a casing is achieved when the yielding of the entire pipe cross-section precedes the pipe failure. Ductile burst requires a limit state model based on the fully plastic section of a casing. As the casing loading, dominated by internal pressure, increases, yielding of the casing body starts at the inner fibre (Johnson and Mellor, 1983; Harvey, 1986). The plastic zone spreads under increasing loads until the outer fibre of the casing yields. Well-executed experiments show that the ultimate burst capacity of a casing is only slightly larger (typically 2 to 3%) than that corresponding to the yielding of the outer fibre of the casing under excessive internal pressure (Gulati et al, 1994). Therefore, yielding of the outer fibre can be considered to represent the ultimate limit state of ductile casing burst. For a cemented section of casing subjected to large internal pressure, a solution is suggested for the calculation of the burst strength (Hill, 1950),

$$P_b = \frac{2\sigma_y}{\sqrt{3}} \ln\left(\frac{R_o}{R_i}\right) \tag{6.8}$$

where σ_y is the yield strength and R_o and R_i are the outer and inner radii of the casing respectively. The wall thickness equals to $(R_o - R_i)$.

An exact solution for an arbitrarily thick end-capped casing on the basis of the Mises yield criterion was derived in an implicit form by Svensson (1958) and discussed in detail by Chakrabarty (1987). It is expressed as follows:

$$P_b = \beta_c \int_{\lambda_i R_i}^{\lambda_o R_o} \left[In\left(\frac{r}{r_o}\right) \right]^n \frac{1}{r} dr \tag{6.9}$$

with

$$\beta_c = k^{n+1}\left(\frac{e}{n}\right)^n \sigma_{uts}$$
$$r_o = \sqrt{r^2 - R_i^{\,2}(\lambda_i^{\,2} - 1)} \tag{6.10}$$

where σ_{uts} is the ultimate tensile strength, n is the material hardening parameter for a assumed Ludwik power law (1909) and λ_i and λ_o are the corresponding inner and outer circumferential stretches.

Klever (1992) developed an analytical model with an isotropic hardening finite strain plasticity based on the Mises yield criterion for the burst strength of thin walled uncorroded casings. The model was further modified to include the Tresca yield criterion and extended to thick walled casings by Stewart (1994). The burst strength is calculated as follows:

$$P_b = k^{(n+1)}\left(\frac{1}{2}\right)^n 2\sigma_{uts}\frac{t}{(D-t)} \tag{6.11}$$

where k is a yield criterion parameter which is unity for the Tresca yield criterion and $2/\sqrt{3}$ for the Mises yield criterion. It is noted that a ductile burst failure is assumed in the derivation of the Stewart model.

In 1994, the DEA (Drilling Engineering Association) adopted the expression of Stewart (1994) for the calculation of the ultimate casing burst strength, which is rewritten to include a temperature effect as:

$$P_b = \mathrm{mod}\,u \cdot \left(2\sigma_{uts}\frac{t_{\min}}{\left(D_o^{loc} - t_{\min}\right)}\right)\left[1 - (T - T_{ref})\frac{t_d}{100}\right] \tag{6.12}$$

where T is the temperature at the point of interest, T_{ref} is the reference temperature for thermal degradation, t_d is the thermal degradation, D_o^{loc} is the local outside diameter and $t_{\min}$ the minimum wall thickness. It is noted that, a modelling uncertainty, $\mathrm{mod}\,u$, is introduced to represent the material term $k^{(n+1)}\left(\frac{1}{2}\right)^n$.

Following Stewart's analytical model, an average burst model was proposed for regular and worn casings (Klever, 1998) as:

$$P_b^{Av} = \frac{t}{(D-t)}\left[\left(\frac{1}{2}\right)^{1+n} + \left(\frac{1}{\sqrt{3}}\right)^{1+n}\right] 2\sigma_{uts} \tag{6.13}$$

where n is the material hardening parameter, which is usually taken as the strain ε_{uts} corresponding to the ultimate tensile strength σ_{uts}.

Considering the effect of axial loading on the basis of conventional work hardening plasticity theory, Paslay (1998) gave another modification to Equation (6.11) as:

$$P_b = 2\sigma_{uts}\frac{t_{\min}}{(D-t_{\min})}\sqrt{1-\left(\frac{\sigma_{ax}}{\sigma_{uts}}\right)^2} \tag{6.14}$$

where $t_{\min}$ is the minimum wall thickness of a worn casing, σ_{ax} is the applied axial stress, which is determined by the external axial force, F_{ext},

$$\sigma_{ax} = \frac{F_{ext}}{\pi(D-t)t} \tag{6.15}$$

The API bulletin 5C3 (1992) provides another equation for the calculation of casing burst strength, which is expressed by:

$$P_b = 0.875\left(\frac{2\,\sigma_y\,t}{D}\right) \tag{6.16}$$

It is noted that the API equation for casing burst is proportional to the yield stress, while the Klever and Stewart equations are proportional to the ultimate tensile strength.

6.4 Finite Element Analysis Of Casing Burst

6.4.1 General

As was done for the case of casing collapse study, finite element analyses are performed to investigate the ultimate burst strength of a thick walled casing using ABAQUS. It is assumed that a regular casing under internal pressure deforms such that its cross section remains circular. Therefore, the membrane forces are essential in the equilibrium equations, while bending does not play any significant role in the problem of casing burst. To obtain an accurate modelling of plasticity and large deformation, a Newton solution technique is used to solve the governing equations of casing burst. A reduced integration technique is employed in the simulation to prevent possible artificial locking in the calculation of stiffness matrices. The modified Riks algorithm is employed to carefully control the internal pressure to the ultimate burst strength. Following the maximum pressure, the program automatically reduces the applied internal pressure so that the casing burst simulation can be continued. In this way, the casing burst process can be simulated. As normally the ratio of casing length to outside diameter is more than 8, the effect of end restraint can be neglected in the simulation of casing burst. Similar to casing collapse, the problem of casing burst is reduced to a case of a plane strain problem, and only one element is necessary in the longitudinal direction.

6.4.2 Modelling Of Geometric Imperfections

There is little in the literature on investigations into the effects of geometrical imperfections, such as ovality and eccentricity, on the casing burst strength. Therefore, these imperfections are constructed in the finite element program to evaluate their effects on the ultimate casing burst strength. As a result, initial ovality and eccentricity are introduced in the same way as was described in Chapter 5.

Similar element type and mesh density studies prove that the second order generalized plane strain continuum element CGPE10R is valid for the problem of casing burst. In particular, six integration points across the wall thickness of a casing were sufficient for an accurate prediction of the ultimate burst strength. However, a detailed description of the element type and mesh studies is omitted here for brevity.

6.4.3 Determination Of Burst Strength

A uniform internal pressure is applied to the faces of the elements on the inner diameter of the casing section. In the simulation, the line direction of the applied internal pressure changes as the casing section deforms and the pressure is increased incrementally. It is noted that, true stress and true strain, instead of engineering stress and strain, are used in the simulation, and no approximation is made in formulating the non-linear equations of the casing burst problem. The internal pressure-strain response of a casing is recorded in the simulation for the determination of ultimate casing burst strength. A typical plot is shown in Fig. 6.1. With the increment of

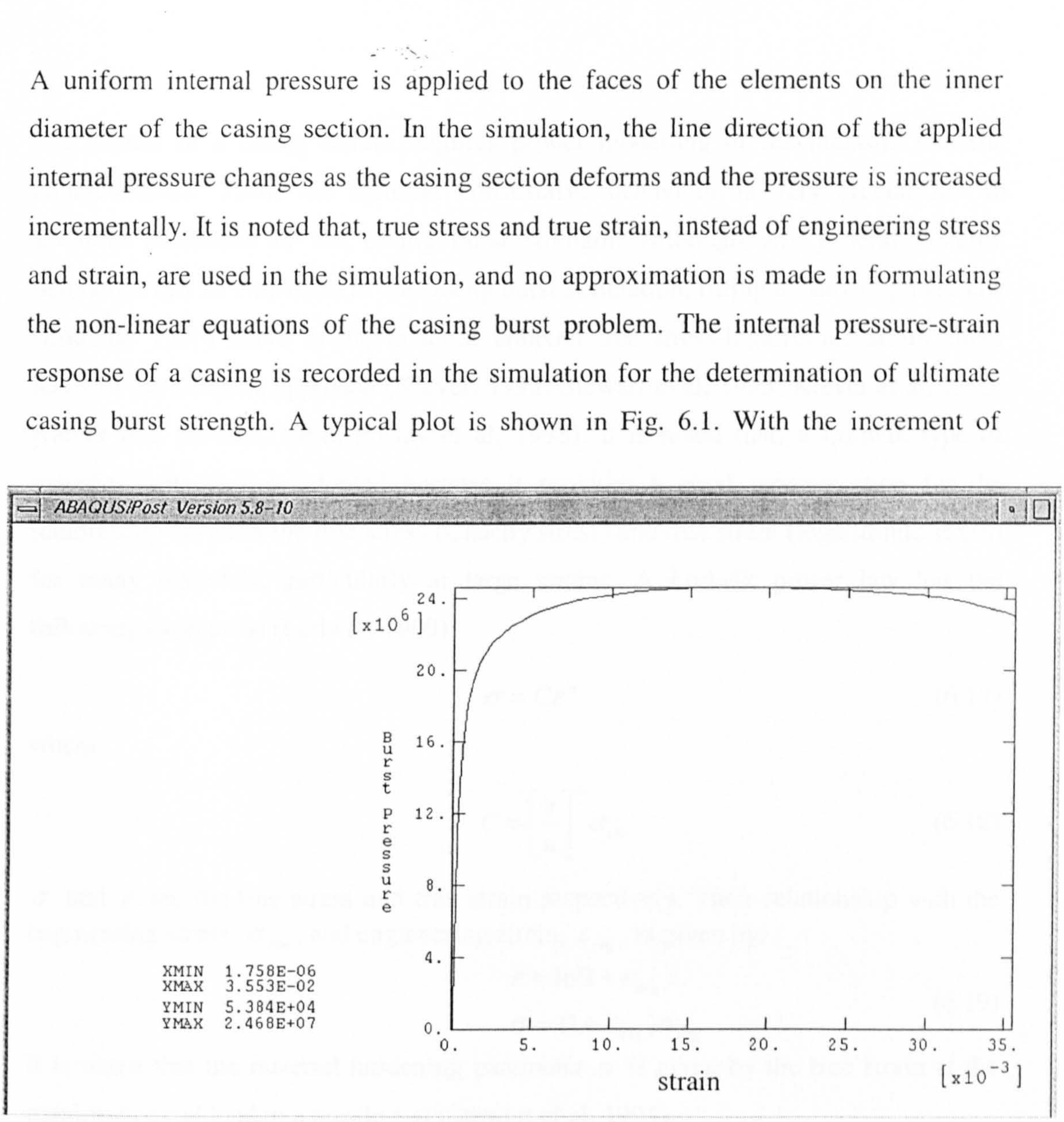

Fig. 6.1 Typical pressure strain plot of casing burst

internal pressure, the measured pressure increases until the maximum pressure is reached and then a decrease in the pressure can be observed with a large increase of deformation. The maximum internal pressure is then taken as the ultimate burst strength of a casing. This is similar to the experiments for burst of the test specimen when a sudden drop of the internal pressure is recorded in the test facility. The above procedures enable the FE program to accurately model the casing burst behaviour.

6.4.4 Material Constitutive Behaviour

The nature of a casing failure requires proper modelling of the inelastic material characteristics. Thus, the material constitutive behaviour is very crucial for an accurate prediction of the casing burst strength. Although any general material behaviour can be employed in the casing burst simulation, fitting a Ludwik power law (Ludwik, 1909) curve to the material uniaxial true stress-logarithmic strain curve leads to the simplest approach (Klever, 1992; Stewart et al, 1993; Klever et al, 1993; Klever and Stewart, 1998; Paslay et al, 1998). It is noted that, a Ludwik type of material behaviour is adopted because it provides a good representation for the relationship between the true stress (Cauchy stress) and true strain (logarithmic strain) for many materials, particularly at large strains. A Ludwik power law has the following expression (Ludwik, 1909):

$$\sigma = C\varepsilon^n \tag{6.17}$$

where

$$C = \left[\frac{e}{n}\right]^n \sigma_{uts} \tag{6.18}$$

σ and ε are the true stress and true strain respectively. Their relationship with the engineering stress, σ_{eng}, and engineering strain, ε_{eng}, is given by,

$$\begin{aligned} \varepsilon &= \ln(1+\varepsilon_{eng}) \\ \sigma &= (1+\varepsilon_{eng})\sigma_{eng} \end{aligned} \tag{6.19}$$

It is noted that the material hardening parameter n is given by the true strain at the maximum axial load in a tensile test (Stewart et al, 1994),

$$n = \ln(1+\varepsilon_{uts}) \tag{6.20}$$

Therefore, the advantage of adopting the Ludwik material model is that it can be easily determined from the tensile test. In the following validation, the individual measured material behaviour including the ultimate tensile stress and strain from the burst test are used to justify the accuracy and reliability of the material model.

A generalized expression of material behaviour needs to be determined in the derivation of a new design equation for casing burst, which should be capable of modelling materials of various yield strength. Because casing burst is controlled by the ultimate tensile strength rather than the yield strength, it is important to have a relationship between the yield strength and ultimate tensile strength in the finite element analysis of casing burst.

Considerable research has been conducted to define the significance of the yield strength to tensile strength ratio (σ_y / σ_{uts}) for casing burst. In the late 1960s and early 1970s, a study by Kiefner et al (1971) was completed, in which a series of burst tests was conducted on 41 pipes ranging from 8 to 42 inches (203 to 1067 mm) in diameter. In 1986, altogether 23 uniaxial tensile tests were performed by Amano et al (1986). Because the casing manufacturing process has been greatly improved, those test data reported in the 1960s and 1970s lost their eligibility for today's casing. Therefore, only the data from the 1980s are selected as shown in Table 6.2 to fit an empirical relationship between the ultimate tensile strength and the yield strength as well as that between the material hardening parameter n and yield strength. The curves are shown in Fig. 6.2 and Fig. 6.3. It is found that the relationship between the ultimate tensile strength and the yield strength can be fairly well represented by a straight line, which is expressed by:

$$\sigma_{uts} = 0.7728\sigma_y + 27.554 \qquad (6.21)$$

While the relationship between the material hardening index n and yield strength is approximated by:

$$n = -0.007\sigma_y + 0.7474 \qquad (6.22)$$

It is noted that the units of σ_y and σ_{uts} in the above equations are in ksi (1 ksi=6.894 MPa).

Therefore, a realistic isotropic hardening material behaviour, which is able to model the casing material of different yield strength, can be constructed and carefully implemented into the finite element program for casing burst.

Table 6.2 Uniaxial ultimate tensile tests on casings

Test No.	σ_y		σ_{uts}		σ_y / σ_{uts}	ε_{uts}	n
	(ksi)	(MPa)	(ksi)	(MPa)			
1	43.6	300.6	66.4	457.8	0.657	0.394	0.332
2	52.3	360.6	67.8	467.4	0.771	0.368	0.313
3	62.3	429.5	69.7	480.5	0.894	0.294	0.258
4	57.3	395.0	77.8	536.4	0.737	0.36	0.307
5	57.8	398.5	77.7	535.7	0.744	0.364	0.31
6	71.4	492.2	81.1	559.1	0.881	0.278	0.245
7	75.9	523.3	82.2	566.7	0.923	0.244	0.218
8	64.9	447.4	78.7	542.6	0.825	0.300	0.262
9	70.2	484.0	79.9	550.8	0.879	0.24	0.215
10	76.2	525.3	81.5	561.9	0.935	0.193	0.176
11	68.0	468.8	80.8	557.0	0.842	0.297	0.26
12	73.5	506.7	82.1	566.0	0.895	0.24	0.215
13	79.7	549.5	84.5	582.5	0.943	0.204	0.186
14	79.8	550.1	93.4	643.9	0.854	0.08	0.077
15	79.6	548.8	93.4	643.9	0.852	0.094	0.09
16	84.3	581.2	93.3	643.2	0.904	0.193	0.176
17	88.4	609.4	93.4	643.9	0.947	0.161	0.149
18	100.2	690.8	101.7	742.5	0.985	0.006	0.005
19	82.9	571.5	92.4	637.0	0.897	0.163	0.151
20	89.3	615.6	94.6	652.2	0.944	0.157	0.146
21	100.8	694.9	102.5	706.6	0.983	0.003	0.003
22	128.4	885.2	130.0	896.2	0.988	0.003	0.003
23	135.6	934.8	137.4	947.2	0.987	0.005	0.005

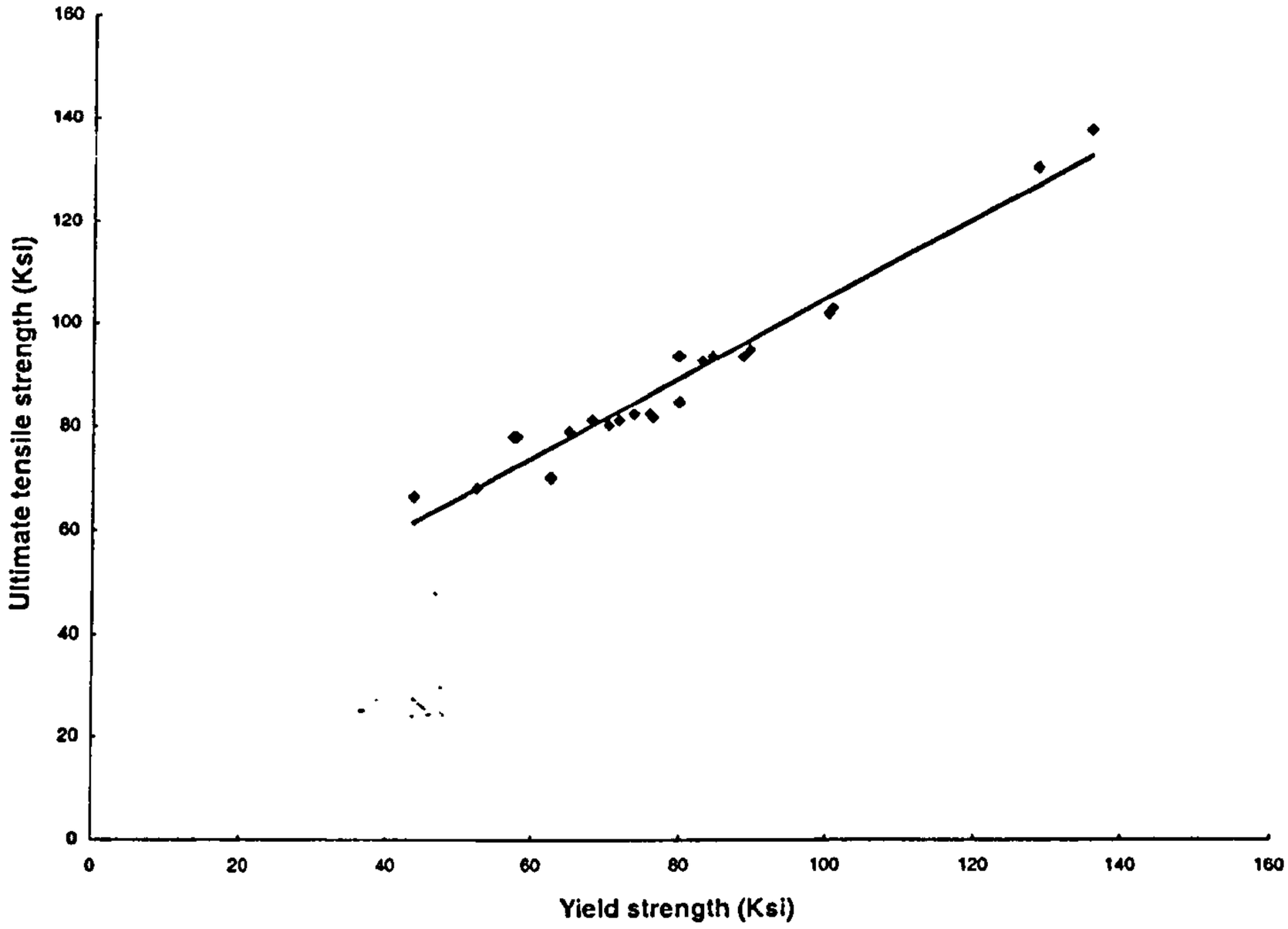

Fig. 6.2 Empirical relationship between ultimate tensile strength and yield strength

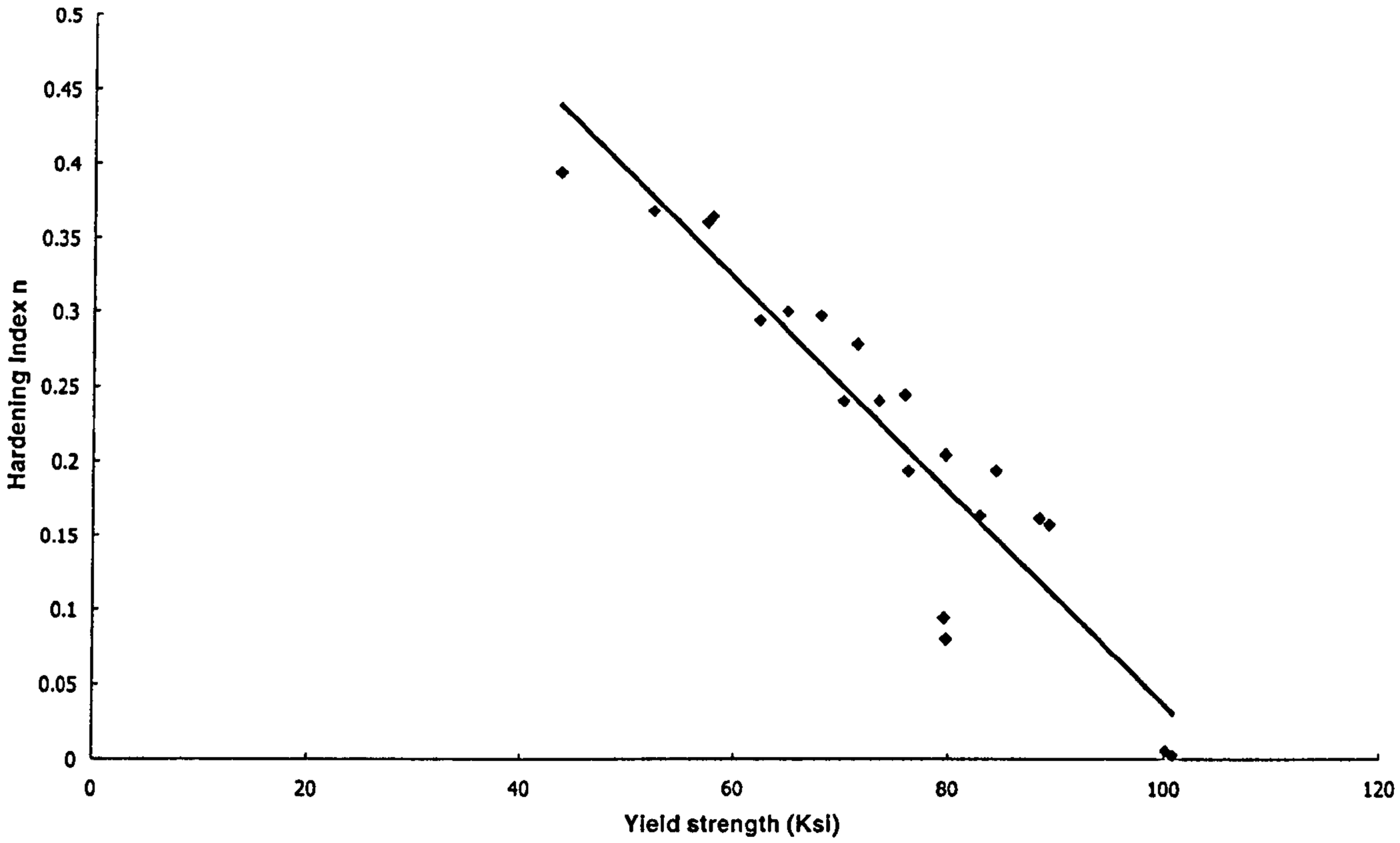

Fig. 6.3 Empirical relationship between material hardening index and yield strength

6.4.5 Validation With Casing Burst Data

The finite element analysis of casing burst has been verified by comparison with burst experimental data. Those experiments were performed on common tubular stock of flawless casings from grades H40 to Q125 (Amano et al, 1986; Stewart et al, 1994; Paslay et al, 1998). Casings were chosen according to their frequencies of application as well as availability from the manufacturers. Each test specimen of casing burst had welded end caps and a length to diameter ratio of at least eight. The welded end caps were used so that the internal pressure could be applied. In the test, the casings were filled with liquid and pressurized until they burst. It is noted that all of the casing materials in the test are ductile.

In an experimental investigation of the significance of yield ratio (yield strength/ultimate tensile strength) to casing burst, Amano et al (1986) performed 12 hydrostatic burst tests on long pipes of the grades of X65 to X70. Stewart et al (1994) provided 29 test data, of which 7 long specimens were selected in the casing burst database. Recently, Paslay et al (1998) tested altogether 22 casings, of which 13 tests on flawless long specimens under internal pressure alone were added in the validation database. It is noted that, the D/t ratio of these test data covers from 6 to 48, casing grade from H40 to Q125, outside diameter from 3.5 inches (89 mm) to 36 inches (914 mm). From the variations of these important parameters, the selected tested data provides a good representation of the casings. Therefore, finite element analysis of casing burst in this research is carefully validated by means of these 32 casing burst tests. In general, casing burst is less important than casing collapse in the casing design process, which is also revealed from the number of published test data for each case. Considering this fact, the 32 burst test data is believed to be sufficient for this research. Furthermore, the casing burst database will be used to evaluate and calibrate potential collapse design equations for the limit state casing design.

The measured geometry and material parameters as well as the reported ultimate burst strength are listed in Table 6.3. The geometry and material behaviour are carefully implemented in the proposed finite element program. The relationship of the applied internal pressure and deformation is recorded in the simulation to determine the ultimate burst strength. Finally, comparisons between the experimental burst strength and predictions are shown in Fig. 6.4. It is clearly demonstrated that the predictions

from the FEM are very close to the actual test burst strength with a maximum predictive deviation less than 7 percent. The possible error comes from the approximation in modelling the material behaviour because of some approximations assumed in the simulation However, the validation does prove that, the finite element simulation in this research can predict the ultimate burst strength of a casing to a satisfactory degree of accuracy.

Table 6.3 Comparison between the FEM and burst tests

No	D (mm)	t (mm)	D/t	σ_y (MPa)	σ_{uts} (MPa)	n	P_{exp} (MPa)	P_{FEM} (MPa)	$\frac{P_{FEM}}{P_{exp}}$
1	493.8	14.3	35.52	508.8	571.0	0.090	34.50	32.16	0.93
2	530.6	13.5	40.30	623.9	624.0	0.010	33.84	32.05	0.95
3	371.0	20.0	38.12	531.5	608.0	0.110	30.63	31.52	1.03
4	371.0	20.0	38.12	555.0	580.0	0.090	31.95	30.34	0.95
5	594.2	15.9	38.34	534.3	653.0	0.110	34.79	33.71	0.97
6	594.2	15.9	38.34	440.5	585.0	0.140	31.76	29.78	0.94
7	594.2	15.9	38.34	511.5	600.0	0.110	31.72	30.89	0.98
8	594.2	15.9	38.34	501.2	581.0	0.130	30.20	29.69	0.98
9	895.0	19.0	48.00	517.1	559.0	0.090	24.85	23.06	0.93
10	895.0	19.0	48.00	457.8	546.0	0.100	23.11	22.42	0.97
11	895.0	19.0	48.00	508.8	604.0	0.100	25.80	24.69	0.96
12	895.0	19.0	48.00	426.7	578.0	0.130	23.17	23.39	1.01
13	591.8	18.2	32.52	636.0	645.0	0.040	41.76	40.86	0.98
14	591.2	18.9	31.28	563.0	589.0	0.090	37.68	37.86	1.00
15	591.2	18.9	31.28	607.0	630.0	0.120	40.79	40.65	1.00
16	893.6	22.5	39.72	526.0	608.0	0.110	27.93	30.22	1.08
17	162.2	9.8	16.55	602.0	776.0	0.180	86.60	94.00	1.09
18	397.6	13.5	29.45	364.0	523.0	0.190	36.50	34.29	0.94
19	390.8	12.8	30.53	807.0	869.0	0.080	59.60	53.27	0.89
20	179.4	8.94	20.07	468.8	737.7	0.115	77.70	69.77	0.90
21	89.7	6.5	13.90	696.3	751.4	0.077	119.27	118.30	0.99
22	198.2	14.6	13.57	903.1	992.7	0.065	173.80	154.80	0.89
23	179.5	13.3	13.49	834.2	903.1	0.061	152.29	141.70	0.93
24	179.7	10.4	17.34	613.6	723.8	0.093	92.17	85.47	0.93
25	179.7	10.3	17.39	848.0	916.9	0.070	118.51	109.00	0.92
26	247.0	9.86	25.06	641.1	717.0	0.102	61.08	57.91	0.95
27	252.2	13.5	18.70	606.7	703.2	0.102	81.56	76.51	0.94
28	89.0	14.4	6.18	606.7	730.8	0.115	294.65	285.10	0.97
29	67.3	3.91	17.20	689.4	834.2	0.065	113.34	103.50	0.91
30	179.6	12.01	14.95	779.0	896.2	0.068	136.09	125.30	0.92
31	198.2	14.7	13.53	903.1	992.7	0.065	171.66	155.40	0.91
32	180.1	14.9	12.12	903.1	992.7	0.065	178.55	175.70	0.98
Coefficient of Variance			0.0024	Standard Deviation		0.0491	Mean		0.962

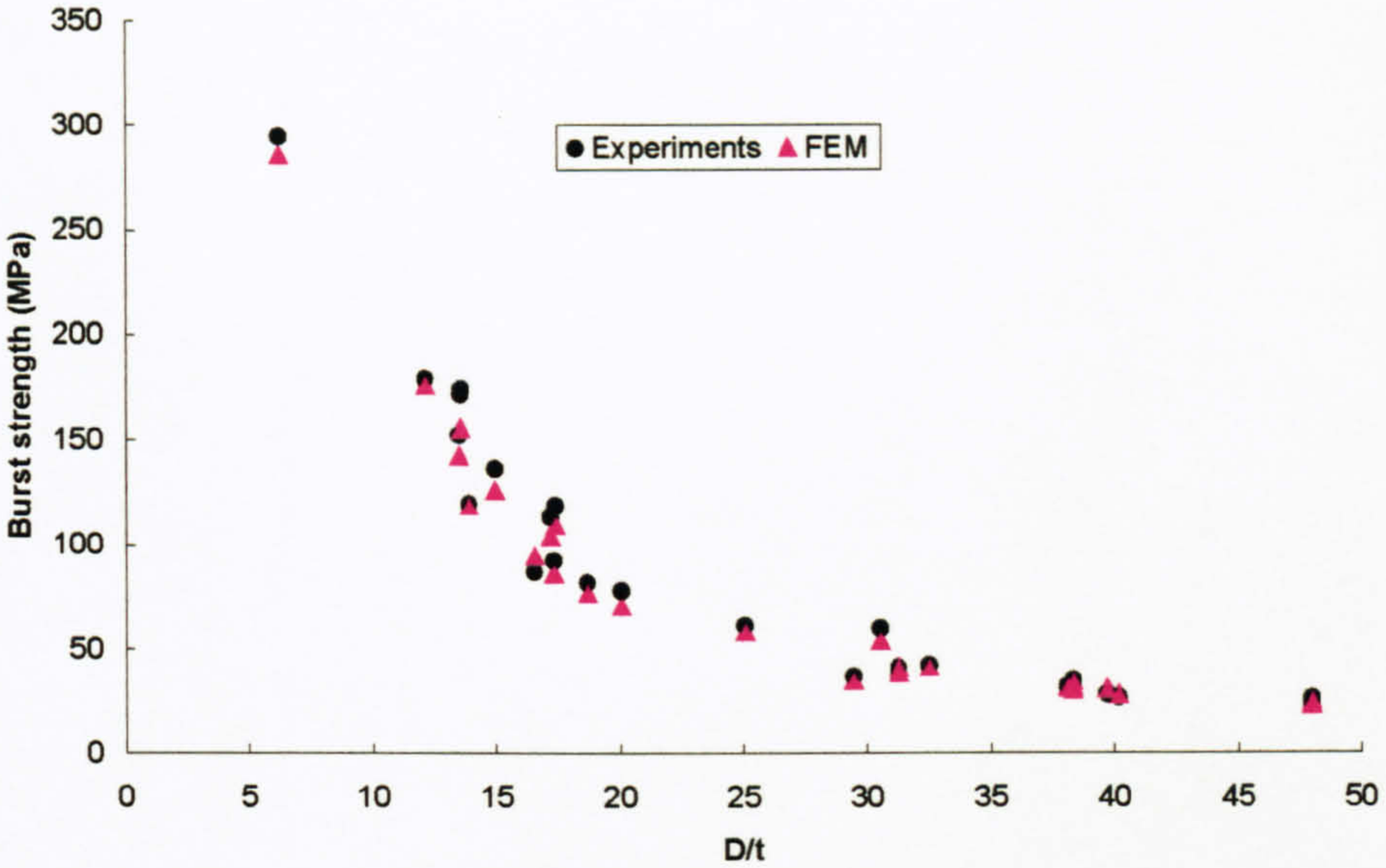

Fig. 6.4 Comparison between casing burst experiments and FEM

6.5 Numerical Results And Discussion

Fig. 6.5 shows the predicted progress of casing burst behaviour. It is seen that the burst occurs when the whole casing section begins to yield. The predicted casing burst process clearly demonstrates that, large deformation occurs during casing burst. A parametric study has been performed to investigate the effects of major factors on the burst strength of a casing.

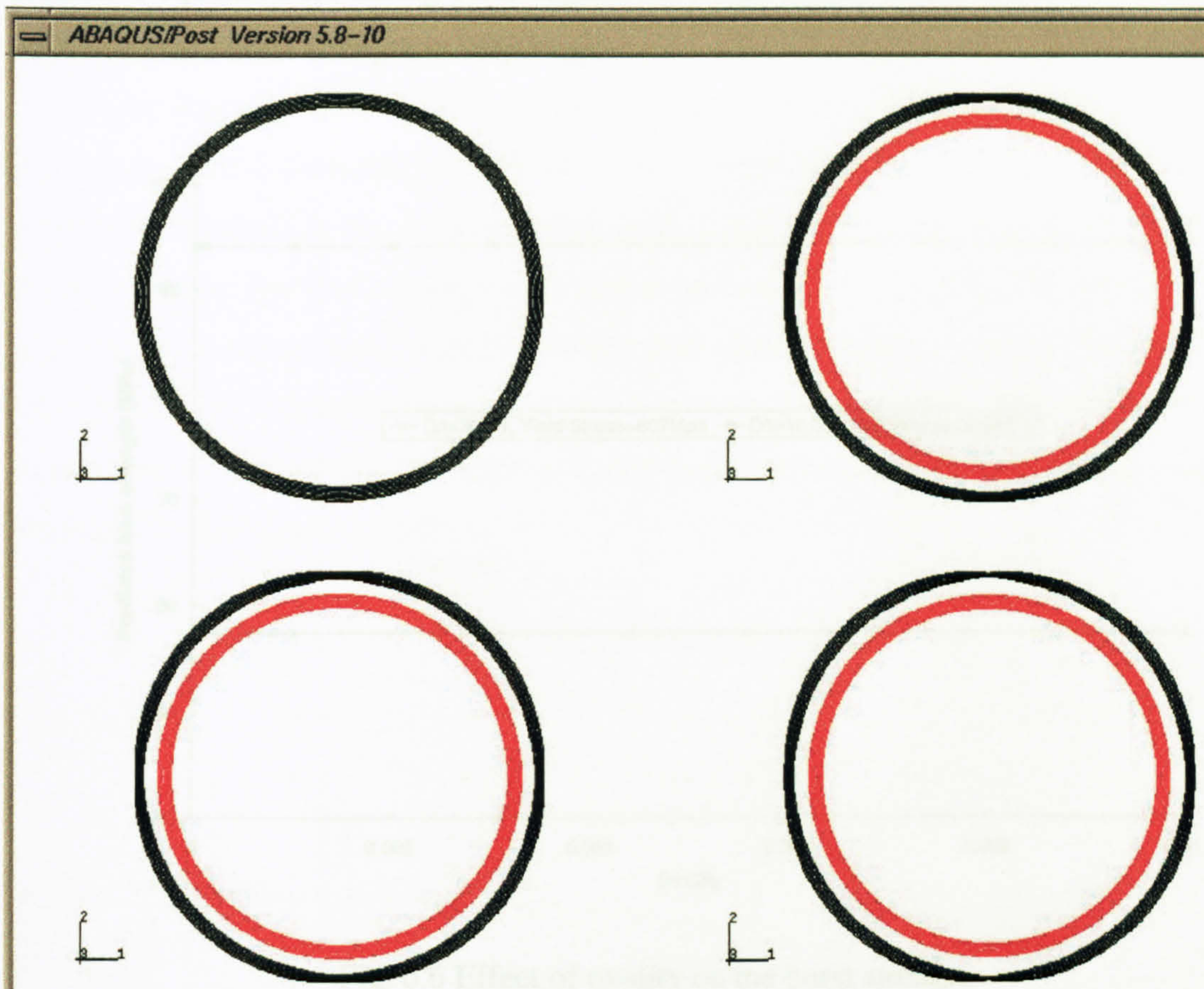

Fig. 6.5 Predicted progress of casing burst
(red denoting the original casing, black denoting deformed casing)

6.5.1 Effects Of Initial Ovality

In contrast to casing collapse, it is found that the effect of initial ovality on the ultimate burst strength is very small as shown in Fig. 6.6. It is well known that the limit load type of instability of a thick casing is caused by the combination of section ovalization and yielding. For casing burst, the presence of internal pressure will reduce the section ovalization. On the other hand, the yield stress in the longitudinal direction is reduced by the circumferential stresses induced by the internal pressure. These reasons make the effect of initial ovality on the burst strength very small, which also explains the obvious scarcity of previous research on this topic. Almost all the

predictive equations for casing burst neglect the initial ovality factor because its effect on the ultimate burst strength is very small.

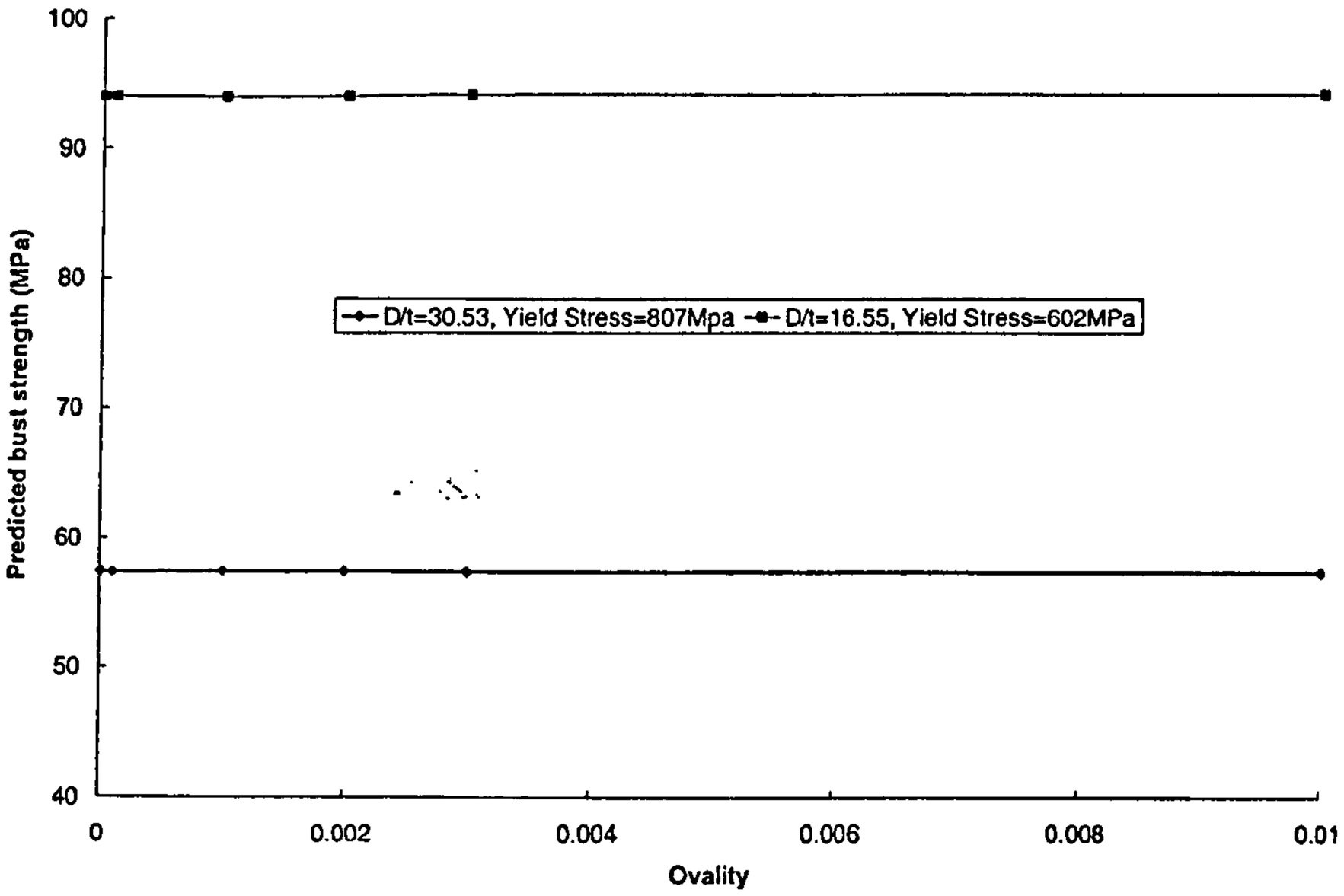

Fig. 6.6 Effect of ovality on the burst strength

6.5.2 Effect Of Initial Eccentricity

The initial eccentricity greatly affects the burst pressure as shown in Fig. 6.7. With eccentricity less than 0.01, very small reduction in the burst pressure is found. With an eccentricity greater than 0.01, the predicted burst strength drops rapidly. In particular, initial eccentricity on the burst strength of a casing with a D/t value of 16.55 has an approximately equivalent reduction in burst strength for a casing with a D/t value of 30.53. As the API maximum allowable wall thickness tolerance is 0.125, the effect of eccentricity is very important on the ultimate burst strength. The range of initial eccentricity considered in this research is from 10^{-4} to 0.4 to account for the fact that there will be some large local wall thickness reductions during the service life of a casing.

Although casings considered in this research are mainly for regular casings without any crack-like defects rather than those casings with localized wall thickness reduction, it is very interesting to investigate if the initial uniform eccentricity model developed in this research remains valid for casings with localized wall thickness reduction. In practice, the localized wall loss in the casing takes a form of a long smooth groove. For those casings with a wear groove, Klever (1998) pointed out that the ultimate burst strength would be lower than these of perfect casings, but higher than the casings with uniform reduced wall thickness. It is therefore, expected that the initial eccentricity model can give a lower bound prediction for the casing with localized wall thickness reduction.

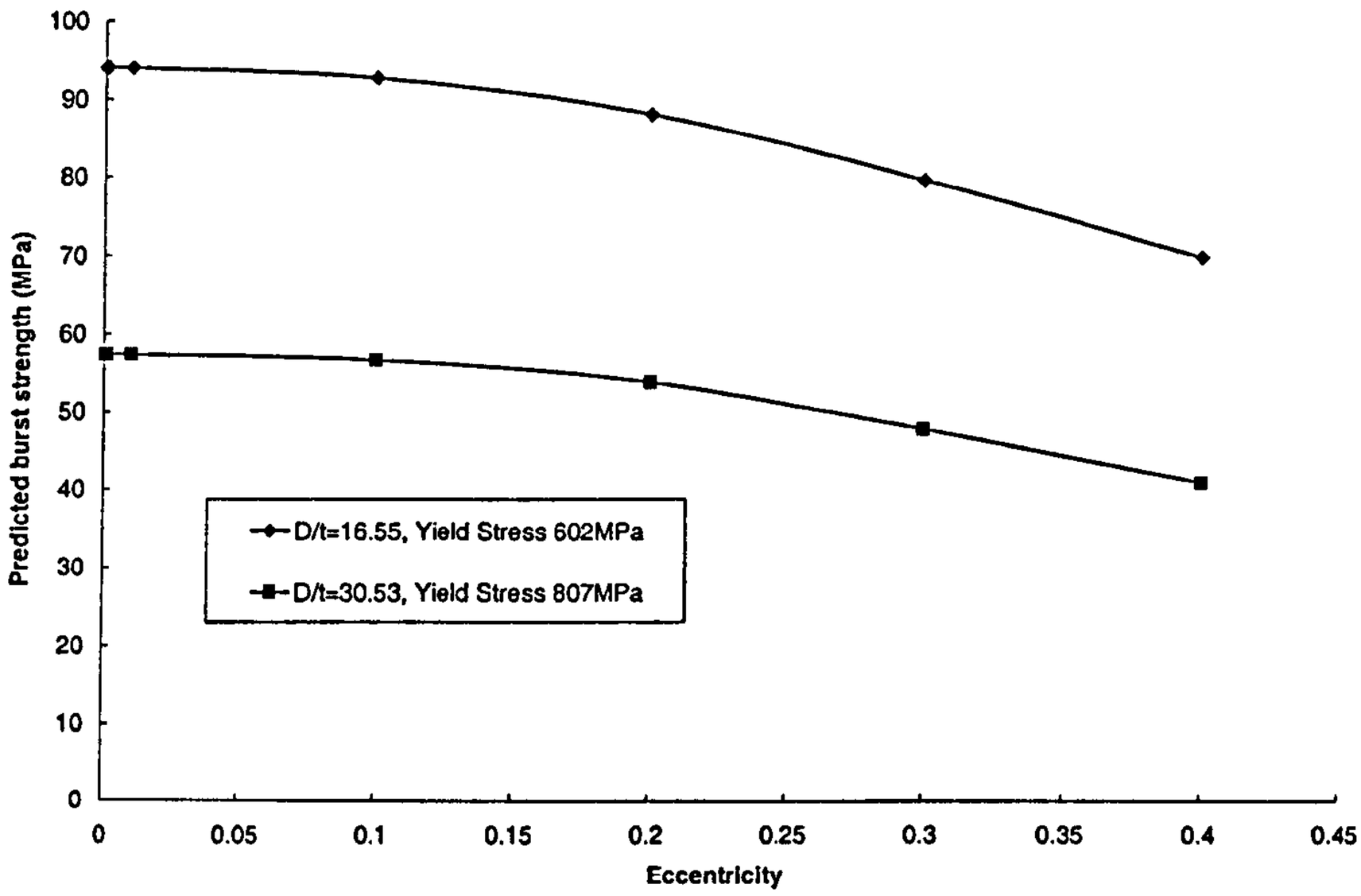

Fig. 6.7 Effect of eccentricity on the burst strength

For this purpose, a series of experimental data have been collected. In 1992, British Gas carried out 8 pressurized ring tests on behalf of Shell (Stewart et al, 1994), of which seven rings were machined internally over 20 percent of the circumference, simulating the reduced wall thickness due to smooth corrosion. It is noted that all eight specimens were cut from a single pipe of grade X60 with $\sigma_{uts} = 563\,MPa$ and material hardening index $n = 0.13$. Klever (1998) further performed eight burst tests on the casings with longitudinal grooves machined at the inside of test specimens, of which four were cut from P110 casings and four from Q125 casings.

It is noted that the minimum wall thickness is used in the simulation instead of the nominal wall thickness. The predictions of ultimate burst strength for each burst test are summarized in Table 6.4. It is clearly demonstrated that the uniform eccentricity model predicts the burst capacity of casings with localized wall thickness reduction extremely well. The mean of the predictions is 0.993 with a standard deviation less than 4 percent as well as a coefficient of variance of 0.001. The spread of the predictions in the ring test is very small, and similar accurate predictions can be observed for these casings with machined long grooves. It is therefore, concluded that the introduction of the additional complexity of localized wall thickness reduction has a minor effect on the ultimate burst strength. The burst strength of a casing with local wall thickness reduction can be predicted to a very satisfactory degree of accuracy if the minimum wall thickness is used in the FE model. Another important message is that, if the empirical relationships for the yield strength, ultimate tensile strength and the material hardening index used in this finite element analysis do not reflect the proper importance of these parameters governing the burst failure mechanism, a wide scatter in the predicted burst strength should be seen in the comparison. If, on the

Table 6.4 Comparison between FEM predictions and burst test

No.	D_{nom} (mm)	t_{nom} (mm)	t_{min} (mm)	σ_y (MPa)	Hardening n	Burst Strength (Mpa)		Predicted / Actual
						Actual	Predicted	
1	892.0	22.20	22.20	563.0	0.130	26.40	27.40	1.038
2	892.0	22.20	15.60	563.0	0.130	18.70	19.06	1.019
3	892.0	22.20	15.80	563.0	0.130	19.50	19.32	0.991
4	892.0	22.20	11.50	563.0	0.130	14.80	13.94	0.942
5	892.0	22.20	10.50	563.0	0.130	13.00	12.73	0.979
6	892.0	22.20	6.94	563.0	0.130	8.56	8.37	0.978
7	892.0	22.20	6.55	563.0	0.130	8.08	7.88	0.975
8	892.0	22.20	6.93	563.0	0.130	8.22	8.36	1.017
9	342.0	13.54	13.30	840.0	0.049	80.60	84.30	1.046
10	342.0	13.54	12.90	840.0	0.049	80.20	80.90	1.009
11	342.0	13.54	11.00	840.0	0.049	74.50	69.50	0.933
12	342.0	13.54	9.90	840.0	0.049	66.10	62.60	0.947
13	252.0	15.73	15.40	1070.0	0.058	143.00	148.00	1.034
14	252.0	15.73	14.30	1070.0	0.058	136.00	138.00	1.013
15	252.0	15.73	13.10	1070.0	0.058	130.00	127.00	0.977
16	252.0	15.73	11.20	1070.0	0.058	110.00	109.00	0.988
COV		0.001	Standard Deviation		0.034	Mean		0.993

other hand, the assumed burst failure mechanism is correct, the predictions should be accurate with a small deviation, which is clearly seen from the comparison as shown in Fig. 6.4 and Table 6.4. Therefore, the proposed finite element analysis is further validated.

6.5.3 Effect Of Material Hardening

In view of the importance of material hardening, a Ludwik type of generalized material behaviour is adopted to carefully simulate the real casing material behaviour in the finite element calculation. The stress-strain behaviour of the material is coded according to Equations (6.21) and (6.22), which is converted to the true stress and true strain. The effect of the material hardening on the burst strength of casing is shown in Fig. 6.8. It demonstrates that the material hardening parameter has an important effect on the casing burst strength. The predicted casing burst strength decreases with the increase of hardening parameter. In particular, the effect of material hardening on the

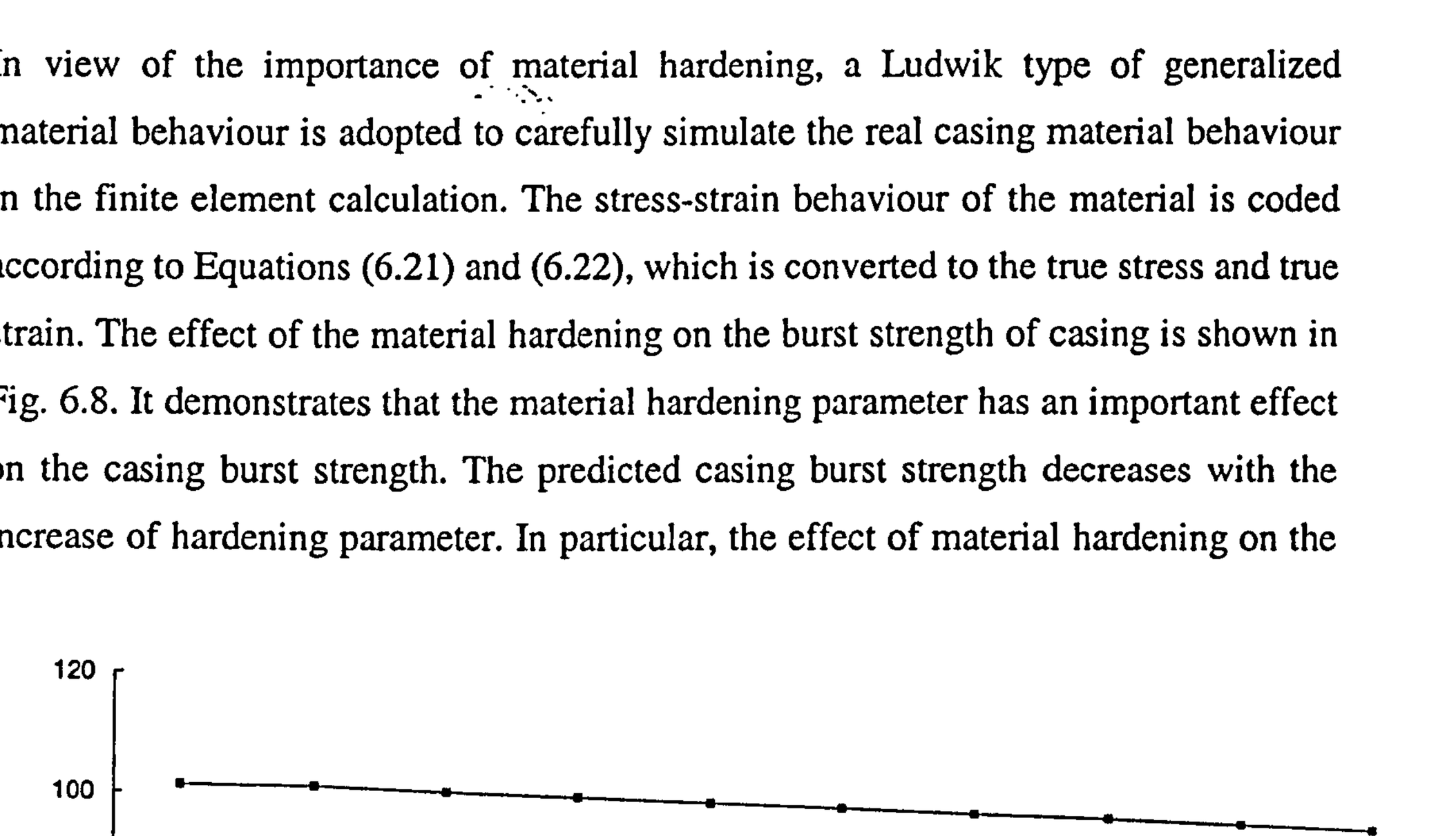

Fig. 6.8 Effect of material hardening on the burst strength

burst strength of a casing with a relatively low D/t value is greater than that of a relatively high D/t casing.

6.6 Development Of A Design Equation For Casing Burst

Although the proposed finite element analysis has been validated to be capable of giving an acceptable prediction for the casing burst strength, it is not convenient to run a computer program in order to obtain a prediction of the casing burst strength in the design process. On the contrary, it is valuable if a straightforward design equation for casing burst were available, which predicts the casing burst strength as a function of the casing dimensions and material properties.

Historically, the ultimate burst strength of a casing is calculated in accordance with the API burst Equation (6.16) given in the API Bulletin 5C3 (1992) in the casing design process for the oil and gas industry, which is for the ductile casing burst failure. However, the API burst equation is based on the working stress design, consequently a safety factor of 0.875 is added to account for the uncertainties in the design process. It is noted that the value of 0.875 is simply chosen from the fact that the minimum wall thickness can be 0.875 times the API nominal wall thickness, giving the API allowable wall thickness tolerance 0.125. During the practical application, it is found that the API design equation for casing burst gives a widely varying predicted failure probability over the D/t range (10 to 40) for well casings (Adams et al, 1998). Under-design can lead to catastrophic failure and over-design leads to costly casing purchase. It is therefore, necessary to develop an improved design equation, in order to remedy the limitations of the widely used API design equation for casing burst. Considerable work has been performed in deriving such an advanced design equation. As a result, several design equations have been proposed for the casing burst design, which are listed below,

- The Hill Equation (6.8) (1950)
- The Stewart Equation (6.11) (1994)
- The Klever Equation (6.13) (1998)

Detailed descriptions of these equations are presented in Section 6.3. Finite element analysis is employed on the development of an improved design equation for casing

burst in the application of limit state casing design after evaluating the above design equations.

6.6.1 Evaluation Of Previous Design Equations

All the aforementioned burst design equations for the calculation of casing burst strength are claimed to be accurate with a very small deviation. A detailed evaluation of these empirical equations against available experimental burst data will tell how accurate and how small the deviations are. Therefore, comparisons have been conducted between these predictions from different design equations and full-scale burst experimental data. It is noted that basically the Stewart equation is identical to the Klever equation when the yield criterion parameter is taken as unity. Therefore, only the Hill equation, the API equation and the Klever equation are assessed in the comparison process.

The predictions from the Hill equation for all 32 casing burst experiments are shown in Fig. 6.9 in comparison with the actual burst strength. It is found that nearly half the predictions from the Hill equation are unconservative and half conservative. Similar conclusion can be drawn for the predictions from the Klever equation as shown in Fig. 6.10, which has a relatively smaller deviation compared to those from the Hill

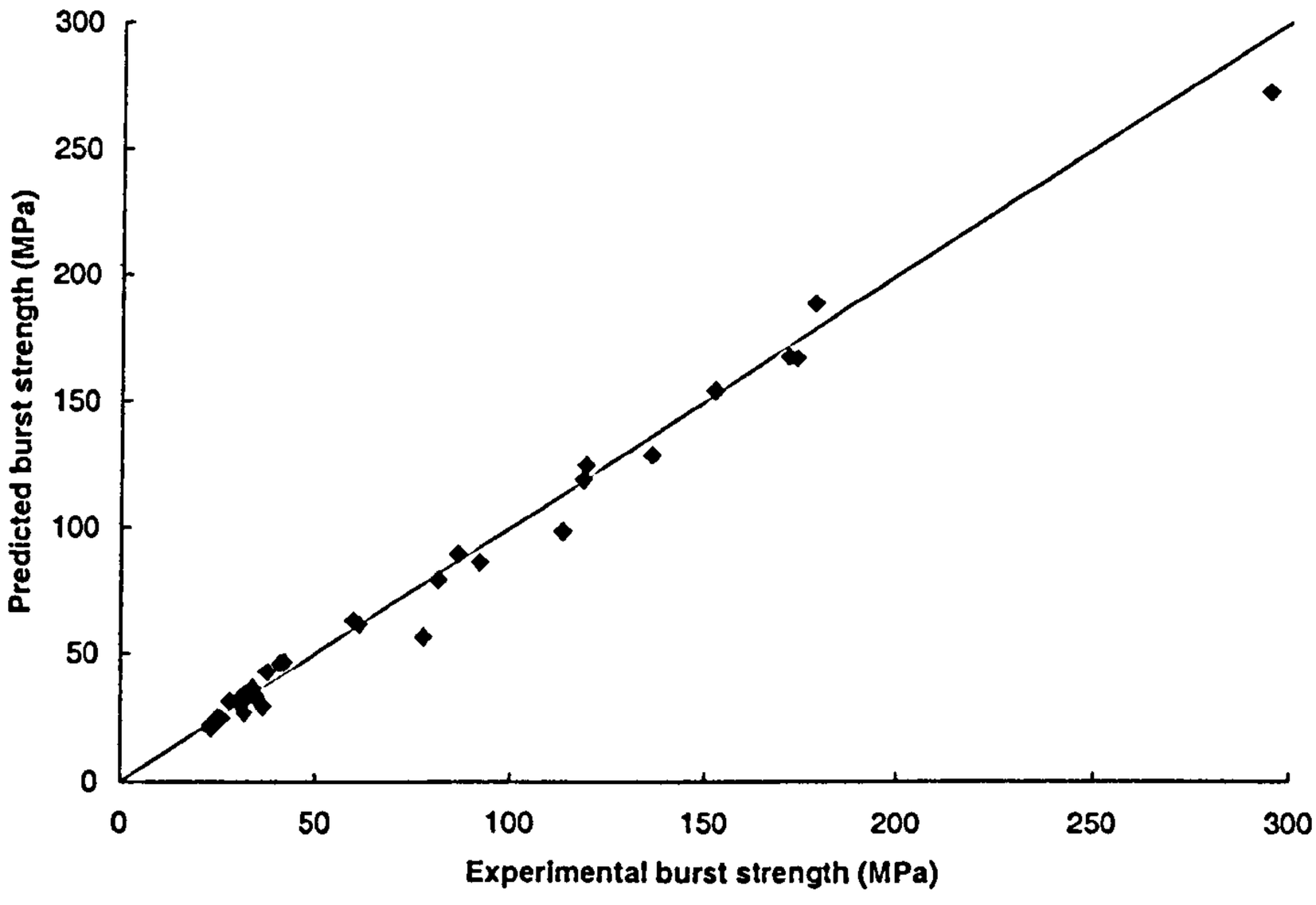

Fig. 6.9 Comparison between experiments and predictions (the Hill equation, 1950)

equation. It is noted that the burst is assumed to occur when the whole casing section begins to yield in the derivation of both the Hill and Klever equations, which may account for the lack of conservatism shown in the comparison. This assumption may not be valid in practice since there are always some material defects, which makes the casing fail before the whole casing section begins to yield. In contrast, the predictions from the API burst equation are wholly conservative for all of the burst experimental data as shown in Fig. 6.11. The conservatism of the API burst equation is expected because it uses a safety factor of 0.875 to account for uncertainties. However, this conservatism is simply too much with a mean of 0.71 and deviation of 0.076. When using the Hill or Klever equations, it is nearly 50 percent possible that an unconservative prediction will be obtained in the design of casing burst, which means potential casing burst failure. When using the API equation, a conservative design can be expected. However, over-conservatism means a large amount of extra purchase on unnecessary high grade of casings. Therefore, it is necessary that an improved equation be obtained for the design of casing burst, which is conservative while more accurate than the API equation. It has been demonstrated that a very accurate finite element model has been built in the previous sections. Using regression analysis, a more accurate whilst realistic conservative equation can be possibly derived.

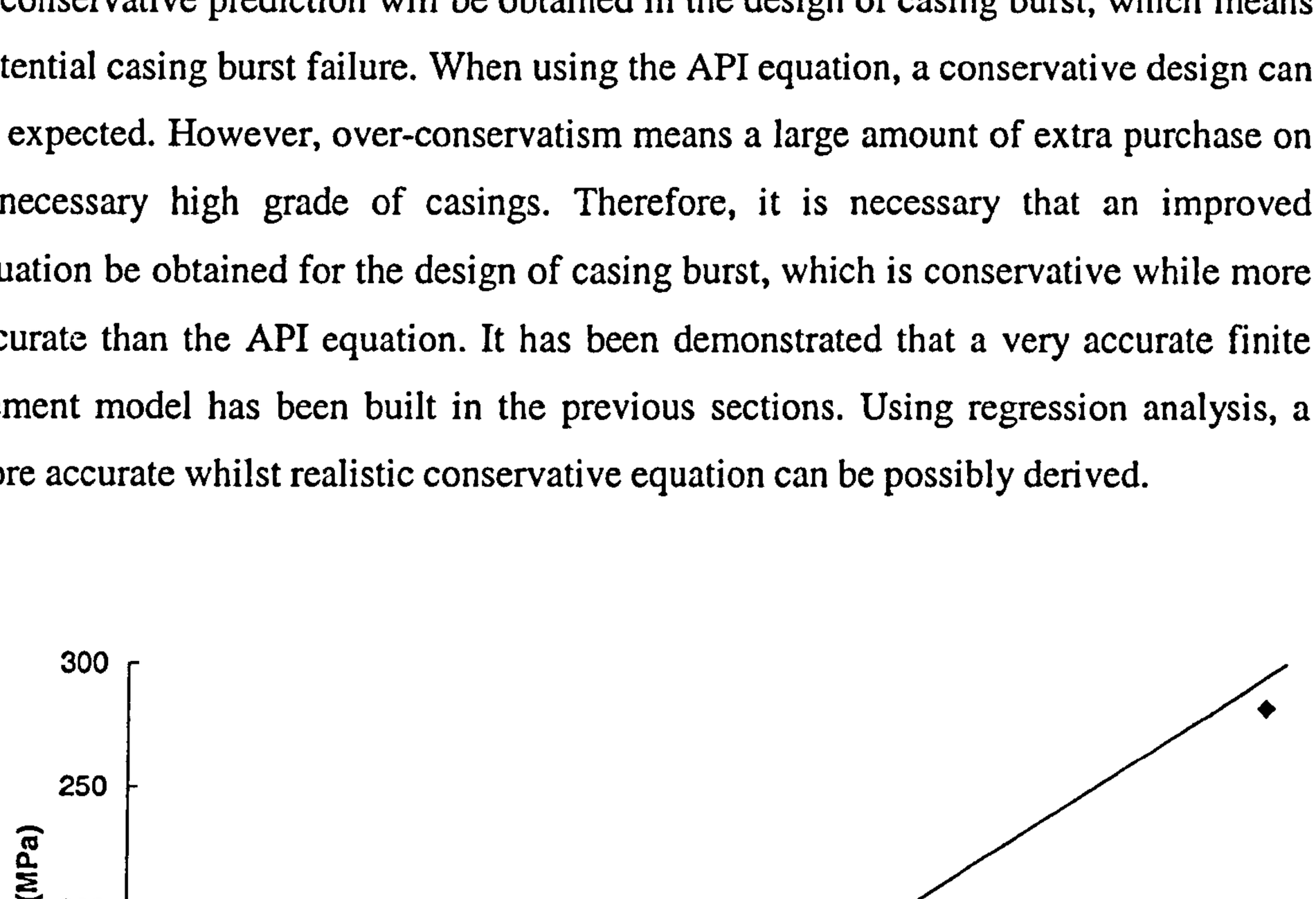

Fig. 6.10 Comparison between experiments and predictions (the Klever equation, 1994)

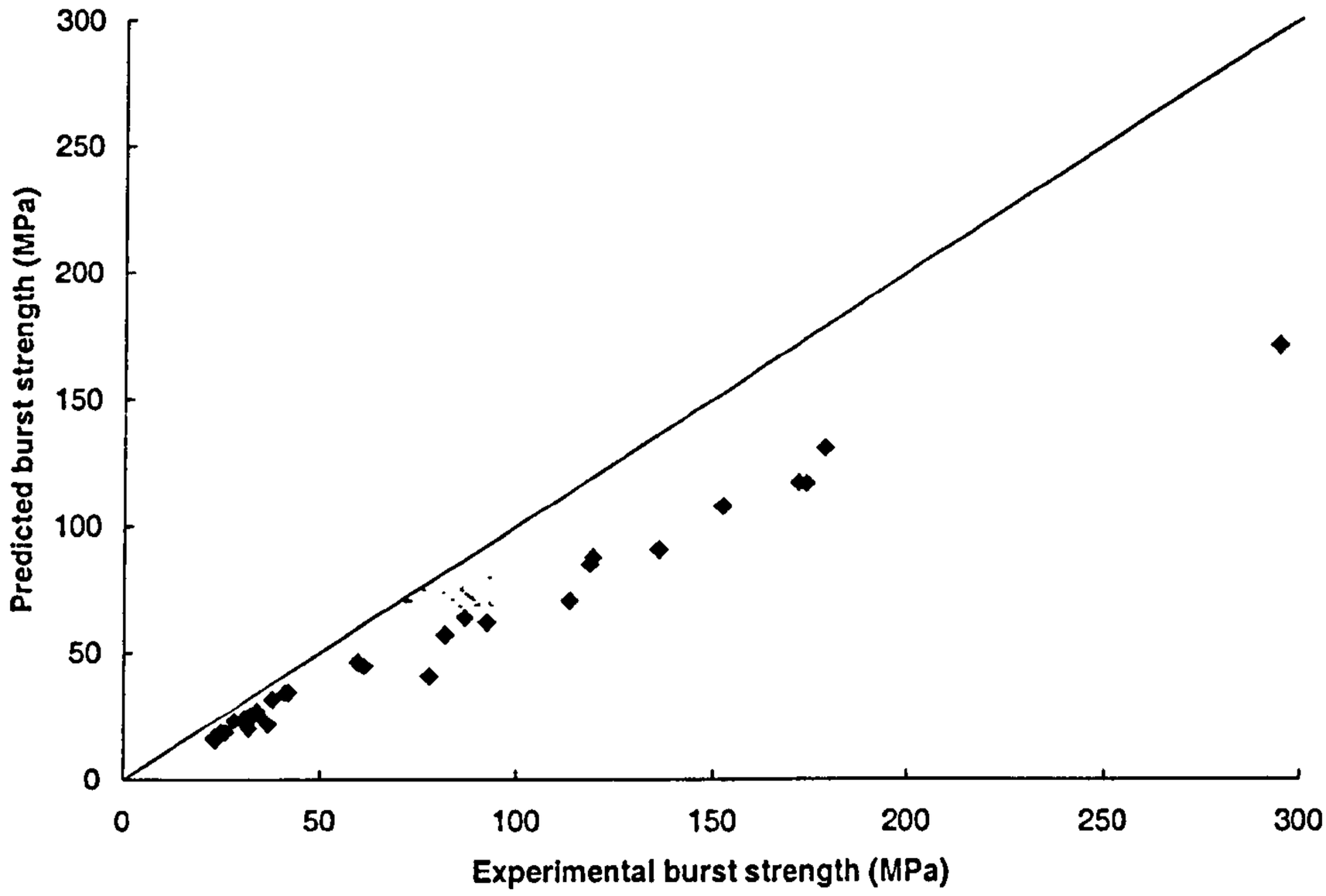

Fig. 6.11 Comparison between experiments and predictions (the API equation, 1992)

6.6.2 Development Of A Burst Predictive Equation

A large number of finite element analyses has been performed to investigate the ultimate burst strength of casings. The predictions from simulation are shown in Fig. 6.12, and regression analyses have been conducted on the basis of the FE predictions. It is very difficult to generate directly a non-linear expression for the casing burst, which is dependent on multiple variables. Trial and test methods are thus used to analysis the predictions from the FEM. Finally it is found that the predicted burst strength divided by $\sigma_y \frac{t}{D}$, as shown in Fig. 6.13, has an approximate linear relationship with the variable t/D as the abscissa. It is noted that, t/D rather than D/t as the abscissa is simply because the curves are more easily fitted in this format. The two variables associated with the linear expression are assumed to have a certain relationship with $\frac{\sigma_y}{E}$, and can be determined by fitting the curve according to the

least square method as shown in Fig. 6.14. Therefore, the design equation for casing burst can be expressed as follows:

$$P_{burst} = \sigma_y \frac{t}{D}(A\frac{t}{D} + B)$$

$$A = -10^8(\frac{\sigma_y}{E})^3 + 10^6(\frac{\sigma_y}{E})^2 - 3680.9 \times \frac{\sigma_y}{E} + 7.2865 \qquad (6.23)$$

$$B = -3 \times 10^7(\frac{\sigma_y}{E})^3 + 400277(\frac{\sigma_y}{E})^2 - 1675.2 \times \frac{\sigma_y}{E} + 4.1703$$

where P_{burst} is the predicted ultimate burst strength, σ_y, E and t/D are the yield strength, Young's modulus and ratio of wall thickness to the outside diameter respectively.

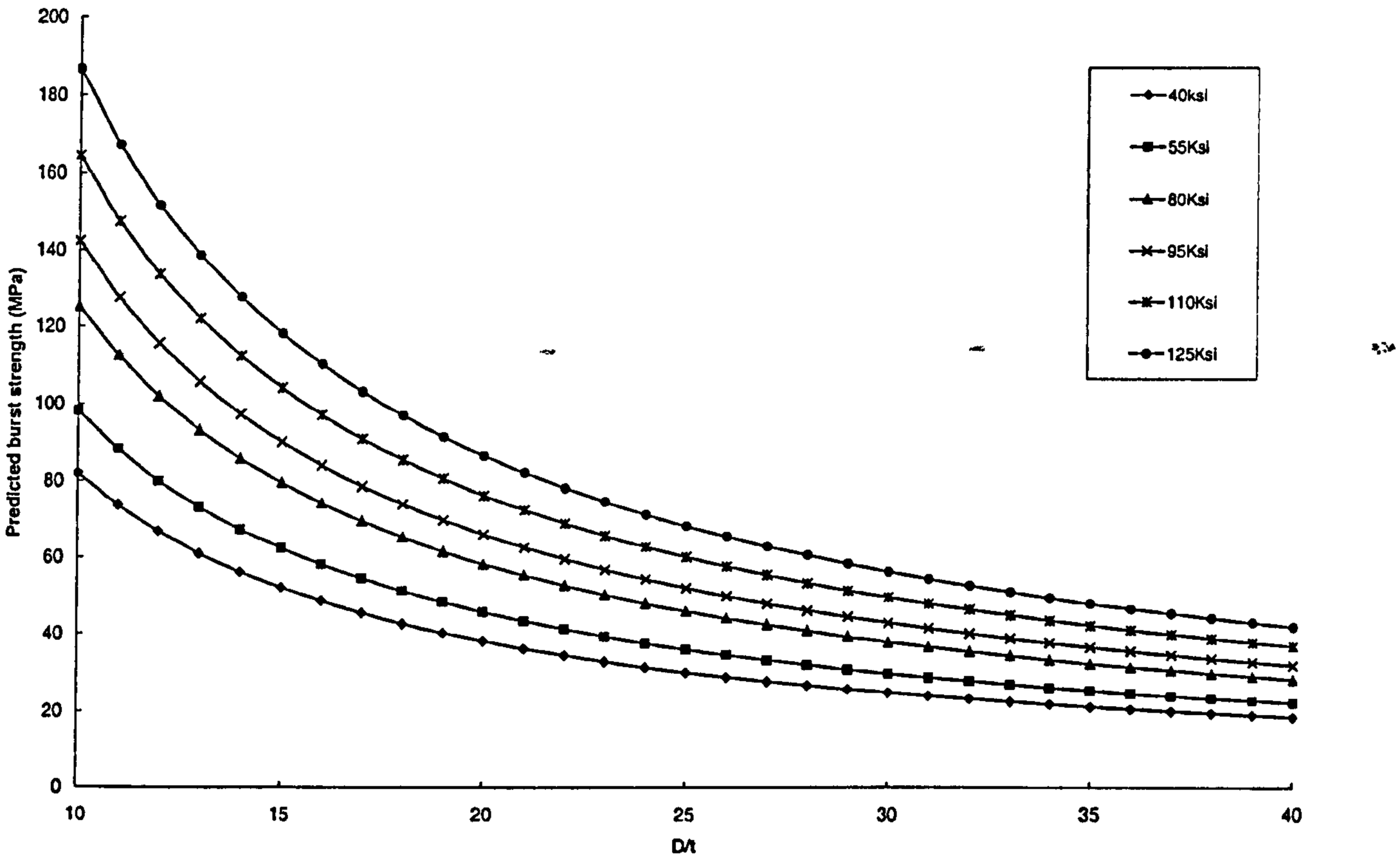

Fig. 6.12 Predicted burst strength of casing from grade K40 to P125

In addition, the predictions from this new design equation for casing burst are compared with experiments as well as the predictions from the API equation as shown in Fig. 6.15. It is evident that the whole predictions from the new burst equation are conservative as expected, and more accurate than those predictions from the API

equation for all experimental data points. In addition, mean values and standard deviations of the predictions from different equations are calculated and summarised in Table 6.5 as well as the coefficient of variation. Although the Hill and Klever equations give better mean values, they are not able to provide a safe design for casing burst. In particular, the predictions from the Klever equation have a smaller deviation than that of the Hill equation, which is in accordance with the observation in the comparison process. In conclusion, the new burst design equation from this research is capable of providing a safe design for casing burst. In the meantime, it is approximately 15 percent more accurate than the API burst equation.

Table 6.5 Prediction error comparison

Parameter	Hill Equation	Klever Equation	API	New Equation
Mean	0.993	0.991	0.718	0.863
Standard Deviation	0.094	0.054	0.076	0.070
COV	0.009	0.003	0.006	0.005

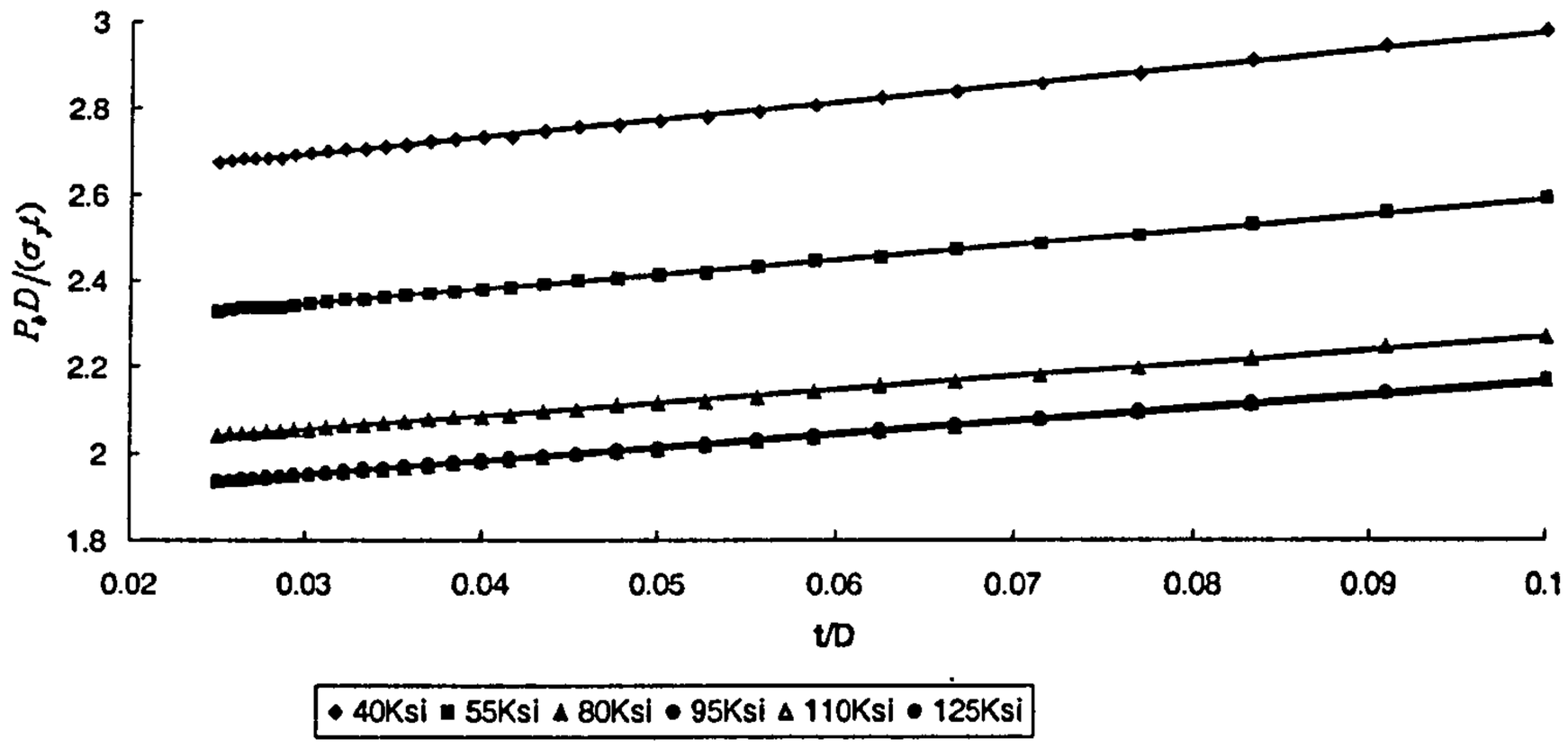

Fig. 6.13 Linear transformation of FEM predictions for casing burst

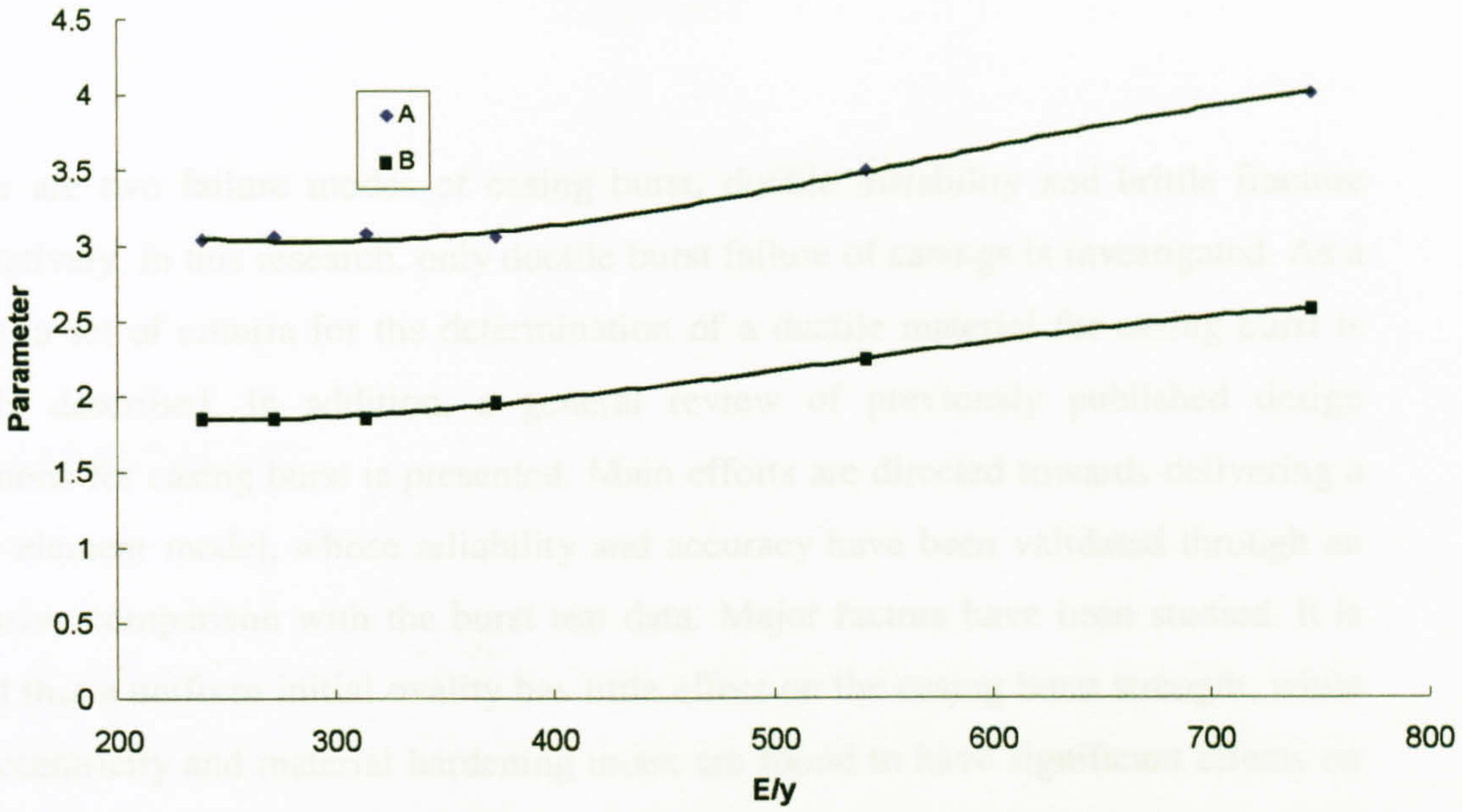

Fig. 6.14 Regression analysis of the variables in the linear expression

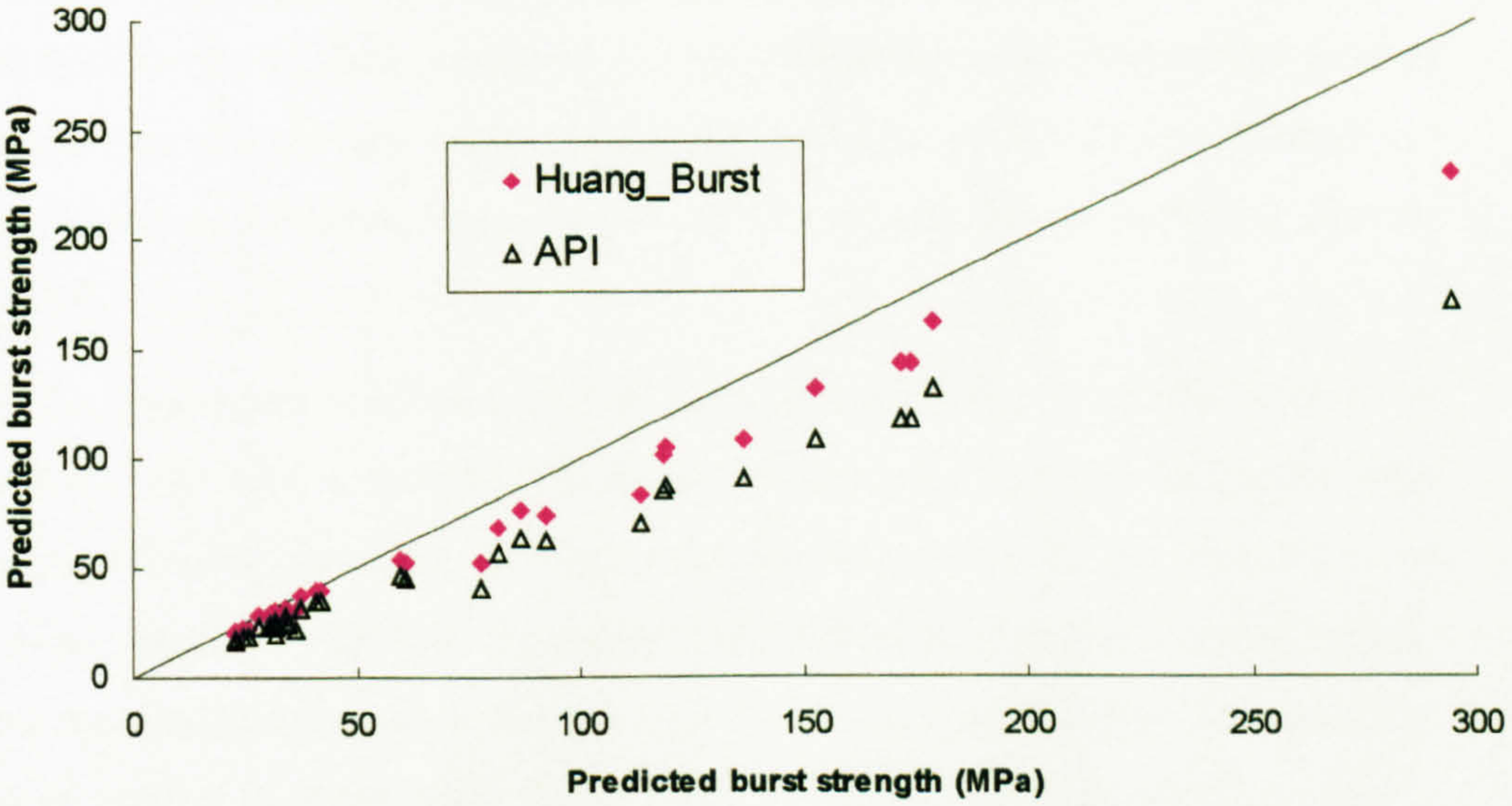

Fig. 6.15 Comparison between burst experiments and predictions from Equations (6.16) and (6.23)

6.7 Summary

There are two failure modes of casing burst, ductile instability and brittle fracture respectively. In this research, only ductile burst failure of casings is investigated. As a result, a set of criteria for the determination of a ductile material for casing burst is briefly described. In addition, a general review of previously published design equations for casing burst is presented. Main efforts are directed towards delivering a finite element model, whose reliability and accuracy have been validated through an extensive comparison with the burst test data. Major factors have been studied. It is found that a uniform initial ovality has little effect on the casing burst strength, while the eccentricity and material hardening index are found to have significant effects on the burst strength. In particular, the eccentricity parameter is capable of giving a good prediction for the remaining burst strength of a casing with localized wall thickness reduction. Detailed comparisons have been performed to assess the accuracy of different design equations for casing burst using the available burst test data. It is found that an improved design equation is necessary for the design of casing burst. As a result, an empirical burst design equation is derived on the basis of regression analysis, which is assessed by the burst test data as well. It is proven from the comparison, that not only is the new burst equation capable of providing a safe design, but also it is 15 percent more accurate than the API burst equation.

Chapter 7

Casing Tension

7.1 Introduction

The oil and gas industry views deep offshore areas as the next frontier for oil exploration and production. With the help of improved drilling techniques, deeper and deeper oil and gas wells can be drilled. A feasibility study (Langner and Ayers, 1985) showed that the technology to explore, drill and produce oil and gas in water depths of 6000 ft (1800 m), and perhaps beyond, could be developed at acceptable costs. As well depth increases, casings receive greater axial tension load due to the weights of the casing strings. Therefore, axial tension design is another consideration in the process of casing design for the oil and gas industry.

Most axial tension load arises from the weight of the casing itself, however, other tension loads of casing can arise due to bending, drag, shock loading and pressure testing during installation. For deep water application, the buoyant force is another important load in the tension design of casings. In practice, the compressive load is less important in comparison with the tensile load and will only be checked for conductor casing as revealed from the British Gas casing design technical manual (Rabia, 1993).

Normally the uppermost joint of a casing string is considered to be the weakest in tension design. The total tensile load must be determined accurately. In the working stress design criterion, casing tensile load is usually designed to be less than the yield strength of the top casing joint. If the casing failure mode is ductile rather than brittle, which is a reasonable assumption for the majority of casings, the material resistance of casing to tension is more likely to be governed by the ultimate tensile strength. Therefore, attention is paid first to investigate the behaviour of a ductile casing under axial tension alone, so called the axial stretch failure (Pattillo and Huang, 1982) due to

excessive axial tensile load. Casing strength is altered under biaxial loadings. In general, collapse strength decreases for a casing loaded in tension, while burst strength increases. The effects, termed biaxial effects, on the casing collapse and burst strength are investigated.

7.2 Casing Failure Under Axial Tension Alone

Under axial tensile loading alone, the casing fails if the induced axial stress exceeds the ultimate tensile stress, providing that the casing is perfect without any material defects. The casing failure under axial tension alone is determined by the material properties in the axial direction. To further demonstrate this point, a three-dimensional FE model is constructed to investigate the casing axial tension problem. Finite element simulations have been performed for casings with an elastic-perfectly-plastic and an elastic-plastic material behaviour under axial tension alone. The relationships between the predicted casing axial strength and deformation are typically shown in Fig. 7.1 for an elastic-perfectly-plastic material with a yield strength of 440 MPa, and Fig. 7.2 for an elastic-plastic material with an ultimate tensile strength of 752 MPa. It is clearly shown in Fig. 7.1 that the predicted ultimate axial tensile strength equals the yield stress in the axial direction for an elastic-perfectly-plastic material. Furthermore, the predicted ultimate axial tensile strength for an elastic-plastic material is very close to the ultimate tensile strength (752 Mpa). Therefore, it is supported from the numerical simulation that the ultimate tensile strength in the axial direction is the limit state strength of a casing in axial tension. The conclusion is in accordance with the findings from the Drilling Engineering Association (DEA), as the following equation is recommended for the casing tension load case (DEA 64, 1994),

$$L_t = \sigma_{uts}[1-(T-T_{ref})\frac{td}{100}] \tag{7.1}$$

where σ_{uts} is the ultimate tensile stress, T is the temperature, T_{ref} is the reference temperature and td is temperature degradation. The other terms are included to account for the effect of temperature variation along the casing length.

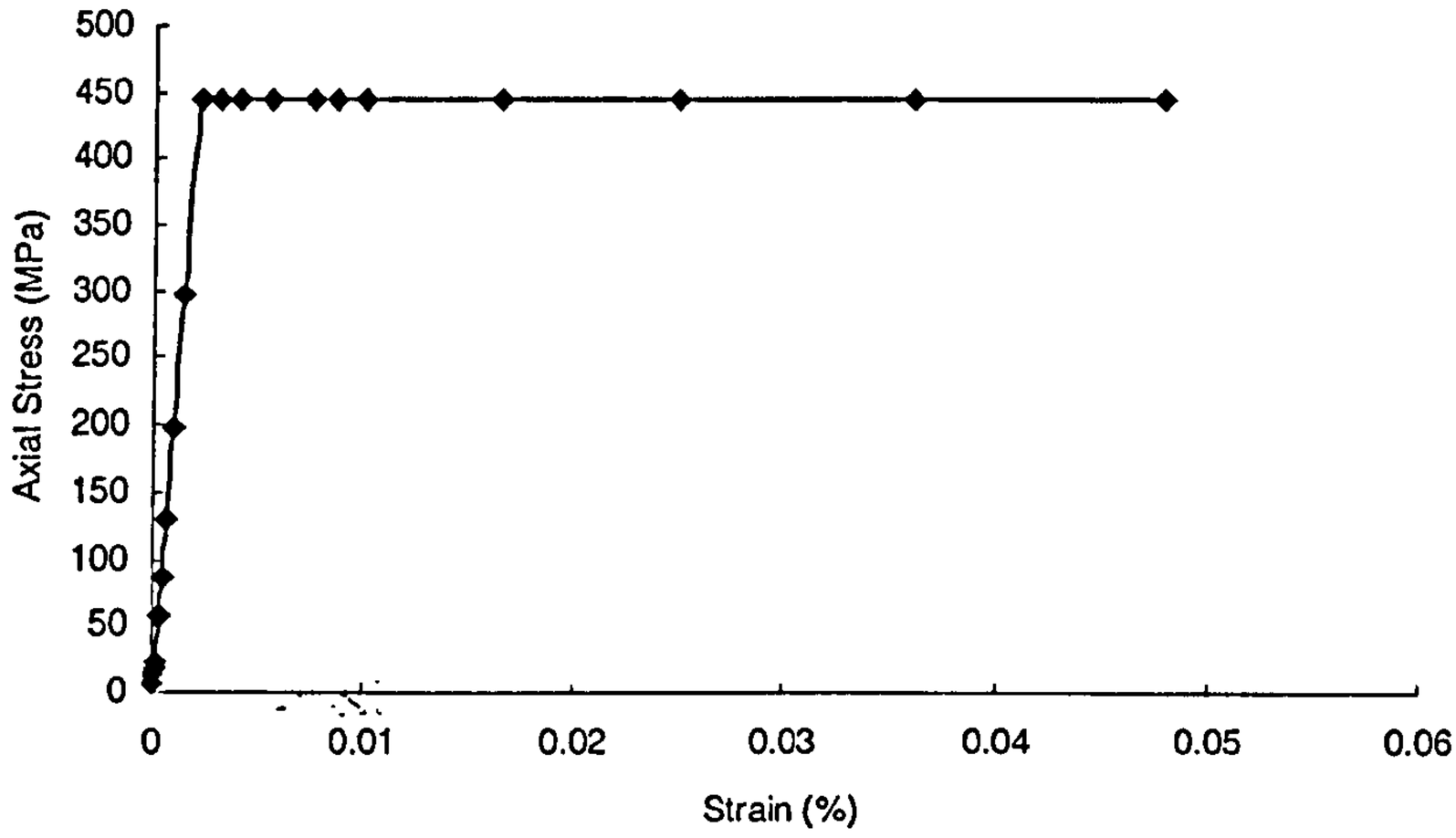

Fig. 7.1 Applied axial tensile stress-strain relationship for a perfect plastic material casing

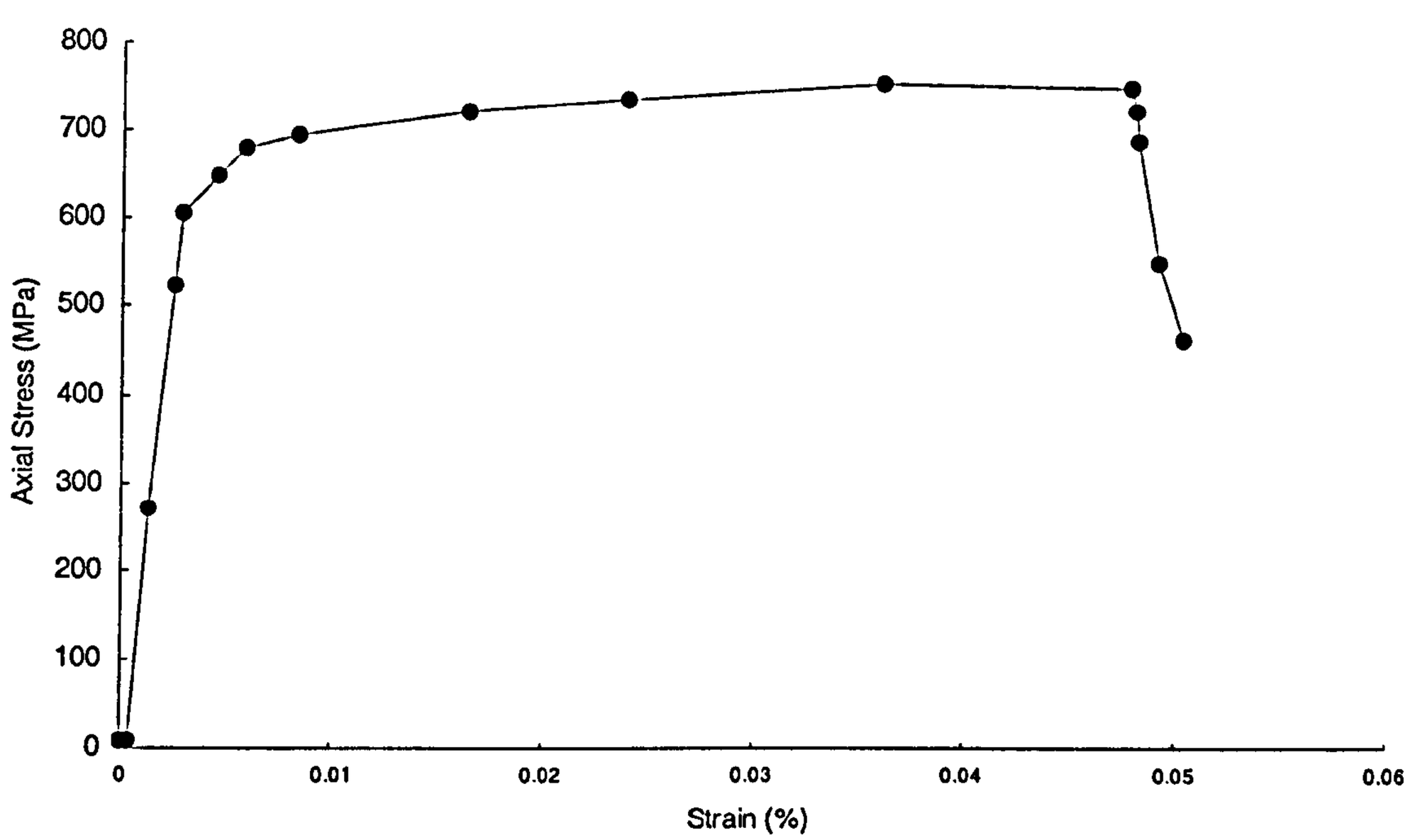

Fig. 7.2 Applied axial tensile stress-strain relationship for an elastic-plastic material casing

7.3 Casing Collapse Under Axial Tension And External Pressure

For elastic collapse under axial tension, theoretical analysis shows that the collapse strength of a casing in tension is the same as that under external pressure alone (Holmquist and Nadai, 1939). This conclusion was further validated experimentally by Kyogoku et al (1982). Therefore, the elastic collapse strength of a casing under axial tension and external pressure is expressed by:

$$P_{ECA} = P_{EC0} = 2\frac{E}{1-\upsilon^2}\frac{1}{D/t\,(D/t-1)} \tag{7.2}$$

where P_{EC0} is the collapse strength under external pressure alone, P_{ECA} is the collapse strength under the combination of external pressure and axial tension, E, υ, D, t are the same parameters defined previously.

For the plastic collapse under axial tension and external pressure, Holmquist and Nadai (1939) derived a yield onset collapse strength under axial loading based on the Mises yield criterion:

$$P_{YA} = P_{Y0}\left[\sqrt{1-0.75\left(\sigma_A/\sigma_y\right)^2} - 0.5\left(\sigma_A/\sigma_y\right)\right] \tag{7.3}$$

where P_{YA} and P_{Y0} are the yield onset collapse strengths with and without axial tension respectively, σ_A is the applied axial stress and σ_y is the yield casing strength.

The American Petroleum Institute (API Bulletin, 1992) summarized the casing collapse data and presented the following formula to calculate the collapse strength under axial stress in the case of plastic collapse,

$$P_{PCA} = P_{PC0}\left[\sqrt{1-0.75\left(\sigma_A/\sigma_y\right)^2} - 0.5\left(\sigma_A/\sigma_y\right)\right] \tag{7.4}$$

where P_{PCA} and P_{PC0} are the plastic collapse strength with and without axial tension respectively.

From the review of the above equations, it can be concluded that for a perfect casing, axial stress has no effect on the elastic collapse strength; its effect on the plastic collapse strength can be included by a correction term as shown in Equations (7.3)

and (7.4). Previous studies have been made for a perfect casing under combined axial tension and external pressure (Pattillo and Huang, 1982; Kyogoku et al, 1982), however, in the presence of geometric imperfections, the effect of axial tensile stress on the casing collapse strength has not been studied sufficiently. Only Tamano et al, (1982 and 1983) investigated the topic on the basis of a small number of casing tests under the combination of axial tension and external pressure. Krug (1983) conducted a large number of casing tests to investigate the casing collapse strength subjected to axial tension and external pressure, including grades K55, N80 and P110 with a casing size from $4\frac{1}{2}$ to $13\frac{3}{8}$ inches (114 mm to 340 mm). Altogether there were 69 specimens tested under tension and external pressure. The geometry data such as outside diameter and wall thickness as well as ovality and eccentricity, material data, exerted axial load and critical test collapse strength are reported as listed in Appendix 4. The test data provides a firm experimental database for the current research investigation into the effect of axial tensile loading on the casing collapse strength in the presence of geometric imperfections. The explicit collapse Equation (5.82) of casing under external pressure alone is employed as P_{C0} in comparison with the test data.

The comparison between the predictions and experiments is shown in Fig. 7.3. It is seen that the effect of axial tension on the collapse strength varies quite smoothly if the applied axial tension load is relatively small. In other words, the effect of axial tension on the ultimate collapse strength is rather small when the applied axial tensile stress is relatively small in comparison with the yield strength of a casing. Therefore, the explicit collapse strength Equation (5.82) under external pressure alone can give a fairly good conservative prediction for casing collapse under a combination of axial tension and external pressure, providing the axial tensile stress is less than $0.45\sigma_y$. A possible reason can be traced back to the implicit conservatism in the derivation of this casing collapse design equation under external pressure alone as already pointed out in Chapter 5. It is therefore, concluded that the derived collapse strength Equation (5.82) under external pressure alone, can be used without any correction even under the combined axial tension and external pressure load case if the applied axial tensile stress is relatively small. When the axial tensile load is greater than $0.45\sigma_y$, a correction term is necessary. If a large axial tensile stress is applied, the casing

collapse strength under the combined loadings decreases very dramatically as shown in Fig. 7.3, which can be approximately estimated using a linear relationship. Therefore, a linear correction term is derived as a lower bound for the ultimate collapse strength of casing under large axial tensile loading, which is expressed as follows:

$$P_{CA} = P_{C0}\left(1.643 - 1.4768\frac{\sigma_A}{\sigma_y}\right) \tag{7.5}$$

where σ_A is the applied axial stress and should be greater than $0.45\sigma_y$ in this empirical correction equation. It is noted that the applied axial stress is calculated according to the applied axial force F_A. For casings, it is calculated by:

$$\sigma_A = \frac{F_A}{\pi(Dt - t^2)} \tag{7.6}$$

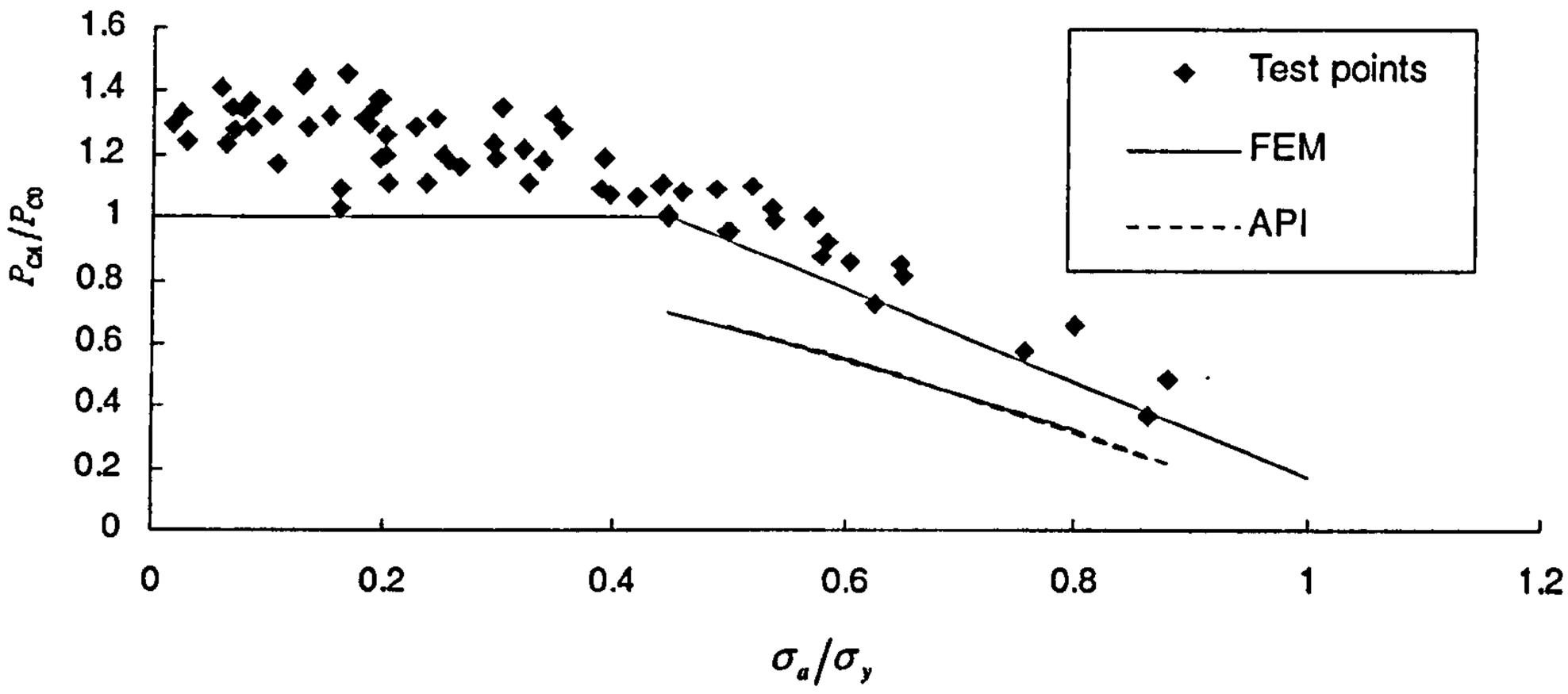

Fig. 7.3 Effect of axial tensile stress on the casing collapse strength

Furthermore, the correction term proposed by the API (1992) is compared with the experimental data and Equation (7.5). It is clearly demonstrated in Fig. 7.3 that the API correction term is more conservative. Although the newly developed correction term is better than the API term, considering the fact that only a limited number of 15 tests with an axial tensile stress greater than $0.45\sigma_y$ were used in the derivation of the correction term, care should be taken when using Equation (7.5). The above correction Equation (7.5) should be further validated by more experiments, it is

therefore suggested by the author, that the API correction term still be used for the calculation of casing collapse strength under a large axial stress.

7.4 Casing Burst Under Axial Tension And Internal Pressure

In general, the presence of an axial tensile load may be beneficial to the casing burst capacity (Adams, 1985; Klever and Stewart, 1998). However, Paslay (1998) proposed the following formula to include the effect of axial tension on the casing burst capacity, which actually means that the presence of internal pressure lowers the ultimate burst strength:

$$P_{BA} = P_{B0} \times \sqrt{1 - \left(\frac{\sigma_A}{\sigma_{uts}}\right)} \tag{7.7}$$

where P_{BA} and P_{B0} are the burst strength with or without axial tensile stress respectively, σ_{uts} is the ultimate tensile strength and σ_A is the applied axial tensile stress calculated from Equation (7.6).

Therefore, it is necessary to clarify the effect of axial tensile stress on the casing burst strength. However, the effect of axial tensile stress on the burst strength has not been studied sufficiently, only a few burst experiments have been carried out so far with an axial tensile stress and internal pressure applied simultaneously. A study has been performed on two casing burst tests (Paslay et al, 1998) under combined axial tension and internal pressure, with the results given in Table 7.1. These two tests were performed with welded end caps and a length to diameter ratio of at least 8. It is noted that the burst strength, P_{B0}, under internal pressure alone is calculated from the newly developed burst design Equation (6.23) and is listed in the table.

It is seen from Table 7.1, that both the experimental measured burst strengths under combined axial tension and internal pressure are greater than those under internal pressure alone. From this limited comparison, it seems that the presence of axial tensile stress is beneficial to the burst strength of a casing without material flaws.

However, a conclusion cannot be easily drawn until more burst test data under combined internal pressure and axial tensile stress become available. If, on the other hand, we consider that welded end caps are used in the burst test under internal pressure alone, the exerted internal pressure would induce some axial tensile stress in the casing wall. Therefore, the experimental burst strength under internal pressure alone was obtained with the presence of a certain amount of axial tensile stress. As a result, the developed burst design equation for casing under internal pressure alone can be used if the applied axial tensile stress is relatively small compared to the yield strength. If, on the other hand, the applied axial tensile stress is relatively large, a further experimental study should be carried out to accurately determine the effect of axial tensile stress on the burst strength.

Table 7.1 Effects of axial tensile stress on the burst strength

No	D (mm)	t (mm)	D/t	σ_y (MPa)	σ_A (MPa)	Test P_{BA} (MPa)	P_{BO} (MPa)
1	88.4	6.1	14.5	695.6	349.0	115.5	100.2
2	172.4	6.5	26.5	466.0	454.6	54.9	38.5

7.5 Summary

.

In this chapter, casing strength under axial tension is studied. It is found that the ultimate tensile strength can be used as the material resistance term in the limit state function for the case of casings under axial tension alone. The casing collapse strength decreases with increasing axial tensile stress. A correction term is proposed to include the effect of axial tension on the collapse strength based on the experimental data. For casing burst under a combination of axial tensile stress and internal pressure, a comparison between experiments and the predictive equation shows that the presence of axial tensile stress is beneficial to the ultimate burst strength. However, further experimental investigations for casing burst in tension will be necessary before a quantitative effect of an axial tensile load on the burst strength can be derived.

Chapter 8

Conclusions And Future Work

8.1 Conclusions

1. The traditional deterministic casing design method, i.e. working stress design (WSD), has a number of shortcomings such as poor economics, inflexibility and uneven risk. The fundamental criticism is that the deterministic design cannot tell how safe a design will be. Therefore, a detailed comparison between deterministic design and reliability-based design is conducted, and applying a full quantitative risk assessment (QRA) methodology in the limit state design is proposed in this thesis. The fundamental difference is that a limit state design equation, which represents the ultimate limit state of the casing for a given load condition, should replace the elasticity-based criteria of working stress design.

2. A set of casing failure modes under casing operating conditions has been identified according to the predominance of a particular load. A set of simple equations has been proposed for the calculation of the load term in a limit state design equation of casing design for the different failure modes. The other term in a limit state design equation, casing material strength depends primarily on the casing dimensions and the material properties.

3. Geometric imperfections can dramatically decrease the ultimate casing strength, however their effects on the casing strength have to be investigated using numerical analysis. Therefore, a comprehensive finite element methodology has been presented to investigate the ultimate strength of casing collapse, casing burst and casing axial tension. Extensive comparisons between the FEM and experiments demonstrate that, if the variables are known, the ultimate strength of a casing can be predicted to a satisfactory degree of accuracy.

4. Detailed parametric studies have been performed to investigate the effects of major factors on the ultimate casing strength. In particular, it is found that for casing collapse, initial ovality and eccentricity exert a considerable influence on the ultimate collapse strength, whereas the effect of residual stresses is negligibly small. For casing burst, the effect of initial ovality is negligibly small, while the initial eccentricity and localized thickness reduction primarily determine the ultimate burst strength. For casings under axial tensile loading alone, the casing strength depends on its material properties.

5. Existing design equations for casing failure have been assessed using full-scale test data. Comparisons in Chapter-5 have shown that, the Tamano equation (1983) over-estimates the ultimate collapse strength of casing, almost every prediction is greater than the actual experimental collapse strength. The Issa (1993) and Tokimasa (1986) equations are generally closer to the actual collapse strength with half the predictions conservative and half unconservative. The API collapse equation (1992) gives almost conservative predictions. However, compared with the actual collapse strength, predictions from the API collapse equation are too conservative.

6. Similar conclusions have been obtained for casing burst. The Klever (1998) and Hill (1950) equations give predictions, that are half conservative and half unconservative. Predictions from the API burst design equation (1992) for casing burst are too conservative in comparison with the experimental burst strength of casing.

7. The concept of a generalized material behaviour is proposed, which is determined on the basis of experiments in the derivation of limit state design equations for the casing collapse and burst. An empirical design Equation (5.75) for casing collapse is proposed based on finite element analysis, which is conservatively close to the actual ultimate collapse strength of casing in comparison with test data. It is noted that the imperfection factors are included implicitly in Equation (5.75). In addition, further refinement has been conducted to improve the performance of the implicit design Equation (5.75) for casing collapse. By combining the implicit design equation together with the Issa equation, an improved prediction of ultimate collapse strength can be obtained. Therefore, the conclusion is drawn that for casing collapse, design Equation (5.75) with imperfections expressed implicitly should be used when

imperfection data are not available. The design Equation (5.82) with imperfections expressed explicitly should be used when imperfection data are available. Comparison with the API equation has proved that the new design equations for casing collapse provide a more accurate prediction. An empirical burst design Equation (6.23) has been derived on the basis of FE analysis of casing burst, which is extensively validated by burst test data. It is proven from the comparison that not only is the new burst equation able to provide a safe design, but also it is 15 percent more accurate than the API burst equation.

8. Casing strength under axial tension alone has been studied. In particular, it is concluded that, the ultimate tensile strength of casings can be used as the material resistance term in the limit state equation for this load case. Furthermore, it has been found that the casing collapse strength decreases with increase of axial tensile stress, while the presence of axial tensile stress is beneficial to the ultimate burst strength.

9. Overall, in this thesis a comprehensive methodology using the finite element method to derive the limit state design equations of casing design for the oil and gas industry has been presented. For three fundamental load cases, i.e. casing collapse, casing burst and casing axial tension, the calculations of the limit state load terms are provided in Chapter 3, while the calculations for the ultimate material resistance terms are given in Chapters 5, 6 and 7 respectively. The ultimate limit state design of casings for each load case is summarised in Tables 8.1, 8.2 and 8.3 respectively. In addition, a design flow chart is given for each load case in Fig. 8.1, 8.2 and 8.3, so that the limit state casing design methodology can be used in a structured way. In this way, engineers with a traditional casing design background can easily access the limit state casing design methodology proposed in this thesis.

Table 8.1 Ultimate Limit State Design for Casing Collapse ($G(Z) = R(Z) - L(Z)$)

A) Resistance Calculation of Casing Collapse

Step 1, $R = P_{est}$ if imperfection data are not available,

$$P_{est} = \frac{2\sigma_y (D/t - 1)}{D/t} e^{(h_1 + h_2 D/t)}$$

$$h_1 = 167.6393 \frac{\sigma_y}{E} - 2.25314 \tag{8.1}$$

$$h_2 = -10.57427 \frac{\sigma_y}{E} - 0.0571617$$

Step 2, continue calculation if imperfection data are available, otherwise go to part B.
Step 3, calculate the elastic collapse strength,

$$P_E = \frac{2E}{1-\upsilon^2} \frac{1}{(D/t)(D/t-1)^2} \tag{8.2}$$

Step 4, calculate the elastic-plastic collapse strength,

$$P_{EP} = \frac{\sigma_y (D/t - 1)}{(D/t)^2} \left[\frac{A_1}{1 + \left[A_2 + A_3 (\sigma_y / E)\right](D/t)} \right] \tag{8.3}$$

$$A_1 = 7.0333 \quad A_2 = 0.1295 \quad A_3 = 12.3298$$

Step 5, calculate the overall collapse strength for a nearly perfect casing,

$$P_{IP} = \left[\frac{1}{2}(P_E + P_{EP}) - \frac{1}{2}\sqrt{(P_E - P_{EP})^2} \right] \tag{8.4}$$

Step 6, calculate the ovality reduction factor,

$$h(u) = \frac{1}{1 + \left[B_1 + B_2 \left(\frac{D}{t} \right) \right] u^{B_3}} \tag{8.5}$$

$$B_1 = 0.1648 \quad B_2 = 0.5972 \quad B_3 = 0.7618$$

Step 7, calculate the eccentricity reduction factor,

$$h(\psi) = (1 - \psi)(1 + C_1 \psi + C_2 \psi^2) \tag{8.6}$$

$$C_1 = 0.8123 \qquad C_2 = -1.1272$$

Step 8, multiply all values together to obtain the final residual collapse strength,

$$R = 0.4951 \times P_{IP} \times h(u) \times h(\psi) + 0.5647 \times P_{est} \tag{8.7}$$

B) Load Calculation of Casing Collapse

a) $L = P_{cs}$ for the design of surface casing,

$$P_{cs} = \rho_m \, H_{CSD} \, g \tag{8.8}$$

b) $L = P_{CSD-L}$ for intermediate and production casings,

$$P_{CSD-L} = \rho_m \, g \left(H_{CSD} - \frac{H_{CSD} \, \rho_f}{\rho_{mi}} \right) \tag{8.9}$$

Table 8.2 Ultimate Limit State Design for Casing Burst ($G = R - L$)

A) Resistance Calculation of Casing Burst

$$P_{burst} = \sigma_y \frac{t}{D}(A\frac{t}{D} + B)$$

$$A = -10^8(\frac{\sigma_y}{E})^3 + 10^6(\frac{\sigma_y}{E})^2 - 3680.9 \times \frac{\sigma_y}{E} + 7.2865 \qquad (8.10)$$

$$B = -3 \times 10^7(\frac{\sigma_y}{E})^3 + 400277(\frac{\sigma_y}{E})^2 - 1675.2 \times \frac{\sigma_y}{E} + 4.1703$$

B) Load Calculation of Casing Burst

Case 1, casing burst due to tube leak

If the annulus fluid is denser than the back-up pressure gradient, load is calculated,

$$P_{b-tl} = [P_{res} - \rho_{pf}\, g\,(d_{perfs} - d_{wh}) + \rho_i\, g\,(d_{packer} - d_{wh})] - \rho_0\, g\, d_{packer} \qquad (8.11)$$

If the annulus fluid is less dense than the back-up pressure gradient, load is calculated,

$$P_{b-tl} = [P_{res} - \rho_{pf}\, g\,(d_{perfs} - d_{wh})] - \rho_0\, g\, d_{wh} \qquad (8.12)$$

Case 2, casing burst due to gas kick

Without formation fracture, the load is calculated,

$$\begin{aligned} &Cased\ \ Hole && P_{b-gk} = P_2 - \rho_o g d_2 \\ &Open\ \ Hole && P_{b-gk} = P_2 \end{aligned} \qquad (8.13)$$

With formation fracture, the load is calculated,

$$P_{b-ff} = \left|P_{fact} - \rho_i\, g\,(d_{shoe} - d_2)\right| - \rho_o\, g\, d_2 \qquad (8.14)$$

Case 3, casing burst due to pressure test

$$\begin{aligned} &Uncemented && P_{b-pt} = P_{test} \\ &Cemented && P_{b-pt} = [P_{test} + \rho_m\, g\,(d_{shoe} - d_{toc})] - \rho_{cement}\, g\,(d_{shoe} - d_{toc}) \end{aligned} \qquad (8.15)$$

Table 8.3 Ultimate Limit State Design for Casing Tension ($G(Z) = R(Z) - L(Z)$)

A) Resistance Calculation of Casing Tension

$$R(Z) = \sigma_{uts} \tag{8.16}$$

B) Load Calculation of Casing Tension

$$L_{at} = (\rho_s A_s g d - \rho_m A_{sshoe} g d + P_{op})\left(\frac{1}{A_s}\right) \tag{8.17}$$

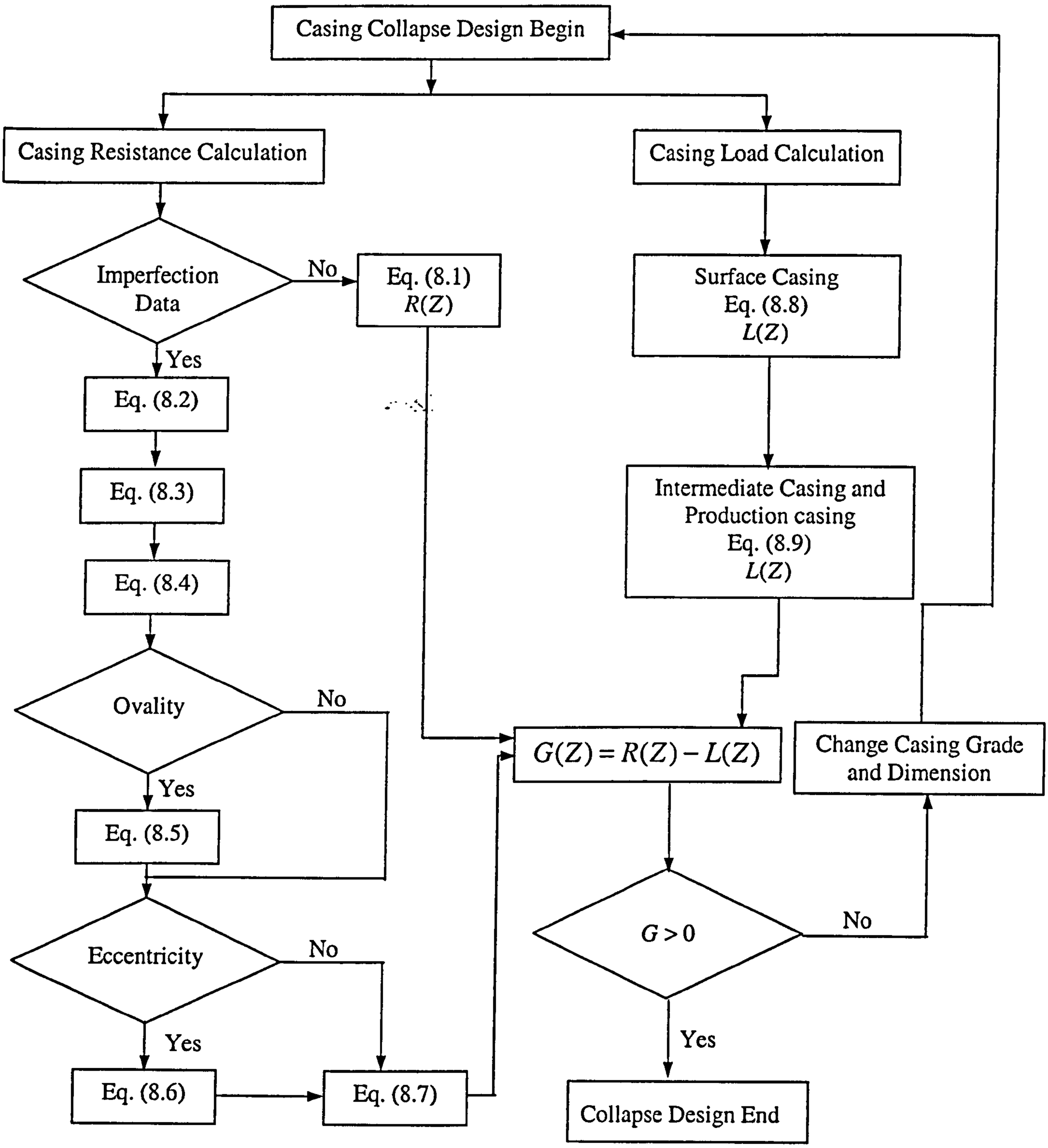

Fig. 8.1 Design flow chart for casing collapse

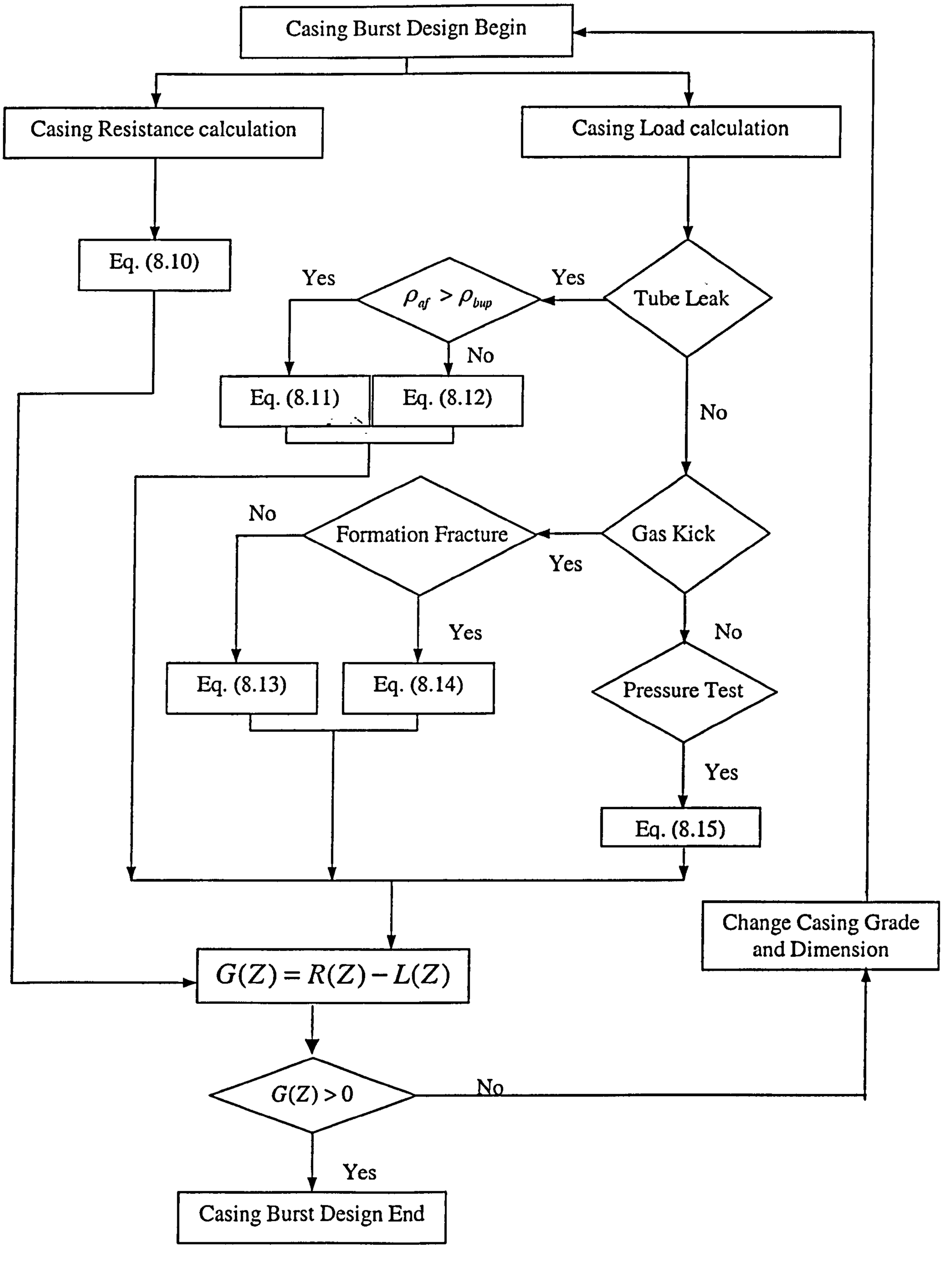

Fig. 8.2 Design flow chart for casing burst

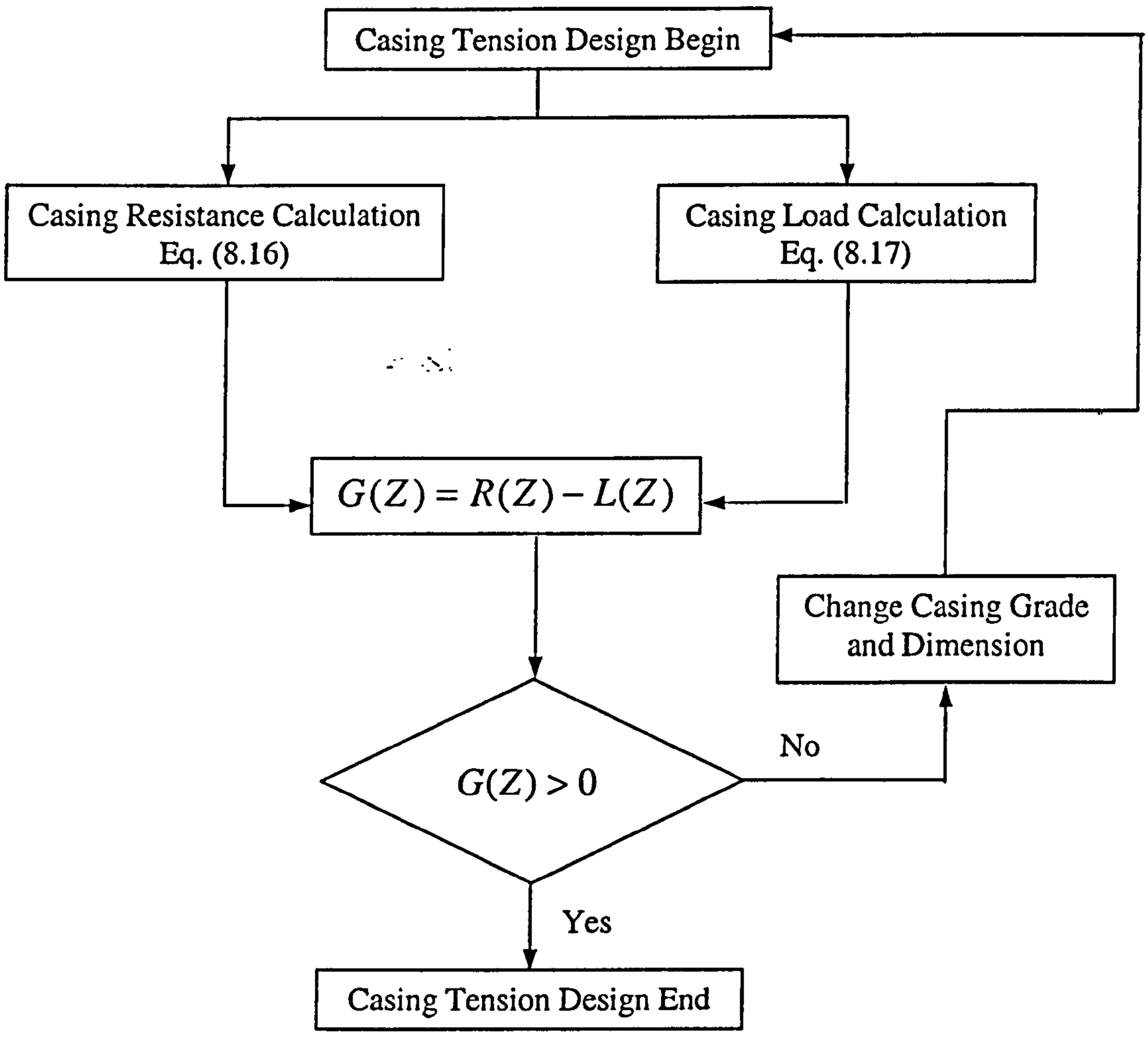

Fig. 8.3 Design flow chart for casing tension

8.2 Recommendations For Future Work

1. Two catalogues of limit states are usually considered in the limit state design. The ultimate limit state (ULS) describes the true maximum load carrying capacity of a structure; while the service limit state (SLS) describes the normal working conditions. As a first step in the development of a limit state casing design, this thesis presents a set of ultimate limit state design equations. Therefore, the service limit state design of casing is recommended for further work after this study. This may include large deflections, vibration due to wind and wave loadings, repairable damage due to fatigue, localized failure due to corrosion, and fracture due to cracks.

2. The ultimate limit state design equations are validated for vertical wells, but effect of bending has not been included. However, in many cases, it is necessary to drill deviated wells, thus the effect of bending on the casing resistance is recommended for further work. Moreover, the external pressure and internal pressure considered in this thesis are uniformly distributed. However in some cases, the load is not uniformly distributed. For example, salt creep behaviour of areas in the North Sea will impose a non-uniform load profile on top of the more usual formation pressure. The refined effect of the non-uniform pressure load is also recommended for further work.

3. An initial investigation of the biaxial effect on the casing strength is conducted in this thesis. A correction term is proposed for casing collapse to include the influence of the axial tension loading provided it is greater than $0.45\sigma_y$. However, this correction term should be used with caution since the experimental collapse data under large tensile loads is insufficient. A similar situation is encountered for casing burst under combined loadings. Therefore, further investigation is necessary to derive more accurate modification terms. Experimental investigations on casing collapse and burst under axial loadings are thus recommended for further work.

REFERENCES

ABAQUS/Standard, User's Manual, Vol. 1-3, Version 5.8, Hibbitt, Karlsson and Sorensen Inc., 1998.

ABAQUS/Standard, Theory Manual, Version 5.8, Hibbitt, Karlsson and Sorensen Inc., 1998.

ABAQUS/Standard, Verification Manual, Version 5.8, Hibbitt, Karlsson and Sorensen Inc., 1998.

ABAQUS/Standard, Example Manual, Vol. 1-2, Version 5.8, Hibbitt, Karlsson and Sorensen Inc., 1998.

Abbassian F and Parfitt S, "Collapse and Post Collapse Behaviour of Tubulars: A Simple Approach", SPE 29458, Proceedings of SPE Production Operations Symposium, Oklahoma City, April 1995.

Adams A, Parfitt S, Reeves T, and Thorogood J, "Casing System Risk Analysis Using Structural reliability", SPE/IADC 25693, Proceedings SPE/IADC Drilling Conference, Amsterdam, Feb. 1993.

Adams A and Glover S, "An Investigation into the Application of QRA in Casing Design", SPE 48319, Applied Technology Workshop on Risk Based Design of Well Casing and Tubing, The Woodlands, Texas, USA, 7-8 May 1998.

Adams A, Warren A and Masson P, "On the Development of Reliability-Based Design Rules for Casing Collapse", SPE 48331, Applied Technology Workshop on Risk Based Design of Well Casing and Tubing, The Woodlands, Texas, USA, 7-8 May 1998.

Adams N, "Drilling Engineering: A Complete Well Planning Approach", Penn Well Publishing Company, Tulsa, Oklahoma, USA.

Allen D, "Criteria for Design Safety Factors and Quality Assurance Expenditure", Proceedings ICOSSAR, Trondheim, Norway, pp 667-678, June 1981.

Amano K, "Significance of Yield Ratio Limitation to Plastic Deformation of Pipeline in High Pressure Proof Test", 7th Symposium on Line Pipe Research, Houston, 1986.

API Bulletin 5C3, "Bulletin on Formulas and Calculations for Casing, Tubing, Drill Pipe and Line Pipe Properties", American Petroleum Institute, 1992.

Arbocz J and Babcock C, "The Effect of General Imperfections on the Buckling of Cylindrical Shells", ASME, Journal of Applied Mechanics, Vol 36, pp 28-38, 1969.

Arbocz J and Williams J, "Imperfection Surveys of a 10 ft Diameter Shell Structures", AIAA Journal, Vol. 15, pp 949-956, 1977.

Assanelli A, Toscano R, Johnson D and Dvorkin E, "Collapse Behaviour of Casings: Measurement Techniques, Numerical Analyses and Full Scale Testing", SPE/ATW Risk Based Design of Well Casing and Tubing, the Woodlands, Texas, 7-8 May 1998.

Assanelli A, Toscano R, Johnson D and Dvorkin E, "Analysis of the Collapse of Steel Tubes under External Pressure", Computational Mechanics new Trends and Applications, Barcelona, Spain 1998.

Assanelli A and Dvorkin E, " Experimental / Numerical Analysis of the Collapse Behaviour of Steel Pipes", Accepted for publication in Engineering Computations, Oct. 1999.

ASTM, "Standard Test Method for Plane Strain Fracture Toughness of Metallic Materials", Annual book of ASTM Standards, Section3, Vol. 3.01, 412-442, 1995.

Bai Y, Igland R and Moan T, "Tube Collapse under Combined Pressure, Tension and Bending Loads", International Journal of Offshore and Polar Engineering, Vol. 3, No. 2, pp 121-129, June 1993.

Babcock C and Arbocz J, " Imperfection Measurements of Large Shell Structures", GALCIT Report No. SM 78-8, Presented at the 8th US Congress of Applied Mechanics, June 1978.

Bai Y, Igland R and Moan T, "Collapse of Thick Tubes under Combined Tension and Bending Loads", Journal of Constructional Steel Research, Vol. 32, pp 233-257, 1995.

Bai Y, Igland R and Moan T, "Tube Collapse under Combined External Pressure, Tension and Bending", Marine Structures, Vol. 10, pp 389-410, 1997.

Brand P and Lewis D, "Load and Resistance Factor Design Case Histories", 27th Annual Offshore Technology Conference, Houston, Texas, USA, 1-4 May 1995.

Brebbia C, "The Boundary Element Method for Engineers", Pentech Press, 1978.

Burres C, Tallin A and Cernocky E, "Determination of Casing and Tubing Burst and Collapse Design Factors to Achieve Target Levels of Risk, Including Influence of Mill Source", SPE 48321, Applied Technology Workshop on Risk Based Design of Well Casing and Tubing, the Woodlands, Texas, 7-8 May 1998.

Chakrabarty J, "Theory of Plasticity", McGraw Hill, New York,1987.

Cheung Y, Lo S and Leung A, "Finite Element Implementation", Blackwell Science, 1996.

Clinedinst W, "A Rational Expression for the Critical Collapsing Pressure of Pipe under External Pressure", Drilling Production Practice, American Petroleum Institute, pp 383-391, 1939.

Clinedinst W, "Analysis of Collapse Test Data and Development of New Collapse Resistance Formulae", API Task Group on Performance Properties Report, 14 Oct. 1977.

Cook R, Malkus D and Plesha M, "Concepts and Applications of Finite Element Analysis"" 3rd Edition, John Wiley and sons, 1989.

DEA (E)-64, "The Use of QRA in Casing Design", Documentation Pack for Third progress Meeting, Newcastle, October 1994.

Donnell L, "Effect of Imperfections on Buckling of Thin Cylinders under External Pressure", Transaction of ASME, Series E, Vol 78, pp 569-575, 1956.

Ellingwood B and Plesha M, "Probability Based Load Criteria: Load Factors and Load Combinations", Journal of Structural Division, ASCE, ST5, Vol. 108, pp 978-997.

Frame W, "Casing Setting Depths Are Not Assured by Physical Properties of the Steel", Drilling and Production Practice, pp 322-329, 1938.

Gulati K and Leung A, "Reliability-Based Design and Application of Drilling Tubulars", 26th Annual Offshore Technology Conference in Houston, Texas, USA, 2-5 May 1994.

Harvey J, "Theory and Design of Modern Pressure Vessels", Van Nostrand reinhold, New York, N. Y. 10001, 1986.

Heise O and Esztergar E, " Elastoplastic Collapse of Tubes under External Pressure", ASME, Journal of Engineering for Industry, Vol. 92, pp 735-742,1970.

Hilderbrand F, "Methods of Applied Mathematics", Prentice-Hall, Second Edition, 1965.

Hill R, "The Mathematical Theory of Plasticity", Oxford University Press, 1950.

Hirakawa K and Tokimasa K, "An Experimental Study on the Critical Collapsing Pressure of Seamless Steel Tube for Well Casing under External Pressure, Part 2: The Effects of L/D on the Collapsing Pressure", Pressure Engineering, Vol. 18, No. 5, pp 247-254, 1980.

Holmquist J and Nadai A, "A Theoretical and Experimental Approach to the Problem of Collapse of Deep-Well Casing", American Petroleum Institute, Drilling and Production Practice, pp 392-420, 1939.

Huang N and Pattillo P, "Collapse of Oil Well Casing", ASME paper No. 80-C2/PVP-89, ASME Pressure Vessel and Piping Conference, San Francisco, August 12-15, 1980.

Huang X, Mihsein M, Kibble K and Hall R, "Ultimate Collapse Strength analysis of Casing Design", Proceeding of ASME Pressure Vessels and Piping Conference, Seattle, Washington, PVP Vol. 399, pp 271-278, July 23-27,2000.

Huang X, Mihsein M, Kibble K and Hall R, "Collapse Strength Analysis of Casing Design Using Finite Element Method", International Journal of Pressure Vessels and Piping, Vol. 77, pp 359-367, Sep. 2000.

Huang X and Mihsein M, " FEM Predictions of The Ultimate Collapse Strength of Casing', Proceedings of Institution of Mechanical Engineers, Part C, Journal of Mechanical Engineering Science, Vol. 214, No. 12, pp 1-13, Dec. 2000.

International Organization for Standardization, "International Standard ISO 2394: General Principles on Reliability for Structures", Second Edition, 1986.

Issa A and Crawford D, "An Improved Design Equation for Tubular Collapse", Society of Petroleum Engineers, SPE 26317, 68th Annual Technical Conference and Exhibition in Houston, Texas, 3-6 Oct. 1993.

Jasper M and Sullivan J, "The Collapsing Strength of Steel Tubes", Transaction of ASME, Vol. 53, APM-53-17b, pp 219-245, 1931.

Jiao G, Mork K, Bruschi R and Sotberg T, "The Superb Project: Reliability Based Design Procedures and Limit State Design Criterion for Offshore Pipelines", OMAE Pipeline Technology ASME, Vol. V, pp 57-68, 1997.

Johnson W and Mellor P, "Engineering Plasticity", Halsted Press, John Wiley and Sons, New York, 1973.

Ju G, Power T and Tallin A, "A reliability Approach to the Design of OCTG Tubulars against Collapse", SPE 48332, Applied Technology Workshop on Risk Based Design of Well Casing and Tubing, The Woodlands, Texas, USA, 7-8 May 1998.

Kanda M, Yazaki Y and Yamamoto K, "Development of NT-Series Oil-Country Tubular Goods", Nippon Steel, Technical Report No. 21, June 1983.

Kapur K and Lamberson L, "Reliability in Engineering Design", John Wiley, New York, 1977.

Keitty I and Rabia H, "Applying Quantitative Risk Assessment to Casing Design", IADC/SPE Drilling Conference , IADC/SPE 35038, New Orleans, Louisiana, USA, 1996.

Kennedy C and Venard J, "Collapse of Tube by External Pressure", Developments of Theoretical and Applied Mechanics, Proceedings of the First Southeast Conference of Theoretical and Applied Mechanics, Gatlinburg, Tenn., May 1962.

Khan A and Huang S, "Continuum Theory of Plasticity", John Wiley and Sons, New York, 1995.

Kiefner J, Maxey W and Duffy A, "The Significance of the Yield-To-Ultimate Strength Ratio of Line Pipe Materials", American Gas Association, NG-18 Report, March 13, 1971.

Klever F, "Burst Strength of corroded pipe: Flow Stress Revisited", Offshore Technology Conference (OTC), Houston, Texas, 1992.

Klever F, Palmer A and Kyriakides S, "Limit State Design of High Temperature Pipelines", KSEPL publication 1196, Dec. 1993.

Klever F and Stewart G, "Analytical Burst Strength Prediction of OCTG with and without Defects", SPE Applied Technology Workshop on Risk Based Design of Well Casing and Tubing, the Woodlands, Texas, 7-8 May 1998.

Krug G, "Testing of Casing under Extreme Loads", Institute of Petroleum Engineering, Technische University Clausthal, 1983.

Kyriakides S and Babcock C, "Large Deflection Collapse Analysis of An Inelastic Inexternal Ring under External Pressure", International Journal of Solid Structures, Vol. 17, pp 981-993, 1981.

Kyriakides S and M Yeh, "Plastic Anisotropy in Drawn Metal Tubes", Journal of Engineering for Industry, Transactions of the ASME, Vol. 110, pp 303-307, 1988.

Kyogoku T, Tokimasa K, Nakanishi H and Okazawa T, "Experimental Study on the Effect of Axial Load on the Collapse Strength of Oilwell Casing", Journal of Society of Petroleum Engineers, Vol. 22, pp 609-615, 1982.

Langner C, "Design of Deep Water Pipelines", Proceedings of the 30th Anniversary Symposium on Underwater Technology, TNO, May 1984.

Langner C and Ayers R, "The Feasibility of Laying pipelines in Deep Waters", ASME, Proceedings of OMAE Symposium, Vol. 1, pp 478-489, Feb. 1985.

Lewis D, Brand P, Hood M and Maes M, "Load and Resistance Factor Design for Oil Country Tubular Goods", 27th Annual Offshore Technology Conference, Houston, Texas, USA, 1-4 May 1995.

Lewis D, Brand P and Maes M, "The Use of QRA Technology in Drilling and Well Operations", SPE 48323, Applied Technology Workshop on Risk Based Design of Well Casing and Tubing, The Woodlands, Texas, USA, 7-8 May 1998.

Ludwik P, " Elementary Technology of Mechanics", Springer-Verlag, 1909.

MacEachran A and Adams A, " Impact on Casing design of Thermal Expansion of Fluids in Confined Annuli", SPE/IADC 21911, Proceedings of Drilling Conference, pp 529-540, Oct. 1991.

Maes M and Breitung K, "Reliability-Based Tail Estimation", Proceedings IVTAM Symposium on Probabalistic Structural Mechanics, San Antonio, TX, June 1993.

Maes M, Breitung K and Dupuis D, "Asymptotic Importance Sampling", Structural Safety, Vol. 12, pp 167-186, Oct. 1993.

Maes M, Gulati K, McKenna D, Brand P, Lewis D and Johnson R, "Reliability-Based Casing Design", ASME Journal of Energy Resources Technology, Vol. 117, pp 93-100, June 1995.

Maruyama K and Yazaki Y, "The influence of shape and residual stress", Journal of Japan Association Petroleum Technology, Vol. 61, pp 292-299, July 1996.

Maxey W, "Y/T Significance in Line Pipe", 7th Symposium on Line Pipe Research, Houston, 1986.

Miller R, "Real World Implementation of QRA Methods in Casing Design", SPE 48325, Applied Technology Workshop on Risk Based Design of Well Casing and Tubing, The Woodlands, Texas, USA, 7-8 May 1998.

Mimura H, Mimaki T and Tamano T, "Finite Element Analysis of Collapse Strength of Casing", Nippon Steel Technical Report No. 34, July 1987.

Nippon Steel Corporation, "Development of High Collapse Casing NT-95 HS", June 1979.

Nishioko K and Mimaki T, "An Experimental Study on the Critical Collapsing Pressure of Seamless Steel Tube for Well Casing under External Pressure, Part 1: The Effects of Yield Strength and the Geometry of Tube on the Collapsing Pressure", Pressure Engineering, Vol. 16, No. 4, pp 195-204, 1978.

Noble B and Daniel J, "Applied Linear Algebra", Prentice-Hall, 1988.

Nordgren R and Murphey C, "Elastic Stability of Circular Tubes of Circumferentially Variable Thickness under External Pressure", ASME Journal of Engineering for Industry, Vol. 90, pp 644-647, 1968.

Owen D and Hinton E, "Finite Elments in Plasticity: Theory and Practice", Pineridge Press Limited, Swansea, UK.

Paslay P, Cernocky E and Wink R, "Burst Pressure Prediction of Thin-Walled, Ductile Tubulars Subjected to Axial Load", SPE Applied Technology Workshop on Risk Based Design of Well Casing and Tubing, the Woodlands, Texas, 7-8 May 1998.

Pattillo P and Hunag N, "The Effect of Axial Load on Casing Collapse", Journal of Petroleum Technology, Vol. 34, pp 159-164, 1982.

Payne L and Swanson J, "Application of Probabilistic Reliability methods to Tubular Designs", SPE Drilling Engineer, pp 299-305, Dec. 1990.

Rabia H, "Fundamentals of Casing Design", Petroleum Engineering and Development Studies, Vol. 1, Graham & Trotman Limited, Alden Press, Oxford, 1987.

Rabia H, "Casing Design Technical manual", British Gas Technology Technical report, 1993.

Raney J, Suryanarayana P, and Maes M, "Implementation of a Reliability-Based Design Procedure for Production Tubing", Offshore Mediterranean Conference Paper No 1897, Ravenna, Italy, March 1997.

Rao S, "The Finite Element Method in Engineering", 2nd Edition, Pergammon Press, 1989.

Ravindra M and Lind N, "Theory of Structural Code Optimization", Jounral of the Structural Division, ASCE, Vol. 99, pp 541-553, 1973.

Reeves T, Parfitt S and Adams A, "Casing System Risk Analysis Using Structural Reliability", Proceedings of the SPE/IADC Drilling Conference, Amsterdam, pp 169-177, SPE 25693, Feb. 1993.

Rice J, "Mathematical Analysis in the Mechanics of Fracture", Fracture, An Advanced Treatise, Vol. II, Academic Press, New York, 1986.

Roberts R and Newton C, "Interpretive Report on Small Scale Test Correlations with K_{1C} Data", Welding Research Council, Bulletin 265, Feb. 1981.

Saunders H and Windenburg D, "Strength of Thin Cylindrical Shells under External Pressure", Transaction of ASME, Vol. 53, APM-53-17a, pp 207-218, 1931.

Small N, "Plastic Collapse of Oval Straight Tubes under External Pressure", Transaction of ASME, Series J, Vol. 100-1, pp 46-51, 1978.

Southwell R, "On the Collapse of Tubes by External Pressure", Part III, Phil. Magazine, Series 6, Vol. 29, pp 67-77, Jan. 1915.

Stewart G, Klever F and Ritchie D, "An Analytical Model to Predict the Burst Capacity of Pipeline", KSEPL Publication 1200, Dec. 1993.

Stewart G, Klever F and Ritchie D, "An Analytical Model to Predict the Burst Capacity of Pipelines", ASME Proceedings of Offshore Mechanics and Arctic Engineering (OMAE) Conference on Pipeline Technology, Houston, Texas, USA, Vol. V, pp 177-188, 1994.

Stewart G and Klever F, "Accounting for Flaws in the Burst Strength of OCTG", SPE Applied Technology Workshop on Risk Based Design of Well Casing and Tubing, the Woodlands, Texas, 7-8 May 1998.

Stewart R, "Collapsing Pressure of Bessemer-Steel Lap-welded Tubes, 3 In. to 10 in. in Diameter", Transaction of ASME, Vol. 27, pp 730-822, 1906.

Strum R, "A Study of the Collapsing Pressure of Thin-Walled Cylinders", Doctorate Thesis, University of Illinois, 1936.

Strum R, "A Study of the Collapsing Pressure of Thin-Walled Cylinders", University of Illinois Engineering Experiment Station, Bulletin No. 329, Vol. 25, pp 41-44, 1941.

Svennson N, " Bursting Pressure of Cylindrical and Spherical Vessels", ASME, Journal of Applied Mechanics, Vol. 25, No. 1 pp 89-96, 1958.

Tallin A, Paslay P, Onyewuenyi O, Burres C and Cernocky E, "The Development of Risk-Based Burst Design for Well Casing and Tubing", SPE Applied Technology Workshop on Risk Based Design of Well Casing and Tubing, the Woodlands, Texas, 7-8 May 1998.

Tamano T, Mimura H and Yanagimoto S, "Examination of Commercial Casing Collapse Strength under Axial Loading", ASME Proceedings of the first Offshore Mechanics, Vol. I, pp 113-118, 1982.

Tamano T, Mimaki T and Yanagimoto S, "A new Empirical Formula for Collapse Resistance of Commercial Casing", ASME Transactions of Energy Resources Technology, pp 489-495, 1983.

Timoshenko S, "Working Stresses for Columns and Thin-Walled Structures", ASME Journal of Applied Mechanics, Vol. 1, pp 173-183, 1933.

Timoshenko S and Gere J, "Theory of Elastic Stability", McGraw-Hill, 1961.

Tokimasa K and Tanaka K, "FEM Analysis of the Collapse Strength of A Tube", ASME, Journal of Pressure Vessel Technology, Vol. 108, pp 158-164, 1986,

Turkstra C, " Theory of Structural Design Decisions", Solid Mechanics Division, SM2, University of Waterloo, Canada, 1970.

Verner E, Langner C and Reifel M, "Collapse of Thick Wall Pipe in Ultra Deep Water", Proceedings of the Conference on Pipelines in Adverse Environments, ASCE, San Diego, pp 159-167, 1983.

Walpole R and Myers R, "Probability and Statistics for Engineers and Scientists", Macmillian, New York, Fifth Edition, 1993.

Yeh M and Kyriakides S, "On the Collapse of Inelastic Thick Walled Tubes under External Pressure", ASME, Journal of Energy Resource Technology, Vol. 108, pp 35-47, March 1986.

Yeh M and Kyriakides S, "Collapse of Deepwater Pipelines", ASME, Journal of Energy Resource Technology, Vol. 110, No. 1, pp 35-47, March 1988.

Zienkiewicz O, "The Finite Element method", McGraw-Hill, 1977

Zienkiewicz O and Taylor R, "The Finite Element Method", Vol. 1-2, 4th Edition, McGraw Hill, Nov. 1989.

APPENDIX 1

Test Data Of Casing Collapse Under External Pressure Alone

No.	σ_y (MPa)	D (mm)	t (mm)	(D/t)	Ovality ($\times 10^{-2}$)	Eccentricity ($\times 10^{-2}$)	Exp. Strength (MPa)
KV16[*1]	533	168.75	9.58	17.61	0.36	10.5	59.2
C1	413	126.90	12.83	9.89	0.39	7.0	84.2
C8	413	126.82	13.07	9.70	0.39	4.6	84.2
D5	412	126.85	13.13	9.66	0.39	6.8	84
E7	414	126.78	13.03	9.73	0.55	3.8	84.8
AP7	416	178.47	7.20	24.79	0.17	9.7	22.9
AP8	416	178.41	7.25	24.61	0.39	11.0	23.2
AQ7	395	178.44	7.25	24.61	0.22	11.0	23.3
AQ8	395	178.68	7.29	24.51	0.34	11.0	23
DV3	648	178.47	9.46	18.87	0.56	14.9	51
DV4	645	178.61	9.49	18.82	1.18	16.7	45
DV9	612	178.02	13.86	12.84	0.45	13.0	89.5
DV10	618	178.00	13.68	13.01	0.79	11.7	92.5
KV15	577	168.79	9.44	17.88	0.42	11.6	56.3
KV17	604	168.72	11.06	15.26	0.36	13.6	70.3
KV18	595	168.76	11.02	15.31	0.36	13.6	73.6
V1	615	89.18	6.83	13.06	0.17	7.3	91.9
V2	615	89.28	6.82	13.09	0.34	7.3	92.2
V3	615	89.20	6.83	13.05	0.11	4.4	92.3
BP7	591	178.73	8.38	21.30	0.28	8.9	38.8
BP8	591	178.60	8.41	21.24	0.22	16.0	38.1
BQ7	596	178.65	8.46	21.11	0.17	10.0	38.6
BQ8	596	178.61	8.48	21.06	0.34	10.6	38.2
CP7	644	178.49	9.40	18.99	0.22	13.3	50.7
CP8	644	178.20	9.31	19.14	0.17	11.3	48.4
CQ7	629	178.41	9.34	19.10	0.45	12.8	48.1
CQ8	629	178.29	9.44	18.87	0.28	13.8	49.9
DP7	576	178.26	10.69	16.67	0.50	5.6	60.8
DP8	576	178.29	10.50	16.98	0.39	8.1	58.8
DQ7	579	178.12	10.59	16.82	0.28	9.0	63.5
DQ8	579	178.12	10.64	16.74	0.28	13.6	63.4
RA7	568	114.13	6.76	16.88	0.44	8.9	54.9
RA8	568	114.14	6.90	16.54	0.35	10.1	58.2
RA9	568	114.11	6.89	16.56	0.61	10.2	58.9
RB7	654	114.19	7.08	16.13	0.61	15.5	67.1
RB8	654	114.25	7.04	16.22	0.79	12.8	67
RB9	654	114.28	7.13	16.03	0.35	11.2	67.5
RC7	589	114.25	8.74	13.07	0.26	13.7	84.9
RC8	589	114.29	8.66	13.20	0.35	9.2	82.3
RC9	589	114.35	8.75	13.07	0.70	12.6	85.6
DV1	686	178.07	8.47	21.02	0.56	22.2	44.5
DV2	736	178.34	8.57	20.81	0.39	17.8	45.5
FV1	755	178.17	12.11	14.71	0.67	7.4	100
FV2	705	178.12	12.12	14.70	0.51	13.1	93
FV3	750	178.30	13.22	13.49	0.39	7.5	104.5
FV4	728	178.35	12.69	14.05	0.34	9.5	97
KV9	752	127.33	9.02	14.12	0.39	8.9	94
KV10	724	127.48	9.26	13.77	0.39	10.8	91
KV11	665	127.30	7.51	16.95	0.39	11.9	60
KV12	686	127.27	7.79	16.34	0.31	10.3	68
KV7	739	139.35	11.32	12.31	0.79	8.8	116
KV8	752	139.21	11.13	12.51	0.36	14.5	110
MV5	677	89.56	6.44	13.91	0.04	6.2	100.5

No.	σ_y (MPa)	D (mm)	t (mm)	(D/t)	Ovality ($\times 10^{-2}$)	Eccentricity ($\times 10^{-2}$)	Exp. Strength (MPa)
MV6	693	89.58	6.39	14.02	0.22	6.2	98
MV7	720	114.94	7.62	15.08	0.44	10.4	87.5
MV8	750	114.51	7.44	15.39	0.79	16.0	84
MV9	720	114.92	7.38	15.57	0.35	18.7	80
Mv10	720	114.83	7.24	15.86	0.17	15.0	79.5
DV8	845	178.44	11.98	14.89	0.45	10.8	98.5
DV11	815	178.16	14.15	12.59	0.79	7.8	116
DV12	811	177.79	14.14	12.57	1.23	7.8	115.5
Z8A	769	178.30	11.54	15.09	0.28	15.8	94.1
Z8B	769	178.42	11.82	14.45	0.28	9.4	93.4
Z9A	810	178.42	12.70	14.04	0.11	10.4	114.2
Z9B	810	178.45	13.16	13.56	0.11	2.3	111.8
Z10A	760	178.56	13.71	13.02	0.22	18.3	120.2
Z10B	760	178.71	13.66	13.08	0.22	23.4	118.9
Z4A	784	244.88	13.90	17.62	0.33	8.6	71.1
Z4B	784	245.01	14.25	17.19	0.33	7.8	74.3
DV5	884	178.52	10.76	16.59	0.91	6.4	84
DV6	904	178.61	10.85	16.46	0.70	7.4	82.5
DV7	863	178.44	12.05	14.81	0.73	10.1	93
Z3A	936	178.49	10.93	16.33	0.28	6.4	94.5
Z3B	936	178.54	11.18	15.96	0.39	13.4	92.9
Z2A	885	244.72	12.98	18.85	0.16	10.8	65.9
Z2B	885	244.88	12.87	19.03	0.16	7.0	67.1
EP7	881	177.88	11.74	15.15	0.34	11.1	96.2
EP8	881	177.14	11.81	15.00	0.40	9.3	96.7
EQ7	891	177.55	11.86	14.97	0.11	15.2	100
EQ8	891	177.66	11.88	14.95	0.73	14.3	96.5
HV3	1015	178.37	11.80	15.12	0.39	10.2	94
HV4	940	178.50	11.52	15.49	0.28	8.6	96
XV1	1022	73.44	5.83	12.60	0.34	5.1	154
XV2	1022	73.50	5.79	12.69	0.27	1.7	160.8
XV3	1022	73.48	5.77	12.73	0.20	3.4	153.5
XV4	1022	73.44	5.84	12.58	0.27	5.1	155.4
XV5	1022	73.45	5.81	12.64	0.34	3.4	154.9
XV6	1022	73.46	5.87	12.52	0.27	5.1	154
S1	1046	340.33	13.43	25.34	0.38	12.7	29.4
S2	1039	341.27	13.21	25.83	0.41	16.3	28.9
HV1	1143	178.62	11.13	16.05	0.45	11.7	105.5
HV2	1150	178.60	11.38	15.69	0.67	7.9	106
FP7	1151	177.48	12.72	13.95	0.34	6.3	136.7
FP8	1151	177.59	12.72	13.83	0.22	5.5	140.8
FQ7	1089	177.40	13.01	13.64	0.34	8.5	132.9
FQ8	1089	177.52	13.04	13.61	0.34	5.4	136.7
A8[*1]	1146	341.16	13.40	25.45	0.32	8	29.1
C01[*2]	840.4	114.61	6.39	17.94	0.175	3.35	70.61
C02	870.8	114.49	6.45	17.75	0.24	4.50	76.49
C03	863.0	114.61	6.41	17.88	0.24	5.20	73.55
C04	859.1	139.90	7.64	18.31	0.055	4.25	55.90
C05	859.1	139.69	7.69	18.17	0.125	4.50	57.86
C06	849.3	140.25	9.33	15.03	0.16	3.45	97.08
C07	849.3	139.83	9.97	14.03	0.07	2.70	93.16
C08	844.4	139.79	10.22	13.68	0.105	2.70	123.56
C09	844.4	140.04	10.36	13.52	0.105	2.55	129.44
C10	878.7	178.57	8.26	21.62	0.14	3.45	47.07

No.	σ_y (MPa)	D (mm)	t (mm)	(D/t)	Ovality ($\times 10^{-2}$)	Eccentricity ($\times 10^{-2}$)	Exp. Strength (MPa)
C11	950.3	178.55	8.18	21.83	0.225	2.80	49.03
C12	962.0	178.52	8.18	21.82	0.18	3.20	49.03
C13	973.8	178.50	8.26	21.61	0.11	3.45	49.03
C14	924.8	178.35	8.25	21.62	0.11	2.40	45.11
C15	882.6	178.84	8.29	21.57	0.11	3.60	42.17
C16	905.2	178.66	10.22	17.48	0.21	2.40	66.69
C17	905.2	178.40	9.40	18.98	0.195	3.80	66.69
C18	735.5	178.50	11.31	15.78	0.24	5.05	81.39
C19	817.9	194.24	10.51	18.48	0.255	3.70	64.72
C20	817.9	194.24	10.42	18.64	0.18	3.75	63.74
C21	861.0	193.96	8.51	22.79	0.05	2.15	45.11
C22	861.0	193.70	8.49	22.82	0.115	3.40	42.17
C23	861.0	194.05	8.53	22.75	0.075	2.85	44.13
C24	861.0	194.11	8.30	23.39	0.075	3.00	44.13
C25	861.0	194.16	9.10	21.34	0.09	2.70	46.09
C26	861.0	194.15	9.00	21.57	0.05	4.45	45.11
C27	861.0	194.13	8.70	22.31	0.065	2.30	42.17
C28[*2]	861.0	194.21	8.51	22.82	0.08	2.45	44.13
Y01[*3]	277.8	-	-	18.66	0.08	3.00	23.63
Y02	357.1	-	-	25.66	0.12	5.05	17.67
Y03	366.8	-	-	28.65	0.15	2.08	14.42
Y04	304.0	-	-	34.67	0.05	2.78	8.962
Y05	330.9	101.60	3.64	27.87	0.05	3.83	18.75
Y06	374.3	101.85	4.28	23.80	0.15	5.04	22.80
Y07	517.1	101.90	3.19	31.97	0.274	3.58	12.16
Y08[*3]	717.0	101.68	4.16	24.44	0.157	2.93	28.87

Note: Data between No KV16[*1] and No. A8[*1] are from Krug (1983); Data between No C01[*2] and No. C28[*2] are from Nishioko et al (1978 ,1980); Data between No. Y01[*3] and No.Y08[*3] are from Yeh and Kyriakides (1986 ,1988)

APPENDIX 2

Fortran Codes To Generate Geometrical Imperfections And Residual Stress

a) Code to generate geometrical imperfections

```
c       This file is written for generation of geometric
c       imperfections, i.e., ovality and eccentricity, for
c       the problem of casing collapse under external pressure.
c       Ovality r=R(1+u*cos(2*SITA)), Eccentricity e=Sigma/t
c       Date:11/04/99  by X.Huang
c       For 3 layers

        Program main
        IMPLICIT REAL*8(A-H,O-Z)
        real xy1(200,2),xy2(200,2),xy3(200,2),xy4(200,2),xy5(200,2)
        real xy6(200,2),xy7(200,2)
        OPEN(11,status='unknown',file='ap7.nod')
C       MESH 100,EVERY RADIAR ANGLE=2*PI/200

        PI=4.*ASIN(1.)
c       actually PI=360 .cetegrade
C       MESH NUMBER=200

        NELS=200
C
        DFI=PI/float(NELS)
```

```
c       1 inch=0.0254 m
        D0=178.68e-3
        ttt=7.29e-3
c       Rinner=.5*D0
        Rout=.5*D0
c       Rinner=Rout-0.06
        Rinner=Rout-ttt
        DT=(2.*Rout)/(Rout-Rinner)
c       eccentricity variable ecc=delta/t,delta must less than t
        ecc=0.11
c       delta=0.00
c       ecc=delta/(Rout-Rinner)
        delta=ecc*(Rout-Rinner)
C       OVALITY A=%, Inner ovality=u1,out ovality=u2
        u1=17e-4
        u2=u1
c     Ovality may be different from inner to outside.
c-----------------------
c     set both data set equal to zero
c     Begin
      do 110 i=1,200
        do 110 j=1,2
          xy1(i,j)=0.0
          xy2(i,j)=0.
          xy3(i,j)=0.
          xy4(i,j)=0.
          xy5(i,j)=0.
          xy6(i,j)=0.
          xy7(i,j)=0.
110       continue
c     data set zero finished
c---------------------------------------
c     constant variable setting
           Ainner=Rinner*(1+u1)
           Binner=Rinner*(1-u1)
c     for  ellipse finished
c ---------------------------------------------------------------
```

```
c     Main calculation
c-------------------------------------------------------------------
       fi=0.
       do 101 i=1,101
c-------------------------------------------------------------------
c          consider the angle=PI/2
c-------------------------------------------------------------------
           if(i.eq.51) then
c-------------------------------------------------------------------
c          first inner layer
c-------------------------------------------------------------------
            xy1(51,1)=0.
            xy1(51,2)=Binner*sqrt(1.-delta**2/Ainner**2)
c           with ellipse equation: (x-delta)^2/a^2+y^2/b^2=1
c           xy1(151,1)=0.
c           xy1(151,2)=-xy1(51,2)
c-------------------------------------------------------------------
c          outside layer
c-------------------------------------------------------------------
           xy7(51,1)=0.
           xy7(51,2)=Rout*(1.-u2)
c          xy7(151,1)=xy6(51,1)
c          xy7(151,2)=-xy6(51,2)
c-------------------------------------------------------------------
c          middle layer,rr=the distance between the points
c-------------------------------------------------------------------
           rr=abs(xy7(51,2)-xy1(51,2))
           xy2(51,1)=0.
           xy2(51,2)=xy7(51,2)-5.*rr/6.
           xy3(51,1)=0.
           xy3(51,2)=xy7(51,2)-4.*rr/6.
           xy4(51,1)=0.
           xy4(51,2)=xy7(51,2)-3.*rr/6.
           xy5(51,1)=0.
           xy5(51,2)=xy7(51,2)-2.*rr/6
           xy6(51,1)=0.
           xy6(51,2)=xy7(51,2)-rr/6.
           fi=fi+dfi
c-------------------------------------------------------------------
c          else
           else if(i.lt.51) then
           xy1(i,1)=(-1.*delta*Binner**2+Ainner*Binner*sqrt(Binner**2
     $        -delta**2*tan(fi)**2+Ainner**2*tan(fi)**2))/(Binner**2+
     $         Ainner**2*tan(fi)**2)
           xy1(i,2)=tan(fi)*xy1(i,1)
           xy7(i,2)=Rout*(1.+u2*cos(2.*fi))*sin(fi)
           xy7(i,1)=Rout*(1.+u2*cos(2.*fi))*cos(fi)
           rr=sqrt((xy7(i,1)-xy1(i,1))**2+(xy7(i,2)-xy1(i,2))**2)
c            define the distance between the terminal points
          Distance=Rout*(1.+u2*cos(2.*fi))
          xy6(i,2)=(Distance-rr/6.)/Distance*xy7(i,2)
          xy6(i,1)=(Distance-rr/6.)/Distance*xy7(i,1)
          xy5(i,1)=(Distance-rr*2./6.)/Distance*xy7(i,1)
          xy5(i,2)=(Distance-rr*2./6.)/Distance*xy7(i,2)
          xy4(i,2)=(Distance-rr*3./6.)/Distance*xy7(i,2)
          xy4(i,1)=(Distance-rr*3./6.)/Distance*xy7(i,1)
          xy3(i,1)=(Distance-rr*4./6.)/Distance*xy7(i,1)
          xy3(i,2)=(Distance-rr*4./6.)/Distance*xy7(i,2)
          xy2(i,2)=(Distance-rr*5./6.)/Distance*xy7(i,2)
          xy2(i,1)=(Distance-rr*5./6.)/Distance*xy7(i,1)
          fi=fi+dfi
```

```
            else
c           xy1(i,1)=(delta-sqrt(Rinner**2+tan(fi)**2*(Rinner**2-
c     $       delta**2)))/(1+tan(fi)**2)
            xy1(i,1)=(-1.*delta*Binner**2-Ainner*Binner*sqrt(Binner**2
     $       -delta**2*tan(fi)**2+Ainner**2*tan(fi)**2))/(Binner**2+
     $       Ainner**2*tan(fi)**2)
            xy1(i,2)=tan(fi)*xy1(i,1)
c             because outside ellipse equation: r=R(1+ucos(20))
            Distance=Rout*(1.+u2*cos(2.*fi))
            xy7(i,2)=Distance*sin(fi)
            xy7(i,1)=Distance*cos(fi)
            rr=sqrt((xy7(i,1)-xy1(i,1))**2+(xy7(i,2)-xy1(i,2))**2)
            xy6(i,2)=(Distance-rr/6.)/Distance*xy7(i,2)
            xy6(i,1)=(Distance-rr/6.)/Distance*xy7(i,1)
            xy5(i,1)=(Distance-rr*2./6.)/Distance*xy7(i,1)
            xy5(i,2)=(Distance-rr*2./6.)/Distance*xy7(i,2)
            xy4(i,2)=(Distance-rr*3./6.)/Distance*xy7(i,2)
            xy4(i,1)=(Distance-rr*3./6.)/Distance*xy7(i,1)
            xy3(i,1)=(Distance-rr*4./6.)/Distance*xy7(i,1)
            xy3(i,2)=(Distance-rr*4./6.)/Distance*xy7(i,2)
            xy2(i,2)=(Distance-rr*5./6.)/Distance*xy7(i,2)
            xy2(i,1)=(Distance-rr*5./6.)/Distance*xy7(i,1)
            fi=fi+dfi
            end if
101           continue
            do 102 i=1,99
               xy1(201-i,1)=xy1(i+1,1)
               xy1(201-i,2)=-xy1(i+1,2)
               xy2(201-i,1)=xy2(i+1,1)
               xy2(201-i,2)=-xy2(i+1,2)
               xy3(201-i,1)=xy3(i+1,1)
               xy3(201-i,2)=-xy3(i+1,2)
               xy4(201-i,1)=xy4(i+1,1)
               xy4(201-i,2)=-xy4(i+1,2)
               xy5(201-i,1)=xy5(i+1,1)
               xy5(201-i,2)=-xy5(i+1,2)
               xy6(201-i,1)=xy6(i+1,1)
               xy6(201-i,2)=-xy6(i+1,2)
               xy7(201-i,1)=xy7(i+1,1)
               xy7(201-i,2)=-xy7(i+1,2)
102         continue
c-------------------------------------------------
c           output nodes
c-------------------------------------------------
c           the first inner layer
            write(11,*)'** DT= ',DT
              write(11,*)'** inner ovality= ',u1
              write(11,*)'** out ovality= ',u2
            write(11,*)'** Delta=', delta
            Write(11,*)'** Eccentricity= ',ecc
            do 103 i=1,200
               knode=1000+i
               write(11,1) knode,xy1(i,1),xy1(i,2)
c1          format(I5,1x,f15.8,1x,f15.8)
1           FORMAT(I5,1H,,F15.8,1H,,F15.8)
103         continue
            do 104 i=1,199,2
            knode=2000+i
            write(11,1) knode,xy2(i,1),xy2(i,2)
104         continue
            do 105 i=1,200
```

```
                knode=3000+i
                write(11,1) knode,xy3(i,1),xy3(i,2)
105             continue
                do 106 i=1,199,2
00              knode=4000+i
                write(11,1) knode,xy4(i,1),xy4(i,2)
106             continue
                do 107 i=1,200
                knode=5000+i
                write(11,1) knode,xy5(i,1),xy5(i,2)
107             continue
                do 108 i=1,199,2
                knode=6000+i
                write(11,1) knode,xy6(i,1),xy6(i,2)
108             continue
                do 109 i=1,200
                knode=7000+i
                write(11,1) knode,xy7(i,1),xy7(i,2)
c1              FORMAT(I5,1H,,F15.8,1H,,F15.8)
109             continue
                REWIND 11
                STOP
                END
```

b) Code to generate residual stress

```
c       This program is written to consider residual stress.
c       since the residual stress is in a polar coodinate and
C       In current model, it is in XY coordinate.
        Program main
       IMPLICIT REAL*8(A-H,O-Z)
        real Alpha1(100,3),SigmaX(3),SigmaY(3),Txy(3),SigmaZ(3)
        OPEN(11,status='unknown',file='res_17_14.nod')
C       first input the desired residual stress field
c       first case, uniform stress field Sigma sita=-0.1 yield stress
c       input yield stress y and passon's ratio P
c       after run the program, it is found that PingJun is not
working
        p=0.3
        Y=200.2e6
        layer=7
c       layer is the layer number of element
c        SigmaR radial stress,SigmaS circumference stress
         SigmaR=0.
         SigmaS=.6*y
         TrS=0.
c
C       MESH 100,EVERY RADIAR ANGLE=2*PI/200

          PI2=4.*ASIN(1.)
c           actually PI2=360 cetegrade
C       MESH NUMBER=200

          NELS=200
C
          DFI=PI2/float(NELS)
c-------------------------
          do i=1,100
               do j=1,3
               alpha1(i,j)=(i-1)*2*DFI+(j-1)*DFI
```

```
                end do
              end do
c--------------------------------------
           Do i=1,100
               do j=1,3
                 SigmaX(j)=.5*(SigmaR+SigmaS)+.5*(SigmaR-SigmaS)*
     &           cos(2*alpha1(i,j))-TrS*sin(2*alpha1(i,j))
                 SigmaY(j)=.5*(SigmaR+SigmaS)-.5*(SigmaR-SigmaS)*
     &           cos(2*alpha1(i,j))+TrS*sin(2*alpha1(i,j))
                 Txy(j)=.5*(SigmaR-SigmaS)*sin(2*alpha1(i,j))+TrS*
     &                    cos(2*alpha1(i,j))
                 SigmaZ(j)=p*(SigmaX(j)+SigmaY(j))
               end do
*              Sx=(SigmaX(i)+SigmaX(2)+SigmaX(3))/3.
               Sx=SigmaX(1)
*              Sy=(SigmaY(i)+SigmaY(2)+SigmaY(3))/3.
               Sy=SigmaY(1)
*              Tt=(Txy(i)+Txy(2)+Txy(3))/3.
               Tt=Txy(2)
               SZ=sigmaZ(1)
*              Sz=(SigmaZ(i)+SigmaZ(2)+SigmaZ(3))/3.
               do j2=1,layer
               Write(11,1) 10*i+J2,Sx,Sy,Sz,Tt
               end do
c-------------------------------------------------------------------
1              FORMAT(I5,1H,,G20.5,1H,,G20.5,1H,,G20.5,1H,,G20.5)
             end do
                 REWIND 11
                 STOP
                 END
```

APPENDIX 3

Typical ABAQUS Input File For Casing Collapse Simulation

```
*HEADING
mesh generation for casing collapse,Unit=SI,m,S,Pa,
**External pressure=11000psi=5.3842327E7Pa,r=R(1+scos(2@))
**1 PSI= 6.894757E3 Pa, 1 Pa=1.450377E-4 PSI
**mesh density=100 elements per layer
*NODE,nset=Mon1
1
2
*node,input=ap7.nod,nset=all
**node data generated by fortran program node.for
*NSET,NSET=YSYM,generate
1001,15001,1000
1101,15101,1000
*nset,nset=xsym,generate
1051,15051,1000
1151,15151,1000
*NSET,NSET=MON
2
*ELEMENT,TYPE=CGPE10r
11,1001,3001,3003,1003,2001,3002,2003,1002,1,2
1001,1199,3199,3001,1001,2199,3200,2001,1200,1,2
*ELGEN,ELSET=ELALL
11,7,2000,1
1001,7,2000,1
11,99,2,10
12,99,2,10
13,99,2,10
14,99,2,10
15,99,2,10
16,99,2,10
17,99,2,10
*ELSET,ELSET=OUT,generate
17,1007,10
*SOLID SECTION,MATERIAL=STEEL,ELSET=ELALL
*MATERIAL,NAME=STEEL
*ELASTIC
204.0624e9,0.3
*PLASTIC
2.916500E+08,    0.000000E+00
3.061276E+08,    1.270903E-06
3.206076E+08,    3.632725E-06
3.350901E+08,    7.319510E-06
3.495754E+08,    1.289600E-05
3.640639E+08,    2.112558E-05
3.785561E+08,    3.302742E-05
3.930526E+08,    4.994542E-05
4.075544E+08,    7.363484E-05
4.220628E+08,    1.063641E-04
4.365794E+08,    1.510400E-04
4.511064E+08,    2.113538E-04
4.656467E+08,    2.919571E-04
4.802039E+08,    3.986681E-04
4.947828E+08,    5.387110E-04
5.093895E+08,    7.209983E-04
*BOUNDARY
xsym,xsymm
**1001,1
ysym,ysymm
**1,1,1
**2,1,2
*initial condition,type=stress,input=res_17_14.nod
```

```
**initial residual stress generated from Fortran code
*RESTART,WRITE,FREQUENCY=1
*STEP,NLGEOM,INC=25
*STATIC,RIKS
.01,1.,1,1,0.0001
*DLOAD
OUT,P2,5.3842327E6
*NODE PRINT,nset=all,FREQUENCY=1
U
RF
*node file,nset=all
u
rf
*monitor,node=1,dof=1
*EL PRINT,ELSET=ELALL,FREQUENCY=1
mises
loads
E
s
PE
*EL FILE,ELSET=ELALL,FREQUENCY=1
loads
s
E
PE
*node file,nset=ALL
U
*END STEP
```

APPENDIX 4

Test Data Of Casing Collapse In Tension

No.	σ_y (MPa)	(D/t)	Ovality ($\times 10^{-2}$)	Eccentricity ($\times 10^{-2}$)	σ_a (MPa)	$\frac{\sigma_a}{\sigma_y}$	Exp. Strength (MPa)
2	740	13.31	0.7	18.6	112.1	0.152	98.0
6	650	13.18	1.40	8.1	208.1	0.320	79.5
7	690	13.24	0.96	20.8	416.4	0.604	59.5
8	690	13.18	1.05	18.4	57.2	0.083	95.0
B7	571	13.45	1.18	6.5	103.1	0.181	72.5
C1	564	13.03	0.44	16.0	127.9	0.227	72.5
C2	564	12.95	0.70	13.1	252.3	0.447	57.5
C3	564	12.86	0.48	15.2	486.4	0.862	21.0
C4	564	12.91	0.57	14.1	426.5	0.756	32.7
C5	564	12.79	0.74	17.9	137.4	0.244	75.5
D1	560	13.31	0.57	8.2	31.7	0.057	77.0
D2	560	13.27	1.14	8.7	189.8	0.339	64.5
D4	560	13.30	0.79	5.8	137.1	0.245	72.0
D5	560	13.33	0.75	8.2	280.2	0.500	52.5
D6	560	13.17	0.70	12.1	104.6	0.187	72.0
D7	560	13.29	0.75	10.5	248.0	0.443	61.0
R1A	445	21.07	0.22	13.0	47.3	0.106	27.8
R1B	445	21.17	0.17	8.1	37.5	0.084	30.4
R2A	436	20.82	0.22	10.5	182.7	0.419	25.1
R2B	436	20.88	0.34	10.9	141.7	0.325	26.3
R3A	441	20.99	0.17	8.3	171.6	0.389	25.8
R3B	441	20.72	0.17	10.7	202.3	0.459	26.1
R4A	416	20.83	0.17	10.6	110.5	0.266	26.5
R5A	444	20.68	0.17	8.2	216.7	0.488	26.5
R5B	444	20.62	0.22	8.0	89.4	0.201	29.4
A2	684	16.43	0.62	10.1	175.1	0.256	60.8
B1	568	16.58	0.22	8.4	197.7	0.348	56.3
B2	595	17.47	0.34	12.8	115.1	0.193	57.2
C1	582	17.48	0.56	7.8	175.1	0.301	54.4
C2	622	17.23	0.51	12.6	48.3	0.078	58.9
D1	544	17.24	0.62	8.7	106.1	0.195	53.3
F2	618	16.50	0.34	18.5	272.1	0.440	51.0
G1	614	16.51	0.56	11.1	41.4	0.067	62.3
G2	599	16.13	0.45	9.0	150.2	0.251	55.9
H2	668	17.80	0.34	9.0	359.3	0.538	44.3
U1A	563	16.57	0.28	8.4	94.2	0.167	61.7
U1B	563	16.85	0.17	6.6	199.9	0.355	52.8
U2A	705	16.34	0.28	16.5	275.4	0.391	64.0
U2B	705	16.28	0.28	13.8	456.9	0.648	46.0
U3A	699	16.28	0.40	13.7	375.6	0.537	55.2
U5A	645	15.58	0.28	17.5	369.1	0.572	52.3
U5B	645	15.31	0.51	17.4	334.1	0.518	59.2
U7A	708	15.63	0.40	15.9	133.0	0.188	77.2
U7B	708	15.67	0.28	15.8	89.6	0.127	81.3
U8A	734	17.09	0.28	23.1	198.2	0.270	67.8
U8B	734	16.69	0.28	22.9	95.9	0.131	77.8
T1A	927	19.60	0.45	15.4	579.3	0.625	36.1
T1B	927	19.11	0.57	14.1	413.0	0.446	53.2
T2A	841	19.28	0.41	13.4	13.1	0.016	62.6
T3A	854	19.44	0.14	18.6	86.6	0.101	63.1
T3B	854	19.45	0.57	10.4	170.8	0.200	60.1
T4A	867	19.36	0.37	11.9	255.9	0.295	60.1

T7A	792	19.42	0.41	18.3	49.3	0.062	55.4
T8A	801	19.06	0.41	17.9	463.7	0.579	41.6
T8B	801	19.66	0.45	12.9	54.9	0.069	57.0
W1A	588	28.75	0.18	6.7	16.2	0.028	19.4
W1B	588	28.73	0.32	14.6	469.3	0.798	10.1
W2B	561	27.08	0.55	13.4	13.6	0.024	23.2
W3A	574	27.15	0.50	6.6	136.3	0.237	19.6
W3B	574	27.46	0.47	13.1	117.3	0.204	19.0
W4A	554	26.87	0.41	15.7	219.2	0.396	18.8
W4B	554	27.65	0.38	16.3	486.4	0.878	7.9
W5A	607	28.61	0.38	14.2	97.4	0.161	17.6
W5B	607	28.48	0.35	13.3	98.6	0.162	16.8
W6A	590	27.17	.26	18.3	78.5	0.133	23.1
W6B	590	26.70	0.73	12.3	176.1	0.298	22.2
W7A	600	25.85	0.32	20.1	351.1	0.585	18.8
W7B	600	25.93	0.29	12.1	292.1	0.487	19.3
W8A	608	28.19	0.15	11.3	394.6	0.649	13.6
W8B	608	27.92	0.29	11.4	119.2	0.196	20.4

Note: Data are from Krug (1983).

APPENDIX 5

Author's Publications And Awards

Finite element prediction of the ultimate collapse strength of casings

X Huang* and **M Mihsein**
School of Engineering and Built Environment, University of Wolverhampton, UK

Abstract: Accurately predicting the ultimate collapse strength is very important for casing design. For an infinitely long thick-walled casing under external pressure, a finite element method (FEM) model has been proposed to obtain a better understanding of the ultimate collapse strength of a casing. A very careful comparison with a series of experimental data has been conducted to verify the accuracy and reliability of the proposed FEM model. In addition, the predicted post-collapse behaviour compares well with the experimental test data. The validation proves that, if the material behaviour and imperfection variables are known, the ultimate collapse strength can be predicted to a satisfactory degree of accuracy. The major factors that affect the ultimate collapse strength of a casing have been fully investigated using the proposed FEM model.

Keywords: finite element analysis, ultimate collapse strength, casing design

NOTATION

D	outside diameter
e	initial eccentricity
E	Young's modulus
n	hardening parameter
P_{EA}	elastic collapse pressure under axial loading
P_{E0}	elastic collapse pressure without axial loading
P_{GA}	general yield pressure under axial loading
P_{G0}	general yield pressure without axial loading
P_{yA}	yield onset pressure under axial loading
P_{y0}	yield onset pressure without axial loading
R, r, θ, δ	dimensions (see Fig. 2)
t	wall thickness
u	initial ovality
λ	anisotropy parameter
ν	Poisson's ratio
σ_A	applied axial stress
σ_y	yield strength
$\sigma_{y,s}$	yield stress in circumferential direction
$\sigma_{y,x}$	yield stress in axial direction
σ'_0	material parameter (see equation (10))

The MS was received on 24 August 1999 and was accepted after revision for publication on 2 February 2000.
**Corresponding author: School of Engineering and Built Environment, University of Wolverhampton, Wolverhampton WV1 1SB, UK.*

1 INTRODUCTION

The casing plays a vital role in drilling operations. Collapse strength under external pressure is one of the most important aspects in casing design process. It is widely known that overdesign leads to costly casing purchase, while underdesign can lead to failures and costly repair operations. Therefore, it is extremely important to have an accurate understanding of the ultimate collapse strength of the casing.

Early work on the collapse of a thick-walled casing under external pressure can be traced back to Timoshenko [1]. With the increasing need in the oil and gas industry, a large amount of experimental and analytical research has been carried out on the collapse of casings. However, the actual problem of casing collapse presents difficulties because there are many important factors that strongly influence the ultimate collapse pressure of the casing. The important geometrical factors are the ratio of outside diameter to wall thickness, D/t, the initial ovality and the eccentricity. The important mechanical properties are the Young's modulus, the Poisson ratio, the proportional limit and the yield criterion. Additionally, residual stress and applied axial stress may be listed as other important factors.

The effects of mechanical properties have been discussed theoretically in previous literature [1–4]. However, imperfections such as ovality and eccentricity will drastically reduce the actual collapse strength of the casing, while their impact on the collapse strength is very difficult to evaluate analytically. In recent years, Tamano and Mimaki [5], Issa and Crawford [6] and

Tokimasa and Tanaka [7] have investigated the effects of imperfections on the collapse strength and presented design equations using numerical analysis. Tamano and Mimaki [5] and Tokimasa and Tanaka [7] claimed that the circumferential residual stress greatly reduced the collapse pressure, while Issa and Crawford [6] thought that its effect was very small, and the effect of residual stress was neglected in their equation. Therefore, it is necessary to clarify what extent the residual stress may affect the collapse strength of the casing. Furthermore, only a single factor was investigated in previous analysis and its effect was then integrated into the final empirical equation. There is a lack of investigation of the effect of the major factors simultaneously. Although these proposed equations might be simple to use, this is not always safe for a specific casing design based on them. Therefore, for the development of casing design, it is necessary to generate a model that is capable of simulating all of the possible factors simultaneously while at the same time giving an accurate prediction of the ultimate collapse strength of the casing. A validated finite element analysis approach can be a tool for casing design since experiments are costly.

In the present paper, a finite element method (FEM) model constructed with major factors is validated through a series of experimental data. The validation process proves that, if the material behaviour and imperfections are known, the ultimate collapse strength can be predicted to a satisfactory degree of accuracy. The effects of major factors such as D/t, ovality, eccentricity, residual stress, material hardening and anisotropy are fully investigated using the proposed FEM model. In addition, FEM analysis was used to assess current existing design equations for casing collapse.

2 COLLAPSE EQUATION REVIEW

There are two modes of collapse, elastic and plastic, for an ideal casing, assuming that it has perfect roundness, with no variation in the wall thickness and no residual stress. Clinedinst [2] derived a theoretical formula, which has been accepted by the American Petroleum Institute (API) as the elastic collapse pressure equation

$$P_{E0} = 2\frac{E}{1-\nu^2}\frac{1}{D/t(D/t-1)^2} \tag{1}$$

where P_{E0} denotes the elastic collapse pressure without axial load and E, ν, D and t are the Young's modulus, the Poisson ratio, the outside diameter and the wall thickness respectively. The elastic collapse pressure under axial loading is equal to that without axial loading [3]. Then

$$P_{EA} = P_{E0} = 2\frac{E}{1-\nu^2}\frac{1}{D/t(D/t-1)^2} \tag{2}$$

where P_{EA} represents the elastic collapse pressure of the casing under axial loading.

As most commonly used casings are moderate-walled or thick-walled casings, their collapse is not just elastic collapse but extends to plastic collapse. A large amount of research effort has concentrated on the plastic collapse behaviour. It is widely assumed that the onset of yield pressure when the inner fibre begins to yield is the plastic collapse pressure for a thick-walled casing and the following plastic collapse pressure equation can be expressed on the basis of the von Mises yield criterion:

$$P_{y0} = 2\sigma_y\frac{D/t-1}{(D/t)^2} \tag{3}$$

where P_{y0} denotes the yield onset pressure without axial loading.

Holmquist [3] presented a modified yield onset pressure for a thick-walled casing under axial loading as follows:

$$P_{yA} = P_{y0}\left[\sqrt{1-0.75(\sigma_A/\sigma_y)^2}-0.5(\sigma_A/\sigma_y)\right] \tag{4}$$

where P_{yA} is the yield onset pressure under axial loading and σ_A is the applied axial stress. Tamano and Mimaki [5] presented a general yield pressure equation for a thick-walled casing under external pressure alone as follows:

$$P_{G0} = 2\sigma_y\frac{D/t-1}{(D/t)^2}\left(1+\frac{1.47}{D/t-1}\right) \tag{5}$$

while, under a combination of axial loading and external pressure, the general yield pressure is

$$P_{GA} = P_{G0}\left[\sqrt{1-0.75(\sigma_A/\sigma_y)^2}-0.5(\sigma_A/\sigma_y)\right] \tag{6}$$

where P_{G0} and P_{GA} represent the general yield pressure without or with axial stress respectively. It is concluded [5] that, for an ideal casing, the plastic collapse pressure is closer to the general yield pressure than to the yield onset pressure.

On the basis of the elastic and plastic collapse theory, five sets of predictive equations have been published [5–9]. Details of these predictive equations can be found in the references. The equations from references [5] and [6] were chosen to compare with the FEM predictions as well as the experimental data in the validation process.

3 FE MODELLING OF CASING COLLAPSE

The problem of casing collapse is a complicated system governed by highly non-linear equations for the stress, strain and displacement because of the large deformation and material non-linearity. Thus, an effective way of accurately obtaining the ultimate collapse strength of

a thick-walled casing is to use numerical analysis. Finite element analysis was performed using the ABAQUS non-linear finite element analysis package [10]. To obtain accurate modelling of plasticity and large deformation, a modified quasi-Newton solution technique was used to solve the non-linear equations. The external pressure was carefully controlled to the ultimate load by a modified Riks algorithm. Following the maximum pressure, the program incrementally reduced the external pressure so that the collapse simulation could be continued. In this way, the post-collapse behaviour of the casing can be investigated and the ultimate collapse strength can be obtained.

The element used in the FEM analysis is a second-order generalized plain strain continuum element. Each element has two extra nodes, which are usually the same nodes in all of the generalized plane strain elements in the proposed FEM model. These two extra nodes enable the program to model the out-of-plane loads such as axial stress and bending moment. To prevent possible artificial locking in the calculation of stiffness matrices, a reduced integration technique is employed in the simulation. From the experiment conducted by Yeh and Kyiakides [11], it is reported that the geometric variables and imperfections do not substantially vary along the length of the casing. Therefore, it is reasonable to assume that all of the geometrical variables involved in the analysis are uniform in the longitudinal direction of the casing. As the ratio of casing length to outside diameter is normally far higher than 10, the effect of end restraint can be neglected. The problem of casing collapse is reduced to a plane strain problem and only one element is necessary in the longitudinal direction.

The casing section is modelled with mean outside diameter D, wall thickness t, initial ovality and eccentricity as shown in Fig. 1. There are 100 elements in the circumferential direction of the casing section and three layers in the radial direction. It has been confirmed that six integration points through the wall thickness are sufficient for casing collapse. The imperfections are introduced to allow the collapse to occur, although they are not plainly visible. Uniform pressure was applied to the faces of the elements on the outside diameter of the casing section. In the simulation, the line direction of applied pressure changes as the casing section deforms, and the pressure is increased incrementally. It is noted that no approximation is made in formulating the non-linear equations of casing collapse. The predicted

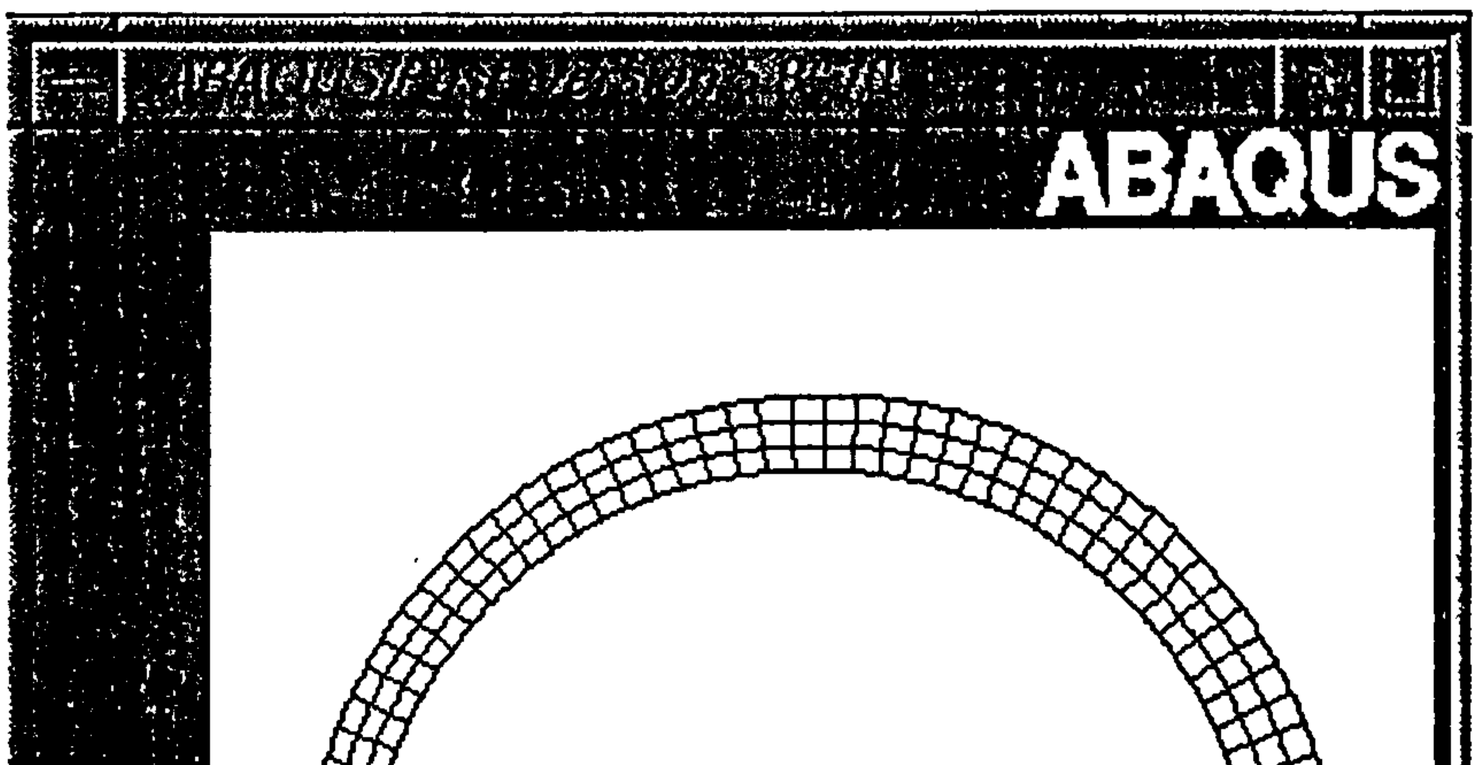

Fig. 1 FEM model with imperfections

collapse pressure in the simulation is recorded when the applied external pressure begins to decrease. This is consistent with the experiments, where collapse of the test specimen was observed when a sudden drop in pressure was recorded in the test facility. The above procedures enable the FEM program accurately to model the collapse behaviour of the casing.

4 MEASUREMENT OF IMPERFECTIONS

4.1 Measurement of ovality

A Fortran program has been written to construct the FEM nodal coordinate system with initial imperfections. Without the imperfections, the collapse process would not occur and the casing section would deform uniformly. According to Timoshenko and Gere [1], initial ovality, u was introduced by the following equation:

$$r = R[1 + u\cos(2\theta)] \tag{7}$$

where

$$u = \frac{(D_{max} - D_{min})}{D_{max} + D_{min}}$$

r = imperfect casing radius
R = nominal perfect casing radius
θ = angular coordinate measured from the centre of the casing as shown in Fig. 2a.

4.2 Measurement of eccentricity

The actual wall thickness of the casing varies along the line of the cross-section. The experiments in reference [12] suggested that the casing section be idealized as

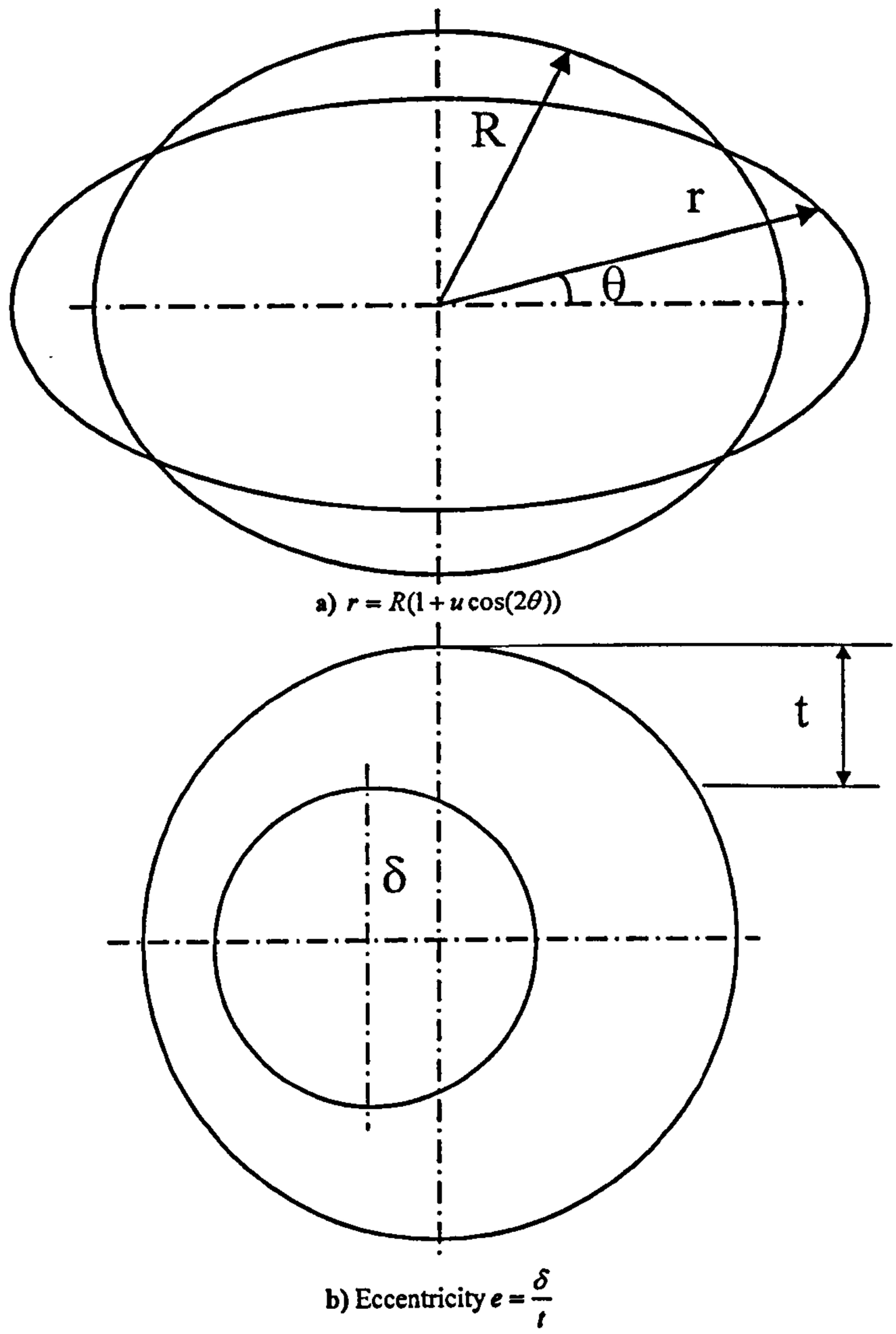

Fig. 2 Measurement of imperfections: (a) $r = R[1 + u\cos(2\theta)]$: (b) eccentricity $e = \delta/t$

shown in Fig. 2b. It can clearly be seen that the centres of the inner and outside circles are not at the same point, since it is reasonable to assume that the section areas of uniform and non-uniform wall thickness casings are the same. The eccentricity parameter e is measured by

$$e = \frac{t_{max} - t_{min}}{t_{max} + t_{min}} \tag{8}$$

For the casing section shown in Fig. 2b it can be seen that the eccentricity parameter is measured as follows:

$$e = \frac{\delta}{t} \tag{9}$$

where δ is the distance between the centres of the inner and outside circles as shown in Fig. 2b.

5 VALIDATION WITH EXPERIMENTS

The proposed FEM model has been validated through a very careful comparison with a series of full-scale experimental data of X-42 and X-65 grade steel casings [11]. A set of 4 in (102 mm) diameter casings used in the experimental programme were manufactured according to the API Spec 5LX specifications [13] by Sumitomo Metal Industry. Two of them were randomly chosen and their specifications are listed in Table 1.

The dimensions of the test specimens were first measured manually using micrometers. Six diametral measurements were made at approximately eight axial positions. The mean values of these measurements as well as the Young's modulus, E, and the API yield stress, σ_y, are listed in Table 2. The accuracy of the measured data is as follows: the wall thickness is within $\pm 0.5 \times 10^{-3}$ in (0.01 mm); the radial imperfections are within $\pm 0.5 \times 10^{-3}$ in (0.01 mm); the axial position is within $\pm 2 \times 10^{-3}$ in (0.5 mm); and the angular position is within $\pm 0.1°$ [11].

The material properties of the test specimens were measured individually. The response of test specimen 1 exhibited an upper and lower yield point followed by an almost perfect plastic response, while the response of test specimen 2 presented a smooth transition from the elastic to inelastic regime, which is found to be a continuously hardening one. The material behaviour of specimen 2 was fitted with a three-parameter Ramberg–Osgood curve as follows:

$$\varepsilon = \frac{\sigma}{E}\left[1 + \frac{3}{7}\left(\frac{\sigma}{\sigma_0'}\right)^{n-1}\right] \tag{10}$$

Table 2 Measured parameters of test specimens

Specimen number	1	2
Material	X-42	X-65
D (in)	4.0000	4.012
(mm)	101.6	101.905
D/t	27.87	31.97
E (10^3 lbf/in^2)	29.6×10^3	29.7×10^3
(GPa)	204.0624	204.7518
σ_y (10^3 lbf/in^2)	48.0	75.0
(MPa)	330.912	517.05
σ_0' (10^3 lbf/in^2)	—	65.0
(MPa)		448.11
n*	—	6.5
λ*	1.3	1.0

*n is the material hardening parameter and λ is the anisotropy parameter.

where σ_0' is the material parameter (its value is listed in Table 2).

In addition, test specimen 1 was found to exhibit substantial inelastic anisotropy. This effect was considered by adopting the anisotropy definitions of equivalent stress and yield function suggested by Hill [14]. It is assumed that the elastic deformation is isotropic but the yield stresses in the two principal directions are different. The measured material hardening parameter and anisotropy are also listed in Table 2.

The geometric and material properties listed in Table 2 were used carefully to simulate the collapse behaviour of the casing tested in order to validate the proposed FEM model. The simulation assumed that the initial geometry of the casing is uniform along its length. This is verified by measuring the initial imperfections of the casing both in the circumferential and in the longitudinal direction in the experiments. From experimental data, the material behaviour of test specimen 1 can be assumed to be elastic–perfectly plastic stress–strain behaviour in the simulation. For specimen 2, the material behaviour is carefully simulated on the basis of its material behaviour measured from experiment.

The predicted collapse pressures of test specimens using the FEM model are compared with experimental test data as well as those from the Tamano and Mimaki [5] and Issa and Crawford [6] equations. The final results are listed in Table 3. It should be noted that the minimum values of elastic collapse pressure [equation (1)] and plastic collapse pressure [equation (3)] are listed in Table 3 as the collapse pressure of a perfect casing. It was reported that in all of the test specimens there was residual stress. However, the residual stress distributions of the tested casings were not

Table 1 Test specimen specifications (API Spec 5LX)

Specimen number	Material	D (in)	t (in)	Finish
1	X-42	4.0	0.14	Cold finished
2	X-65	4.0	0.12	Cold finished

available. For this particular study, a linear residual stress distribution along the circumference was assumed in the validation.

The validation proves that, if the imperfection variable and material behaviour are known, the collapse pressure can be predicted to a satisfactory degree of accuracy with a maximum deviation of less than 3.2 per cent using the proposed FEM model. The predicted error is defined as follows:

$$\text{Error} = \frac{P_{\text{FEM}} - P_{\text{experiment}}}{P_{\text{experiment}}} \cdot \tag{11}$$

It should be noted that the predictions from the Issa and Crawford equation are all conservative, while the

Table 3 Comparison of calculated and experimental collapse pressure

FEM model		Specimen number 1	2
Perfect geometry	D (in)	4.000	4.012
	(mm)	101.600	101.905
	t (in)	0.1435	0.1255
	(mm)	3.645	3.1877
	D/t	27.87	31.97
	P_{co}* (MPa)	22.29	14.68
	P_{Tamano} (MPa)	22.28	14.68
	P_{Issa} (MPa)	15.58	14.68
Idealized imperfection	Ovality, u	0.00050	0.00274
Pure ovality	Eccentricity, e	0	0
	P_{Tamano} (MPa)	22.27	14.67
	P_{Issa} (MPa)	14.82	12.08
	P_{FEM} (MPa)	20.23	13.28
Both ovality and eccentricity	Ovality, u	0.00050	0.00274
	Eccentricity, e	0.0383	0.0358
	P_{Tamano} (MPa)	22.25	14.67
	P_{Issa} (MPa)	14.67	11.97
	P_{FEM} (MPa)	19.62	13.12
	Ovality, u	0.00050	0.00274
	Eccentricity, e	0.0383	0.0358
	P_{Tamano} (MPa)	22.25	14.67
	P_{Issa} (MPa)	14.67	11.97
	P_{FEM} (MPa)	19.62	13.12
Experimental collapse pressure (lbf/in^2)		2720	1764
(MPa)		18.75	12.16
No residual stress			
$\text{Error}_{\text{Tamano}}$ (%)		18.7	20.6
$\text{Error}_{\text{Issa}}$ (%)		−21.8	−1.6
$\text{Error}_{\text{FEM}}$		4.64	7.9
With residual stress			
P_{Tamano} (MPa)		20.29	13.28
$\text{Error}_{\text{Tamano}}$ (%)		8.2	9.2
P_{FEM} (MPa)		19.55	12.97
$\text{Error}_{\text{FEM}}$ (%)		4.3	6.7
FEM with hardening			
P_{FEM} (MPa)		19.62	11.78
$\text{Error}_{\text{FEM}}$ (%)		4.64	−3.2
FEM with anisotropy			
P_{FEM} (MPa)		18.87	11.78
$\text{Error}_{\text{FEM}}$ (%)		0.7	−3.2

* P_{co} is the lower of the theoretical elastic collapse pressure and plastic pressure.

predictions from the Tamano and Mimaki equation are all unconservative. Especially for specimen 2, the predicted collapse pressure from the Issa and Crawford equation is very accurate with a −1.6 per cent deviation, which may stem from the fact that the Issa and Crawford equation was derived from an elastic–plastic material model. For an almost perfect plastic material behaviour, the Issa and Crawford prediction of specimen 1 is inaccurate with a large error of −21.8 per cent. As for the Tamano and Mimaki equation, the predictions are unacceptable for the test specimens, with the largest deviation of 21 per cent. Even when considering the residual stress, the largest predicted deviation of the Tamano and Mimaki equation is 9.2 per cent. It is therefore noted that great attention will be necessary in the design of casing collapse when using these predictive equations.

6 FEM ANALYSIS

In addition to predicting the ultimate collapse pressure, it is important that a good FEM model is capable of predicting the post-collapse behaviour of the casing. For test specimen 2, after collapse, deformation was compared with the predicted deformation from the FEM as shown in Fig. 3. In the simulation, half of the test specimen 2 was modelled. The excellent agreement between the collapse test data and the predictions of the proposed FEM model as well as the post-collapse behaviour justifies a satisfactory degree of confidence in using the FEM model for accurate simulation of the problem of casing collapse. It has been confirmed that the two-dimensional FEM model is accurate enough to predict the ultimate collapse strength of the casing. Figure 4 shows the predicted progress of casing collapse behaviour and Fig. 5 gives the pressure deformation response from the FEM simulation. As shown in Fig. 5, with the increment of external pressure, the pressure increases until the maximum pressure is reached, and then a decrease in pressure can be observed with a large increase of deformation. The maximum pressure was then taken as the ultimate collapse pressure. This is consistent with the experiment, where collapse of the test specimen was observed when a sudden drop in pressure was recorded in the test facility.

6.1 Effect of the ratio of outside diameter to wall thickness, D/t

The ratio of outside diameter to wall thickness, D/t, of the casing considered in the FEM analysis is 10–40. The simulations performed are with small initial imperfections. From the results shown in Fig. 6, with an increase in D/t values, the collapse pressure of the casing decreases. In general, the smaller the D/t, the larger is the ultimate collapse strength. The curve fluctuates when multiple factors are considered simultaneously, possibly because of the interaction between the imperfections. A further investigation will be necessary regarding this point.

6.2 Effect of ovality

Initial ovality is dependent on several operational factors but generally is always present in a seamless casing

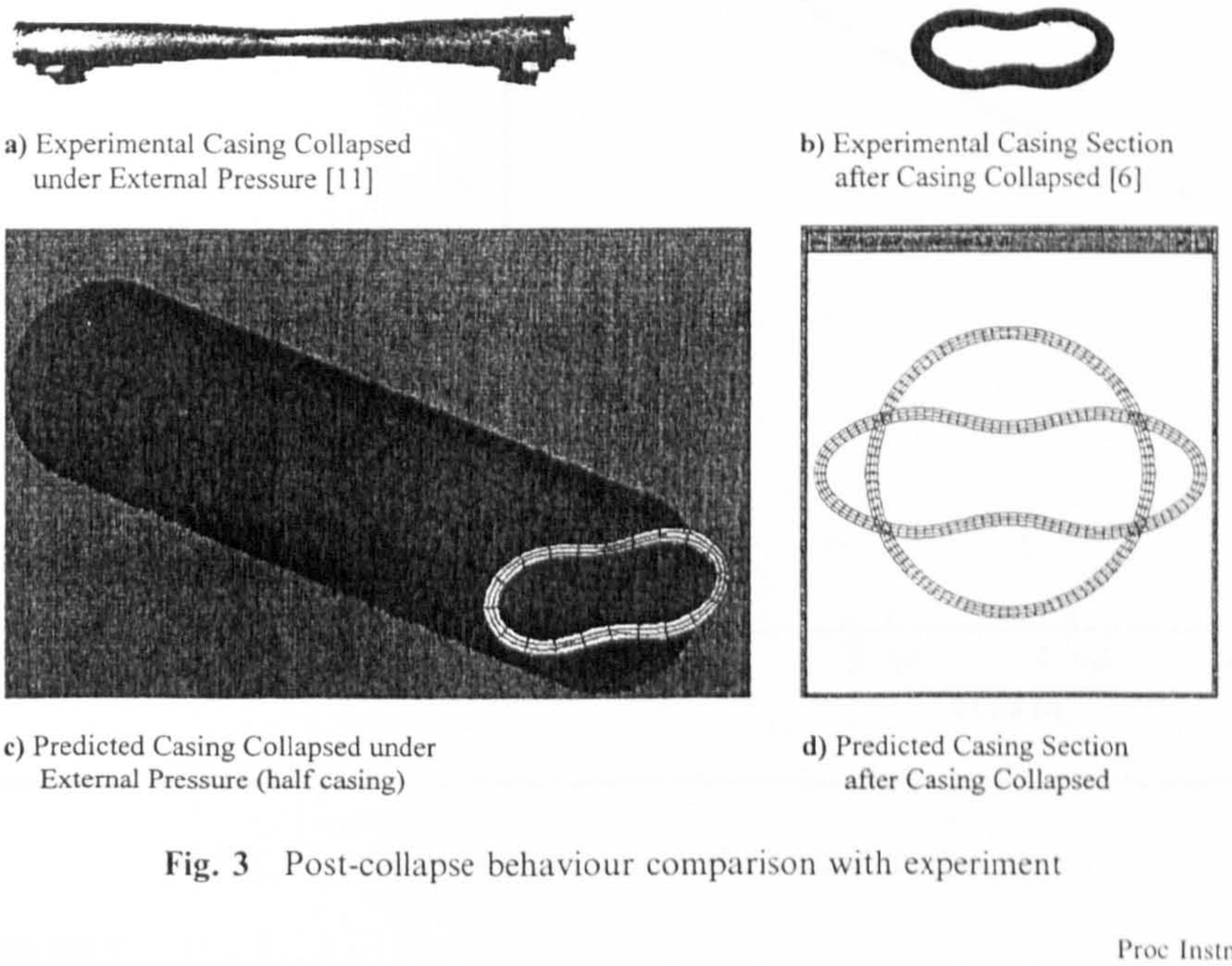

a) Experimental Casing Collapsed under External Pressure [11]

b) Experimental Casing Section after Casing Collapsed [6]

c) Predicted Casing Collapsed under External Pressure (half casing)

d) Predicted Casing Section after Casing Collapsed

Fig. 3 Post-collapse behaviour comparison with experiment

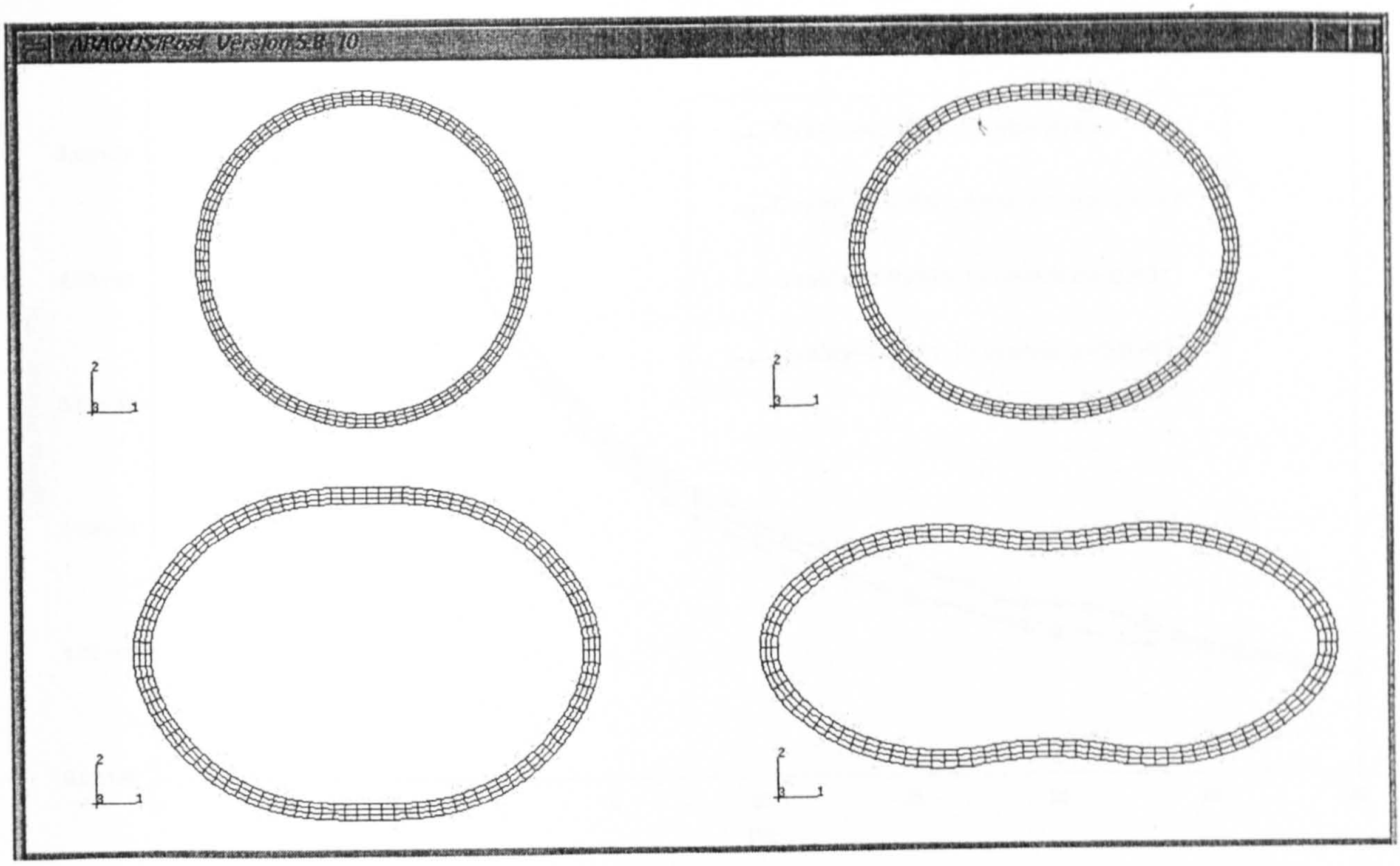

Fig. 4 Predicted progress of casing collapse

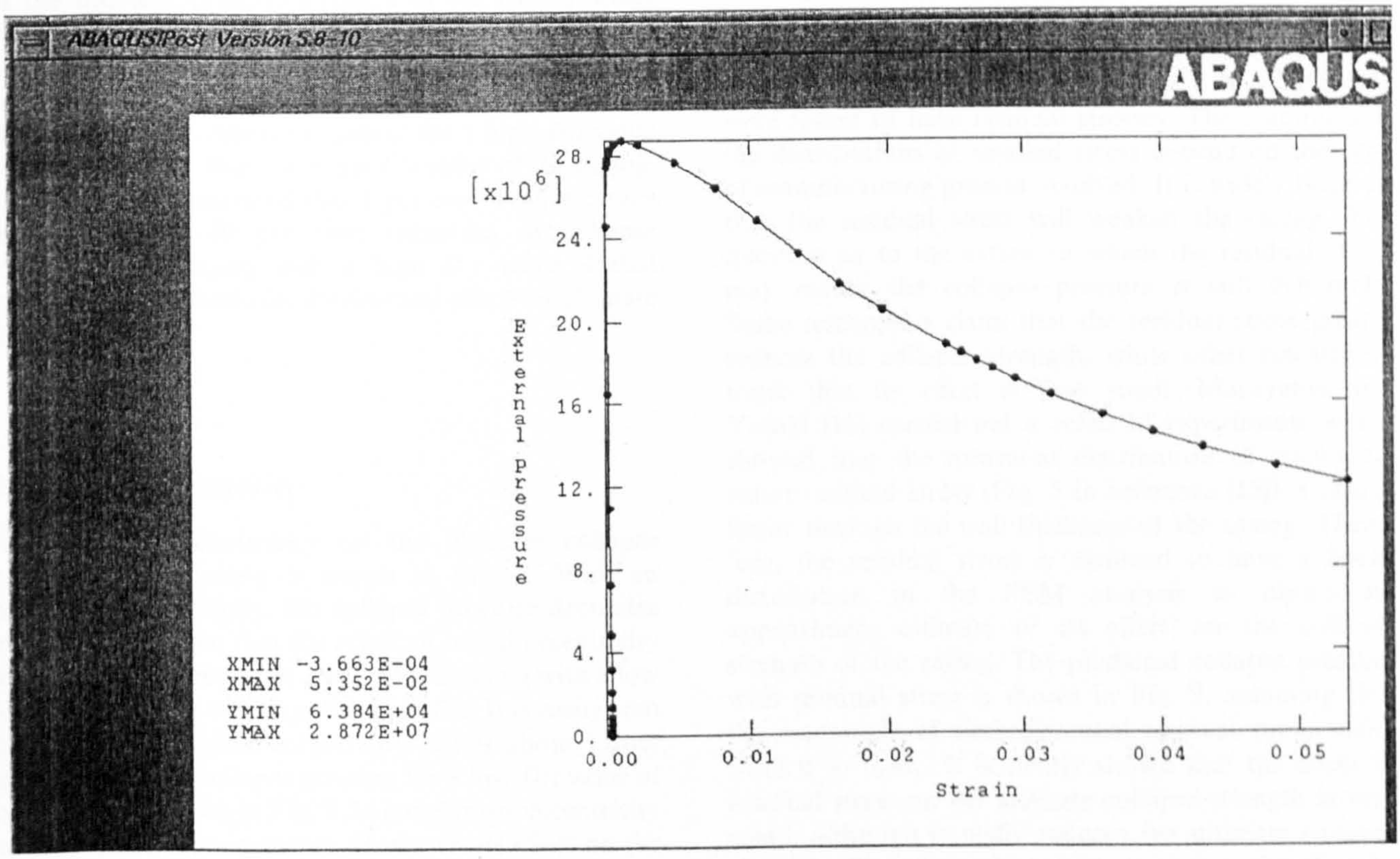

Fig. 5 Predicted pressure and deformation relationship

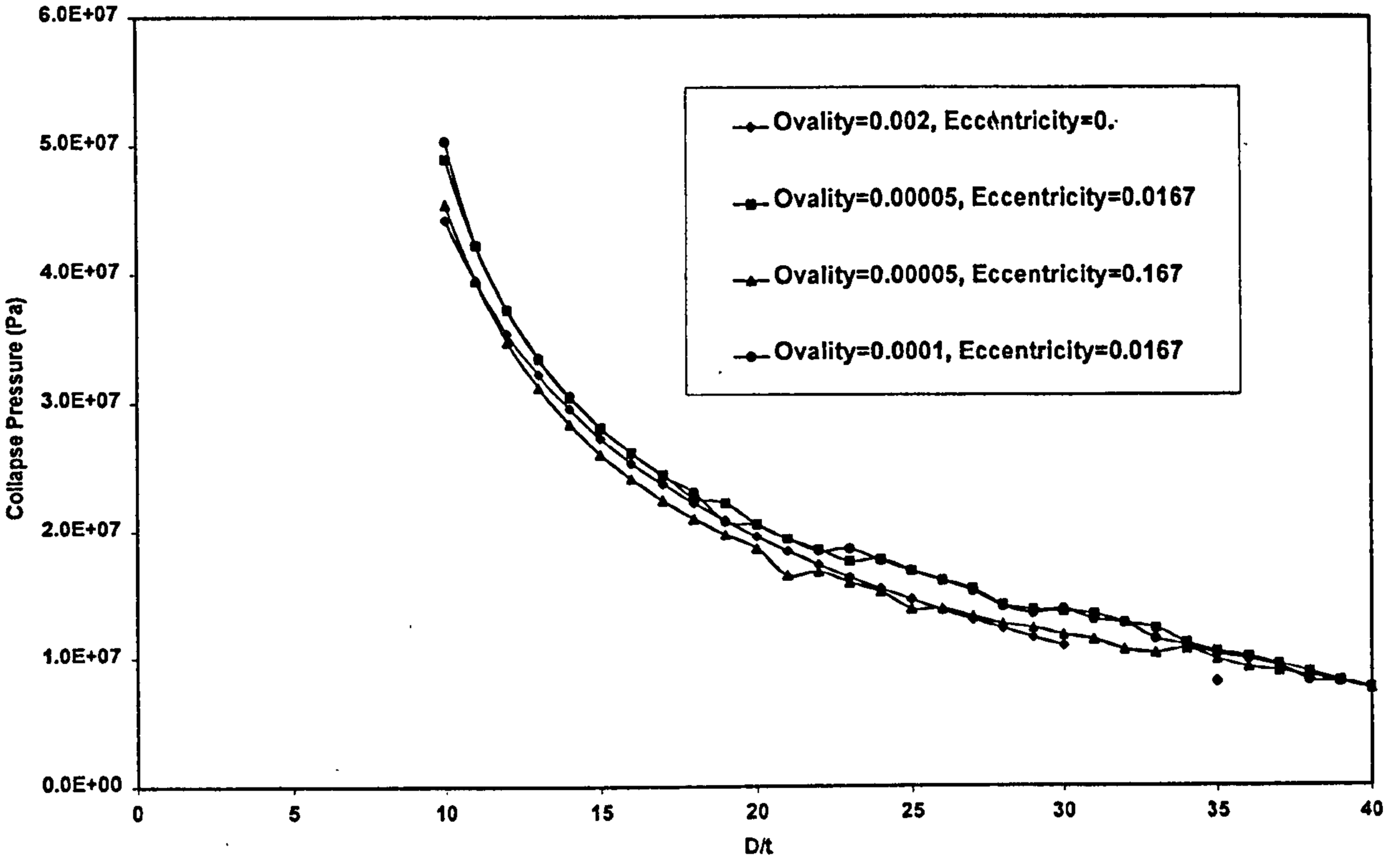

Fig. 6 Effect of D/t on the collapse strength

and even in a welded casing. The effect of initial ovality on the ultimate collapse strength of the casing under external pressure is shown in Fig. 7 with ovality varying from 10^{-5} to 10^{-2}. With an increase in ovality, the collapse pressure decreases greatly. It is shown that the effect of ovality is relatively greater for a high D/t value of the casing than that for a low D/t value of the casing. It is clearly demonstrated that 1 per cent ovality causes an approximate 50 per cent reduction in collapse pressure for a casing with a high D/t value. Initial ovality has a dramatically detrimental effect on ultimate collapse strength.

6.3 Effect of eccentricity

The effect of eccentricity on the ultimate collapse strength of the casing is shown in Fig. 8. With an increase in eccentricity, the collapse pressure decreases greatly. It is shown that the effect of initial eccentricity on the collapse strength is greater for a casing with a low D/t value than for a casing with high D/t. It is easily seen that 30 per cent initial eccentricity causes about 15 per cent reduction in collapse pressure for a low D/t value of the casing, as shown in Fig. 8. In conclusion, eccentricity reduces the collapse pressure. However, its effect on the ultimate collapse strength of the casing is relatively lower than that of initial ovality.

6.4 Effect of residual stress

Manufacturing processes that do not involve annealing will leave residual stresses in the tubes. For example, all of the test specimens tested by Yeh and Kyiakides [11] were found to have residual stresses. The amount and the distributions of residual stress depend on the type of manufacturing process involved. It is widely believed that the residual stress will weaken the casing. The question as to the extent to which the residual stress may reduce the collapse pressure is still debatable. Some researchers claim that the residual stress greatly reduces the collapse strength, while other researchers think that its effect is very small. Maruyama and Yazaki [15] carried out a series of experiments which showed that the measured distribution of circumferential residual stress (Fig. 5 in reference [15]) is nearly linear through the wall thickness of the casing. Therefore, the residual stress is assumed to have a linear distribution in the FEM analysis to obtain an approximate estimate of its effect on the collapse strength of the casing. The predicted collapse pressure with residual stress is shown in Fig. 9, assuming that the magnitude of circumferential residual stress varies from 0 to $0.4\sigma_y$. It is clearly shown that the effect of residual stress on the ultimate collapse strength is very small, although it really reduces the ultimate collapse strength. The effect of residual stress may therefore be neglected in the process of casing design.

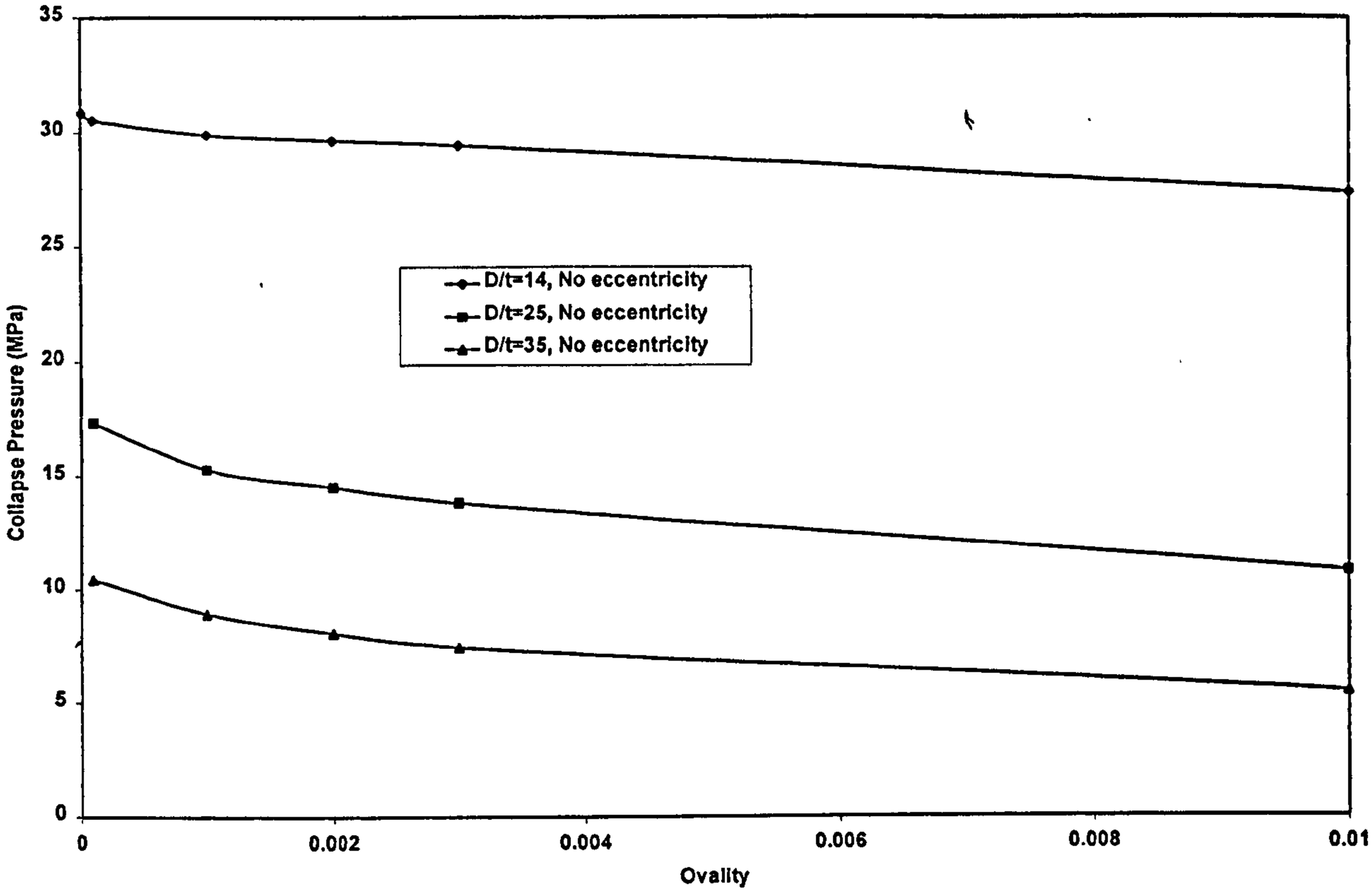

Fig. 7 Effect of initial ovality on the collapse strength

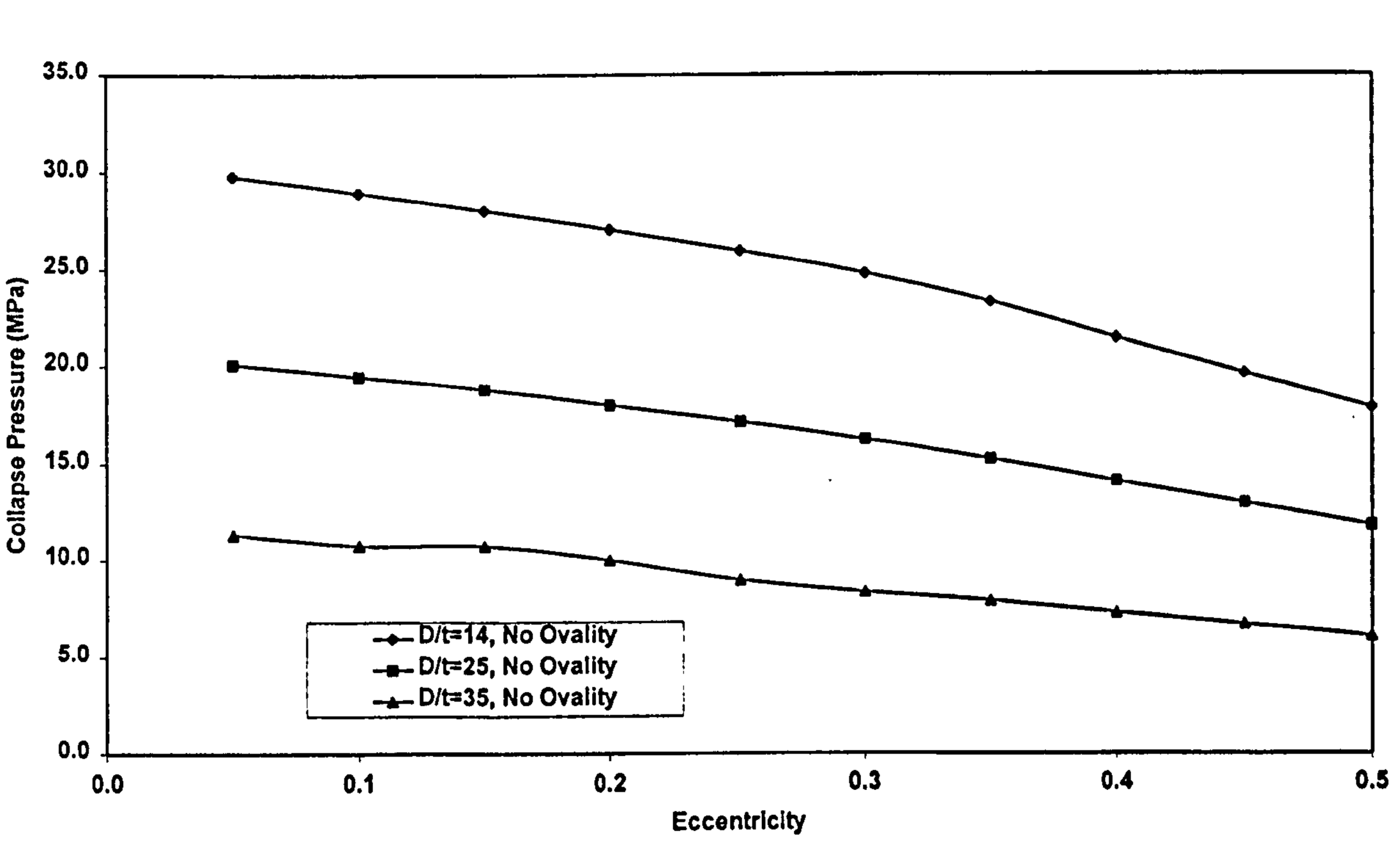

Fig. 8 Effect of initial eccentricity on the collapse strength

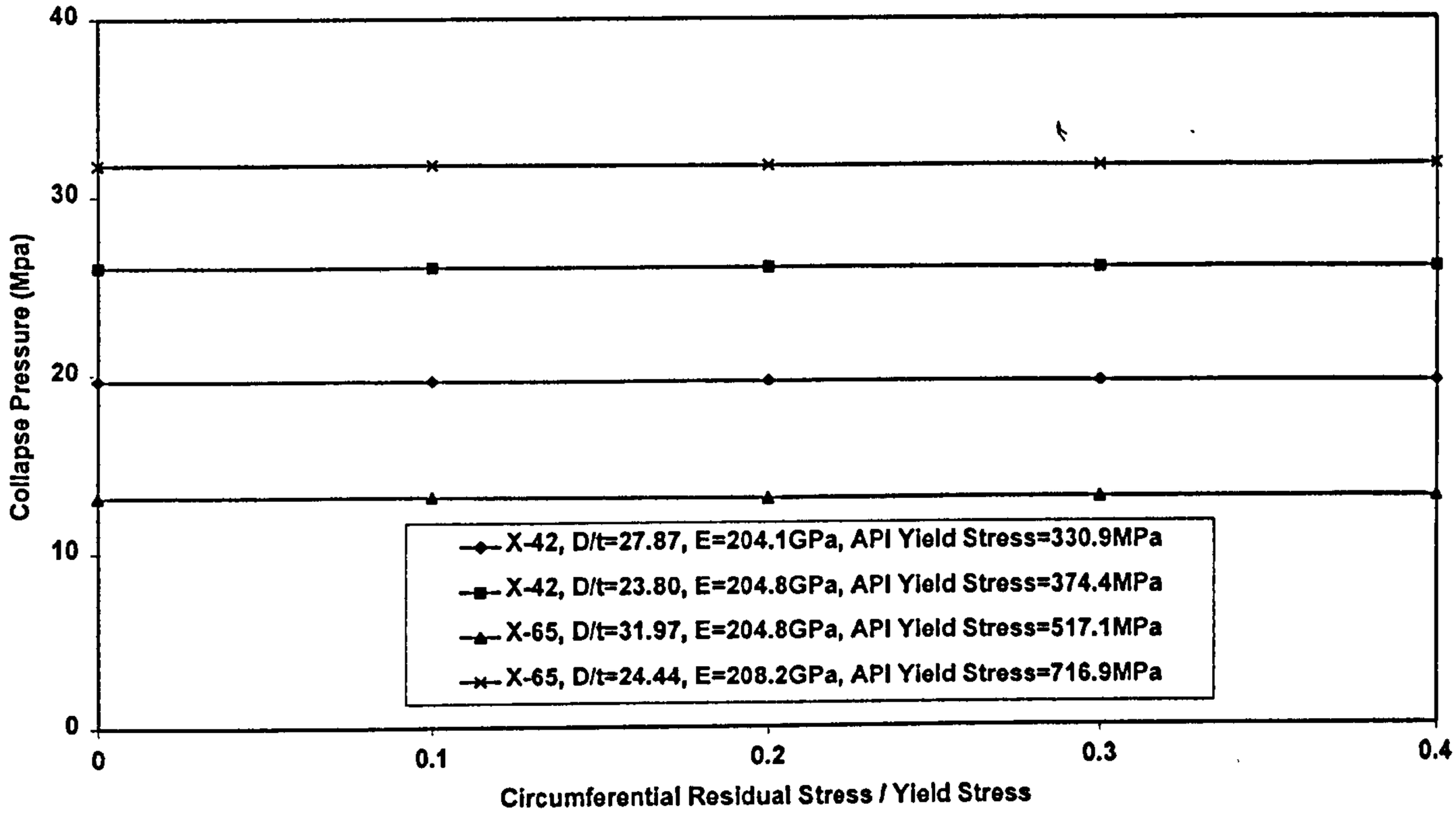

Fig. 9 Effect of residual stress on the collapse strength

6.5 Effect of material hardening parameter

It is generally known from experimental evidence that, during the process of incremental plastic deformation, the loading surface changes size, shape and location. A rule governing this aspect of behaviour, defining the manner of construction of the subsequent loading surface, is called the hardening rule. Mathematically, hardening is characterized by parameters that vary with the plastic load history. The hardening parameter may vary in form from material to material. The choice of a specific hardening rule depends primarily on the case to which it can be applied and its ability to represent the hardening behaviour of a particular material.

The stress–strain relationship used in FEM is crucial for accurate prediction of the collapse behaviour of the casing under external pressure. The nature of the problem requires proper modelling of the inelastic material characteristics. On the basis of the experiments conducted by Yeh and Kyiakides [11], the stress–strain behaviour of test specimen 2 is carefully fitted with a three-parameter Ramberg–Osgood curve [equation (10)]. Though test specimen 2 exhibited only smooth hardening, if an elastic–perfectly plastic material model is used, the predicted collapse strength will be 7.9 per cent higher than the experimental collapse strength. The predicted error will be reduced to −3.2 per cent when the carefully fitted Ramberg–Osgood material model is used, as can be seen in Table 3. Furthermore, the effect of material hardening on the collapse strength is shown in Fig. 10. It can be seen that the predicted collapse pressure of a casing with a relatively low D/t value decreases dramatically as the hardening parameter increases. However, it is found that the predicted collapse pressure of a casing with a relative high D/t value increases with increase in the hardening parameter, though the effect of material hardening on collapse strength is much smaller for a casing with a high D/t value.

6.6 Effect of anisotropy

Many thick casings are drawn, and many plates used for welded tubes are rolled. These manufacturing processes tend to induce material anisotropy. As reported in an earlier experiment [11], half of the test specimens exhibited material anisotropy. In addition, it is reported that the yield stresses measured in the circumferential and the radial direction are the same but different from the yield stress in the axial direction. In the majority of cases, the material anisotropy can be modelled by a yield anisotropy parameter, λ, which is established by adopting Hill's yield theory [14]:

$$\left(\frac{1+\lambda}{2}\right)^{1/2} = \frac{\sigma_{yx}}{\sigma_{ys}} \tag{12}$$

where σ_{yx} is the yield stress in the axial direction and σ_{ys} is the yield stress in the circumferential direction. In the FEM analysis, the effect of material anisotropy is carefully simulated using parameter λ.

The effect of material anisotropy on the collapse strength of casings with different D/t values is shown in Fig. 11. It is clearly shown that the material anisotropy

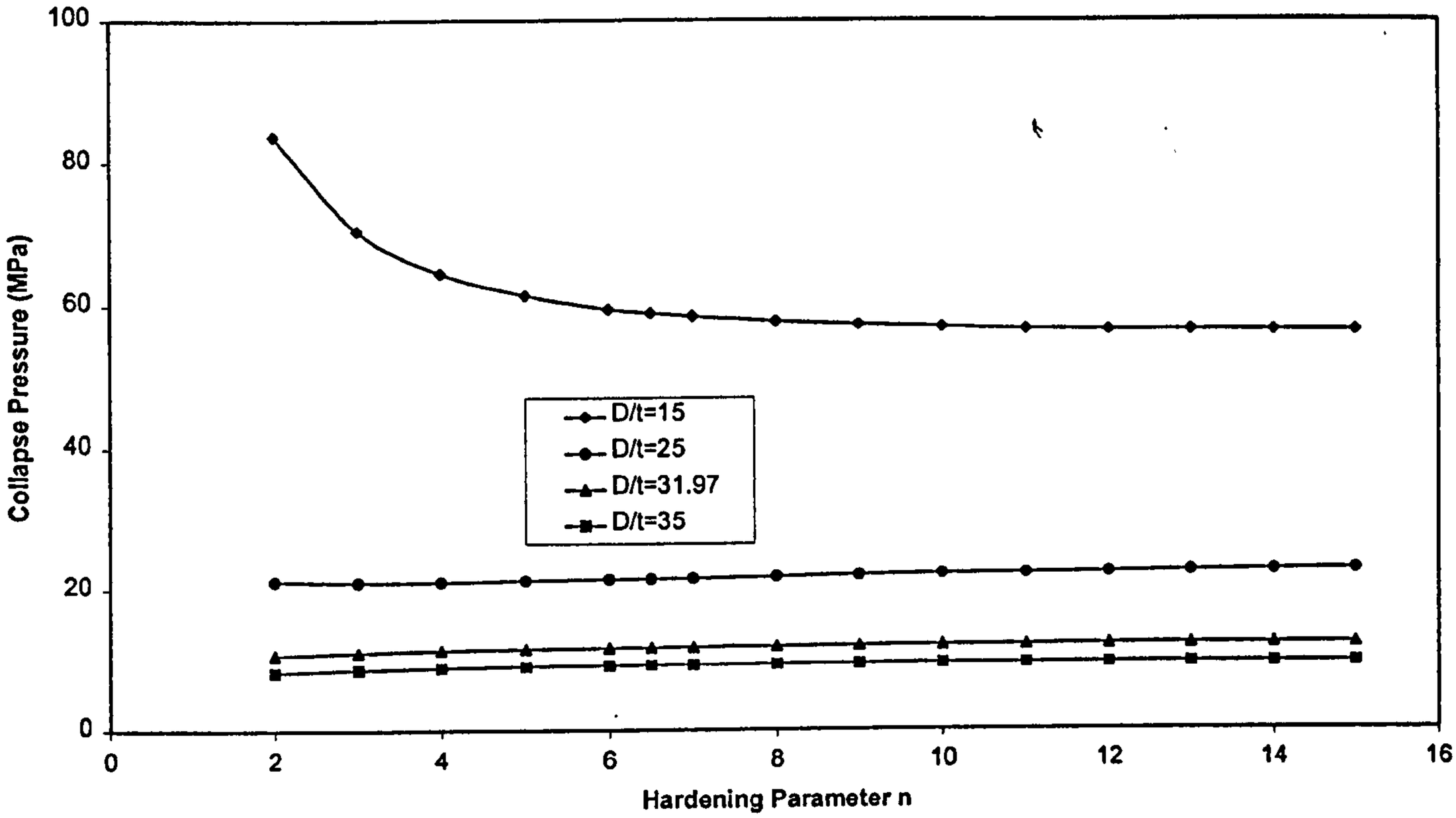

Fig. 10 Effect of material hardening on the collapse strength

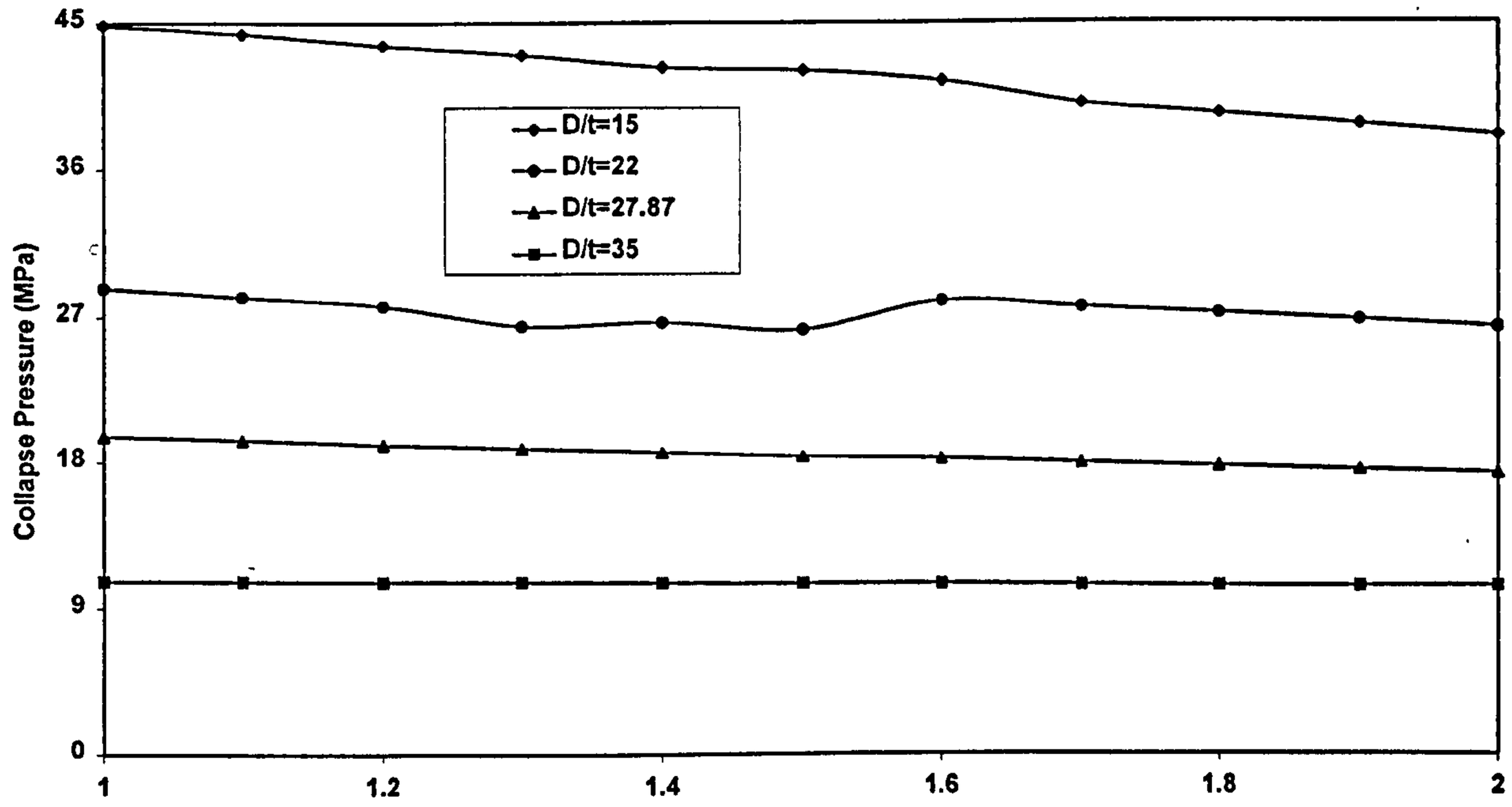

Fig. 11 Effect of the material anisotropy parameter on the collapse strength

directly affects the collapse strength. Its effect is greater for a casing with a relatively low D/t value. Note that the deviation between experiment and FEM predictions of the ultimate collapse strength can be reduced greatly when the anisotropy parameter is considered as shown in Table 3. This proves that the material anisotropy is a very important factor for casing failure in the plastic range. Thus, in the simulation it is obvious that accurate

predictions can be obtained if a stress–strain behaviour obtained from a circumferential test is used in the analysis.

7 CONCLUSIONS

An FEM model has been developed to investigate the ultimate collapse strength of casings under external pressure. The major factors such as initial ovality, eccentricity, residual stress, material hardening and anisotropy were modelled in the analysis. The accuracy and reliability of the proposed FEM model have been validated through a very careful comparison with a series of full-scale experimental data of casings that satisfied the API Spec 5LX specification. Meanwhile, two sets of current existing equations for casing design were used in comparison with the FEM predictions. The geometric imperfections and material behaviour are carefully simulated in the FEM program. It is shown that, if the material behaviour and imperfection variables are known, the ultimate collapse strength can be predicted to a satisfactory degree of accuracy. A parametric study of the ultimate collapse strength of casings was carried out using the proposed FEM model. The following conclusions can be made:

1. The ultimate collapse strength of the casing is sensitive to the geometric imperfections. Significant reduction in the ultimate collapse strength occurs when a small imperfection is introduced. The orientation of eccentricity with respect to ovality has little effect on the ultimate collapse strength, as shown in Table 3.
2. Although most casings are found to have residual stress due to the manufacturing process, the effect of residual stress on the ultimate collapse strength seems to be very small and may be neglected in the design of casing collapse.
3. It is found that material properties (material hardening and anisotropy) are crucial in accurate prediction of the ultimate collapse strength of casings. It is very important to model the material behaviour as accurately as possible.
4. Based on the proposed FEM model, an accurate prediction of the ultimate collapse strength can be obtained for casing design.

ACKNOWLEDGEMENTS

The authors would like to thank BG Technology for the financial support of this research. In addition, the authors would like to thank Marc Nunn, senior engineer of BG Technology, and Dr Kevin Kibble, Senior Lecturer of the University of Wolverhampton, for their kind advice.

REFERENCES

1 **Timoshenko, S. P.** and **Gere, J. M.** *Theory of Elastic Stability*, 2nd edition, 1961 (McGraw-Hill, New York).
2 **Clinedinst, W. O.** A rational expression for the critical collapsing pressure of pipe under external pressure. *Drilling Prod. Pract., API*, 1939, 383–391.
3 **Holmquist, J. L.** and **Nadai, A.** A theoretical approach to the problem of collapse of deep well casing. *Drilling Prod. Pract., API*, 1939, 392–420.
4 **Huang, N. C.** and **Pattillo, P. D.** Collapse of oil well casing. In ASME Meeting San Francisco, August 1980, pp. 12–15.
5 **Tamano, T.** and **Mimaki, T.** A new empirical formula for collapse resistance of commercial casing. *Trans. ASME, Energy Resour. Technol.*, 1983, 489–495.
6 **Issa, J. A.** and **Crawford, D. S.** An improved design equation for tubular collapse. In Proceedings of SPE Annual Technical Conference, Houston, October 1993.
7 **Tokimasa, K.** and **Tanaka, K.** FEM analysis of the collapse strength of a tube. *Trans. ASME, J. Pressure Vessel Technol.*, May 1986.
8 API Bulletin 5C3 on *Formulas and Calculations for Casing, Tubing, Drill Pipe and Line Pipe Properties*, 5th edition, July 1989.
9 **Abbassian, F.** and **Parfitt, S. H. L.** Collapse and post collapse behaviour of tubular: a simple approach. SPE 29458, April 1995.
10 ABAQUS manual, Version 5.8.
11 **Yeh, M. K.** and **Kyiakides, S.** Collapse of deepwater pipelines. *Trans. ASME, J. Energy Resour. Technol.*, 1988, **110**, 1–11.
12 **Qiu, W.** and **Zhao, H.** Major factors having influence on the ultimate collapse strength of casing. *J. Petrol.*, April 1996, **17**.
13 *API Specification 5A*, 39th edition, 31 May 1987.
14 **Hill, R.** *The Mathematical Theory of Plasticity*, 1950 (Oxford University Press, London).
15 **Maruyama, K.** and **Yazaki, Y.** The influence of shape and residual stress. *J. Jap. Ass. Petrol. Technol.*, July 1996, **61**, 292–299.

ELSEVIER

International Journal of Pressure Vessels and Piping 77 (2000) 359–367

INTERNATIONAL JOURNAL OF
Pressure Vessels and Piping

www.elsevier.com/locate/ijpvp

Collapse strength analysis of casing design using finite element method

X. Huang*, M. Mihsein, K. Kibble, R. Hall

Engineering Research Group, School of Engineering and Built Environment, University of Wolverhampton, Wolverhampton WV1 1SB, UK

Received 20 January 2000; revised 11 May 2000; accepted 28 June 2000

Abstract

Accurately predicting the ultimate collapse strength is very important in the design of casings for the oil and gas industry. For an infinitely long thick walled casing subjected to external pressure, a finite element model has been proposed to achieve a better understanding of the ultimate collapse strength of casing. Careful comparison with a series of full-scale experiments has been conducted to verify the accuracy and reliability of the finite element model. In addition, several current predictive equations for casing design have been assessed using those available test data. The validation proves that, if the material behaviour and imperfection variables are known, the ultimate collapse strength of casing can be predicted to a satisfactory degree of accuracy. Major factors, which affect the collapse strength of casing, were studied and their effects on the collapse strength of casing were summarized. Regression analysis has been conducted on the basis of finite element predictions and a new design equation for casing collapse is presented.

Keywords: Collapse strength analysis; Casing design; Finite element method

1. Introduction

The casing is widely used as a protective conduit during all phases of drilling operations and productions for the oil and gas industry. Casings for deepwater applications must be designed to withstand the high ambient external pressure. This implies use of tubes with lower diameter to thickness ratio (D/t) and, when possible, use of higher strength materials. During installation, sections of the casing can experience combined pressure, bending and axial loads. However, when the casing reaches the sea floor eventually, the casing can be considered to be relatively free of other loads but the external pressure, in most cases. It is reasonable to state that collapse strength of the casing under the large hydrostatic pressure on the outside surface is one of the most important considerations in the design of casings. It is widely known that over-design leads to costly tubular purchases while under-design can lead to failures and costly repair operations. Therefore, it is extremely necessary to develop a more accurate method for predicting collapse strength of casings.

The practical design of casing strings for collapse has been based mainly on the empirical solutions, which relate the collapse pressure and important factors affecting the resistance of a casing to collapse. Early work on the collapse strength of a casing under external pressure can be traced back to Clinedinst [1], Holmquist [2] and Timoshenko [3]. With the increasing need in the oil and gas industry, a large amount of experimental and analytical research work has been carried out on the collapse of casings up to date. However, the actual problem of casing collapse presents difficulties because there are many important factors, which strongly influence the collapse strength of casings. The important geometrical factors are the ratio of outside diameter to wall thickness (D/t), the initial ovality and eccentricity. The important mechanical properties are Young's modulus, Possion's ratio and the yield strength. Residual stress and applied axial stress should be listed as other important factors

In recent years, Tamano [4], Issa [5] and Tokimasa [6] investigated the effects of geometric imperfections on the collapse strength of casings, and presented their empirical equations using numerical analyses. However, whether those equations are safe to use for a specific casing design still remains unanswered. Therefore, it is necessary to assess the accuracy of these predictive equations in the design of casing collapse. This study has been initiated and guided by the need to establish a clear and accurate design criterion for casing collapse in the oil and gas industry.

Furthermore, casings with D/t values between 10–40 are widely used for deepwater applications in the oil and gas wells nowadays. For this D/t region of casing, the collapse pressure is largely determined by the inelastic behaviour of

* Corresponding author. Tel.: +44-1902-322-273; fax: +44-1902-322-680.

E-mail address: x.huang@wlv.ac.uk (X. Huang).

0308-0161/00/$ - see front matter
PII: S0308-0161(00)00045-4

Nomenclature

D	casing outside diameter
E	Young's modulus
n	hardening parameter
P_E	elastic collapse pressure under external pressure alone
P_{gp}	general yield pressure without axial loading
P_y	yield onset collapse pressure under external pressure alone
R, r, θ, δ	dimensions (see Fig. 1)
t	wall thickness
u	initial ovality
ν	Poisson's ratio
ξ	initial eccentricity
λ	anisotropy parameter
σ_y	API yield stress (0.5% offset)
σ_{yx}	yield stress in the axial direction
σ_{ys}	yield stress in the circumference direction

tube material. In addition, manufacturing processes such as rolling and drawing tend to induce material anisotropy. However, no predictive equation so far is derived from a numerical model with material anisotropy. In the present study, an elasto-plastic FEM model with material hardening and anisotropy as well as geometric imperfections is proposed to accurately predict the collapse strength of an infinitely long unstiffened thick walled casing subjected to external pressure. The proposed finite element analysis has been validated through an extensive comparison with a series of full-scale test data.

2. Theoretical collapse analysis of an ideal casing

There are two modes of collapse, elastic and plastic, for an ideal infinitely long unstiffened casing under external pressure alone, assuming that it has perfect roundness, with no variation in the wall thickness, and no residual stress. Clinedinst [1] derived a theoretical formula in 1939, which has been accepted by the American Petroleum Institute (API) as the elastic collapse pressure equation

$$P_E = 2\frac{E}{1-\nu^2}\frac{1}{D/t(D/t-1)^2} \tag{1}$$

As most of commonly used casings belong to moderate walled or thick walled casings, their collapses are not just elastic collapses, but extend to plastic collapses. Large amounts of research efforts have concentrated on the plastic collapse behaviour. It is widely assumed that the onset of yield pressure when the inner fibre begins to yield is the plastic collapse pressure for a thick walled casing, and the following plastic collapse pressure equation can be expressed based on the Mises yield criterion:

$$P_y = 2\sigma_y\frac{D/t-1}{(D/t)^2} \tag{2}$$

However, this yield onset pressure typically underestimates the collapse strength, because failure does not occur until the elastic–plastic boundary has penetrated some way through the wall thickness. Tamano [5] investigated this effect by presenting a general yield pressure equation for a thick walled casing under external pressure alone as follows:

$$P_{gp} = 2\sigma_y\frac{(D/t-1)}{(D/t)^2}\left(1+\frac{1.47}{D/t-1}\right) \tag{3}$$

Based on the elastic and plastic collapse theory, four sets of predictive equations were evaluated as below:

- Tamano [4]
- Issa [5]
- Tokimasa [6]
- API Bulletin 5C3 [7]

Details of these predictive equations can be found in references. Detailed comparisons between these equations and full-scale experimental data have been conducted to assess the accuracy of those collapse equations in the design of casing for the oil and gas industry.

3. FE Modelling of casing collapse

The problem of casing collapse is a complicated system governed by highly non-linear equations for the stress, strain and displacement because of the large deformation and material non-linearity involved in the process of casing collapse. Thus, the effective way of obtaining the ultimate collapse pressure of a thick walled casing is to use numerical analysis. Finite element analysis was performed using ABAQUS [8]. To obtain an accurate modelling of plasticity and large deformation, a modified Quasi-Newton solution technique was used to solve the non-linear equations of casing collapse. In particularly, a modified Riks algorithm

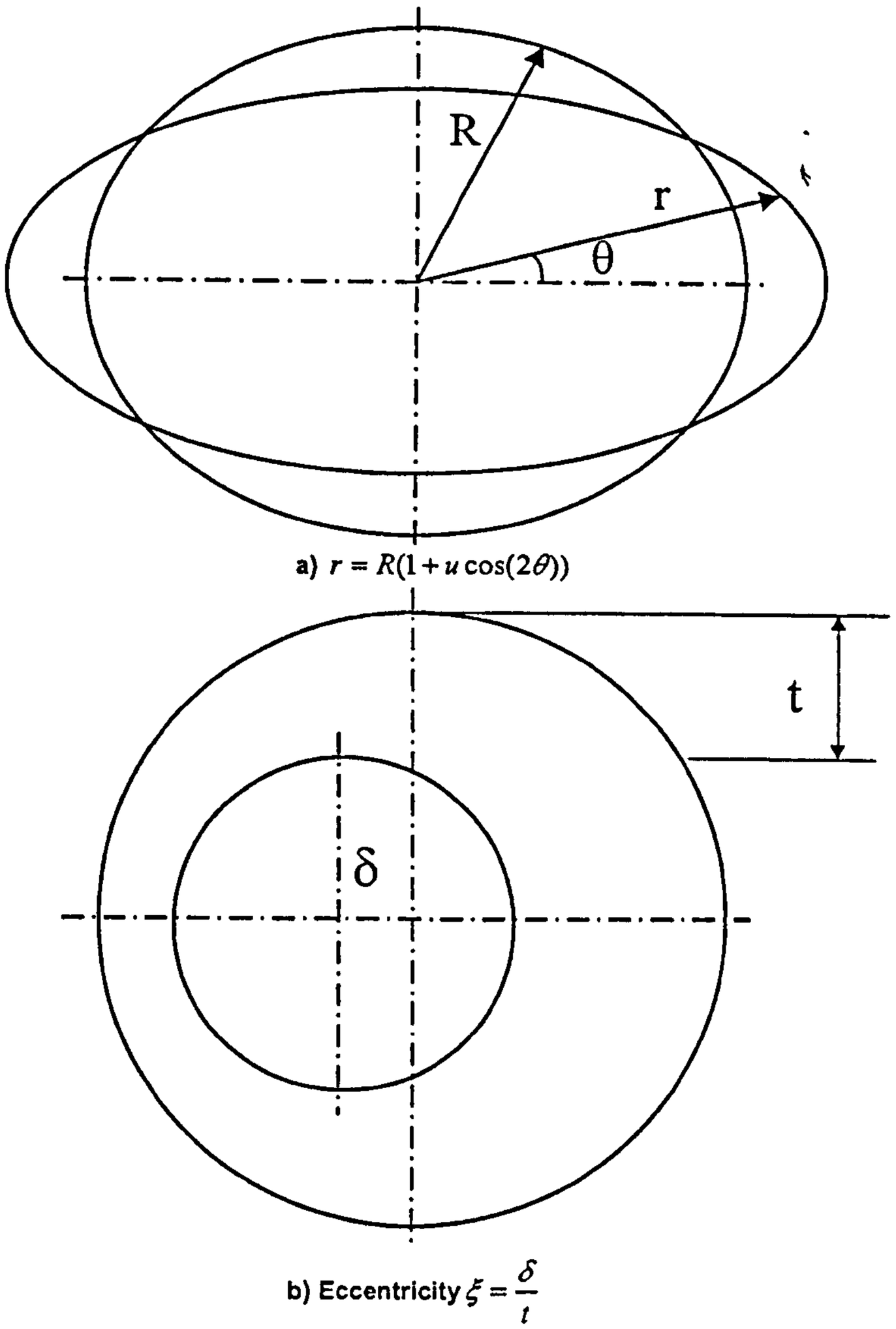

a) $r = R(1 + u\cos(2\theta))$

b) Eccentricity $\xi = \frac{\delta}{t}$

Fig. 1. Measurement of imperfections: (a) $r = R(1 + u\cos(2\theta))$; (b) eccentricity $\xi = \delta/t$.

[8] was employed to carefully control the external pressure to the ultimate load. Following the maximum pressure, the program incrementally reduced the external pressure so that the collapse simulation could be continued. In this way, the post collapse behaviour of the casing can be investigated and the ultimate collapse strength can be obtained.

3.1. Modelling of geometric imperfections

Without the imperfections, the collapse process would not occur and the casing section would deform uniformly. According to the Timoshenko assumption [3], the initial ovality u was introduced by the following equation,

$$r = R(1 + u\cos(2\theta)) \tag{4}$$

where

$$u = \frac{(D_{max} - D_{min})}{D_{max} + D_{min}}$$

r is the imperfect casing radius, R is the nominal perfect casing radius, θ is the angular coordinate measured from the centre of the casing as shown in Fig. 1a.

The real wall thickness of a casing varies along the line of cross-section. The eccentricity parameter ξ is established as below:

$$\xi = \frac{t_{max} - t_{min}}{t_{max} + t_{min}} \tag{5}$$

For the casing section shown in Fig. 1b, the eccentricity

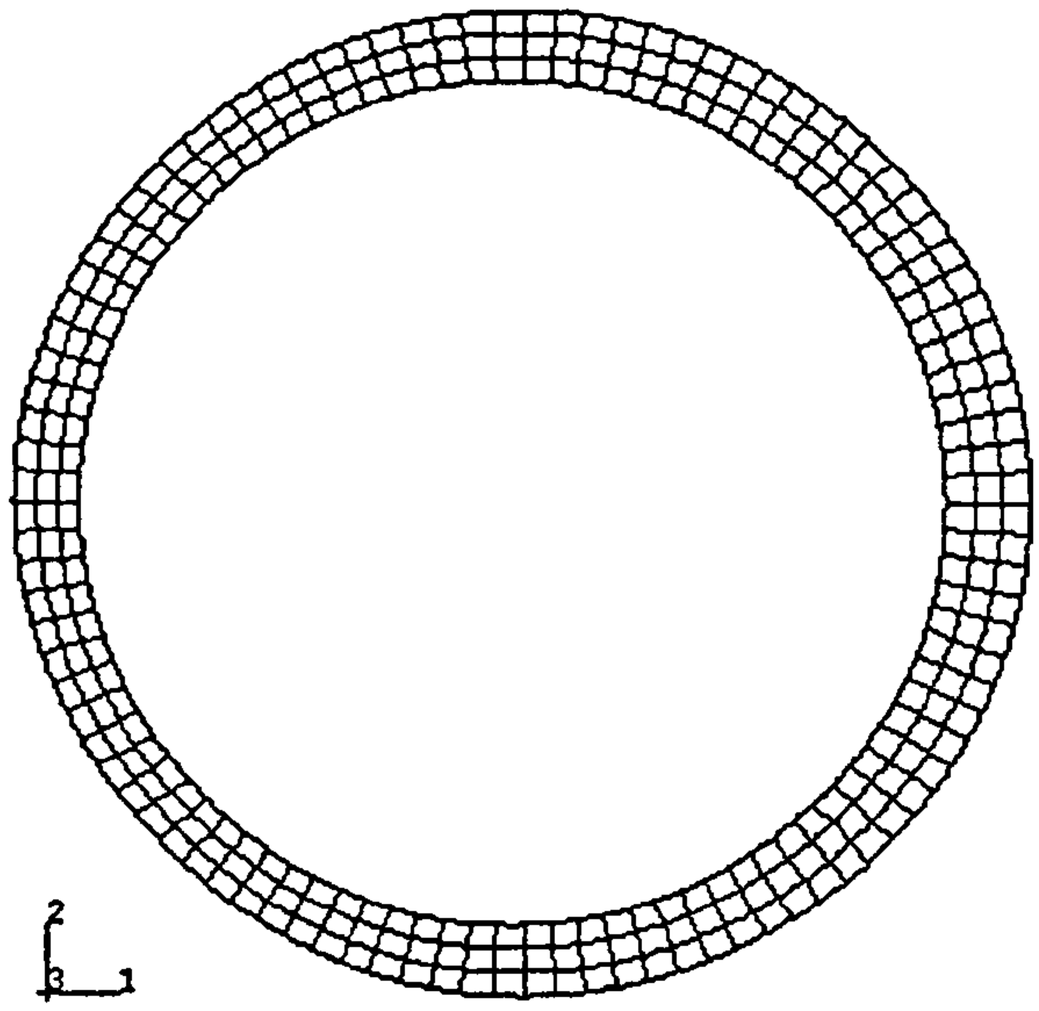

Fig. 2. FEM Model with imperfections.

parameter is described as follows:

$$\xi = \frac{\delta}{t} \tag{6}$$

where δ is the distance between the centres of inner and outside circles, t is the nominal wall thickness.

It is assumed that all of the geometrical variables involved in the analysis are uniform as it is found that the geometric variables and imperfections do not substantially vary along the length of a casing [11]. The imperfections are introduced to allow the collapse to occur, although they are not plainly visible.

The casing section is modelled with outside diameter D, wall thickness t, initial ovality and eccentricity as shown in Fig. 2. The element used in the FEM analysis is a second order generalized plane strain continuum element. To prevent possible artificial locking in the calculation of stiffness matrices, a reduced integration technique [8] is employed in the simulation. The proposed element is of a satisfactory accuracy to predict the collapse pressure after a detailed element type study including two-dimensional shell elements and three-dimensional continuum elements, however, detailed comparisons of predictions from different type of elements are beyond the scope of this paper.

Mesh convergence studies have demonstrated that six integration points across the wall thickness are sufficient for casing collapse. As normally the ratio of casing length to outside diameter is more than 10, the effect of end restraint can be neglected in the simulation [11]. Thus, the problem of casing collapse is reduced to a case of a plane strain problem, and only one element is necessary in the longitudinal direction. The 3D simulation for a long casing yields the same result as that from the proposed plane strain simulation. In addition, the above simplification is supported in the experiment where the measured collapse pressure is reported to be independent of the casing length at $(L/D) \cong 10$ [11].

3.2. Determination of collapse strength

The uniform pressure was applied to the faces of the elements on the outside diameter of the casing section, as shown in Fig. 2. In the simulation, the line direction of the

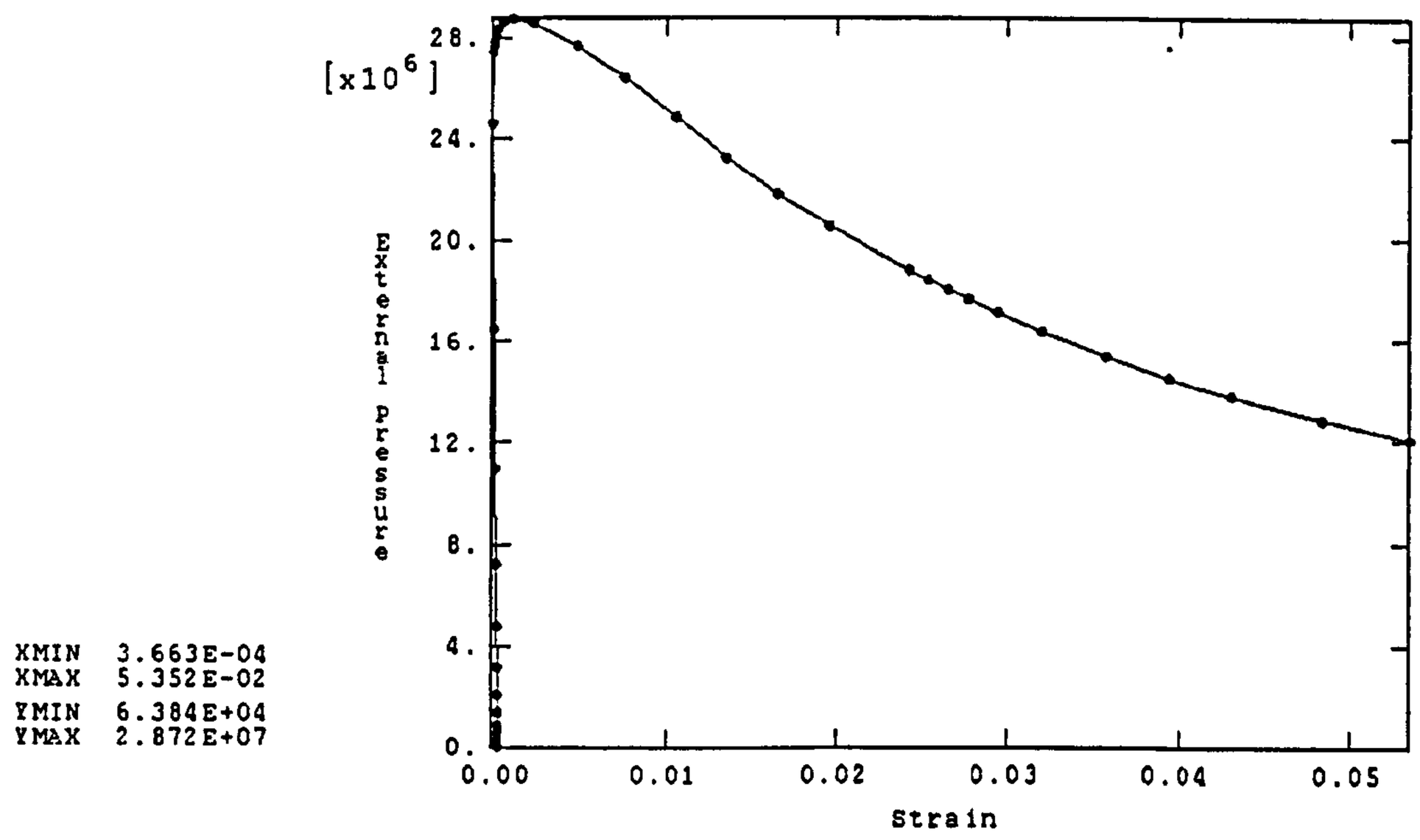

Fig. 3. Predicted external pressure versus strain.

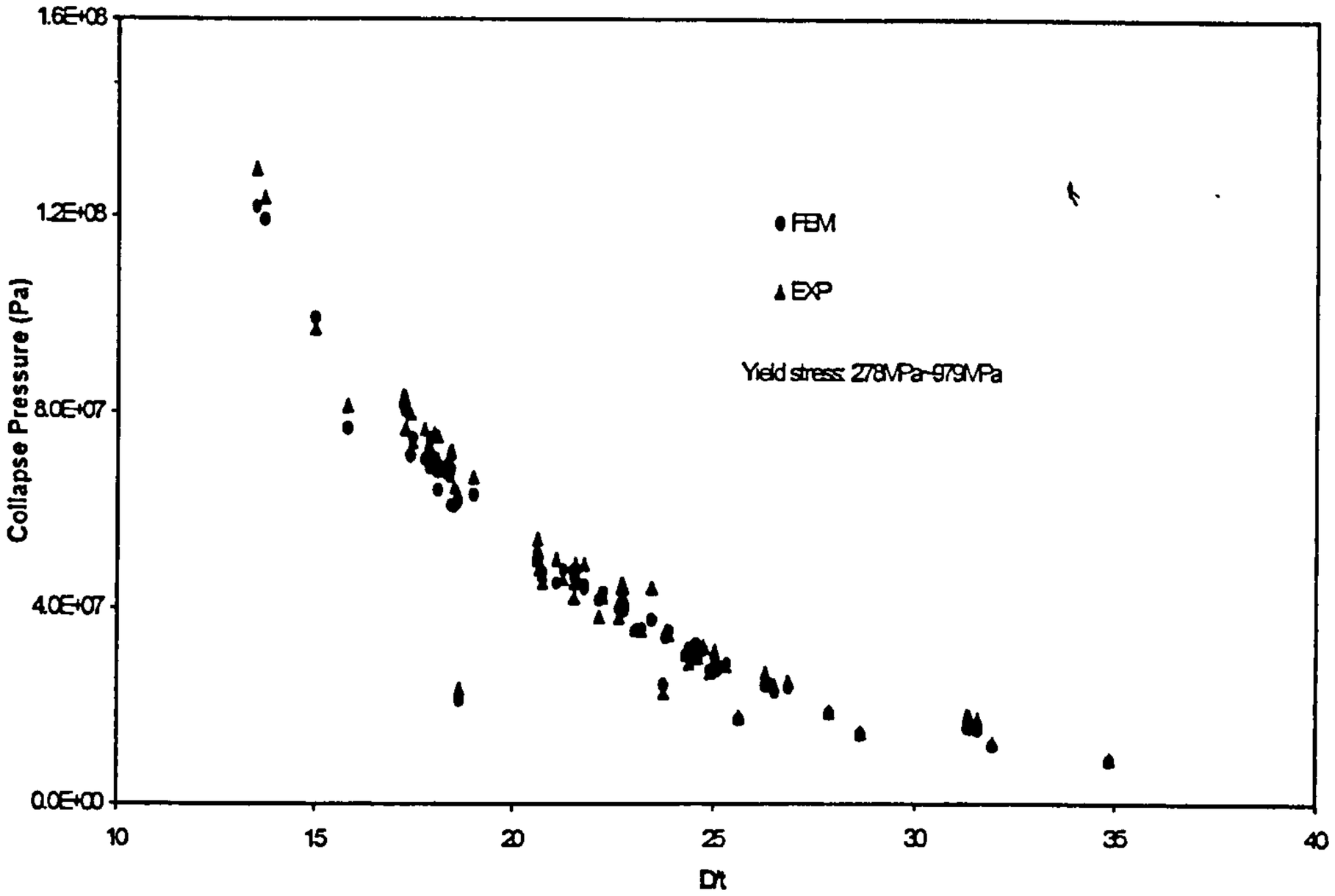

Fig. 4. Comparison between FEM and experiment (97 samples).

applied external pressure changes as the casing section deforms and the pressure is increased incrementally. It is noted that the Cauchy stress and the logarithmic strain [8], instead of engineering stress and strain, are used in the simulation, and no approximation is made in formulating the non-linear equations of casing collapse problem. The external pressure–strain response of the casing was recorded in the simulation. A typical pressure–strain plot is shown in Fig. 3. With the increment of external pressure, the measured pressure increases until the maximum pressure is reached and then a decrease in the pressure can be observed with a large increase of deformation. The maximum pressure was then taken as the collapse pressure of casing. It is the same as in the experiments that collapse of the test specimen is observed when a sudden drop of the pressure is recorded in the test facility. The above procedures enable the FEM program to accurately model the collapse behaviour of casings.

Experimental collapsed Casing Section (Issa, 1993)

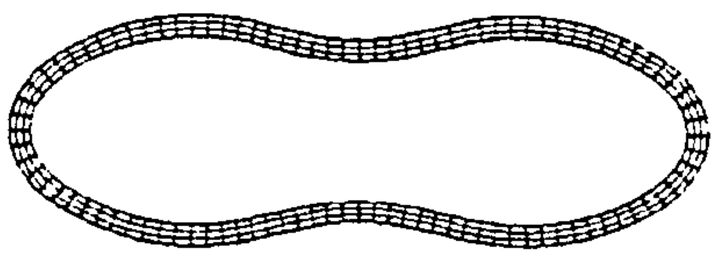

Predicted casing section

Fig. 5. Post collapse behaviour comparison with experiment.

3.3. Material constitutive behaviour

The nature of casing collapse requires proper modelling of the inelastic material characteristics. Thus, the material constitutive behaviour is very crucial for accurately predicting the collapse behaviour of a casing. In the validation, the measured material behaviour from the test is used to justify the accuracy and reliability of the FEM model as shown in Section 4. However, a generalized expression of material behaviour needs to be determined in the derivation of a new design equation for casing collapse, which should be capable of modelling materials of various yield strength. In this study, the interested yield strength of casing ranges from 275.8 Mpa (40 Ksi) to 861.8 MPa (125 Ksi). As a result, the form of the material behaviour was determined by a very careful selection from tensile tests of material properties of commercial seamless steel well casings, and the variables associated with that expression were determined from the experimental data. It is found that the most suitable material behaviour can be expressed in a

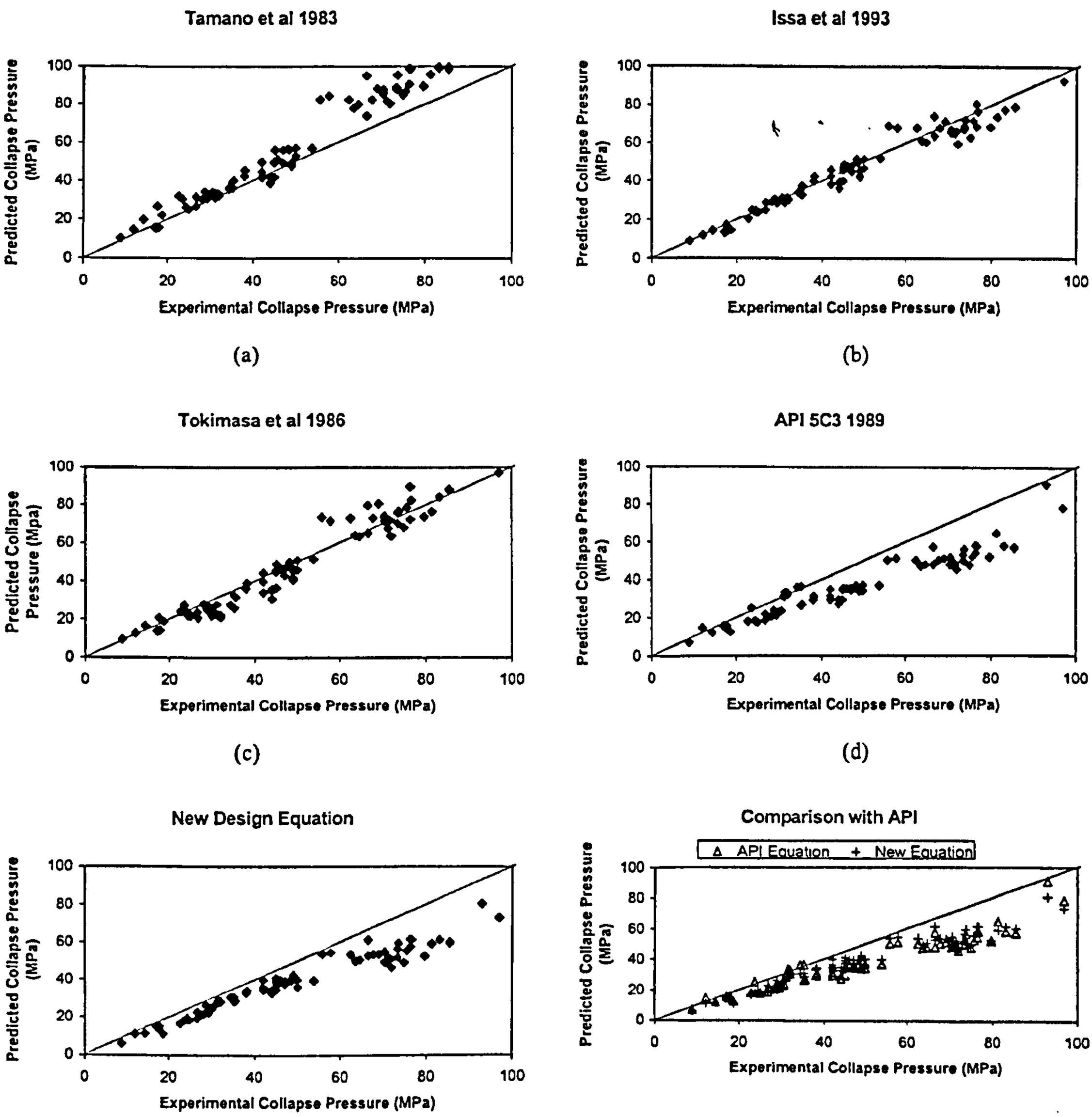

Fig. 6. Comparisons between predicted strength and experimental collapse strength.

Ramberg–Osgood curve as below:

$$\epsilon = \frac{\sigma}{E}\left[1 + \frac{3}{7}\left(\frac{\sigma}{\sigma_0}\right)^{n-1}\right] \tag{7}$$

where σ_0 is a material parameter, which can be determined from the API yield stress σ_y as shown below:

$$\sigma_0 = \frac{\sigma_y}{\left[\frac{7}{3}\left(\frac{0.005 \times E}{\sigma_y} - 1\right)\right]^{1/(n-1)}} \tag{8}$$

In addition, another important factor, the material anisotropy parameter λ, is also included in the proposed generalized material model according to Hill's assumption as defined below [15]:

$$\left(\frac{1+\lambda}{2}\right)^{1/2} = \frac{\sigma_{yx}}{\sigma_{ys}} \tag{9}$$

It is assumed that the yield stresses in the radial and circumferential direction are equal but different from that in the axial direction.

Therefore, a realistic elasto-plastic material model with material hardening and anisotropy was constructed and carefully implemented into the finite element program in the derivation of a new design equation for casing design.

4. Validation with experimental data

The proposed finite element analysis has been validated through an extensive comparison with a series of full-scale experimental data of commercial steel seamless casings [9–11,14]. The steel seamless casings used in the experimental programs were manufactured according to API Spec 5LX. As the casings are often designed to withstand many severe operating conditions, the test data of casing collapse is collected to contain a wide variation in yield strength to meet the potential requirements in the casing design process. The ratios of length to outside diameter (L/D) of the casings tested were larger than 10. Following the imperfection measurements, the test specimens were sealed at both ends and placed in a high-pressure test facility. The collapse experiments were carried out under volume controlled loading conditions. The applied external pressure was continuously monitored using a calibrated pressure transducer and analogue time-based recording equipment. The pressurization rate was low enough to avoid strain rate effects.

The geometry data as well as material behaviour from experiments were carefully coded into the validation programs. The comparison between FEM and experiments is shown in Fig. 4 with the biggest deviation less than 5%. Such an error level can be acceptable because of assumptions regarding material properties. It is crucial for any simulation using FEM to simulate the circumferential material properties as accurately as possible because material anisotropy might be induced in the manufacturing process. However, such data were not included in the available experimental data and the axial material properties were used in the current validation. Some error is also introduced by the fact that geometric imperfections are idealized, such as a uniform ovality. Those factors can be further refined in a more complete treatment of the casing collapse problem. The validation does, however, clearly demonstrate that the collapse strength can be predicted to a satisfactory degree of accuracy.

In addition to predicting the collapse pressures, it is important that a good FEM model is capable of predicting the post collapse behaviour of a casing. For one of the test specimens [11], a picture after collapse was used for comparison with the predicted deformation from FEM as shown in Fig. 5. The excellent agreement between the collapse test data and the predictions from the proposed FEM model as well as the post collapse behaviour justify a satisfactory degree of confidence in using the proposed FEM model to investigate the problem of casing collapse. It has been confirmed that the two-dimensional FEM model is accurate enough to predict the collapse strength of casings.

5. The effects of major factors on the collapse strength

The effects of major factors on the collapse strength of casings have been investigated to study parametric dependence of the collapse strength [12,13]. For a basic idea of their effects on the collapse pressure, a brief summary is given below.

- In general, collapse pressure decreases with the increase of D/t.
- Initial ovality is the most important factor, which dramatically reduces the collapse strength. It is found that a 1% initial ovality causes about 50% of reduction in casing collapse pressure for casings with relatively high D/t.
- The effect of eccentricity on the collapse pressure is the second important factor. With the increase of eccentricity, the collapse pressure decreases greatly. A 30% of initial eccentricity causes about 15% reduction for relatively low D/t value of casing.
- The effect of circumferential residual stress on the collapse pressure is very small, and may be neglected in the engineering casing design.
- The collapse pressure of relatively low D/t value of casing decreases dramatically as the hardening parameter increases. However, it is found that the predicted collapse pressure of relative high D/t value of casing increases with the increase of the hardening parameter, though the effect of material hardening on the collapse strength is much smaller for high D/t value of casing.
- Material anisotropy directly affects the collapse strength of casing. Its effect is bigger for the relatively low D/t value of casings.

6. Development of a new design equation for casing collapse

As mentioned in the previous section, there are four sets of predictive equations worth evaluating. Detailed comparisons have been conducted between these predictions from different design equations and the full-scale experimental data as shown in Fig. 6.

It is found that almost all of the predictions from the Tamano equation are unconservative as shown in Fig. 6a. The potential risk using the Tamano equation for casing design is unacceptably high. The possible reason for its high risk arises from the fact that the material model is assumed to be isotropic without material hardening. Another reason may come from the assumption that the plastic collapse pressure is taken when the whole casing section begins to yield. However, these assumptions may not be valid for the problem of real casing collapse.

Therefore, the Tamano equation overestimates the collapse strength of a real casing.

The predictions from the Issa and Tokimasa equations are relatively closer to the experimental data with approximately half the predictions conservative and half unconservative as shown in Fig. 6b and c, compared with those of the Tamano equation. It is observed that the Issa equation is better than the Tokimasa equation with a smaller deviation from the experiments. Though an elastic perfect plastic material model is used in the derivation of the Tokimasa equation, the effect of material hardening on the collapse strength is considered using a reduction coefficient, which may be the reason why its predictions are more conservative than the Tamano equation. Different from the Tamano and Tokimasa equations, the Issa equation was developed on the basis of a strain hardening elasto-plastic material model fitted from tensile tests of the axial properties of commercial casing, which made its predictions closer to the experimental data than those of the Tamano and Tokimasa equations. However, its material model is still assumed to be isotropic and the axial material properties are used to derive the Issa equation rather than the circumferential material properties.

The predictions from the API equations for the collapse casing design are compared with experimental data as shown in Fig. 6d. It is found that it is conservative in the high-collapse strength region, while unconservative in the relatively lower-collapse strength region. In addition, API equations are the most complicated system among the predictive equations, derived from statistical analysis rather than theoretic deduction.

From the evaluation of those existing design equations for casing collapse, it is necessary to establish a new design criterion for casing collapse, which will give a more accurate prediction of collapse strength of casing while conservative at the same time. Based on the finite element analysis described in the previous section, over 180 finite element models were used to investigate the casing collapse strength. After a detailed non-linear regression analysis has been conducted, the best function that fits the simulation data can be expressed as below:

$$P_{\text{est}} = \frac{2\sigma_y(D/t - 1)}{D/t}\, e^{(h_1 + h_2 D/t)} \tag{10}$$

$$h_1 = 167.6393\frac{\sigma_y}{E} - 2.25314$$

$$h_2 = -10.57427\frac{\sigma_y}{E} - 0.0571617$$

Comparison has been performed against available test data as shown in Fig. 6e. It is shown that the predictions from the new design equation are wholly conservative as expected. In addition, the predictions are more accurate than predictions of the API equation in the relatively lower collapse strength region as shown in Fig. 6f. However, the new design equation is relatively too conservative in the very high collapse strength region, corresponding to the thick casings with D/t values less than 15. The main reason arises from the fact that little data is available around that region. As a result, the ranges of the parameter values in the foregoing Eq. (10) where it can be applied are given as follows:

$$15 \le D/t \le 40 \tag{11}$$

$$10^{-4} \le u \le 2.74 \times 10^{-3}$$

$$8.5 \times 10^{-3} \le \xi \le 8.4 \times 10^{-2}$$

$$277.8\ \text{MPa} \le \sigma_y \le 861.8\ \text{MPa}$$

Further development will be needed when more experimental data becomes available.

7. Conclusions

A methodology using finite element analysis has been developed to investigate the problem of casing collapse under external pressure. Major factors such as initial ovality, eccentricity, material hardening and anisotropy are modelled in the analysis. The accuracy and reliability of the proposed FEM model have been validated through a very careful comparison with a series of full-scale test data. There is a high degree of confidence in using the method to accurately model the problem of casing collapse. At the same time, several current existing predictive equations have been assessed in comparison with available experimental data. After conducting a detailed non-linear regression analysis, a new design equation is presented for the casing design. Further improvement of the proposed design equation of casing collapse is currently being conducted at the University of Wolverhampton.

Acknowledgements

The authors would like to thank BG Technology for the financial support for this research work and permission to publish this paper.

References

[1] Clinedinst WO. A rational expression for the critical collapsing pressure of pipe under external pressure. Drilling Production Practice, API 1939:383–91.

[2] Holmquist JL, Nadai A. A theoretical approach to the problem of collapse of deep well casing. Drilling Production Practice, API 1939:392–420.

[3] Timoshenko SP, Gere JM. Theory of elastic stability. 2nd ed. New York: McGraw-Hill, 1961.

[4] Tamano T, et al. A new empirical formula for collapse resistance of commercial casing. ASME Transactions of Energy Resources Technology 1983:489–95.

[5] Issa JA, et al. An improved design equation for tubular collapse. SPE

26317, Proceedings of SPE Annual Technical Conference, Houston, Oct. 1993.
[6] Tokimasa K, et al. FEM analysis of the collapse strength of a tube. Journal of Pressure Vessel Technology, ASME 1986.
[7] API Bulletin 5C3 on Formulas and Calculations for Casing, Tubing, Drill Pipe and Line Pipe Properties. Fifth edition, July 1989.
[8] ABAQUS manual. Version 5.4, 1998.
[9] Nishioka K, et al. An experimental study on the critical collapsing pressure of seamless steel tube for well casing under external pressure (part 1). Pressure Engineering 1978;16(4):195–204.
[10] Hirakawa K. An experimental study on the critical collapsing pressure of seamless steel tube for well casing under external pressure (part 2). Pressure Engineering 1980;18(5):247–54.
[11] Yeh M, Kyiakides S. Collapse of deep water pipelines. Journal of Energy Research Technology, ASME 1988;110:1–11.
[12] Huang XG, Mihsein M, Kibble K, Hall R. Ultimate collapse strength of casing design. Accepted for ASME Pressure Vessel and Piping Conference, Seattle, Washington, 23–27 July 2000.
[13] Huang XG, Mihsein M. FEM Predictions of the ultimate collapse strength of casing. Journal of Mechanical Engineering Science 2000 (in press).
[14] Yeh M, Kyiakides S. On the collapse of inelastic thick walled tubes under external pressure. Journal of Energy Research Technology, ASME; 1986;108:35–47.
[15] Hill R. The mathematical theory of plasticity. Oxford: Oxford University Press, 1950.

TEXT BOUND INTO

THE SPINE

ASME International

Three Park Avenue
New York, NY 10016-5990
U.S.A.
www.asme.org

September 15, 2000

Reply to:

W. E. Short II, P.E.
Pressure Systems Engineering Inc.
1201 Kirkwood Highway, Suite A
Wilmington, DE 19805
Tel/Fax: 302-683-0490/0493
E-mail: PSEIncDE@aol.com

Mr. Xiaoguang Huang
University of Wolverhampton
Engineering Division
School of Engineering & Built Environment
Wulfruna Street
Wolverhampton, West Midlands
UK WV1 1SB

RE: **ASME PVP DIVISION 2000 STUDENT PAPER COMPETITION**
"ULTIMATE COLLAPSE STRENGTH ANALYSIS OF CASING DESIGN"

Dear Mr. Huang:

Congratulations on being the student author of a 2nd Place Graduate Level paper in the 2000 Student Paper Competition of the ASME Pressure Vessels and Piping Division.

The finalists' papers were very competitive in both technical content and presentation. Placing Second in the Graduate Level Category is a significant achievement.

In recognition of this achievement, enclosed is a Certificate of Recognition awarded by the Senate of the PVP Division. Also enclosed is a $300 award check.

Again, on behalf of the Senate of Past Chairs of the ASME PVP Division, congratulations on your 2nd Place Graduate Level Paper Award in the 8th Annual PVP Division Student Paper Competition.

Very truly yours,

William E. Short II, P.E.
PVP Division Senate

WES:ksk

Enclosures

c: T. H. Liu, Senate President*
S. Y. Zamrik, VP ASME M&S*
Executive Committee*
Prof. M. Mihsein, Univ. of Wolverhampton*
Dr. K. Kibble, Univ. of Wolverhampton*
R. Hall, Univ. of Wolverhampton*
*cover only

HUANG CERT CHK WEW

ASME INTERNATIONAL

The American Society of Mechanical Engineers

Founded 1880

CERTIFICATE OF RECOGNITION

This Certificate is Awarded by
the Senate of the Pressure Vessels and Piping Division to

Xiaoguang Huang

University of Wolverhampton

In Recognition for being a Finalist in the

Student Paper Competition
2000 ASME Pressure Vessels and Piping Conference

"Ultimate Collapse Strength Analysis of Casing Design"

W. E. Short

William E. Short, II

J. Sinnappan

Joseph Sinnappan

ASME INTERNATIONAL

The American Society of Mechanical Engineers

Founded 1880

CERTIFICATE OF RECOGNITION

This Certificate is Awarded by
the Senate of the Pressure Vessels and Piping Division to

Xiaoguang Huang

University of Wolverhampton

In Recognition as the Author of the
2nd Place Graduate Level Paper in the

Student Paper Competition
2000 ASME Pressure Vessels and Piping Conference
"Ultimate Collapse Strength Analysis of Casing Design"

W. E. Short

William E. Short, II
President, PVPD Senate

J Sinnappan

Joseph Sinnappan
Chair, Honors & Awards Committee